

**Kinetics of nitrogenase
from *Azotobacter vinelandii***

Promotor: dr. C. Veeger
emeritus hoogleraar in de Biochemie

Co-promotor: dr. H. Haaker
universitair hoofddocent, vakgroep Biochemie

Kinetics of nitrogenase from *Azotobacter vinelandii*

Martina Gezina Duyvis

Proefschrift
ter verkrijging van de graad van doctor
op gezag van de rector magnificus
van de Landbouwniversiteit Wageningen,
dr. C. M. Karssen,
in het openbaar te verdedigen
op vrijdag 30 mei 1997
des namiddags te half twee in de Aula

UW AG 1725

BIBLIOTHEEK
LANDBOUWUNIVERSITEIT
WAGENINGEN



The research described in this thesis was carried out at the Department of Biochemistry, Wageningen Agricultural University, The Netherlands. The investigations were supported by The Netherlands Foundation for Chemical Research (SON), with financial aid from The Netherlands Organization for Scientific Research (NWO).

ISBN 90-5485-663-7

aan mama, oma en oma

Stellingen

1. Het nitrogenase ijzer-eiwit is een 'molecular switch' eiwit.

Dit proefschrift

2. Dissociatie van het nitrogenase complex is niet noodzakelijk voor de nitrogenase katalyse.

Dit proefschrift, hoofdstuk 6

3. De geldigheid van het model waarmee Lowe *et al.* de absorptieveranderingen bij 430 nm tijdens de reactie van *Klebsiella pneumoniae* nitrogenase verklaren, is onvoldoende aangetoond.

Lowe, D. J., Fisher, K. & Thorneley, R. N. F. (1993) *Biochem. J.* 292, 93-98
Dit proefschrift, hoofdstuk 4

4. De conclusie van Mukund & Adams dat de omzetting van glucose tot acetaat door *Pyrococcus furiosus* 4 mol ATP per mol glucose oplevert, getuigt van een nieuwe kijk op bio-energetische processen, maar is onjuist.

Mukund, S. & Adams, M. W. W. (1995) *J. Biol. Chem.* 270, 8389-8392

5. Ten onrechte wordt nog steeds gesuggereerd dat intramoleculaire transacyleringsreacties tussen lipoylgroepen snel genoeg zijn om een significante bijdrage te leveren aan de overall activiteit van 2-oxozuurdehydrogenase complexen.

Perham, R. N. (1991) *Biochemistry* 30, 8501-8512

Voet, D. & Voet, J. G. (1995) *Biochemistry* (John Wiley & Sons, Inc., New York, USA)

Mathews, C. K. & van Holde, K. E. (1996) *Biochemistry* (The Benjamin/Cummings Publishing Company, Inc., Menlo Park, USA)

6. De benaming 'diazotroof' voor een organisme dat in staat is N_2 te benutten als stikstofbron, suggereert dat een dergelijk organisme in zijn energiebehoefte voorziet door middel van de afbraak van N_2 . Men kan beter spreken van 'chemodiazotroof' of 'fotodiazotroof'.
7. Het huidige gebruik om 'een stuk(je)' in plaats van 'een beetje' te zeggen, doet uitdrukkingen als 'een stuk verdriet' hun duidelijkheid verliezen.
8. Het openhartig onthullen van hun handelen en gevoelens door sommige mensen, juist voor het oog van de televisiecamera - in programma's als 'Het spijt me' - trekt onbedoeld de door hen aangevoerde beweegredenen in twijfel.
9. Het verdient aanbeveling de zeilterm 'fok bak' te vervangen door 'fok te loevert'.
10. Het experiment dat alle andere experimenten overbodig maakt wordt meestal pas bedacht wanneer al die andere experimenten al zijn uitgevoerd.

Stellingen behorende bij het proefschrift
'Kinetics of nitrogenase from *Azotobacter vinelandii*'

Martina G. Duyvis
Wageningen, 30 mei 1997

Contents

| | |
|--|-----|
| Symbols and abbreviations | 9 |
| Chapter 1 Introduction | 11 |
| Chapter 2 Pre-steady-state MgATP-dependent proton production and electron transfer by nitrogenase from <i>Azotobacter vinelandii</i> | 39 |
| Chapter 3 Formation and characterization of a transition state complex of <i>Azotobacter vinelandii</i> nitrogenase | 59 |
| Chapter 4 Pre-steady-state kinetics of nitrogenase from <i>Azotobacter</i> <i>vinelandii</i> . Evidence for an ATP-induced conformational change of the nitrogenase complex as part of the reaction mechanism | 71 |
| Chapter 5 Evidence for multiple steps in the pre-steady-state electron transfer reaction of nitrogenase from <i>Azotobacter vinelandii</i> | 87 |
| Chapter 6 Kinetics of nitrogenase from <i>Azotobacter vinelandii</i> : is dissociation of the nitrogenase complex necessary for catalysis? | 105 |
| Chapter 7 Summary and concluding remarks | 131 |
| Samenvatting | 139 |
| Curriculum vitae | 147 |
| Publications | 149 |
| Nawoord | 151 |

Symbols and abbreviations

Av1 and Av2, Kp1 and Kp2, Ac1 and Ac2: MoFe protein and Fe protein from *Azotobacter vinelandii* (Av), *Klebsiella pneumoniae* (Kp), *Azotobacter chroococcum* (Ac), respectively.

| | |
|----------------------|--|
| Å | angstrom (0.1 nm) |
| Av1* | one of two independently functioning halves of Av1 |
| A_x | absorbance at x nm |
| $\Delta A_{x(\max)}$ | maximal absorbance change at x nm |
| ADP | adenosine 5'-diphosphate |
| ATP | adenosine 5'-triphosphate |
| CD | circular dichroism |
| cresol red | <i>o</i> -cresolsulphonphthalein |
| DEAE | diethylaminoethyl |
| DNA | deoxyribonucleic acid |
| e^- | electron |
| ϵ_x | molecular absorbance coefficient at x nm |
| ELISA | enzyme linked immunosorbent assay |
| E_m | redox midpoint potential |
| E_n | one of two independently functioning halves of the MoFe protein, reduced by n electrons |
| EPR | electron paramagnetic resonance |
| FeFeco | iron-iron cofactor |
| FeMoco | iron-molybdenum cofactor |
| FeVaco | iron-vanadium cofactor |
| Fld _{SQ} | flavodoxin semiquinone |
| Fld _{HQ} | flavodoxin hydroquinone |
| GDP | guanosine 5'-diphosphate |
| GTP | guanosine 5'-triphosphate |
| HPLC | high performance liquid chromatography |
| k | rate constant |
| k_{obs} | observed rate constant |
| K | equilibrium constant |
| K_d | dissociation constant |

| | |
|------------|---|
| kDa | kilodalton |
| MSE | mean square error |
| n | number of electrons |
| NMR | nuclear magnetic resonance |
| ox | oxidized |
| PEEK | polyetheretherketone |
| P_i | inorganic phosphate |
| PMS | phenazine methosulphate |
| red | reduced |
| S | electron spin |
| $s_{20,w}$ | sedimentation coefficient at 20 °C in water |
| t | time |
| TCA | trichloroacetic acid |
| Tes | 2-[[2-hydroxy-1,1-bis(2-hydroxymethyl)ethyl]amino]ethanesulfonic acid |
| Tris | 2-amino-2-hydroxymethylpropane-1,3-diol |
| v | rate |

Chapter 1

Introduction

Nitrogen is an essential element in biological macromolecules such as proteins and nucleic acids, and is therefore indispensable to life. As for all bio-elements, a cycle can be imagined (the nitrogen cycle) which describes the circulation of nitrogen through soil and water, living organisms and atmosphere. Dinitrogen, N_2 , is abundant in the atmosphere but is kinetically inert towards reduction or oxidation and is thus not metabolically usable for most organisms. When nitrogen is available in a reduced form (such as in ammonia, NH_3) or an oxidized form (like in nitrate, NO_3^-), it can be utilized by plants and microorganisms for the biosynthesis of amino acids and other biomolecules, via glutamate and glutamine. The so-called denitrifying bacteria use nitrate as electron acceptor in their respiration, and thereby deplete the earth's supply of metabolically usable nitrogen.

The discovery of nitrogen fixation - which is the utilization of dinitrogen as a nitrogen source - by leguminous plants was published by Hellriegel and Wilfarth in 1888. Shortly after this discovery it was understood that the biological fixation of nitrogen must be ascribed to the microorganisms (*Rhizobium*) living in symbiosis with the plant, and not to the plant itself (Beijerinck, 1888). In the following years other microorganisms were found to fix nitrogen as well. The diazotrophs, as the nitrogen fixers are called, constitute a group of physiologically diverse microorganisms: among them are free-living bacteria, bacteria living in symbiosis with specific host plants (e.g. *Rhizobium*), obligate anaerobes (e.g. *Clostridium*), facultative aerobes (e.g. *Klebsiella*) and obligate aerobes (e.g. *Azotobacter*), cyanobacteria (e.g. *Anabaena*), photosynthetic bacteria (e.g. *Rhodospirillum*) and archaea (e.g. *Methanobacterium*). No eukaryotic organisms are known to fix nitrogen. Comprehensive lists of the diazotrophs are given by Postgate (1982) and Young (1992). However diverse the diazotrophs are, they all possess a similar enzyme system, **nitrogenase**, which enables them to reduce dinitrogen to ammonia. Some nitrogen fixation occurs by lightning and ultraviolet radiation, and in the industrial Haber-Bosch process dinitrogen is converted to ammonia at temperatures between 300 and 500 °C and pressures over 300 atmospheres. From the ecological point

of view, all organisms are, ultimately, mainly dependent on the relatively small group of diazotrophic organisms for their supply of biologically usable nitrogen.

Nitrogenase

Nitrogenase consists of two oxygen-sensitive metalloproteins that cooperate in catalysis (Mortenson, 1965; Bulen & LeComte, 1966; Mortenson et al., 1967): the molybdenum-iron protein (MoFe protein or Av1 - if, as in this thesis, nitrogenase from the obligate aerobe *Azotobacter vinelandii* is concerned) and the iron protein (Fe protein or Av2). The separate nitrogenase proteins do not have any nitrogenase activity. If MgATP is present, the Fe protein acts as a specific electron donor to the MoFe protein, which contains the active site. Other low potential electron donors do not reduce the MoFe protein further than the 'as-isolated' (dithionite-reduced) state (Mortenson et al., 1972; Orme-Johnson et al. 1972; Smith et al., 1972, 1973; Zumft et al., 1974). The Fe protein from one organism and the MoFe protein from another organism often are catalytically active together, which indicates a large homology between the nitrogenase proteins from the different diazotrophs (Detroy et al., 1968; Emerich & Burris, 1978). Exceptions are the nitrogenase proteins from *Clostridium pasteurianum* in combination with the nitrogenase proteins from, amongst others, *A. vinelandii* (Emerich & Burris, 1976, 1978). The general pathway of the electrons through nitrogenase is:

electron donor \rightarrow Fe protein \rightarrow MoFe protein \rightarrow substrate

In vivo ferredoxin (D'Eustachio & Hardy, 1964; Mortenson, 1964a) or flavodoxin (Knight & Hardy, 1966) serves as the electron donor to the Fe protein, *in vitro* sodium dithionite is used (Bulen et al., 1965). The reduction of dinitrogen requires MgATP (McNary & Burris, 1962; Hardy & D'Eustachio, 1964; Mortenson, 1964b; Burns & Bulen, 1965), which is hydrolysed during the reaction (Hardy & Knight, 1966). Under optimal conditions, 2 molecules of MgATP are hydrolysed per electron transferred to the substrate (Ljones & Burris, 1972). Hydrogen is an inevitable side product of the reduction of dinitrogen (Hardy et al., 1964; Bulen et al., 1965; Burns & Bulen, 1965; Simpson & Burris, 1984). The overall reaction catalysed by nitrogenase may be written as follows:



The reaction is thermodynamically favourable (Watt et al., 1975; Orme-Johnson, 1985; Alberty, 1994) but a high activation barrier has to be overcome in breaking the $\text{N}\equiv\text{N}$ triple bond. The turnover time of the reduction of N_2 to 2NH_3 and H_2 is approximately 1.3 s (at 23 °C); the concentration of nitrogenase *in vivo* is about 100 μM (Thorneley & Lowe, 1984b). The rate of substrate reduction is sensitive to pH (Winter & Burris, 1968; Hadfield & Bulen, 1969; Pham & Burgess, 1993), temperature (Burns, 1969; Thorneley et al., 1975; Watt & Burns, 1977) and the ratio of the nitrogenase proteins (Eady et al., 1972; Davis, 1975; Thorneley, 1975; Thorneley & Lowe, 1984b).

Besides the reduction of dinitrogen to ammonia and the reduction of protons to hydrogen, nitrogenase reduces a number of small unsaturated molecules (Burgess, 1985), such as acetylene (Dilworth, 1966), cyanide and azide (Hardy & Knight, 1967). All substrates of nitrogenase are reduced by a multiple of two electrons and equivalent numbers of electrons and protons are required (Burgess, 1985; Burris, 1991). The electron flux through nitrogenase is independent of the substrate; however, under conditions of a low electron flux (for example in the case of a low ratio $[\text{Av}2]/[\text{Av}1]$) products requiring few electrons, like H_2 , are favoured at the cost of products like N_2 (Hageman & Burris, 1980; Wherland et al., 1981). Acetylene reduction is widely used as a convenient and sensitive assay of nitrogenase activity.

Each of the substrates of nitrogenase inhibits the reduction of the other substrates since they compete for the same pool of reduced Fe protein (Rivera-Ortiz & Burris, 1975). The nitrogenase reaction is inhibited by MgADP (Moustafa & Mortenson, 1967). H_2 is an inhibitor of the reduction of N_2 (Lockshin & Burris, 1965; Koch et al., 1967; Strandberg & Wilson, 1967), but does not affect the reduction of the other nitrogenase substrates (Hwang et al., 1973; Burgess, 1985). CO is not a substrate of nitrogenase, but inhibits all nitrogenase-catalysed reductions except the production of H_2 (Lockshin & Burris, 1965; Hwang et al., 1973; Burgess, 1985). Salts inhibit the reduction of the various nitrogenase substrates by an, as yet, unidentified mechanism (Bulen & LeCompte, 1966; Shah et al., 1970; Burns et al., 1985; Deits & Howard, 1990).

The MoFe protein

The nitrogenase MoFe protein is an $\alpha_2\beta_2$ -tetramer, of approximately 230 kDa. The α -subunit is ~50 kDa, the β -subunit ~60 kDa (Eady et al., 1972; Zumft et al., 1972). The crystal structure of the MoFe protein from *A. vinelandii* was determined at 2.7 Å resolution by Kim & Rees (1992a,b) and refined later, to 2.2 Å resolution (Chan et al., 1993), see Figure 1. The α -subunit and the β -subunit each consist of three domains of the α -helix/ β -sheet type, with a cleft at the interface of the three domains. Between the

two $\alpha\beta$ -dimers is an open channel of ~ 8 Å diameter and length ~ 35 Å (Kim & Rees, 1992b). Each $\alpha\beta$ -dimer of the MoFe protein has one binding site for the Fe protein (Kim & Rees, 1992b) and is supposed to function independently from the other $\alpha\beta$ -dimer during catalysis (Thorneley & Lowe, 1984a). The MoFe protein contains two different metal-sulphur clusters per $\alpha\beta$ -dimer: the FeMo cofactor (FeMoco) and the P-cluster. Within the $\alpha\beta$ -dimer the distance between FeMoco and the P-cluster is approximately 19 Å; the distance between the metal-sulphur clusters on the separate $\alpha\beta$ -dimers is ~ 67 Å (Kim & Rees, 1992a). FeMoco is thought to be the site of substrate binding and reduction (Hawkes et al., 1984; Imperial et al., 1989). Recent studies indicated that the P-cluster is probably involved in mediating the electron transfer from the Fe protein to FeMoco (Peters et al., 1995; Ma et al., 1996); the Fe protein transfers a single electron to the P-cluster if the P-cluster is oxidized by two electron equivalents (Lanzilotta & Seefeldt, 1996).

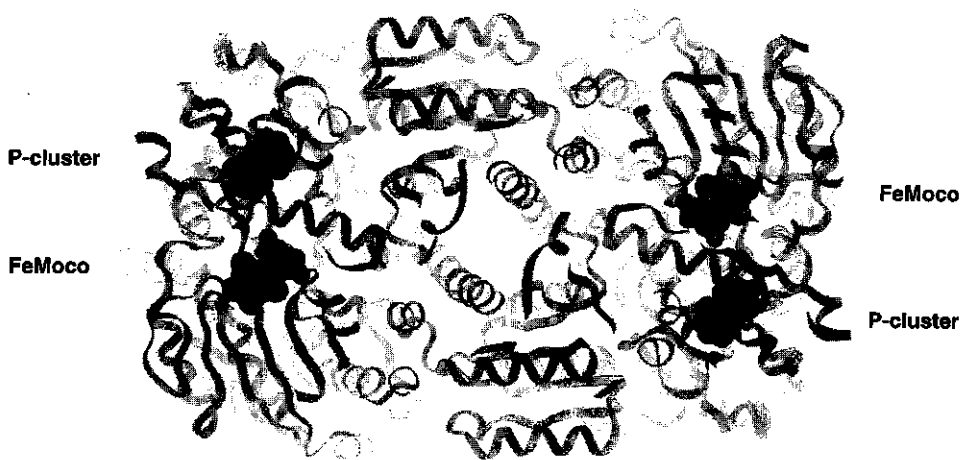


Figure 1. Polypeptide fold of the MoFe protein from *A. vinelandii* (Kim & Rees, 1992a,b). A slice of the protein, including the metal-sulphur clusters, is shown. The FeMo cofactors and P-clusters are represented by space-filling models. (Figure prepared with Insight II.)

The FeMo cofactor (with approximate composition MoFe_3S_6) was first isolated by Shah & Brill, in 1977. The cofactors from various nitrogen fixing organisms appeared to be very similar (Shah & Brill, 1977). An essential component of FeMoco is homocitrate (Hoover et al., 1987; Madden et al., 1990). From the crystallographic analysis of the

MoFe protein from *A. vinelandii*, Kim & Rees (1992a) concluded that FeMoco consists of a [4Fe-3S] cluster bridged by probably three (non-protein) sulphur ligands to a [1Mo-3Fe-3S] cluster, see Figure 2 (Kim & Rees, 1992a; Chan et al., 1993). Bolin et al. (1993) established from (2.2 Å resolution) crystallographic analysis that all three bridging atoms in FeMoco of *C. pasteurianum* are sulphur. Six of the seven iron atoms of FeMoco have an unusual three-coordinated geometry; the seventh Fe is liganded to the side chain of Cys^{α275}. The molybdenum atom has an octahedral coordination geometry, being liganded by two oxygens from homocitrate, three sulphurs of FeMoco and the imidazole side chain of His^{α442}. Cys^{α275} and His^{α442} are the only ligands from the protein to FeMoco. Several proposals have been offered for the binding mode of the substrate to FeMoco (Kim & Rees, 1992a; Chan et al., 1993). If the Mo atom is the active site, it will lose a ligand when it binds the substrate (Leigh, 1995). Another possibility is that the substrate interacts with the trigonally coordinated Fe sites, and binds on the exterior of FeMoco. Small substrates like N₂ might occupy the central cavity of FeMoco, which has a diameter of ~4 Å: the interaction with the three-coordinated Fe atoms would weaken the N≡N bond. There is no experimental evidence for any of these suggestions. The function of homocitrate might be to protonate reaction intermediates or to participate in the electron transfer between the P-cluster and FeMoco (Kim & Rees, 1992a).

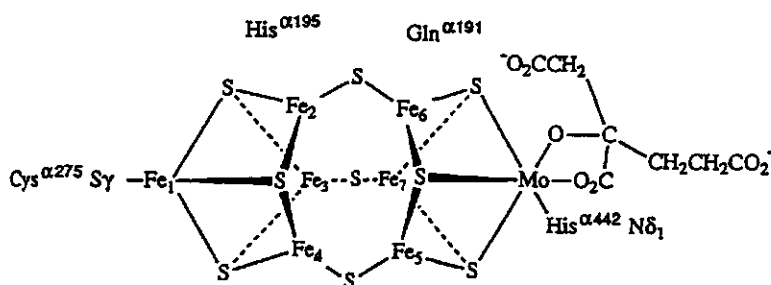


Figure 2. Schematic representation of the FeMo cofactor of the MoFe protein (after Kim & Rees, 1992a; Chan et al., 1993).

FeMoco is located in the α -subunit of the MoFe protein, buried at least 10 Å beneath the protein surface in the cleft between the three domains of the α -subunit (Kim & Rees, 1992b; Kim et al., 1993). Structural fluctuations might provide the passage for the entry and exit of substrates and products. The protein environment of FeMoco consists primarily of hydrophilic residues (Kim & Rees, 1992b). In the dithionite-

reduced MoFe protein FeMoco exhibits an EPR $S = 3/2$ signal with g -values 4.3, 3.7 and 2.0 (Davis et al., 1972; Orme-Johnson et al., 1972; Palmer, 1972; Smith et al., 1972). This EPR signal is lost when the MoFe protein is further reduced during catalysis (Orme-Johnson et al., 1972; Smith et al., 1972, 1973; Zumft et al., 1974) and when the protein is oxidized (Palmer et al., 1972); $E_m \approx -42$ mV for oxidation of the MoFe protein of *A. vinelandii* (Pierik et al., 1993).

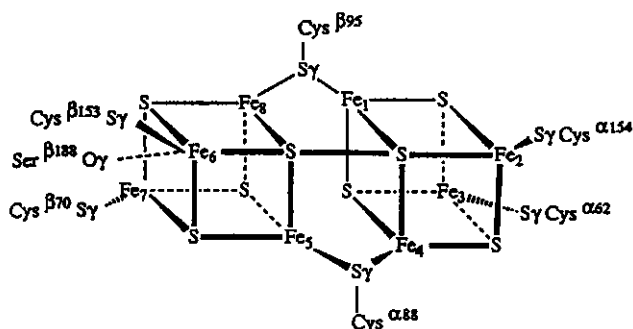


Figure 3. Schematic representation of the P-cluster of the MoFe protein from *A. vinelandii* (after Kim & Rees, 1992a; Chan et al., 1993). Bolin et al. (1993) suggested that the subclusters of the P-cluster (of the MoFe protein of *C. pasteurianum*) are bridged by a single shared S atom instead of by a disulphide bridge.

The P-cluster is located on the interface of the α -subunit and the β -subunit, about 10 Å below the MoFe protein surface (Kim & Rees, 1992a,b). The protein environment of the P-cluster mainly consists of hydrophobic residues (Kim & Rees, 1992b). There is still discussion about the structure of the P-cluster. From the crystallographic analysis of the MoFe protein Kim & Rees (1992a) concluded that the P-cluster from *A. vinelandii* nitrogenase is an [8Fe-8S] cluster (as was first proposed by Hagen et al. (1987)) that consists of two [4Fe-4S] clusters bridged by two cysteine thiol ligands (Cys ^{α 88} and Cys ^{β 95}); the remaining four Fe are liganded by Cys ^{α 62}, Cys ^{α 154}, Cys ^{β 70} and Cys ^{β 153}. In addition Ser ^{β 188} coordinates the same iron atom as Cys ^{β 153}, or is hydrogen bonded to a sulphur of the cluster (Kim & Rees, 1992a; Bolin, 1993), see Figure 3. Recently it was shown that the two bridging cysteine ligands can each be replaced by the non-coordinating amino acid alanine (Yousafzai et al., 1996). From the crystallographic analysis of the MoFe protein of *A. vinelandii* (2.2 Å) Chan et al. (1993) concluded that two sulphurs of the different subclusters of the P-cluster probably form a disulphide bond (see Figure 3), considering the small distance between these sulphurs (about

2.1 Å); one of these sulphurs might be labile. It was suggested that the P-cluster might act as a two-electron redox group and might provide a site for H_2 evolution during catalysis (Chan et al., 1993; Howard & Rees, 1994). However, Bolin et al. (1993) analysed the MoFe protein of *C. pasteurianum* (2.2 Å) and found that the separation between two sulphurs from the different subclusters was only 1 Å. Because of this the authors suggested that the subclusters are bridged by a single shared S atom (rather than by a disulphide bond), which would define the P-cluster as an [8Fe-7S] cluster (Bolin et al., 1993). Spectroscopic studies of the dithionite-reduced MoFe protein indicate that all eight Fe atoms of the P-cluster are probably in the ferrous state (Surerus et al., 1992). In the dithionite-reduced MoFe protein the P-clusters are diamagnetic (Zimmermann et al., 1978); according to Pierik et al. (1993), oxidation of the P-cluster by two electron equivalents ($E_m \approx -307$ mV) yields a redox state which exhibits an EPR $S = 3$ signal with a g -value 12.0; further oxidation, by one electron equivalent ($E_m \approx +90$ mV), leads to a redox state with an $S = 7/2$ signal with g -values 10.4, 5.8 and 5.5 (Hagen et al., 1987) and an $S = 1/2$ signal with g -values 1.97, 1.88 and 1.68. Tittsworth and Hales (1993), on the other hand, proposed that the oxidation of the P-clusters occurs by one-electron steps; it was found that one electron equivalent oxidized P-clusters exhibit an $S = 5/2$ signal with g -values 7.3, 6.67 and 5.3, and an $S = 1/2$ signal with g -values 2.06, 1.95 and 1.82; further oxidation yields the two electron equivalents oxidized state of the P-cluster with an $S \geq 3$ signal with g -value 11.6.

Studies on the binding of nucleotides to the MoFe protein have yielded somewhat contradictory results. From 1H NMR relaxation studies on the binding of Mn^{2+} to the MoFe protein from *Klebsiella pneumoniae* (Kp1) Kimber et al. (1982) concluded that Kp1 has four binding sites for MgATP. Robson (1984) proposed, on the basis of amino acid sequence analysis, that the β -subunit of the MoFe protein from *A. vinelandii* possibly contains one nucleotide binding site. Weak binding of 4 mol MgATP per mol Kp1 has been reported (Miller, 1980); however, no significant binding of MgATP to dithionite-reduced Av1 (Cordewener et al., 1985) or to the dye-oxidized or dithionite-reduced MoFe protein from *Azotobacter chroococcum*, Ac1, has been demonstrated (Miller & Eady, 1989).

Both dye-oxidized and dithionite-reduced Ac1 tightly bind 2 mol MgADP per mol protein (Miller & Eady, 1989), but dithionite-reduced Av1 (Cordewener et al., 1983) and dithionite-reduced Kp1 (Miller et al., 1989) do not bind MgADP; however, Kp1 with oxidized P-clusters tightly binds 4 mol MgADP per mol protein (Miller et al., 1993). Eady et al. (1995) reported that the reaction of MgADP with Kp1 results in covalent binding of MgAMP to Kp1, without loss of Kp1 activity.

It has been proposed that MgATP binds to the nitrogenase complex in a bridging configuration between the Fe protein and the MoFe protein (Kimber et al., 1982; Miller et al., 1989, 1993). The significance of nucleotide binding by the MoFe protein with respect to the catalytic mechanism of nitrogenase is not understood.

Alternative nitrogenases

If molybdenum is not available, alternative nitrogenase systems may be induced (Bishop et al., 1980). Besides the molybdenum nitrogenase, *A. vinelandii* and the closely related species *A. chroococcum* both have a vanadium nitrogenase, which is expressed only if molybdenum is absent. In addition, *A. vinelandii* has an iron-only nitrogenase which functions if both molybdenum and vanadium are scarce. The photosynthetic *Rhodobacter capsulatus* possesses the iron-only nitrogenase system besides the Mo nitrogenase. The alternative nitrogenase proteins are believed to be highly similar to the Mo nitrogenase, with analogous metal-sulphur clusters: in the alternative systems molybdenum is replaced by vanadium or iron, resulting in a VaFe cofactor or a FeFe cofactor. The three nitrogenase systems have similar requirements for nitrogenase activity and the efficiency of coupling of MgATP hydrolysis to electron transfer is the same. The existence of the alternative nitrogenase systems indicates that molybdenum is not uniquely required for nitrogen fixation. However, the substrate reduction characteristics of the systems differ in some aspects. For example, the catalytic activity of the alternative nitrogenases is lower than the activity of Mo nitrogenase, and more electrons are directed towards H_2 production at the cost of N_2 reduction. The alternative nitrogenases have been reviewed by Smith & Eady (1992) and Kim & Rees (1994).

The Fe protein

The nitrogenase Fe protein is a γ_2 -dimer with a molecular mass of ~63 kDa (Eady et al., 1972). The crystal structure (2.9 Å resolution) of the Fe protein from *A. vinelandii* was determined by Georgiadis et al. (1992), see Figure 4. At the top of the two-fold axis of the Fe protein, exposed to the solvent, the subunits are connected by a single [4Fe-4S] cluster which is coordinated by Cys⁹⁷ and Cys¹³² from each subunit (Hausinger & Howard, 1983; Howard et al., 1989). The solvent exposure of the cluster might contribute to the Fe protein's sensitivity to inactivation by oxygen. The [4Fe-4S] cluster is a one electron donor (Ljones & Burris, 1978a) and cycles between the oxidation states +1 and +2. The reduced [4Fe-4S] cluster has an $S = 1/2$ EPR spectrum with g -values at

1.85, 1.94 and 2.06 (Orme-Johnson et al., 1972; Palmer et al., 1972; Smith et al., 1973; Braaksma et al., 1982; Hagen et al., 1985a) and in addition exhibits an $S = 3/2$ EPR signal, with g -values around 5 (Hagen et al., 1985b; Lindahl et al., 1985; Watt & McDonald, 1985). The Fe protein can bind two molecules of MgATP or MgADP. Numerous methods have been used to determine the binding constants of these nucleotides to the Fe protein, with a considerable variation in the results: approximately, MgATP and MgADP bind to the Fe protein with dissociation constants $\sim 100 \mu\text{M}$. In general, MgADP binds more tightly to the Fe protein than does MgATP, and both MgATP and MgADP bind more tightly to oxidized Fe protein than to reduced Fe protein (reviewed by: Yates, 1992). Although the Fe protein binds MgATP (Bui & Mortenson, 1968), it cannot hydrolyse MgATP in the absence of the MoFe protein (Bulen & LeComte, 1966). Besides its function as the electron donor to the MoFe protein, the Fe protein is also involved in the biosynthesis of FeMoco and the insertion of FeMoco in the MoFe protein (Filler et al., 1986; Robinson et al., 1987, 1989).



Figure 4. The polypeptide fold of the Fe protein from *A. vinelandii* (Georgiadis et al., 1992). A slice of the protein, including the [4Fe-4S] cluster and the MgADP molecule, is shown. The [4Fe-4S] cluster (on top) and the MgADP molecule are represented by space-filling models. (Figure prepared with Insight II.)

The residues 9-16 of the Fe protein have an amino acid sequence known as Walker's motif A (Walker et al., 1982), which is characteristic of the phosphate binding sites found in many nucleotide binding proteins (Schulz, 1992). Analysis of the amino

acid sequence of Av2 (Hausinger & Howard, 1982) suggested a possible involvement of this region in nucleotide binding (Robson, 1984). This was confirmed by side-directed mutagenesis studies on Lys¹⁵ (Seefeldt et al., 1992; Ryle et al., 1995) and Ser¹⁶ (Seefeldt & Mortenson, 1993) and by the finding of molybdate ions at this region in the crystal structure of Av2 (Georgiadis et al., 1992). Asp¹²⁵ is a ligand to Mg²⁺ (Wolle et al., 1992a) and is part of Walker's motif B (found at residues 125-128 of Av2), which completes the phosphate binding region in other nucleotide binding proteins (Georgiadis et al., 1992). A remarkable structural similarity between the nucleotide binding regions of Av2 and the proto-oncogenic H-Ras p21 protein was found. This protein has GTPase activity, and its MgGTP and MgGDP binding properties have been well characterized (Brünger et al., 1990; Milburn et al., 1990; Pai et al., 1990; Tong et al., 1991). The side chains of the residues that constitute the Walker's motifs A and B of the H-Ras p21 protein and Av2 closely superimpose. However, the nucleotide binding regions of Av2 and the H-Ras p21 protein appeared to be different with respect to the orientation of the nucleotide: one of the nucleotide binding sites of Av2 was found to be occupied by a molecule of MgADP, oriented across the subunit interface (Georgiadis et al., 1992) - in a Ras-like binding mode the orientation of the nucleotide would be along the subunit interface. However, later refinements of the crystallographic analysis of Av2 (2.3 Å resolution) did no longer reveal the presence of a bound MgADP at the nucleotide binding site (J. Schlessmann, personal communication to Dr. H. Haaker).

The nucleotide binding sites of the Fe protein are located some 20 Å away from the [4Fe-4S] cluster (Georgiadis et al., 1992). Nevertheless, the binding of MgATP or MgADP to the Fe protein leads to significant changes of the properties of the [4Fe-4S] cluster. The protein conformational changes initiated at the nucleotide binding sites upon the binding of MgATP or MgADP somehow propagate to the environment of the [4Fe-4S] cluster. Binding of MgATP enhances the oxygen-sensitivity of the Fe protein and causes a highly increased accessibility of the [4Fe-4S] cluster to Fe chelating reagents (Walker & Mortenson, 1973, 1974; Ljones & Burris, 1978b; Deits & Howard, 1989); the latter effect is inhibited by MgADP, by salt and by the MoFe protein. The rate of reduction of oxidized Fe protein by sodium dithionite is much lower when the Fe protein is bound to MgADP (Ashby & Thorneley, 1987). The redox potential of the Fe protein decreases from ~ -375 mV (free Av2) to ~ -435 mV upon binding of MgATP and to ~ -473 mV upon binding of MgADP (Zumft et al., 1974; Braaksma et al., 1982; Watt et al., 1986). Binding of MgATP or MgADP to the Fe protein changes the shape of the $S = 1/2$ EPR signal (Orme-Johnson et al., 1972; Zumft et al., 1972, 1973, 1974; Braaksma et al., 1982) and the distribution of the Av2 $S = 1/2$ and $S = 3/2$ spin-states (Hagen et al., 1985b); nucleotide binding changes the CD spectrum of oxidized Fe protein (Stephens et al., 1979; Watt et al., 1986; Ryle et al., 1996a), the ¹H NMR

spectrum of the reduced Fe protein (Meyer et al., 1988; Lanzilotta et al., 1995a) and the Mössbauer spectrum of the oxidized Fe protein (Lindahl et al., 1985). (Fe K-edge) X-ray absorption spectroscopy studies indicated that the Fe-Fe and Fe-S distances in the [4Fe-4S] cluster do not significantly change by the binding of MgATP or MgADP to the Fe protein (Lindahl et al., 1987; Ryle et al., 1996a).

The nitrogenase complex

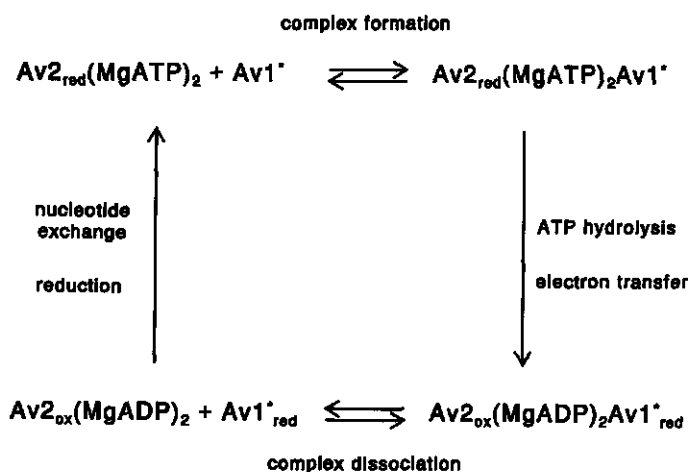
The formation of a (transient) complex between the Fe protein and the MoFe protein is essential for nitrogenase activity. Little is known about the interactions between the Fe protein and the MoFe protein in the nitrogenase complex. Some amino acid residues, located on the top surface of the Fe protein close to the [4Fe-4S] cluster, are involved in the association with the MoFe protein: Arg¹⁰⁰ (Murrell et al., 1988; Lowery et al., 1989; Wolle et al., 1992b), Glu¹¹² (Willing et al., 1989; Willing & Howard, 1990), Arg¹⁴⁰ and Lys¹⁴³ (Seefeldt, 1994). An anionic loop, defined by residues 59 through 67 at the top surface of the Fe protein, is also involved in the component protein interaction (Peters et al., 1994). Ionic interactions appear to contribute largely to formation of the complex between the nitrogenase proteins (Willing et al., 1989; Deits & Howard, 1990; Wolle et al., 1992b). At the MoFe protein, to either side of the P-cluster, are two wide and shallow clefts which may provide the binding site for the Fe protein (Kim & Rees, 1992b). Two residues of the MoFe protein that possibly participate in complex formation are Phe⁸¹²⁵ and Asp^{α161} (Dean et al., 1993; Howard & Rees, 1994). A docking model for the nitrogenase proteins was proposed, based on the crystal structures of the proteins and the knowledge of the residues involved in complex formation (Kim & Rees, 1992b). In this model the top surface of the Fe protein containing the [4Fe-4S] cluster and the residues Arg¹⁰⁰ and Glu¹¹², is directed towards the MoFe protein in such a way that the distance between the [4Fe-4S] cluster and the P-cluster is ~18 Å (Kim & Rees, 1992b; 1994).

The Fe protein cycle and the MoFe protein cycle

The Fe protein is a one-electron donor to the MoFe protein (Ljones & Burris, 1978a); only the Fe protein can reduce the MoFe protein and thus cause substrate reduction. Hageman & Burris proposed that the nitrogenase complex dissociates after the transfer of each electron from the Fe protein to the MoFe protein (Hageman & Burris, 1978a,b; 1979). This concept was further developed by Lowe and Thorneley into a

comprehensive model for the mechanism of action of nitrogenase, which was based entirely on (steady-state) kinetic data for *Klebsiella pneumoniae* nitrogenase, with sodium dithionite as the reductant (Lowe & Thorneley, 1984a,b; Thorneley & Lowe, 1984a,b). This model consists of two coupled cycles of electron transfer: the Fe protein cycle and the MoFe protein cycle.

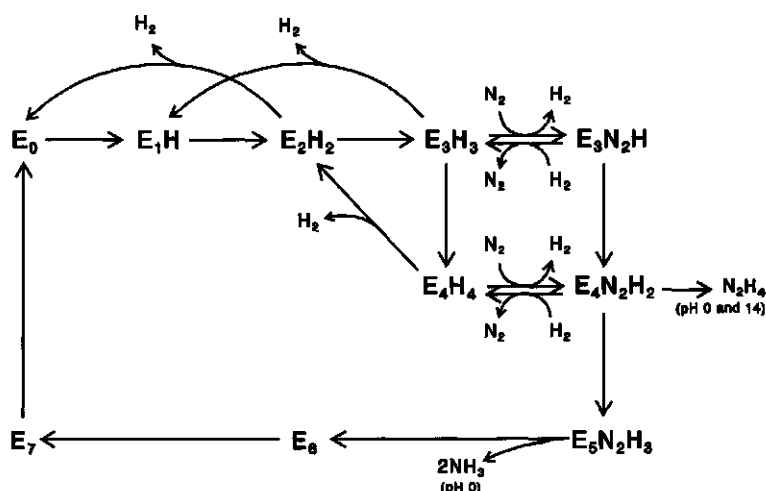
Scheme 1 shows the Fe protein cycle (Thorneley & Lowe, 1983), which starts with the formation of the nitrogenase complex by association of the reduced Fe protein (with 2 MgATP bound) and the MoFe protein. After formation of the nitrogenase complex a single electron is transferred from the Fe protein to the MoFe protein, with concomitant hydrolysis of MgATP (Eady et al., 1978; Hageman et al., 1980). The dissociation of the nitrogenase complex after electron transfer and MgATP hydrolysis, is considered to be the rate-limiting step of the nitrogenase reaction, if all other reactants are saturating (Thorneley & Lowe, 1983). After dissociation of the nitrogenase complex the Fe protein is reduced again and finally MgADP is replaced by MgATP (Ashby & Thorneley, 1987).



Scheme 1. The Fe protein cycle (after Thorneley & Lowe, 1983). Av1^* is one of the two independently functioning halves of the MoFe protein; $\text{Av1}^*_{\text{red}}$ is the MoFe protein after one-electron reduction by the Fe protein; Av2_{red} and Av2_{ox} are reduced and oxidized Fe protein, respectively (N.B. the redox change between Av2_{red} and Av2_{ox} concerns one electron).

The MoFe protein cycle (Scheme 2) describes the stepwise reduction of the MoFe protein through eight consecutive Fe protein cycles, necessary to supply the eight electrons for the reduction of N_2 to 2NH_3 and H_2 . (In this scheme - one of the two

independently functioning halves of - the MoFe protein is depicted as E_n : the subscript n indicates the amount of electrons that has been transferred from the Fe protein to the MoFe protein.) This mechanism was formulated based on the observed pre-steady-state kinetics of the formation of H_2 , NH_3 and an intermediate that yields N_2H_4 (hydrazine) upon quenching of the nitrogenase reaction (Thorneley & Lowe, 1984a). The rate constants of the reactions that constitute the Fe protein cycle were assumed to be independent of the level of reduction of the MoFe protein. The observation that the rate of formation of the nitrogenase complex and the rate of electron transfer are the same for the E_0 and E_1 state of the MoFe protein, supports this assumption (Fisher et al., 1991).



Scheme 2. The MoFe protein cycle (after Lowe & Thorneley, 1984a). E_n is one of the two independently functioning halves of the MoFe protein; the subscript n refers to the amount of electrons which has been transferred from the Fe protein to the MoFe protein (by way of n Fe protein cycles).

In order to explain and to be able to simulate the observation that the measured specific H_2 production activity of the *Klebsiella pneumoniae* Fe protein, Kp2, is only 45% of the calculated maximum specific activity, Thorneley and Lowe assumed that only 45% of all Kp2 present is active (Thorneley & Lowe, 1984b). The remaining 55% of total Kp2 is considered to be inactive with respect to electron transfer to Kp1, but is still capable of binding to Kp1 (with lower rate constants for binding to and dissociation from Kp1 than active Kp2 (Thorneley & Lowe, 1984b)). This assumption also explains

the observation that a ratio $[Kp2]/[Kp1] \geq 4.5$ is needed to obtain maximum electron transfer from the Fe protein to the MoFe protein: if all Kp2 would be active a ratio $[Kp2]/[Kp1] = 2$ would be sufficient (Ashby & Thorneley, 1987).

The hydrolysis of MgATP

Hydrolysis of MgATP is required for electron transfer from the Fe protein to the MoFe protein, rather than for the reduction of the nitrogenase substrates (Hageman & Burris, 1978b). MgATP hydrolysis is not stoichiometric with substrate reduction. Under optimal conditions 2 MgATP are hydrolysed per electron transferred (Ljones & Burris, 1972), but this $ATP/2e^-$ value varies with the pH (Winter & Burris, 1968; Imam & Eady, 1980), the temperature (Hadfield & Bulen, 1969; Watt et al., 1975; Watt & Burns, 1977), the redox potential of the reaction mixture (Hallenbeck, 1983), the substrate (Li et al., 1982; Robinson et al., 1983) and the ratio of the nitrogenase proteins (Ljones & Burris, 1972). For the H_2 evolution by the heterologous complex of the *K. pneumoniae* MoFe protein and the *C. pasteurianum* Fe protein an $ATP/2e^-$ value of 50 was obtained (Smith et al., 1976). In the absence of an electron donor nitrogenase still hydrolyses MgATP, which is called the reductant-independent ATPase activity of nitrogenase (Bui & Mortenson, 1969; Hadfield & Bulen, 1969; Yeng et al., 1970; Ljones & Burris, 1972; Imam & Eady, 1980; Cordewener et al., 1987, 1988).

The molecular switch proteins

When the crystal structure of the Fe protein from *A. vinelandii* was solved, a close structural similarity was found between the nucleotide binding regions of Av2 and the H-Ras p21 protein (Georgiadis et al., 1992), which is a member of the large and diverse family of the molecular switch proteins. These proteins use the binding and hydrolysis of nucleotides (ATP/GTP) as a mechanism to switch between different protein conformations. The conformation of the molecular switch protein (ATP/GTP-bound or ADP/GDP-bound) determines whether another protein, the "effector protein", is triggered and catalyses some biochemical process ("switch on") or not ("switch off"). The binding of the effector protein often induces hydrolysis of ATP/GTP, which alters the conformation of the molecular switch protein and thereby ends the biochemical process.

To the group of molecular switch proteins belong, among others, GTPases (Bourne et al., 1991) like the H-Ras p21 protein (Marshall, 1993), bacterial elongation factors (Nierhaus, 1996) and the α -subunits of the heterotrimeric signal transducing G proteins

(Rens-Domiano & Hamm, 1995); and ATPases like the recA protein (Story & Steitz, 1992) and the muscle protein myosin (Rayment et al., 1993a,b; Fisher et al., 1995).

Like the molecular switch proteins, nitrogenase could be using MgATP binding and hydrolysis to switch between different conformations (Georgiadis et al., 1992; Howard & Rees, 1994).

The catalytic mechanism of nitrogenase

One of the major, unanswered questions about the mechanism of nitrogenase action concerns the role of MgATP. How is the hydrolysis of MgATP coupled to electron transfer from the Fe protein to the MoFe protein? Hydrolysis of MgATP only occurs if the Fe protein interacts with the MoFe protein. Since the putative docking site on the Fe protein is some 20 Å away from the nucleotide binding site, it must be through alterations of the Fe protein conformation that the MoFe protein induces MgATP hydrolysis. It is conceivable that the formation of the nitrogenase complex and the binding of MgATP to the Fe protein cause conformational changes in the nitrogenase complex that result in electron transfer, e.g. by affecting the redox properties of the metal-sulphur clusters of the nitrogenase proteins (Dean et al., 1993; Howard & Rees, 1994).

Although the nucleotide binding regions of the *A. vinelandii* Fe protein and the H-Ras p21 protein closely superimpose, the orientation of the MgADP molecule which (originally) co-crystallized with Av2 was different from the orientation of the nucleotide H-Ras p21 protein. In Av2 the binding mode of the MgADP molecule was across the subunit interface (Georgiadis et al., 1992), whereas in the H-Ras p21 protein the nucleotide (MgGDP and MgGTP) is oriented parallel to the twofold symmetry axis of the protein. It has been proposed that the Fe protein could also adopt the H-Ras p21 nucleotide binding mode and that this different binding mode represents the MgATP-bound conformation of the Fe protein (Georgiadis et al., 1992). In the gating mechanism proposed by Wolle et al. (1992a) the hydrolysis of MgATP would then lead to a transition state from which electron transfer occurs. After MgATP hydrolysis, the conformational change to the MgADP-bound state of the Fe protein would prevent backflow of the previously transferred electron from the MoFe protein to the Fe protein (Wolle et al., 1992a). A possible pathway for the communication between the nucleotide binding site and the [4Fe-4S] cluster might be provided by the protein chain from Asp¹²⁵ in the nucleotide binding site, to Cys¹³² which is a ligand to the [4Fe-4S] cluster (Wolle et al., 1992a; Howard & Rees, 1994; Lanzilotta et al., 1995b, 1996; Ryle & Seefeldt, 1996; Ryle et al., 1996b). Asp¹²⁹ is probably involved in the hydrolysis of MgATP

(Lanzilotta et al., 1995b). Phe¹³⁵, located ~5 Å from the [4Fe-4S] cluster, has an important role in defining the redox potential and the MgADP-induced (but not the MgATP-induced) redox change of the [4Fe-4S] cluster (Ryle et al., 1996b). Deletion of Leu¹²⁷ results in a conformation resembling the MgATP-bound state of the Fe protein, as judged by the electronic properties of the [4Fe-4S] cluster (Ryle & Seefeldt, 1996); the altered protein was found to transfer a single electron to the MoFe protein in the absence of MgATP (Lanzilotta et al., 1996).

Outline of this thesis

The aim of the work described in the following chapters of this thesis was to obtain a deeper insight in nitrogenase catalysis. For that purpose, reactions between the Fe protein and the MoFe protein during nitrogenase turnover were studied, mainly by rapid kinetic methods.

In order to understand the role of MgATP in nitrogenase catalysis, the pre-steady-state MgATP hydrolysis has been studied extensively by various techniques. Rapid-quench studies (Eady et al., 1978; Hageman et al., 1980; Cordewener et al., 1987) suggested that P_i release due to the hydrolysis of MgATP, occurs concomitant with electron transfer. These investigations do not agree on the amount of MgATP hydrolysed per electron transferred. Thorneley et al. (1989) concluded from their stopped-flow calorimetry experiments (at 6 °C) that the hydrolysis of MgATP precedes electron transfer. The reliability of the use of the rapid-quench technique as a means to study pre-steady-state MgATP-dependent P_i production was questioned by Mensink et al. (1992), who subsequently studied MgATP-dependent proton production using a pH indicator. It was concluded that the hydrolysis of MgATP, as judged by the proton release, occurs at a lower rate than electron transfer. Lowe et al. (1995) recently studied pre-steady-state MgATP-dependent P_i release using a fluorescent probe and observed that P_i release takes place at a lower rate than electron transfer. *Chapter 2* describes the dependence of the pre-steady-state MgATP-dependent proton production on the redox state of the nitrogenase proteins, monitored by the absorbance changes of the pH indicator cresol red during the nitrogenase reaction.

When the structural similarities between the nucleotide-binding regions of the Fe protein from *A. vinelandii* and the H-Ras p21 protein were discovered, it was suggested that the Fe protein might act as a molecular switch protein (Georgiadis et al., 1992; Wolle et al., 1992b). In several studies on the working mechanism of various molecular switch proteins, aluminium fluoride has been used as an analogue of the terminal phosphate of ATP/GTP: the combination of aluminium fluoride and ADP/GDP

is thought to mimic ATP/GTP (Chabre, 1990). *Chapter 3* describes the formation of a stable, inactive complex of both nitrogenase proteins, MgADP and aluminium fluoride, locked in a conformation that might be like a transition state of the (normally transient) nitrogenase complex during MgATP hydrolysis (before P_i release).

The electron transfer from the Fe protein to the MoFe protein is accompanied by absorbance changes at 430 nm. The absorbance increase observed immediately after mixing of both nitrogenase proteins with MgATP, is mainly due to the oxidation of the Fe protein in the electron transfer reaction (Thorneley, 1975; Thorneley & Cornish-Bowden, 1977). The pre-steady-state absorbance changes that are observed during the reaction of nitrogenase of *K. pneumoniae* were simulated by Lowe et al. (1993). The absorbance changes observed after the initial absorbance increase were explained as being caused by the consecutive redox changes of the MoFe protein (see Scheme 2). A role for the P-cluster in mediating electron transfer to the substrate was proposed. In *Chapter 4* the absorbance curves associated with electron transfer and the ATPase reaction of nitrogenase from *A. vinelandii* are described. These absorbance curves differ significantly from the curves observed for *K. pneumoniae* nitrogenase, and could not be simulated as proposed by Lowe et al. (1993).

The pre-steady-state absorbance changes associated with electron transfer are influenced by (among others) the temperature and the salt concentration of the reaction mixture. A low reaction temperature or a high salt concentration decreases the amplitude and rate of initial absorbance increase in, apparently, a comparable way, suggesting a diminished transfer of electrons from the Fe protein to the MoFe protein. The effect of a low reaction temperature has been explained by reversible electron transfer between the nitrogenase proteins (Thorneley et al., 1989; Mensink & Haaker, 1992). In *Chapter 5* stopped-flow and rapid-freeze EPR experiments are described by which this hypothesis is tested. The rapid-freeze EPR data showed that the effect of salt on the initial absorbance increase cannot be attributed to a diminished reduction of FeMoco. The kinetics of the FeMoco reduction indicated that the electron transfer reaction is not a one-step process.

The Fe protein cycle (Scheme 1) is based on kinetic data obtained with the nitrogenase proteins from *K. pneumoniae*, with sodium dithionite as reductant (Thorneley et al., 1983). *Chapter 6* describes a study on the rate-limiting step of the Fe protein cycle, using three different reductants: sodium dithionite, flavodoxin hydroquinone and titanium (III) citrate. It is shown that dissociation of the nitrogenase complex is not obligatory in the nitrogenase catalytic cycle. An essentially different version of the Fe protein cycle is proposed.

Chapter 7 summarizes and discusses the preceding chapters.

References

- Alberty, R. A. (1994) Thermodynamics of the nitrogenase reaction, *J. Biol. Chem.* 269, 7099-7102.
- Ashby, G. A. & Thorneley, R. N. F. (1987) Nitrogenase of *Klebsiella pneumoniae*. Kinetic studies on the Fe protein involving reduction by sodium dithionite, the binding of MgADP and a conformation change that alters the reactivity of the 4Fe-4S centre, *Biochem. J.* 246, 455-465.
- Beijerinck, M. W. (1888) Die Bakterien der Papilionaceen-Knöllchen, *Bot. Ztg.* 46, 725-735.
- Bishop, P. E., Jarlenski, D. M. L. & Hetherington, D. R. (1980) Evidence for an alternative nitrogen fixation system in *Azotobacter vinelandii*, *Proc. Natl. Acad. Sci. USA* 77, 7342-7346.
- Bolin, J. T., Campobasso, N. Muchmore, S. W., Morgan, T. V. & Mortenson, L. E. (1993) Structure and environment of metal clusters in the nitrogenase molybdenum-iron protein from *Clostridium pasteurianum*, in: *Molybdenum enzymes, cofactors and model systems* (Stiefel, E. I., Coucouvanis, D. & Newton, W. E., eds.) pp. 186-195, American Chemical Society, Washington.
- Bourne, H. R., Sanders, D. A. & McCormick, F. (1991) The GTPase superfamily: conserved structure and molecular mechanism, *Nature* 349, 117-127.
- Braaksma, A., Haaker, H., Grande, H. J. & Veeger, C. (1982) The effect of the redox potential on the activity of the nitrogenase and on the Fe protein of *Azotobacter vinelandii*, *Eur. J. Biochem.* 121, 483-491.
- Brünger, A. T., Milburn, M. V., Tong, L., deVos, A. M., Jancarik, J., Yamaizumi, Z., Nishimura, S., Ohtsuka, E. & Kim, S.-H. (1990) Crystal structure of an active form of RAS protein, a complex of a GTP analog and the HRAS p21 catalytic domain, *Proc. Natl. Acad. Sci. USA* 87, 4849-4853.
- Bui, P. T. & Mortenson, L. E. (1968) Mechanism of the enzymic reduction of N_2 : the binding of adenosine 5'-triphosphate and cyanide to the N_2 -reducing system, *Proc. Natl. Acad. Sci. USA* 61, 1021-1027.
- Bui, P. T. & Mortenson, L. E. (1969) The hydrolysis of adenosine triphosphate by purified components of nitrogenase, *Biochemistry* 8, 2462-2465.
- Bulen, W. A., Burns, R. C. & LeComte, J. R. (1965) Nitrogen fixation: hydrosulfite as electron donor with cell-free preparations of *Azotobacter vinelandii* and *Rhodospirillum rubrum*, *Proc. Natl. Acad. Sci. USA*, 53, 532-539.
- Bulen, W. A. & LeComte, J. R. (1966) The nitrogenase system from *Azotobacter*: two-enzyme requirement for N_2 reduction, ATP-dependent H_2 evolution and ATP hydrolysis, *Proc. Natl. Acad. Sci.* 56, 979-986.
- Burgess, B. K. (1985) Substrate reactions of nitrogenase, in: *Molybdenum enzymes* (Spiro, T. G., ed.) pp. 1610-217, Wiley & Sons, New-York.
- Burns, R. C. (1969) The nitrogenase system from *Azotobacter*. Activation energy and divalent cation requirement, *Biochim. Biophys. Acta* 171, 253-259.
- Burns, R. C. & Bulen, W. A. (1965) ATP-dependent hydrogen evolution by cell-free preparations of *Azotobacter vinelandii*, *Biochim. Biophys. Acta* 105, 437-445.
- Burns, A., Watt, G. D. & Wang, Z. C. (1985) Salt inhibition of nitrogenase catalysis and salt effects on the separate protein components, *Biochemistry* 24, 3932-3936.
- Burris, R. H. (1991) Nitrogenases, *J. Biol. Chem.* 266, 9339-9342.
- Chabre, M. (1990) Aluminofluoride and berylliofluoride complexes: new phosphate analogs in enzymology, *Trends Biochem. Sci.* 15, 6-10.

- Chan, M. K., Kim, J. & Rees, D. C. (1993) The nitrogenase FeMo-cofactor and P-cluster pair: 2.2 Å resolution structures, *Science* 260, 792-794.
- Cordewener, J., ten Asbroek, A., Wassink, H., Eady, R., Haaker, H. & Veeger, C. (1987) Binding of ADP and orthophosphate during the ATPase reaction of nitrogenase, *Eur. J. Biochem.* 162, 265-270.
- Cordewener, J., Haaker, H., van Ewijk, P. & Veeger, C. (1985) Properties of the MgATP and MgADP binding sites on the Fe protein of nitrogenase from *Azotobacter vinelandii*, *Eur. J. Biochem.* 148, 499-508.
- Cordewener, J., Haaker, H. & Veeger, C. (1983) Binding of MgATP to the nitrogenase proteins from *Azotobacter vinelandii*, *Eur. J. Biochem.* 132, 47-54.
- Cordewener, J., Krüse-Wolters, M., Wassink, H., Haaker, H. & Veeger, C. (1988) The role of MgATP hydrolysis in nitrogenase catalysis, *Eur. J. Biochem.* 172, 739-745.
- Davis, L. C., Shah, V. K., Brill, W. J. & Orme-Johnson, W. H. (1972) Nitrogenase. II. Changes in the EPR signal of component I (iron-molybdenum protein) of *Azotobacter vinelandii* nitrogenase during repression and derepression, *Biochim. Biophys. Acta* 256, 512-523.
- Davis, L. C., Shah, V. K. & Brill, W. J. (1975) Nitrogenase. VII. Effect of component ratio, ATP and H₂ on the distribution of electrons to alternative substrates, *Biochim. Biophys. Acta* 256, 67-78.
- Dean, D. R., Bolin, J. T. & Zheng, L. (1993) Nitrogenase metalloclusters: structures, organization, and synthesis, *J. Bact.* 175, 6737-6744.
- Deits, T. L. & Howard, J. B. (1989) Kinetics of MgATP-dependent iron chelation from the Fe-protein of the *Azotobacter vinelandii* nitrogenase complex, *J. Biol. Chem.* 264, 6619-6628.
- Deits, T. L. & Howard, J. B. (1990) Effect of salts on *Azotobacter vinelandii* nitrogenase activities. Inhibition of iron chelation and substrate reduction, *J. Biol. Chem.* 265, 3859-3867.
- Detroy, R. W., Witz, D. F., Parejko, R. A. & Wilson, P. W. (1968) Reduction of N₂ by complementary functioning of two components from nitrogen-fixing bacteria, *Proc. Natl. Acad. Sci. USA* 61, 537-541.
- Dilworth, M. J. (1966) Acetylene reduction by nitrogen-fixing preparations from *Clostridium pasteurianum*, *Biochim. Biophys. Acta* 127, 285-294.
- Eady, R. R., Lowe, D. J. & Thorneley, R. N. F. (1978) Nitrogenase of *Klebsiella pneumoniae*: a pre-steady-state burst of ATP hydrolysis is coupled to electron transfer between the component proteins, *FEBS Lett.* 95, 211-213.
- Eady, R. R., Miller, R. W., Gormal, C., Fairhurst, S. & Smith, B. E. (1995) Covalent modification of nitrogenase MoFe protein by ADP, in: *Nitrogen fixation, fundamentals and applications* (Tikhonovich, I. A., Provorov, N. A., Romanov, V. I. & Newton, W. E., eds.), pp. 147, Kluwer Academic Publishers, Dordrecht, The Netherlands.
- Eady, R. R., Smith, B. E., Cook, K. A. & Postgate, J. R. (1972) Nitrogenase of *Klebsiella pneumoniae*. Purification and properties of the component proteins, *Biochem. J.* 128, 655-675.
- Emerich, D. W. & Burris, R. H. (1976) Interactions of heterologous nitrogenase components that generate catalytically inactive complexes, *Proc. Natl. Acad. Sci. USA* 73, 4369-4373.
- Emerich, D. W. & Burris, R. H. (1978) Complementary functioning of the component proteins of nitrogenase from several bacteria, *J. Bacteriol.* 134, 936-943.
- D'Eustachio, A. J. & Hardy, R. W. F. (1964) Reductants and electron transport in nitrogen fixation, *Biochem. Biophys. Res. Commun.* 15, 319-323.
- Filler, W. A., Kemp, R. M., NG, J. C., Hawkes, T. R., Dixon, R. A. & Smith, B. E. (1986) The *nifH* gene product is required for the synthesis or stability of the iron-molybdenum

- cofactor of nitrogenase from *Klebsiella pneumoniae*, *Eur. J. Biochem.* 160, 371-377.
- Fisher, A. J., Smith, C. A., Thoden, J., Smith, R., Sutoh, K., Holden, H. M. & Rayment, I. (1995) Structural studies of myosin:nucleotide complexes: a revised model for the molecular basis of muscle contraction, *Biophys. J.* 68, 19s-28s.
- Fisher, K., Lowe, D. J. & Thorneley, R. N. F. (1991) *Klebsiella pneumoniae* nitrogenase. The pre-steady-state kinetics of MoFe-protein reduction and hydrogen evolution under conditions of limiting electron flux show that the rates of association with the Fe-protein and electron transfer are independent of the oxidation level of the MoFe-protein, *Biochem. J.* 279, 81-85.
- Georgiadis, M. M., Komiya, H., Chakrabarti, P., Woo, D., Kornuc, J. J. & Rees, D. C. (1992) Crystallographic structure of the nitrogenase iron protein from *Azotobacter vinelandii*, *Science* 257, 1653-1659.
- Hadfield, K. L., & Bulen, W. A. (1969) Adenosine triphosphate requirement of nitrogenase from *Azotobacter vinelandii*, *Biochemistry* 8, 5103-5108.
- Hageman, R. V. & Burris, R. H. (1978a) Kinetic studies on electron transfer and interaction between nitrogenase components from *Azotobacter vinelandii*, *Biochemistry* 17, 4117-4124.
- Hageman, R. V. & Burris, R. H. (1978b) Nitrogenase and nitrogenase reductase associate and dissociate with each catalytic cycle, *Proc. Natl. Acad. Sci. USA* 75, 2699-2702.
- Hageman, R. V. & Burris, R. H. (1979) Changes in the EPR signal of dinitrogenase from *Azotobacter vinelandii* during the lag period before hydrogen evolution begins, *J. Biol. Chem.* 254, 11189-11192.
- Hageman, R. V. & Burris, R. H. (1980) Electron allocation to alternative substrates of *Azotobacter* nitrogenase is controlled by the electron flux through dinitrogenase, *Biochim. Biophys. Acta* 591, 63-75.
- Hageman, R. V., Orme-Johnson, W. H. & Burris, R. H. (1980) Role of magnesium adenosine 5'-triphosphate in the hydrogen evolution reaction catalyzed by nitrogenase from *Azotobacter vinelandii*, *Biochemistry* 19, 2333-2342.
- Hagen, W. R., Dunham, W. R., Braaksma, A. & Haaker, H. (1985a) On the prosthetic group(s) of component II from nitrogenase, *FEBS Lett.* 187, 146-150.
- Hagen, W. R., Eady, R. R., Dunham, W. R. & Haaker, H. (1985b) A novel $S = 3/2$ EPR signal associated with native Fe-proteins of nitrogenase, *FEBS Lett.* 189, 250-254.
- Hagen, W. R., Wassink, H., Eady, R. R., Smith, B. E. & Haaker, H. (1987) Quantitative EPR of an $S = 7/2$ system in thionine-oxidized MoFe proteins of nitrogenase. A redefinition of the P cluster concept, *Eur. J. Biochem.* 169, 457-465.
- Hallenbeck, P. C. (1983) Nitrogenase reduction by electron carriers: influence of redox potential on activity and the ATP/2e⁻ ratio, *Arch. Biochem. Biophys.* 220, 657-660.
- Hardy, R. W. F. & D'Eustachio, A. J. (1964) The dual role of pyruvate and the energy requirement in nitrogen fixation, *Biochem. Biophys. Res. Commun.* 15, 314-318.
- Hardy, R. W. F., Knight, E. & D'Eustachio, A. J. (1965) An energy-dependent hydrogen evolution from dithionite in nitrogen-fixing extracts from *Clostridium pasteurianum*, *Biochem. Biophys. Res. Commun.* 20, 539-544.
- Hardy, R. W. F. & Knight, E. (1966) Reductant-dependent adenosine triphosphatase of nitrogen-fixing extracts of *Azotobacter vinelandii*, *Biochim. Biophys. Acta* 132, 520-531.
- Hardy, R. W. F. & Knight, E. (1967) ATP-dependent reduction of azide and HCN by N₂-fixing enzymes of *Azotobacter vinelandii* and *Clostridium pasteurianum*, *Biochim. Biophys. Acta* 139, 69-90.
- Hausinger, R. P. & Howard, J. B. (1982) The amino acid sequence of the nitrogenase iron protein from *Azotobacter vinelandii*, *J. Biol. Chem.* 257, 2483-2490.
- Hausinger, R. P. & Howard, J. B. (1983) Thiol reactivity of the nitrogenase Fe-protein from

- Azotobacter vinelandii*, *J. Biol. Chem.* 258, 13486-13492.
- Hawkes, T. R., McLean, P. A. & Smith, B. E. (1984) Nitrogenase from *nifV* mutants of *Klebsiella pneumoniae* contains an altered form of the iron-molybdenum cofactor, *Biochem. J.* 217, 317-231.
- Heilriegel, H. & Wilfarth, H. (1888) Untersuchungen über die Stickstoffnahrung der Gramineen und Leguminosen, in: *Beilageheft der Zeitschrift des Vereins für die Rübenzuckerindustrie des Deutschen Reiches*, pp. 1-234.
- Hoover, T. R., Robertson, A. D., Cerny, R. L., Hayes, R. N., Imperial, J., Shah, V. K. & Ludden, P. W. (1987) Identification of the V factor needed for synthesis of the iron-molybdenum cofactor of nitrogenase as homocitrate, *Nature* 329, 855-857.
- Howard, J. B., Davis, R., Moldenhauer, B., Cash, V. L. & Dean, D. R. (1989) Fe:S cluster ligands are the only cysteines required for nitrogenase Fe-protein activities, *J. Biol. Chem.* 264, 11270-11274.
- Howard, J. B. & Rees, D. C. (1994) Nitrogenase: a nucleotide-dependent molecular switch, *Annu. Rev. Biochem.* 63, 235-264.
- Hwang, J. C., Chen, C. H. & Burris, R. C. (1973) Inhibition of nitrogenase-catalyzed reductions, *Biochim. Biophys. Acta* 292, 256-270.
- Imam, S. & Eady, R. R. (1980) Nitrogenase of *Klebsiella pneumoniae*: reductant-independent ATP hydrolysis and the effect of pH on the efficiency of coupling of ATP hydrolysis to substrate reduction, *FEBS Lett.* 110, 35-38.
- Imperial, J., Hoover, T. R., Madden, M. S., Ludden, P. W. & Shah, V. K. (1989) Substrate reduction properties of dinitrogenase activated in vitro are dependent upon the presence of homocitrate or its analogues during iron-molybdenum cofactor synthesis, *Biochemistry* 28, 7796-7799.
- Kim, J. & Rees, D. C. (1992a) Structural models for the metal centers in the nitrogenase molybdenum-iron protein, *Science* 257, 1677-1682.
- Kim, J. & Rees, D. C. (1992b) Crystallographic structure and functional implications of the nitrogenase molybdenum-iron protein from *Azotobacter vinelandii*, *Nature* 360, 553-560.
- Kim, J. & Rees, D. C. (1994) Nitrogenase and biological nitrogen fixation, *Biochemistry* 33, 389-397.
- Kim, J., Woo, D. & Rees, D. C. (1993) X-ray crystal structure of the nitrogenase molybdenum-iron protein from *Clostridium pasteurianum* at 3.0 Å resolution, *Biochemistry* 32, 7104-7115.
- Kimber, S. J., Bishop, E. O. & Smith, B. E. (1982) Evidence on the role(s) of ATP in the mechanism of nitrogenase from proton NMR relaxation studies on metal and nucleotide binding to the molybdenum-iron protein, *Biochim. Biophys. Acta* 705, 385-395.
- Knight, E. & Hardy, R. W. F. (1996) Isolation and characteristics of flavodoxin from nitrogen-fixing *Clostridium pasteurianum*, *J. Biol. Chem.* 241, 2752-2756.
- Koch, B., Evans, H. J. & Russell, S. (1967) Properties of the nitrogenase system in cell-free extracts of bacteroids from soybean root nodules, *Proc. Natl. Acad. Sci. USA* 58, 1343-1350.
- Lanzilotta, W. N., Fisher, K. & Seefeldt, L. C. (1996) Evidence for electron transfer from the nitrogenase iron protein to the molybdenum-iron protein without MgATP hydrolysis: characterization of a tight protein-protein complex, *Biochemistry* 35, 7188-7196.
- Lanzilotta, W. N., Holz, R. C. & Seefeldt, L. C. (1995a) Proton NMR investigation of the [4Fe-4S]¹⁺ cluster environment of nitrogenase iron protein from *Azotobacter vinelandii*: defining nucleotide-induced conformational changes, *Biochemistry* 34, 15646-15653.
- Lanzilotta, W. N., Ryle, M. J. & Seefeldt, L. C. (1995b) Nucleotide hydrolysis and protein conformational changes in *Azotobacter vinelandii* nitrogenase iron protein: defining the

- function of aspartate 129, *Biochemistry* 34, 10713-10723.
- Lanzilotta, W. N. & Seefeldt, L. C. (1996) Electron transfer from the nitrogenase iron-protein to the [8Fe-(7/8)S] clusters of the molybdenum-iron protein, *Biochemistry* 35, 16770-16776.
- Leigh, G. J. (1995) The mechanism of dinitrogen reduction by molybdenum nitrogenase, *Eur. J. Biochem.* 229, 14-20.
- Li, J.-G., Burgess, B. K. & Corbin, J. L. (1982) Nitrogenase reactivity: cyanide as substrate and inhibitor, *Biochemistry* 21, 4393-4402.
- Lindahl, P. A., Day, E. P., Kent, T. A., Orme-Johnson, W. H. & Münck, E. (1985) Mössbauer, EPR and magnetization studies of the *Azotobacter vinelandii* Fe protein, *J. Biol. Chem.* 260, 11160-11173.
- Lindahl, P. A., Boon-Keng, T. & Orme-Johnson, W. H. (1987) EXAFS studies of the nitrogenase iron protein from *Azotobacter vinelandii*, *Inorg. Chem.* 26m, 3912-3916.
- Ljones, T. & Burris, R. H. (1972) ATP hydrolysis and electron transfer in the nitrogenase reaction with different combinations of the iron protein and the molybdenum-iron protein, *Biochim. Biophys. Acta* 275, 93-101.
- Ljones, T. & Burris, R. H. (1978a) Evidence for one-electron transfer by the Fe protein of nitrogenase, *Biochem. Biophys. Res. Commun.* 80, 22-25.
- Ljones, T. & Burris, R. H. (1978b) Nitrogenase: the reaction between the Fe protein and bathophenanthrolinedisulfonate as a probe for interactions with MgATP, *Biochemistry* 17, 1866-1872.
- Lockshin, A. & Burris, R. H. (1965) Inhibitors of nitrogen fixation in extracts from *Clostridium pasteurianum*, *Biochim. Biophys. Acta* 111, 1-10.
- Lowe, D. J., Ashby, G. A., Brune, M., Knights, H., Webb, M. R. & Thorneley, R. N. F. (1995) ATP hydrolysis and energy transduction by nitrogenase, in: *Nitrogen fixation, fundamentals and applications* (Tikhonovich, I. A., Provorov, N. A., Romanov, V. I. & Newton, W. E., eds.), pp. 103-108, Kluwer Academic Publishers, Dordrecht, The Netherlands.
- Lowe, D. J., Fisher, K. & Thorneley, R. N. F. (1993) *Klebsiella pneumoniae* nitrogenase: pre-steady-state absorbance changes show that redox changes occur in the MoFe protein that depend on substrate and component protein ratio; a role for P-centers in reducing dinitrogen? *Biochem. J.* 292, 93-98.
- Lowe, D. J. & Thorneley, R. N. F. (1984a) The mechanism of *Klebsiella pneumoniae* nitrogenase action. Pre-steady-state kinetics of H₂ formation, *Biochem. J.* 224, 877-886.
- Lowe, D. J. & Thorneley, R. N. F. (1984b) The mechanism of *Klebsiella pneumoniae* nitrogenase action. The determination of rate constants required for the simulation of the kinetics of N₂ reduction and H₂ evolution, *Biochem. J.* 224, 895-901.
- Lowery, R. G., Chang, C. L., Davis, L. C., McKenna, M.-C., Stephens, P. J. & Ludden, P. W. (1989) Substitution of histidine for arginine-101 of dinitrogenase reductase disrupts electron transfer to dinitrogenase, *Biochemistry* 28, 1206-1212.
- Ma, L., Brosius, M. A. & Burgess, B. K. (1996) Construction of a form of the MoFe protein of nitrogenase that accepts electrons from the Fe protein but does not reduce substrate, *J. Biol. Chem.* 271, 10528-10532.
- Madden, M. S., Kindon, N. D., Ludden, P. W. & Shah, V. K. (1990) Diastereomer-dependent substrate reduction properties of a dinitrogenase containing 1-fluorohomocitrate in the iron-molybdenum cofactor, *Proc. Natl. Acad. Sci. USA* 87, 6517-6521.
- Marshall, M. S. (1993) The effector interactions of p21^{ras}, *Trends Biochem. Sci.* 18, 250-254.
- McNary, J. E. & Burris, R. H. (1962) Energy requirement for nitrogen fixation by cell-free preparations from *Clostridium pasteurianum*, *J. Bact.* 84, 598-599.
- Mensink, R. E., Wassink, H. & Haaker, H. (1992) A reinvestigation of the pre-steady-state

- ATPase activity of nitrogenase from *Azotobacter vinelandii*, *Eur. J. Biochem.* 208, 289-294.
- Mensink, R. E. & Haaker, H. (1992) Temperature effects on the MgATP-induced electron transfer between the nitrogenase proteins from *Azotobacter vinelandii*, *Eur. J. Biochem.* 208, 295-299.
- Meyer, J., Gaillard, J. & Moulis, J.-M. (1988) Hydrogen-1 nuclear magnetic resonance of the nitrogenase iron protein (Cp2) from *Clostridium pasteurianum*, *Biochemistry* 27, 6150-6156.
- Milburn, M. V., Tong, L., deVos, A. M., Brünger, A., Yamaizumi, Z., Nishimura, S. & Kim, S.-H. (1990) Molecular switch for signal transduction: structural differences between active and inactive forms of protooncogenic *ras* proteins, *Science* 247, 939-945.
- Miller, R. W. & Eady, R. R. (1989) Molybdenum nitrogenase of *Azotobacter chroococcum*. Tight binding of MgADP to the MoFe protein, *Biochem. J.* 263, 725-729.
- Miller, R. W., Robson, R. L., Yates, M. G. & Eady, R. R. (1980) Catalysis and exchange of terminal phosphate groups of ATP and ADP by purified nitrogenase proteins, *Can. J. Biochem.* 58, 542-548.
- Miller, R. W., Smith, B. E. & Eady, R. R. (1993) Energy transduction by nitrogenase: binding of MgADP to the MoFe protein is dependent on the oxidation state of the iron-sulphur 'P' clusters, *Biochem. J.* 291, 709-711.
- Mortenson, L. E. (1964a) Ferredoxin requirement for nitrogen fixation by extracts of *Clostridium pasteurianum*, *Biochim. Biophys. Acta* 81, 473-478.
- Mortenson, L. E. (1964b) Ferredoxin and ATP, requirements for nitrogen fixation in cell-free extracts of *Clostridium pasteurianum*, *Proc. Natl. Acad. Sci. USA* 52, 272-279.
- Mortenson, L. E. (1965) Nitrogen fixation in extracts of *Clostridium pasteurianum*, in: *Non-heme iron proteins: role in energy metabolism* (San Pietro, A., ed.) pp. 243-259, The Antioch Press, Yellow Springs, Ohio.
- Mortenson, L. E., Morris, J. A. & Yeng, D. Y. (1967) Purification, metal composition and properties of molybdoferredoxin and azoferredoxin, two of the components of the nitrogen-fixing system of *Clostridium pasteurianum*, *Biochim. Biophys. Acta* 141, 516-522.
- Mortenson, L. E., Zumft, W. G. & Palmer, G. (1972) Electron paramagnetic resonance studies on nitrogenase. III. Function of magnesium adenosine 5'-triphosphate and adenosine 5'-diphosphate in catalysis by nitrogenase, *Biochim. Biophys. Acta* 292, 422-435.
- Moustafa, E. & Mortenson, L. E. (1967) Acetylene reduction by nitrogen fixing extracts of *Clostridium pasteurianum*: ATP requirement and inhibition by ADP, *Nature* 216, 1241-1242.
- Murrell, S. A., Lowery, R. G. & Ludden, P. W. (1988) ADP-ribosylation of dinitrogenase reductase from *Clostridium pasteurianum* prevents its inhibition of nitrogenase from *Azotobacter vinelandii*, *Biochem. J.* 251, 609-612.
- Nierhaus, K. N. (1996) An elongation factor turn-on, *Nature* 379, 491-492.
- Orme-Johnson, W. H. (1985) Molecular basis of biological nitrogen fixation, *Ann. Rev. Biophys. Biophys. Chem.* 14, 419-459.
- Orme-Johnson, W. H., Hamilton, W. D., Ljones, T., Tso, M.-Y., Burris, R. H., Shah, V. K. & Brill, W. J. (1972) Electron paramagnetic resonance of nitrogenase and nitrogenase components from *Clostridium pasteurianum* WS and *Azotobacter vinelandii* OP, *Proc. Natl. Acad. Sci. USA* 69, 3142-3145.
- Pai, E. F., Krengel, U., Petsko, G. A., Goody, R. S., Kabsch, W. & Wittinghofer, A. (1990) Refined crystal structure of the triphosphate conformation of H-ras p21 at 1.35 Å resolution: implications for the mechanism of GTP hydrolysis, *EMBO J.* 9, 2351-2359.
- Palmer, G., Multani, J. S., Cretny, W. C., Zumft, W. G. & Mortenson, L. E. (1972) Electron

- paramagnetic resonance studies on nitrogenase. I. The properties of molybdoferredoxin and azoferredoxin, *Arch. Biochem. Biophys.* 153, 325-332.
- Peters, J. W., Fisher, K., Newton, W. E. & Dean, D. R. (1994) Identification of a nitrogenase protein-protein interaction site defined by residues 59 through 67 within the *Azotobacter vinelandii* Fe protein, *J. Biol. Chem.* 269, 28076-28083.
- Peters, J. W., Fisher, K., Newton, W. E. & Dean, D. R. (1995) Involvement of the P-cluster in intramolecular electron transfer within the nitrogenase MoFe protein, *J. Biol. Chem.* 270, 27007-27013.
- Pham, D. N. & Burgess, B. K. (1993) Nitrogenase activity: effects of pH on substrate reduction and CO inhibition, *Biochemistry* 32, 13725-13731.
- Pierik, A. J., Wassink, H., Haaker, H. & Hagen, W. R. (1993) Redox properties and EPR spectroscopy of the P clusters of *Azotobacter vinelandii* MoFe protein, *Eur. J. Biochem.* 212, 51-61.
- Postgate, J. R. (1982) *The fundamentals of nitrogen fixation*, Cambridge University Press, London.
- Rayment, I., Rypniewski, W. R., Schmidt-Bäse, K., Smith, R., Tomchick, D. R., Benning, M. M., Winkelmann, D. A., Wesenberg, G. & Holden, H. M. (1993a) Three-dimensional structure of myosin subfragment-1: a molecular motor, *Science* 261, 50-58.
- Rayment, I., Holden, H. M., Whittaker, M., Yohn, C. B., Lorenz, M., Holmes, K. C. & Milligan, R. A. (1993b) Structure of the actin-myosin complex and its implications for muscle contraction, *Science* 261, 58-65.
- Rens-Domiano, S. & Hamm, H. E. (1995) Structural and functional relationships of heterotrimeric G-proteins, *FASEB J.* 9, 1059-1066.
- Rivera-Ortiz, J. M. & Burris, R. H. (1975) Interactions among substrates and inhibitors of nitrogenase, *J. Bact.* 123, 537-545.
- Robinson, A. C., Dean, D. R. & Burgess, B. K. (1987) Iron-molybdenum cofactor biosynthesis in *Azotobacter vinelandii* requires the iron protein of nitrogenase, *J. Biol. Chem.* 262, 14327-14332.
- Robinson, A. C., Chun, T. W. & Burgess, B. K. (1989) Iron-molybdenum cofactor insertion into the apo-MoFe protein of nitrogenase involves the iron protein-MgATP complex, *J. Biol. Chem.* 264, 10088-10095.
- Robson, R. L. (1984) Identification of possible adenine nucleotide-binding sites in nitrogenase Fe- and MoFe-proteins by amino acid sequence comparison, *FEBS Lett.* 173, 394-398.
- Rubinson, J. F., Corbin, J. L. & Burgess, B. K. (1983) Nitrogenase reactivity: methyl isocyanide as substrate and inhibitor, *Biochemistry* 22, 6260-6268.
- Ryle, M. J., Lanzilotta, W. N., Mortenson, L. E., Watt, G. E. & Seefeldt, L. C. (1995) Evidence for a central role of lysine 15 of *Azotobacter vinelandii* nitrogenase iron protein in nucleotide binding and protein conformational changes, *J. Biol. Chem.* 270, 13112-13117.
- Ryle, M. J., Lanzilotta, W. N., Seefeldt, L. C., Scarrow, R. C. & Jensen, G. M. (1996a) Circular dichroism and X-ray spectroscopies of *Azotobacter vinelandii* nitrogenase iron protein, *J. Biol. Chem.* 271, 1551-1557.
- Ryle, M. J., Lanzilotta, W. N. & Seefeldt, L. C. (1996b) Elucidating the mechanism of nucleotide-dependent changes in the redox potential of the [4Fe-4S] cluster in nitrogenase iron-protein: the role of phenylalanine 135, *Biochemistry* 35, 9424-9434.
- Ryle, M. J. & Seefeldt, L. C. (1996) Elucidation of a MgATP signal transduction pathway in the nitrogenase iron protein: formation of a conformation resembling the MgATP-bound state by protein engineering, *Biochemistry* 35, 4766-4775.
- Schulz, G. E. (1992) Binding of nucleotides by proteins, *Curr. Opin. Struct. Biol.* 2, 61-67.
- Seefeldt, L. C. (1994) Docking of nitrogenase iron- and molybdenum-iron proteins for electron

- transfer and MgATP hydrolysis: the role of arginine 140 and lysine 143 of the *Azotobacter vinelandii* iron protein, *Protein Sci.* 3, 2073-2081.
- Seefeldt, L. C., Morgan, T. V., Dean, D. R. & Mortenson, L. E. (1992) Mapping the site(s) of MgATP and MgADP interaction with the nitrogenase of *Azotobacter vinelandii*, *J. Biol. Chem.* 267, 6680-6688.
- Seefeldt, L. C. & Mortenson, L. E. (1993) Increasing nitrogenase catalytic efficiency for MgATP by changing serine 16 of its Fe protein to threonine: use of Mn^{2+} to show interaction of serine 16 with Mg^{2+} , *Protein Sci.* 2, 93-102.
- Shah, V. K. & Brill, W. J. (1977) Isolation of an iron-molybdenum cofactor from nitrogenase, *Proc. Natl. Acad. Sci. USA* 74, 3249-3253.
- Shah, V. K., Davis, L. C. & Brill, W. J. (1970) Nitrogenase. I. Repression and derepression of the iron-molybdenum and iron proteins of nitrogenase in *Azotobacter vinelandii*, *Biochim. Biophys. Acta*, 256, 498-511.
- Simpson, F. B. & Burris, R. H. (1984) A nitrogen pressure of 50 atmospheres does not prevent evolution of hydrogen by nitrogenase, *Science* 224, 1095-1097.
- Smith, B. E. & Eady, R. R. (1992) Metalloclusters of the nitrogenases, *Eur. J. Biochem.* 205, 1-15.
- Smith, B. E., Lowe, D. J. & Bray, R. C. (1972) Nitrogenase of *Klebsiella pneumoniae*: electron-paramagnetic-resonance studies on the catalytic mechanism, *Biochem. J.* 130, 641-643.
- Smith, B. E., Lowe, D. J. & Bray, R. C. (1973) Studies by electron paramagnetic resonance on the catalytic mechanism of nitrogenase of *Klebsiella pneumoniae*, *Biochem. J.* 135, 331-341.
- Smith, B. E., Thorneley, R. N. F., Eady, R. R. & Mortenson, L. E. (1976) Nitrogenases from *Klebsiella pneumoniae* and *Clostridium pasteurianum*. Kinetic investigations of cross-reactions as a probe of the enzyme mechanism, *Biochem. J.* 157, 439-447.
- Stephens, P. J., McKenna, C. E., Smith, B. E., Nguyen, H. T., McKenna, M.-C., Thomson, A. J., Devlin, F. & Jones, J. B. (1979) Circular dichroism and magnetic circular dichroism of nitrogenase proteins, *Proc. Natl. Acad. Sci. USA* 76, 2585-2589.
- Story, R. M. & Steitz, T. A. (1992) Structure of the *recA* protein-ADP complex, *Nature* 355, 374-376.
- Strandberg, G. W. & Wilson, P. W. (1967) Molecular H_2 and the pN_2 function of *Azotobacter*, *Proc. Natl. Acad. Sci.* 58, 1404-1409.
- Surerus, K. K., Hendrich, M. P., Christie, P. D., Rottgardt, D., Orme-Johnson, W. H. & Münck, E. (1992) Mössbauer and integer-spin EPR of the oxidized P-clusters of nitrogenase: P^{ox} is a non-Kramers system with a nearly degenerate ground doublet, *J. Am. Chem. Soc.* 114, 8579-8590.
- Thorneley, R. N. F. (1975) Nitrogenase of *Klebsiella pneumoniae*. A stopped-flow study of magnesium-adenosine-triphosphate-induced electron transfer between the component proteins, *Biochem. J.* 145, 391-396.
- Thorneley, R. N. F., Ashby, G., Howarth, J. V., Millar, N. C. & Gutfreund, H. (1989) A transient kinetic study of the nitrogenase of *Klebsiella pneumoniae* by stopped-flow calorimetry, *Biochem. J.* 264, 657-661.
- Thorneley, R. N. F. & Cornish-Bowden, A. (1977) Kinetics of nitrogenase of *Klebsiella pneumoniae*. Heterotrophic interactions between magnesium-adenosine 5'-diphosphate and magnesium-adenosine 5'-triphosphate, *Biochem. J.* 165, 255-262.
- Thorneley, R. N. F., Eady, R. R. & Yates, M. G. (1975) Nitrogenases of *Klebsiella pneumoniae* and *Azotobacter chroococcum*. Complex formation between the component proteins, *Biochim. Biophys. Acta* 403, 269-284.
- Thorneley, R. N. F. & Lowe, D. J. (1983) Nitrogenase of *Klebsiella pneumoniae*. Kinetics of the

- dissociation of oxidized iron protein from molybdenum-iron protein: identification of the rate-limiting step for substrate reduction, *Biochem. J.* 215, 393-403.
- Thorneley, R. N. F. & Lowe, D. J. (1984a) The mechanism of *Klebsiella pneumoniae* nitrogenase action. Pre-steady-state kinetics of an enzyme-bound intermediate in N_2 reduction and of NH_3 formation, *Biochem. J.* 224, 887-894.
- Thorneley, R. N. F. & Lowe, D. J. (1984b) The mechanism of *Klebsiella pneumoniae* nitrogenase action. Simulation of the dependencies of H_2 -evolution rate on component-protein concentration and ratio and sodium dithionite concentration, *Biochem. J.* 224, 903-909.
- Tittsworth, R. C. & Hales, B. J. (1993) Detection of EPR signals assigned to the 1-equiv-oxidized P-clusters of the nitrogenase MoFe-protein from *Azotobacter vinelandii*, *J. Am. Chem. Soc.* 115, 9763-9767.
- Tong, L., deVos, A. M., Milburn, M. V. & Kim, S.-H. (1991) Crystal structures at 2.2 Å resolution of the catalytic domains of normal *ras* protein and an oncogenic mutant complexed with GDP, *J. Mol. Biol.* 217, 503-516.
- Walker, G. A. & Mortenson, L. E. (1973) An effect of magnesium adenosine 5'-triphosphate on the structure of azoferredoxin from *Clostridium pasteurianum*, *Biochem. Biophys. Res. Commun.* 53, 904-909.
- Walker, G. A. & Mortenson, L. E. (1974) Effect of magnesium adenosine 5'-triphosphate on the accessibility of the iron of Clostridial azoferredoxin, a component of nitrogenase, *Biochemistry* 13, 2382-2388.
- Walker, J. E., Saraste, M., Runswick, M. J. & Gay, N. J. (1982) Distantly related sequences in the α - and β -subunits of ATP synthase, myosin, kinases and other ATP-requiring enzymes and a common nucleotide binding fold, *EMBO J.* 1, 945-951.
- Watt, G. D., Bulen, W. A., Burns, A. & Hadfield, K. L. (1975) Stoichiometry, ATP/2e values and energy requirements for reactions catalyzed by nitrogenase from *Azotobacter vinelandii*, *Biochemistry* 14, 4266-4272.
- Watt, G. D. & Burns, A. (1977) Kinetics of dithionite ion utilization and ATP hydrolysis for reactions catalyzed by the nitrogenase complex from *Azotobacter vinelandii*, *Biochemistry* 16, 264-270.
- Watt, G. D. & McDonald, J. W. (1985) Electron paramagnetic resonance spectrum of the iron protein of nitrogenase: existence of a $g = 4$ spectral component and its effect on spin quantization, *Biochemistry* 24, 7226-7231.
- Watt, G. D., Wang, Z.-C. & Knotts, R. R. (1986) Redox reactions of and nucleotide binding to the iron protein of *Azotobacter vinelandii*, *Biochemistry* 25, 8156-8162.
- Wherland, S., Burgess, B. K., Stiefel, E. I. & Newton, W. E. (1981) Nitrogenase reactivity: effects of component ratio on electron flow and distribution during nitrogen fixation, *Biochemistry* 20, 5132-5140.
- Willing, A. H. & Howard, J. B. (1990) Cross-linking site in *Azotobacter vinelandii* complex, *J. Biol. Chem.* 265, 6596-6599.
- Willing, A. H., Georgiadis, M. M., Rees, D. C. & Howard, J. B. (1989) Cross-linking of nitrogenase components. Structure and activity of the covalent complex, *J. Biol. Chem.* 264, 8499-4503.
- Winter, H. C. & Burris, R. H. (1968) Stoichiometry of the adenosine triphosphate requirement for N_2 fixation and H_2 evolution by a partially purified preparation of *Clostridium pasteurianum*, *J. Biol. Chem.* 243, 940-944.
- Wolfe, D., Dean, D. R. & Howard, J. B. (1992a) Nucleotide-iron-sulphur cluster signal transduction in the nitrogenase iron-protein: the role of Asp¹²⁵, *Science* 258, 992-995.
- Wolfe, D., Kim, C.H., Dean, D. & Howard, J. B. (1992b) Ionic interactions in the nitrogenase

- complex. Properties of Fe-protein containing substitutions for Arg¹⁰⁰, *J. Biol. Chem.* 267, 3667-3673.
- Yates, M. G. (1992) The enzymology of molybdenum-dependent nitrogen fixation, in: *Biological nitrogen fixation* (Stacey, G., Burris, R. H. & Evans, H. J., eds.), pp. 685-735, Chapman & Hall, New-York.
- Yeng, D. Y., Morris, J. A. & Mortenson, L. E. (1970) The effect of reductant in inorganic phosphate release from adenosine 5'-triphosphate by purified nitrogenase of *Clostridium pasteurianum*, *J. Biol. Chem.* 245, 2809-2813.
- Young, J. P. W. (1992) Phylogenetic classification of nitrogen-fixing organisms, in: *Biological nitrogen fixation* (Stacey, G. Burris, R. H. & Evans, H. J., eds.), pp. 43-86, Chapman & Hall, New-York/London.
- Yousafzai, F. K., Buck, M. & Smith, B. E. (1996) Isolation and characterization of nitrogenase MoFe protein from the mutant strain pHK17 of *Klebsiella pneumoniae* in which the two bridging cysteine residues of the P-clusters are replaced by the non-coordinating amino acid alanine, *Biochem. J.* 318, 111-118.
- Zimmermann, R., Münck, E., Brill, W. J., Shah, V. K., Henzl, M. T., Rawlings, J. & Orme-Johnson, W. H. (1978) Nitrogenase. X. Mössbauer and EPR studies on reversibly oxidized MoFe protein from *Azotobacter vinelandii*, *Biochim. Biophys. Acta* 537, 185-207.
- Zumft, W. G., Cretney, W. C., Huang, T. C., Mortenson, L. E. & Palmer, G. (1972) On the structure and function of nitrogenase from *Clostridium pasteurianum* W5, *Biochem. Biophys. Res. Commun.* 48, 1525-1532.
- Zumft, W. G., Mortenson, L. E. & Palmer, G. (1974) Electron-paramagnetic-resonance studies on nitrogenase. Investigation of the oxidation-reduction behaviour of azoferredoxin and molybdoferredoxin with potentiometric and rapid-freeze techniques, *Eur. J. Biochem.* 46, 525-535.
- Zumft, W. G., Palmer, G. & Mortenson, L. E. (1973) Electron paramagnetic resonance studies on nitrogenase. Interaction of adenosine 5'-triphosphate with azoferredoxin, *Biochim. Biophys. Acta* 292, 413-421.

Chapter 2

Pre-steady-state MgATP-dependent proton production and electron transfer by nitrogenase from *Azotobacter vinelandii*

Abstract

MgATP-dependent pre-steady-state proton production by nitrogenase from *Azotobacter vinelandii* was studied by monitoring the absorbance changes at 572 nm of the pH indicator *o*-cresolsulphonphthalein in a weakly buffered solution. The absorbance changes are characterized by a constant phase, a single exponential decrease and a linear decrease. The observed rate constant for the single exponential MgATP-dependent proton production by reduced nitrogenase proteins at 20.0 °C was $14 \pm 4 \text{ s}^{-1}$. No proton production with a rate constant comparable to the observed rate constant of electron transfer ($k_{\text{obs}} \approx 100 \text{ s}^{-1}$) was detected. The extent of the observed MgATP-dependent proton production is determined by the redox state of the nitrogenase proteins before mixing with MgATP: less protons are produced when more electrons are transferred from the Fe protein to the MoFe protein. Values of $2.7 \pm 0.3 \text{ mol H}^+ \text{ produced/mol Av1}$ with oxidized Fe protein, and $1.1 \pm 0.1 \text{ mol H}^+ \text{ produced/mol Av1}$ with reduced Fe protein, were found. The data are interpreted that protons are taken up after electron transfer from the Fe protein to the MoFe protein; the ratio electrons transferred/ H^+ uptake was calculated to be 1.2 ± 0.2 .

After mixing of the nitrogenase proteins with MgADP proton production takes place as well. The proton production curve did not have a constant phase and the observed rate constant of the single exponential reaction is higher, compared to MgATP-dependent proton production: $k_{\text{obs}} \approx 35 \text{ s}^{-1}$. The amount of protons produced depends also on the redox state of the Fe protein; no proton production was observed with the oxidized Fe protein; with dithionite-reduced Fe protein a value of $3.1 \pm 0.4 \text{ mol H}^+ \text{ produced/mol Av1}$ was found (or $0.5 \pm 0.1 \text{ mol H}^+ \text{ produced/mol Av2}$). Similar results were obtained when only the Fe protein was mixed with MgADP, but the observed absorbance changes were smaller; mixing of dithionite reduced Av2 with MgADP resulted in the production of $0.17 \pm 0.05 \text{ mol H}^+ \text{ produced/mol Av2}$.

All reported absorbance changes were absent when the experiments were performed in a buffered solution.

The series of events that occur after mixing of the nitrogenase proteins with MgATP will be presented and discussed. In case of reduced Fe protein electron transfer takes place at a rate of 100 s^{-1} , which is followed by H^+ production ($k_{\text{obs}} \approx 14\text{ s}^{-1}$). When there is no electron transfer (oxidized Fe protein) the rate constant of the MgATP-induced proton production decreases. When electrons are transferred stoichiometrically less protons are produced.

Introduction

Nitrogenase is the enzyme system which catalyses the reaction of nitrogen fixation, in which dinitrogen is reduced to ammonia. Nitrogenase consists of two distinct oxygen-sensitive metalloproteins, which are both necessary for the catalytic activity (Burris, 1991; Smith & Eady, 1992; Dean et al., 1993). The molybdenum containing nitrogenase was studied in the present investigation. The largest one of the nitrogenase proteins is the (molybdenum-iron) MoFe protein (Av1): it contains two types of metal-sulphur clusters: an Fe, Mo and S containing cofactor, called FeMoco, and the P-clusters, which are $[\text{8Fe-8S}]$ clusters (Hagen et al., 1987). Kim and Rees (1992a) have proposed structural models for FeMoco and the P-clusters, based on (2.7 \AA resolution) crystallographic analysis of the MoFe protein of *Azotobacter vinelandii* nitrogenase (Kim & Rees, 1992a,b), which structures were confirmed (2.2 \AA resolution) by Chan et al. (1993). FeMoco is generally agreed to be the site where substrate reduction takes place; the function of the P-clusters is not known. Based on pre-steady-state kinetic data and EPR measurements, Lowe et al. (1993) recently proposed that at the point in nitrogenase catalysis when dinitrogen is committed to be reduced to ammonia, the P-clusters are oxidized and the electron density on N_2 , bound to FeMoco, is increased; this might be the crucial event in the catalysis to give nitrogenase the ability to reduce N_2 . The other protein of the nitrogenase system is the (iron) Fe protein (Av2), a homodimer which contains one $[\text{4Fe-4S}]$ cluster. Georgiadis et al. (1992) determined the crystallographic structure of the nitrogenase Fe protein of *A. vinelandii* (2.9 \AA resolution). The Fe protein has two nucleotide binding sites. Binding of MgATP or MgADP to the Fe protein results in a decrease of the redox potential (Watt et al., 1986), changes in the EPR spectrum (Hagen et al., 1985) and conformational changes (Ashby & Thorneley, 1987; Georgiadis et al., 1992).

For catalytic activity, the presence of both the MoFe protein and the Fe protein is needed, as well as the presence of a strong reductant (such as a flavodoxin or ferredoxin

in vivo, or sodium dithionite ($\text{Na}_2\text{S}_2\text{O}_4$) *in vitro*) and MgATP, which is hydrolysed during catalysis. In the nitrogenase reaction electrons are transferred from the Fe protein to the MoFe protein, where the substrate is reduced. The accepted model for the mechanism of electron transport through nitrogenase was developed by Thorneley and Lowe (1983, 1985; Lowe & Thorneley, 1984a). They proposed an Fe protein cycle and a MoFe protein cycle for the catalytic mechanism of nitrogenase. In the Fe protein cycle, after the association of the reduced Fe protein and the MoFe protein a single electron is transferred from the Fe protein to the MoFe protein, with concomitant hydrolysis of MgATP. Hereafter, the nitrogenase complex dissociates into the separate proteins (which is the rate limiting step in the catalytic cycle), MgADP is replaced by MgATP, P_i released and the Fe protein is reduced again by the present electron donor (for example dithionite). The Fe protein cycle is now completed, and the MoFe protein is reduced by one electron. For the reduction of N_2 to NH_3 the MoFe protein has to be reduced another seven times in the Fe protein cycle: the sequence of eight Fe protein cycles constitutes the MoFe protein cycle (Lowe & Thorneley, 1984a; Thorneley & Lowe, 1983, 1985).

Under optimal steady-state conditions two molecules of MgATP are hydrolysed for each electron transferred from the Fe protein to the MoFe protein (Smith & Eady, 1992). There is no agreement about the rate constant of MgATP hydrolysis and the value of the molar ratio MgATP hydrolysed/electrons transferred in the pre-steady-state phase of the reaction (Mensink et al., 1992).

Reinvestigating the role of MgATP in nitrogenase catalysis, Mensink et al. (1992) showed that it is possible to use the pH indicator *o*-cresolsulphonphthalein (cresol red) to monitor MgATP-dependent pre-steady-state proton production by nitrogenase. It was observed that MgATP-dependent proton production occurred at a much lower rate than electron transfer. From these observations Mensink et al. (1992) concluded that proton production due to MgATP hydrolysis happens after electron transfer from the Fe protein to the MoFe protein has occurred, in contradiction with the general opinion about the order in which these processes take place. It is suggested in the literature that electron transfer from the Fe protein to the MoFe protein is coupled to MgATP hydrolysis in the catalytic cycle of nitrogenase (Burris, 1991; Smith & Eady, 1992). Thorneley et al. (1989) concluded from their stopped-flow calorimetry and stopped-flow absorbance experiments of the pre-steady-state kinetics of MgATP hydrolysis by nitrogenase from *Klebsiella pneumoniae*, that (at 6 °C) hydrolysis of MgATP even precedes electron transfer. They proposed a mechanism in which both MgATP hydrolysis and electron transfer are reversible. Based on stopped-flow experiments on the temperature dependence of the pre-steady-state MgATP-dependent electron transfer, Mensink & Haaker (1992) have proposed an alternative explanation for the data of Thorneley et al.

(1989). They suggested that the interaction of MgATP with the nitrogenase complex, but not necessarily the hydrolysis of MgATP to MgADP and P_i , is a fast and irreversible reaction, which is followed by a reversible electron transfer within the protein complex (Mensink & Haaker, 1992).

There are some molecular models for a mechanism of the ATPase activity of nitrogenase, suggesting how the energy from ATP hydrolysis is used in nitrogenase catalysis. Cordewener et al. (1987) have shown that Av2 tightly binds one molecule of MgATP or MgADP. Later it was found that a single ADP molecule co-crystallized with Av2, bound in the interface region between the two subunits, and is separated about 20 Å from the [4Fe-4S] cluster (Georgiadis et al., 1992). This distance is too large to permit direct chemical coupling of electron transfer and ATP hydrolysis. A close structural similarity has been found between the nucleotide binding regions of the nitrogenase Fe protein and the H-Ras p21 protein (Georgiadis et al., 1992; Wolle et al., 1992), which has GTPase activity and of which the MgGTP and MgGDP binding properties have been well characterized. The nucleotide binding regions of the Fe protein and the H-Ras p21 protein are different with respect to the orientation of the nucleotide. In the Fe protein the binding mode for MgADP is across the subunit interface, whereas in the H-Ras p21 protein the binding mode is parallel to the twofold symmetry axis of the protein. Binding of MgGDP or MgGTP alters the conformational state of the protein, but the orientation in the protein of either nucleotide is the same (Milburn et al., 1990; Pai et al., 1990; Bourne et al., 1991). It has been proposed (Georgiadis et al., 1992; Wolle et al., 1992) that the Fe protein could also adopt the H-Ras binding mode, and that this different binding mode represents the MgATP bound conformation. In the gating mechanism proposed by Wolle et al. (1992) hydrolysis of MgATP, bound to the Fe protein in the H-Ras p21 protein mode, would lead to a transition state from which electron transfer occurs; MgADP could move to the intersubunit binding mode resulting in such a conformational change that backflow from the electrons to the Fe protein is prevented. Another view on the interaction of the nucleotides with nitrogenase was put forward by Miller et al. (1993). They observed that MgADP binding to the MoFe protein of *K. pneumoniae* (Kp1) depends on the oxidation state of the P-clusters: MgADP only binds tightly to the MoFe protein when the P-clusters are oxidized. It is proposed that MgADP originally bound as MgATP to the Fe protein, binds to MgADP binding sites on the MoFe protein that are transiently generated during catalysis, and that hydrolysis of MgATP occurs on a bridging site on the MoFe protein - Fe protein complex.

As indicated above, several proposals have been put forward for a molecular mechanism of MgATP hydrolysis by nitrogenase, but there are still no conclusive kinetic data available to support these models. In this paper the ATPase activity of nitrogenase is studied by its proton production in the Fe protein cycle. Mensink et al. (1992)

reported the time course of the MgATP-dependent proton production of nitrogenase. It was concluded that the hydrolysis rate of MgATP, as judged by proton release, is lower than the rate of electron transfer from the Fe protein to the MoFe protein. In this paper new results concerning the redox dependency of the pre-steady-state ATPase activity, judged as H^+ production, will be presented. A more detailed kinetic model based on our results, for the Fe protein cycle of nitrogenase will be presented.

Materials and methods

Cell growth and isolation and preparation of nitrogenase

Azotobacter vinelandii ATCC strain 478 was grown and the separate nitrogenase proteins were isolated as described by Mensink et al. (1992). Protein concentrations were measured by the microbiuret method (Goa, 1953) after a precipitation step with deoxycholic acid and trichloroacetic acid (Bensadoun & Weinstein, 1976). The molar concentrations of the nitrogenase proteins Av1 and Av2 were determined from their molecular masses of 230 kDa and 63 kDa, respectively. The activities of the nitrogenase components were determined from their specific acetylene reduction activity, as was described by Braaksma et al. (1982). The specific activities of the Av1 and Av2 preparations used in the experiments were at least 8 mol ethylene produced $\cdot s^{-1} \cdot (mol\ Av1)^{-1}$ and 2 mol ethylene produced $\cdot s^{-1} \cdot (mol\ Av2)^{-1}$, respectively. Av1 contained 1.8 ± 0.2 mol Mo/mol Av1; the Fe content of Av2 was 3.6 ± 0.3 mol Fe/mol Av2 (Mensink et al., 1992).

Dithionite-free nitrogenase complex was prepared by running both nitrogenase components together at the indicated ratio over a Biogel P-6DG column (Biorad, 1 cm x 8 cm), which was equilibrated with argon-saturated 10 mM $MgCl_2$ in 1 mM Tes/NaOH, pH 7.8.

Chemicals

ADP and ATP (special quality) were obtained from Boehringer; *o*-cresolsulphonphthalein (cresol red) was obtained from Sigma.

Measurement of electron transfer and proton production

For the measurements of the pre-steady-state proton production and electron transfer by the nitrogenase complex, a Hi-TECH SF-51 stopped-flow spectrofluorimeter, equipped with an anaerobic kit and a data acquisition and analysis system, was used.

Electron transfer from the Fe protein to the MoFe protein was measured in the absence of cresol red, at 430 nm. The molecular absorbance coefficient for electron transfer, $\epsilon_{430} = 4.85 \text{ mM}^{-1} \cdot \text{cm}^{-1}$, was calculated from the maximal absorbance change for electron transfer as found by Mensink & Haaker (1992). One syringe in the stopped-flow spectrophotometer contained Av1 and Av2 at the indicated concentrations, and 10 mM MgCl_2 in 1 mM Tes/NaOH, pH 7.8. The other syringe contained 10 mM ATP or ADP and 10 mM MgCl_2 in 1 mM Tes/NaOH, pH 7.8. The mixing ratio was 1:1. Just before the measurements dithionite was added to the protein solution, or to both the protein and the MgATP/MgADP solution (as indicated in Results). After measuring the electron transfer, to the same protein solution 100 μM cresol red was added and the pre-steady-state proton production was monitored at 572 nm by the absorbance changes of the pH indicator cresol red. All experiments were performed at $20.0 \pm 0.1^\circ\text{C}$, under argon.

The buffer capacities ($\Delta A_{572}/\Delta[\text{H}^+]_{\text{added}}$) of the reaction mixtures were determined under anaerobic conditions, by titration of solutions of various concentrations of the nitrogenase proteins with known quantities of argon-saturated HCl and measurement of the subsequent absorbance change of cresol red at 572 nm. The reaction mixture had the same composition as the reaction mixture used in the stopped-flow experiments, with the difference that dithionite was omitted and ATP was replaced by ADP. For a solution of 6 μM Av1 and 36 μM Av2 the buffer capacity was calculated to be $3100 \pm 200 \text{ M}^{-1}$, for 36 μM Av2 this value is $4100 \pm 200 \text{ M}^{-1}$. The buffer capacity of these solutions is mainly determined by the concentration of the nitrogenase proteins, especially of Av2 (Mensink et al., 1992).

Analysis of the proton production curves

In the proton production curves (measured at 572 nm) obtained after mixing of the nitrogenase complex with MgATP, three phases can be discerned: a constant phase during which no absorbance changes occur, a single exponential decrease and a linear decrease. Starting after the constant phase, the proton production curves were fitted to a function consisting of a single exponential and a slope: $\Delta A_{572} = A \cdot \exp(-k_{\text{obs}} \cdot t) - m \cdot t$. From the amplitude A of the single exponential reaction (and the buffer capacity

of the reaction mixture) the amount of protons produced (with a rate constant k_{obs}) in the pre-steady-state phase of the reaction of the nitrogenase complex with MgATP, was calculated. From the slope the amount of protons produced per second in the linear phase of the reaction was calculated. The constant phase at the beginning of the proton production curves was never included in the fit.

Results

Mensink et al. (1992) have shown that it is possible to monitor the pre-steady-state MgATP-dependent proton production by nitrogenase, following the absorbance changes in time of the pH indicator cresol red. One control experiment was mentioned by Mensink et al. (1992): they observed that mixing of Av2 with a solution containing MgATP and cresol red gave rise to absorbance changes, which were subsequently subtracted from the proton production curves obtained from the reaction of the nitrogenase complex with MgATP. During the present study it appeared that one important control experiment, namely mixing a solution containing both Av1 and Av2 with a cresol red solution, resulted also in an absorbance decrease (see Figure 1). We therefore tested all mixing possibilities to obtain a condition with low background reactions of cresol red with the nitrogenase proteins. When cresol red was present in the protein solution only a small background absorbance decrease is observed after mixing of the nitrogenase/cresol red solution with buffer (see Figure 1). Therefore in subsequent experiments cresol red was always pre-mixed with the proteins.

It was also verified whether the observed absorbance changes of cresol red were not due to a reaction of cresol red with the nucleotides or dithionite. When 100 μM cresol red with or without 50 μM sodium dithionite (in 10 mM MgCl_2 + 1 mM Tes/NaOH, pH 7.8) was mixed with 10 mM ATP or ADP (in 10 mM MgCl_2 + 1 mM Tes/NaOH, pH 7.8), the linear decrease was less than 0.004 in 1 s. This is about 4% of the linear phase of the ATPase activity of nitrogenase.

It was found that all reported cresol red absorbance changes were absent when 25 mM Tes/NaOH, pH 7.8, was present in the reaction mixture; this shows that the observed absorbance changes at 572 nm in a weakly buffered solution, must be attributed to pH changes of the reaction mixture and not to changes of the absorbance coefficient of cresol red (data not shown).

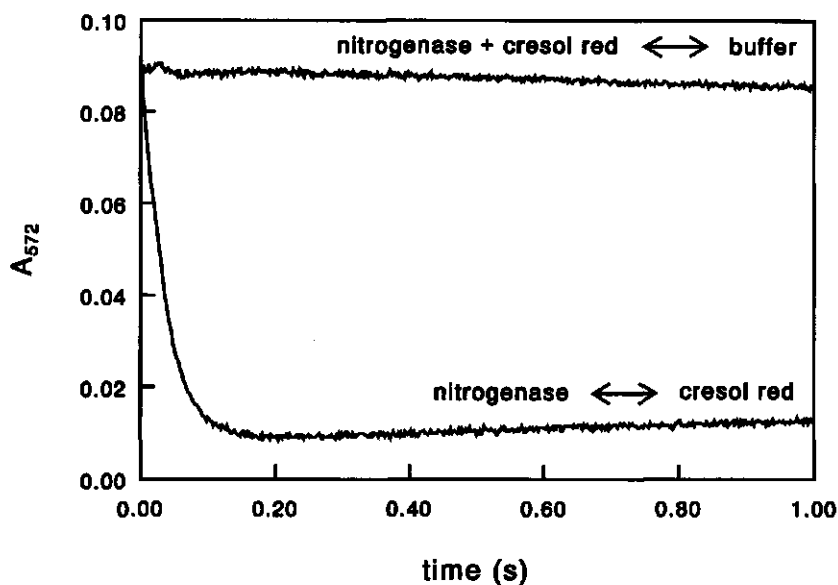


Figure 1. Reaction of cresol red with the nitrogenase proteins. Trace 'nitrogenase \leftrightarrow cresol red': absorbance changes (572 nm) after mixing of the nitrogenase proteins with cresol red. Syringe one contained: $[Av1] = 12 \mu\text{M}$, $[Av2] = 80 \mu\text{M}$, 10 mM MgCl_2 and 1 mM Tes/NaOH , pH 7.8. Syringe two contained: $[\text{cresol red}] = 100 \mu\text{M}$, 10 mM MgCl_2 and 1 mM Tes/NaOH , pH 7.8. To the protein solution 50 μM dithionite was added. Trace 'nitrogenase + cresol red \leftrightarrow buffer': absorbance changes (572 nm) after mixing of the nitrogenase proteins and cresol red with buffer. Syringe one: $[Av1] = 12 \mu\text{M}$, $[Av2] = 72 \mu\text{M}$, $[\text{cresol red}] = 100 \mu\text{M}$, 10 mM MgCl_2 and 1 mM Tes/NaOH , pH 7.8. Syringe two: 10 mM MgCl_2 and 1 mM Tes/NaOH , pH 7.8. To both solutions 50 μM dithionite was added.

MgATP-induced electron transfer and proton production

Figure 2 shows the absorbance changes associated with proton production and electron transfer after mixing of the nitrogenase proteins and cresol red with MgATP. The nitrogenase solution and the MgATP solution each contained 50 μM dithionite. The data curve for electron transfer from Av2 to Av1 (Figure 2) in this experiment could be fitted to a single exponential with an amplitude $\Delta A_{430} = 0.047$ and a rate constant $k_{\text{obs}} = 102 \text{ s}^{-1}$. Using $\epsilon_{430} = 4.85 \text{ mM}^{-1} \cdot \text{cm}^{-1}$, the amount of electrons transferred from Av2 to Av1 was calculated to be 9.7 μM electrons. This corresponds to a ratio of 1.6 mol electrons/mol Av1 ($[Av1] = 6 \mu\text{M}$). As can be seen from Figure 2, electron transfer started immediately after mixing of nitrogenase with MgATP.

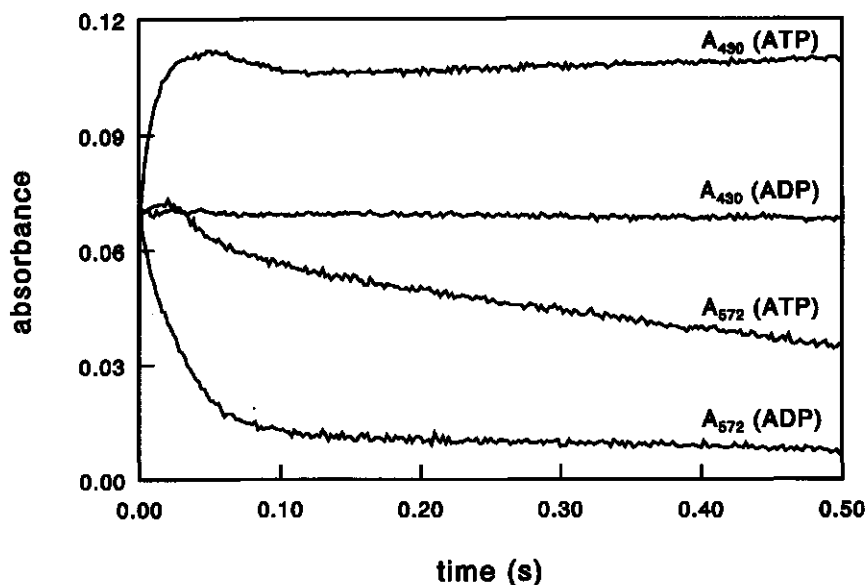


Figure 2. Absorbance changes at 430 nm and at 572 nm after mixing of the nitrogenase proteins with MgATP or MgADP. ' $A_{430}(\text{ATP})$ ': electron transfer (A_{430}) after mixing with MgATP; ' $A_{572}(\text{ATP})$ ': proton production (A_{572}) after mixing with MgATP; ' $A_{572}(\text{ADP})$ ': proton production (A_{572}) after mixing with MgADP; ' $A_{430}(\text{ADP})$ ': A_{430} after mixing with MgADP. Syringe one: $[\text{Av1}] = 12 \mu\text{M}$, $[\text{Av2}] = 72 \mu\text{M}$, 10 mM MgCl_2 and 1 mM Tes/NaOH , pH 7.8. Syringe two: $[\text{MgA(T)(D)P}] = 10 \text{ mM}$, 10 mM MgCl_2 and 1 mM Tes/NaOH , pH 7.8. To both syringes 50 μM dithionite was added. For measurement of proton production (' $A_{572}(\text{ATP})$ ' and ' $A_{572}(\text{ADP})$ ') 100 μM cresol red was added to the protein solution.

The MgATP-dependent proton production started after a constant phase of about 25 ms. After this constant phase the progression curve for MgATP-dependent proton production fitted: $\Delta A_{572} = 0.016 \cdot \exp(-18.2t) - 0.045t$; the plateau formed by the constant phase of the curve is considered to represent the maximal absorbance and was not included in the fit. From these data, it was calculated, with $\Delta A_{572}/\Delta[\text{H}^+]_{\text{added}} = 3100 \text{ M}^{-1}$, that 5.2 μM H^+ were produced in the (single exponential) pre-steady-state phase of the reaction (with a rate constant of 18.2 s^{-1}), which corresponds to a ratio of 0.87 mol H^+ /mol Av1.

The constant phase of the MgATP-dependent proton production trace (Figure 2) started with a small increase of the absorbance in case of reduced Av2. This increase is caused by electron transfer, since the absorbance coefficient of electron transfer is about $0.5 \text{ mM}^{-1} \cdot \text{cm}^{-1}$ when measured at 572 nm, which is about 10% of its value at 430 nm. When this value was taken into account and 10% of the electron transfer curve was

subtracted from the proton production curve, the absorbance increase at the start of the constant phase of the proton production curve disappeared, whereas the rest of the proton production curve remained unaltered (data not shown).

From Figure 2, it can be seen that mixing of the nitrogenase proteins with MgADP also induces absorbance changes at 572 nm. The MgADP-induced proton production curve differed from the MgATP-induced curve: it did not have a constant phase, but proton production started immediately after mixing and the absorbance decrease in the first phase of the curve was faster. The progression curve for MgADP-dependent proton production fitted: $\Delta A_{572} = 0.059 \cdot \exp(-35.3t) - 0.010t$. So 19.0 μM H^+ were produced during the pre-steady-state phase of this reaction (with a rate constant of 35.3 s^{-1}), corresponding to a ratio of 3.2 mol H^+ / mol Av1. At 430 nm no absorbance changes were observed after mixing of the nitrogenase proteins with MgADP (Figure 2).

Dependence of MgATP-induced proton production on the redox state of Av2

Figure 3A shows that the single exponential phase of MgATP-dependent proton production depends on the redox state of the nitrogenase proteins before mixing with MgATP. When Av2 or a mixture of Av1 and Av2 was made dithionite-free, as described in Materials and Methods, it was measured spectrophotometrically that at least 80% of the Av2 present is oxidized at the time of the experiment. It is thought that this is caused by the process of spontaneous oxidation or self-oxidation of Av2 as described by Watt et al. (1986). With EPR measurements it was found that in dithionite-free Av1 the P-clusters are not oxidized to the $S = 3$ spin state (Pierik et al., 1993), and that FeMoco is not oxidized (data not shown). Therefore, the dithionite-free nitrogenase proteins were reduced with various amounts of dithionite just before the experiment and subsequently mixed with MgATP.

Reduction of Av2 by low dithionite concentrations causes a decrease of the amplitude of the MgATP-dependent proton production. It was observed that 25 or 50 μM dithionite added to the protein solution gave, within the experimental error, similar electron transfer and proton production curves. In case of the dithionite-free nitrogenase complex the proton production curve fitted to: $\Delta A_{572} = 0.034 \cdot \exp(-5.9t) - 0.013t$, so 11.0 μM H^+ were produced in the pre-steady-state phase of the reaction (which corresponds to 2.7 mol H^+ /mol Av1, with $[\text{Av1}] = 4 \mu\text{M}$); when 50 μM dithionite was added to the nitrogenase proteins the proton production curve fitted to: $\Delta A_{572} = 0.014 \cdot \exp(-10.3t) - 0.033t$, corresponding to 4.5 μM H^+ produced during the pre-steady-state (and 1.1 mol H^+ /mol Av1).

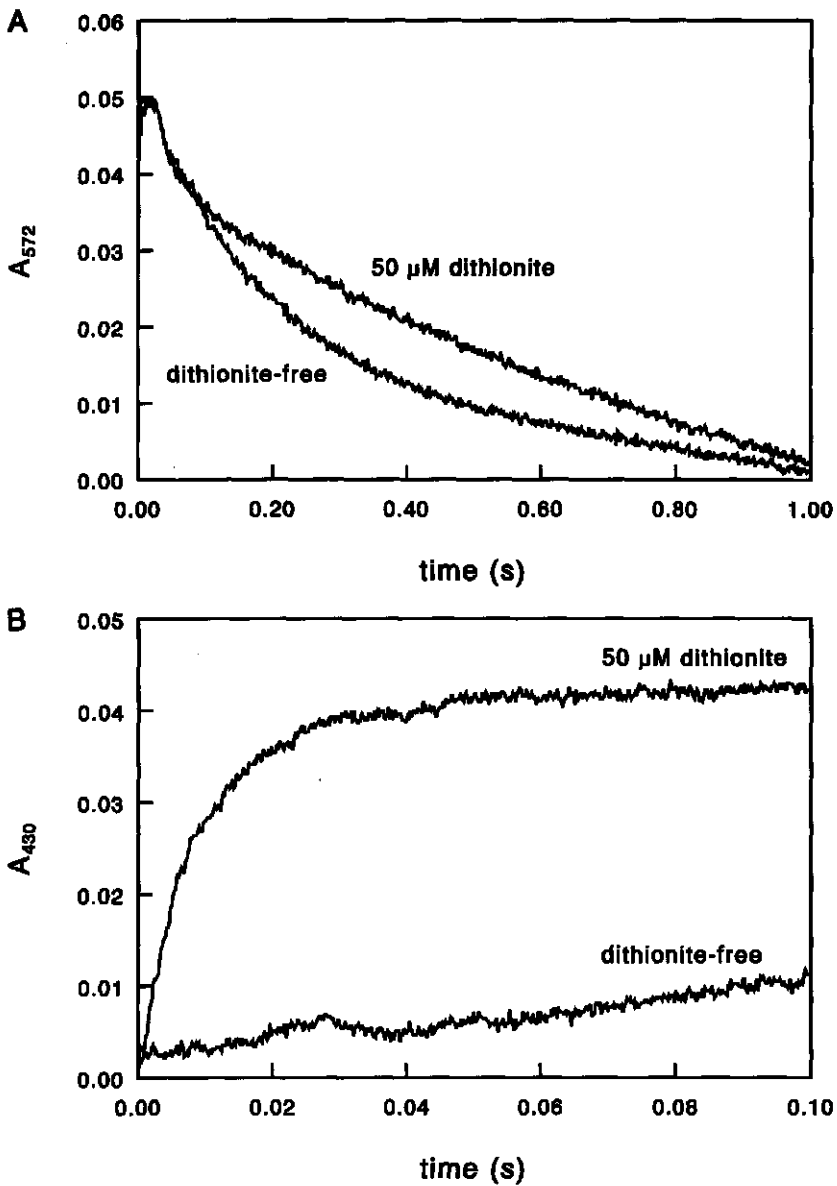


Figure 3. Reactions of dithionite-free nitrogenase proteins with MgATP compared with reactions of 50 μ M dithionite reduced nitrogenase proteins with MgATP. (A) Proton production (A_{572}). (B) Electron transfer (A_{430}). Syringe one: $[Av1] = 8 \mu$ M, $[Av2] = 48 \mu$ M, 10 mM $MgCl_2$ and 1 mM Tes/NaOH, pH 7.8. To acquire the traces labelled 'dithionite-free' and '50 μ M dithionite', no dithionite and 50 μ M dithionite, respectively, was added to the protein solution. Syringe two: 10 mM ATP, 10 mM $MgCl_2$ and 1 mM Tes/NaOH, pH 7.8. For measurement of proton production (A) 100 μ M cresol red was added to the protein solution.

Measurements at 430 nm (see Figure 3B) showed almost no absorbance changes after mixing of the dithionite-free nitrogenase proteins with MgATP. When the dithionite-free nitrogenase complex was reduced with 50 μM dithionite electron transfer took place with an absorbance amplitude $\Delta A_{430} = 0.039$ (which corresponds to the transfer of 8.0 μM electrons, or 2.0 mol electrons/mol Av1) and rate constant $k_{\text{obs}} = 113 \text{ s}^{-1}$.

Table 1. Absorbance changes ΔA_{430} and ΔA_{572} after mixing of dithionite-free and dithionite (50 μM) reduced nitrogenase proteins with MgATP.

| | $[\text{Na}_2\text{S}_2\text{O}_4]$ (μM) | ΔA_{430} | $[\text{e}^-]$ (μM) | ΔA_{572} | $[\text{H}^+]$ (μM) | $\Delta[\text{H}^+]$ (μM) | $[\text{e}^-]/\Delta[\text{H}^+]$ |
|-------|--|------------------|-------------------------------------|------------------|-------------------------------------|---|-----------------------------------|
| exp.1 | - | - | - | 0.034 | 11.0 | - | - |
| | 50 | 0.039 | 8.0 | 0.014 | 4.5 | 6.5 | 1.2 |
| exp.2 | - | - | - | 0.034 | 11.0 | - | - |
| | 25 | 0.027 | 5.6 | 0.021 | 6.8 | 4.2 | 1.3 |
| | 50 | 0.026 | 5.4 | 0.017 | 5.5 | 5.5 | 1.0 |

$[\text{Na}_2\text{S}_2\text{O}_4]$: amount of dithionite added to the nitrogenase proteins; $[\text{e}^-]$: amount of electrons transferred; $[\text{H}^+]$: amount of protons produced (calculated from the amplitude of the single exponential fit); $\Delta[\text{H}^+] = [\text{H}^+]_{\text{dithionite-free}} - [\text{H}^+]_{\text{dithionite}}$ (the difference between proton production by dithionite-free nitrogenase proteins and proton production by reduced nitrogenase proteins). In experiment 1 (exp. 1), one syringe contained: $[\text{Av1}] = 8 \mu\text{M}$, $[\text{Av2}] = 48 \mu\text{M}$. The other syringe contained 10 mM ATP; both syringes contained 10 mM MgCl_2 and 1 mM Tes/NaOH , pH 7.8; 100 μM cresol red was added to the protein solution for measurement of proton production. In experiment 2, one syringe contained: $[\text{Av1}] = 7 \mu\text{M}$, $[\text{Av2}] = 42 \mu\text{M}$. The other syringe contained 10 mM ATP; both syringes contained 10 mM MgCl_2 and 1 mM Tes/NaOH , pH 7.8; 100 μM cresol red was added to the protein solution for measurement of proton production.

MgATP-dependent proton production by Av2 and Av1 separately

Mixing of Av1 (plus cresol red) with MgATP did not lead to any absorbance changes of the pH indicator. It was observed that mixing of dithionite-free (= oxidized) Av2 or Av2 reduced with 50 μM dithionite with MgATP, did not lead to significant proton production. Also at 430 nm almost no absorbance changes were observed. Data not shown.

Summarized, our data show that pre-steady-state proton production by the nitrogenase complex is determined by the redox state of the Fe protein before mixing with MgATP. From two different stopped-flow experiments, it was calculated that the electron transfer as measured by the absorbance increase at 430 nm, divided by the observed decrease in the pre-steady-state burst proton production ($[\text{H}^+]_{\text{dithionite-free}} - [\text{H}^+]_{\text{dithionite}}$) is 1.2 ± 0.2 (see Table 1).

Dependence of MgADP-induced proton production on the redox state of Av2

The pre-steady-state proton production induced by MgADP also depends on the redox state of Av2, see Figure 4A. The dithionite-free nitrogenase proteins were reduced with several concentrations of dithionite and after that mixed with MgADP. When the dithionite-free nitrogenase proteins were mixed with MgADP, hardly any proton production was observed. An increase of the amount of dithionite added to the nitrogenase solution resulted in a larger absorbance decrease after mixing with MgADP: when the complex was reduced with 50 μM dithionite the absorbance decrease was $\Delta A_{572} = 0.053$ (amplitude of single exponential fit), which corresponds to the production of 17.1 μM H^+ , and 3.1 mol H^+ /mol Av1 ($[\text{Av1}] = 5.5 \mu\text{M}$), or 0.5 mol H^+ /mol Av2 ($[\text{Av2}] = 33 \mu\text{M}$). No significant absorbance changes were observed at 430 nm (data not shown).

MgADP-dependent proton production of Av2 and Av1 separately

Proton production was also observed when Av2 was mixed with MgADP, see Figure 4B. There is a large similarity with the MgADP-dependent proton production of the nitrogenase proteins: when dithionite-free Av2 was mixed with MgADP, hardly any proton production was observed; when Av2 was reduced, proton production took place after mixing with MgADP. When 50 μM dithionite was added to the Av2 solution, the absorbance decrease was $\Delta A_{572} = 0.016$, which corresponds to 3.9 μM H^+ produced, and 0.17 mol H^+ /mol Av2 ($[\text{Av2}] = 23 \mu\text{M}$). At 430 nm hardly any absorbance changes were observed (data not shown).

Mixing of Av1 (plus cresol red) with MgADP did not lead to any absorbance changes of the pH indicator (data not shown).

The MgADP-dependent proton production by the nitrogenase proteins and by Av2 alone is also determined by the redox state of the Fe protein before mixing with MgADP. When Av2 is reduced, the observed proton production is larger.

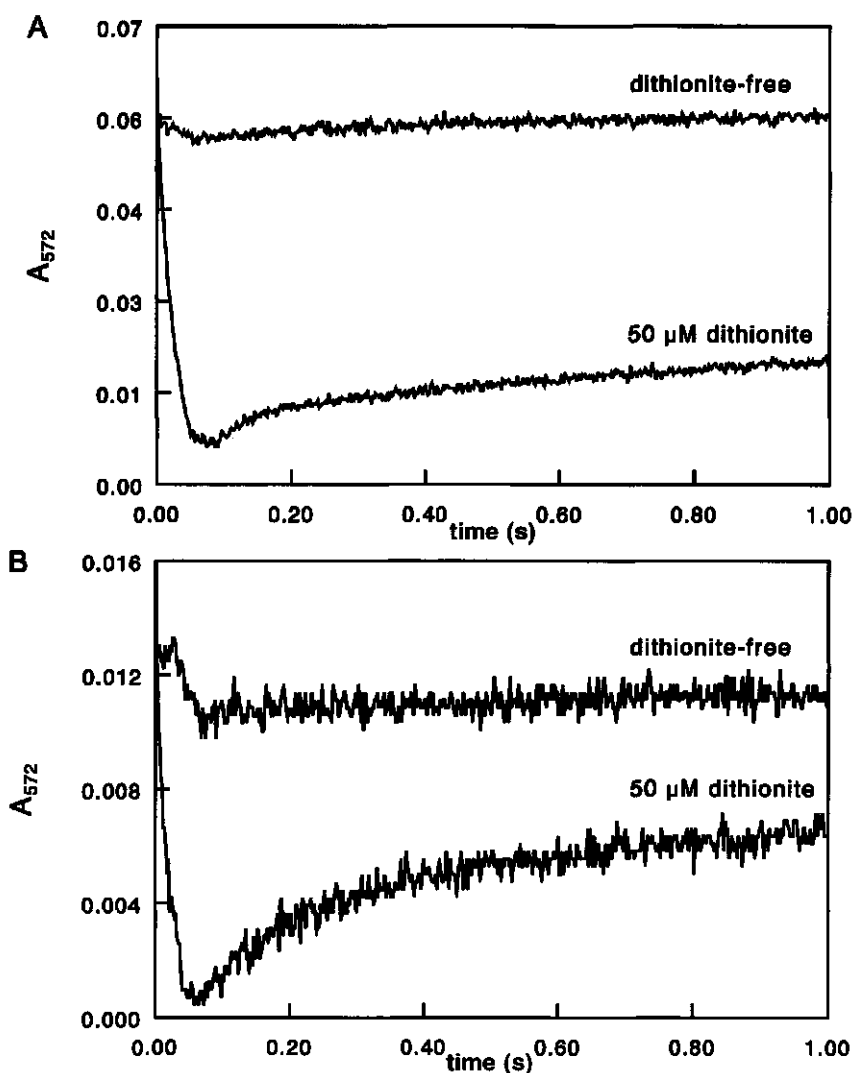


Figure 4. Reaction of dithionite-free nitrogenase proteins with MgADP compared with the reaction of 50 μ M dithionite reduced nitrogenase proteins with MgADP (A), and reaction of dithionite-free Av2 with MgADP compared with the reaction of 50 μ M dithionite reduced Av2 with MgADP (B). (A) Syringe one: [Av1] = 11 μ M, [Av2] = 66 μ M, 10 mM MgCl_2 and 1 mM Tes/NaOH, pH 7.8. To acquire the traces labelled 'dithionite-free' and '50 μ M dithionite', no dithionite and 50 μ M dithionite, respectively, was added to the protein solution. Syringe two: 10 mM ADP, 10 mM MgCl_2 and 1 mM Tes/NaOH, pH 7.8; 100 μ M cresol red was added to the protein solution. (B) Syringe one: [Av2] = 46 μ M, 10 mM MgCl_2 and 1 mM Tes/NaOH, pH 7.8. To acquire the traces labelled 'dithionite-free' and '50 μ M dithionite', no dithionite and 50 μ M dithionite respectively was added to the protein solution. Syringe two: 10 mM ADP, 10 mM MgCl_2 and 1 mM Tes/NaOH, pH 7.8; 100 μ M cresol red was added to the Av2 solution.

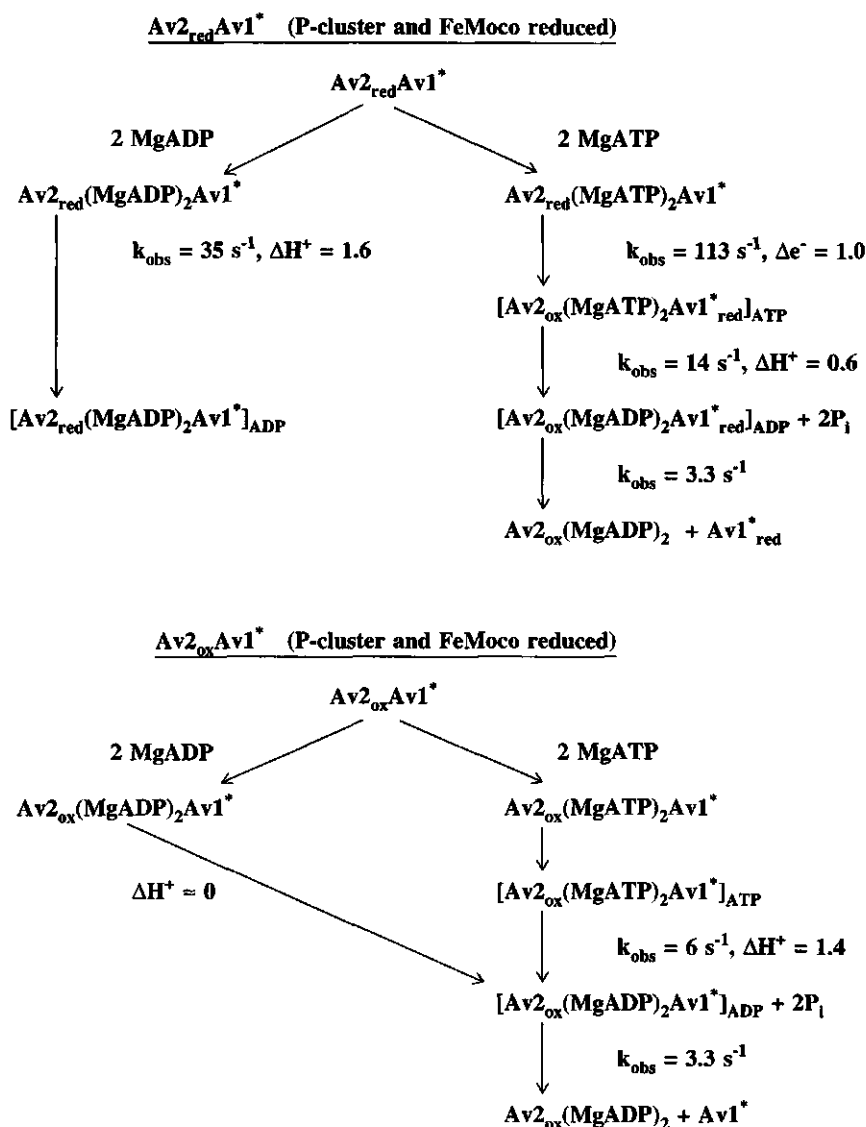
Discussion

The presence of MgATP is an absolute requirement for electron transfer from the Fe protein to the MoFe protein. The binding of MgATP to the nitrogenase complex is a fast process, $k > 5 \cdot 10^7 \text{ M}^{-1} \cdot \text{s}^{-1}$ (Lowe & Thorneley, 1984b); no proton production or uptake during this process can be observed within the time range of stopped-flow measurements. Electron transfer can be measured and is generally thought to be coupled with MgATP hydrolysis. Our data however cannot prove or disprove that on-enzyme MgATP hydrolysis does take place at the same time scale as electron transfer. But our data can exclude the possibility that ATP hydrolysis followed by P_i and H^+ dissociation from the protein complex takes place during electron transfer, because the observed rate constant for electron transfer was $\sim 100 \text{ s}^{-1}$, and no proton production with a comparable or a higher rate constant was observed after mixing of the nitrogenase proteins with MgATP.

The proton production observed after mixing of the nitrogenase proteins with MgATP is a unique property of the nitrogenase complex and not of Av2, since the only reaction of Av2 that leads to proton production is the binding of MgADP to reduced Av2 (see Figure 4B). This reaction will not occur in the part of the catalytic cycle that is studied because, according to our data, protons are produced after electron transfer has taken place, at which time Av2 is already thought to be oxidized.

The next possibility that will be considered to explain the MgATP-induced proton production is a change of the nitrogenase complex to a MgADP conformation. It should be realised that both in the MgATP and MgADP experiments the reaction starts with the 'as isolated' conformation of the protein complex. This means that three conformations of the nitrogenase complex must be considered: an 'as isolated' conformation, a MgATP conformation and a MgADP conformation. The 'as isolated' conformation must be different from the MgATP conformation since electron transfer depends upon the presence of MgATP. Because the binding of MgATP and MgADP to nitrogenase itself occurs within the mixing time of the stopped-flow apparatus, the data acquisition starts with complexes which still might have the 'as isolated' conformation with MgATP/MgADP bound, but not yet changed to their MgATP/MgADP conformation.

The observed proton production traces, induced by MgATP, cannot be the result of a change of the nitrogenase complex in the 'as isolated' conformation to a MgADP conformation, since the only reaction of the nitrogenase complex with MgADP that produced protons is the reaction of the reduced complex with MgADP, but this reaction does not occur in the catalytic cycle. A possible explanation for the MgATP-induced proton production might be a conformational change of the nitrogenase complex from the MgATP conformation to the MgADP conformation.



Scheme 1. Pre-steady-state reactions of nitrogenase with MgATP and MgADP. Av1^* represents one of two independently functioning halves of the tetrameric MoFe protein of nitrogenase. Each Av1^* is assumed to contain one FeMo cofactor and one Av2 binding site. $[\text{Av2}(\text{MgATP})_2\text{Av1}^*]_{\text{ATP}}$: nitrogenase protein complex in the MgATP conformation; $[\text{Av2}(\text{MgADP})_2\text{Av1}^*]_{\text{ADP}}$: nitrogenase protein complex in the MgADP conformation; $\text{Av1}^*_{\text{red}}$: Av1^* with a super-reduced FeMo cofactor. The amount of electrons (Δe^-) transferred and the amount of protons (ΔH^+) produced are expressed per Av1^* .

The amount of protons produced in the reaction of MgATP with the nitrogenase complex depends on the redox state of Av2 before mixing with MgATP. It was calculated (see Table 1) that the amount of electrons transferred, divided by the observed decrease in the pre-steady-state proton production ($[H^+]_{\text{dithionite-free}} - [H^+]_{\text{dithionite}} \approx 1$). The difference between the proton production of oxidized Av2 and reduced Av2 (in the nitrogenase complex) might be explained by the assumption that electron transfer from the Fe protein to the MoFe protein is coupled with uptake of protons (after a constant phase), in the ratio: one proton taken up per one electron transferred. Also the observed rate constant of the pre-steady-state proton production by the nitrogenase complex is determined by the redox state of Av2; when Av2 was reduced, the rate of proton production was faster than in case of oxidized Av2.

We suggest that the following events occur when the nitrogenase complex is mixed with MgATP (see Scheme 1). When the nitrogenase proteins are mixed with MgATP, MgATP binds to the protein complex within the mixing time of the stopped-flow apparatus (Lowe & Thorneley, 1984b). After MgATP binding the protein complex changes to the MgATP conformation ($[Av2_{\text{red}}(MgATP)_2Av1^*]_{\text{ATP}}$), followed by a rapid electron transfer ($k_{\text{obs}} \approx 100 \text{ s}^{-1}$) ($[Av2_{\text{ox}}(MgATP)_2Av1^*]_{\text{ATP}}$). This reaction is not associated with a net proton production. No data are available about the molecular events that facilitate this reaction. After electron transfer MgATP is hydrolysed and the protein complex changes its conformation to the MgADP conformation ($[Av2_{\text{ox}}(MgADP)_2Av1^*]_{\text{ADP}}$). This reaction is associated with a net proton production ($k_{\text{obs}} \approx 14 \text{ s}^{-1}$). It is also possible that the proton production is caused by dissociation of P_i from the protein complex. Our experiments cannot prove or disprove this possibility. The protein complex in the MgADP conformation dissociates with a rate of 3.3 s^{-1} . This reaction is supposed to be the rate-limiting step of the Fe protein cycle and has been determined from the steady-state rate under optimal conditions with saturating reductant (5 mM dithionite plus 100 μM flavodoxin). After reduction of the Fe protein and exchange of MgADP for MgATP both proteins can enter the Fe protein cycle again.

In the case of electron transfer a stoichiometric amount of protons stays at the protein complex. It is postulated by us that the reducing equivalents stored in the MoFe protein are present as H-atoms.

Hydrolysis of MgATP to MgADP and P_i , or the release of P_i from the nitrogenase complex after the change of the protein conformation, might be a requirement for dissociation of the nitrogenase complex. The mechanism of action of MgATP hydrolysis by nitrogenase resembles the mechanisms of action of molecular switch proteins, like MgATP hydrolysis by the muscle protein myosin (Rayment et al., 1993a,b) and recA protein (Story & Steitz, 1992), and MgGTP hydrolysis by the guanosine triphosphatase

proteins (Milburn et al., 1990; Pai et al., 1990; Bourne et al., 1991) (like the elongation factor EF-Tu (Bourne et al., 1991) and the before mentioned H-Ras p21 protein (Georgiadis et al., 1992; Wolle et al., 1992)), in this respect that they have in common the use of nucleotide hydrolysis as a kinetic mechanism to temporary switch between two different conformations.

Acknowledgements

We thank Prof. C. Veeger for critically reading the manuscript, Dr. A. J. Pierik for performing the EPR measurements and Dr. S. P. J. Albracht for providing access to the parallel-mode EPR facility at the E. C. Slater Institute for Biochemical Research, University of Amsterdam. This investigation was supported by the Netherlands Foundation for Chemical Research (SON) with financial aid from the Netherlands Organization for Scientific Research (NWO) and by the Commission of the European Communities in the framework of the program 'Stimulation of European Cooperation and Scientific and Technical Interchange' SC1-0179-C(TT).

References

- Ashby, G. A. & Thorneley, R. N. F. (1987) Nitrogenase of *Klebsiella pneumoniae*. Kinetic studies on the Fe protein involving reduction by sodium dithionite, the binding of MgADP and a conformation change that alters the reactivity of the 4Fe-4S centre, *Biochem. J.* 246, 455-465.
- Bensadoun, A. & Weinstein, D. (1976) Assay of proteins in the presence of interfering materials, *Anal. Biochem.* 70, 241-250.
- Bourne, H. R., Sanders, D. A. & McCormick, F. (1991) The GTPase superfamily: conserved structure and molecular mechanism, *Nature* 349, 117-127.
- Braaksma, A., Haaker, H., Grande, H. J. & Veeger, C. (1982) The effect of the redox potential on the activity of the nitrogenase and on the Fe protein of *Azotobacter vinelandii*, *Eur. J. Biochem.* 121, 483-491.
- Burris, R. H. (1991) Nitrogenases, *J. Biol. Chem.* 266 (15), 9339-9342.
- Chan, M. K., Kim, J. & Rees, D. C. (1993) The nitrogenase FeMo-cofactor and P-cluster pair: 2.2 Å resolution structures, *Science* 260, 792-794.
- Cordewener, J., ten Asbroek, A., Wassink, H., Eady, R., Haaker, H. & Veeger, C. (1987) Binding of ADP and orthophosphate during the ATPase reaction of nitrogenase, *Eur. J. Biochem.* 162, 265-270.
- Dean, D. R., Bolin, J. T. & Zheng, L. (1993) Nitrogenase metallocusters: structures, organization, and synthesis, *J. Bact.* 175, 6737-6744.
- Georgiadis, M. M., Komiya, H., Chakrabarti, P., Woo, D., Kornuc, J. J. & Rees, D. C. (1992) Crystallographic structure of the nitrogenase iron protein from *Azotobacter vinelandii*, *Science* 257, 1653-1659.
- Goa, J. (1953) A micro biuret method for protein determination. Determination of total protein in cerebrospinal fluid, *Scand. J. Clin. Lab. Invest.* 5, 218-222.
- Hagen, W. R., Eady, R. R., Dunham, W. R. & Haaker, H. (1985) A novel $S = 3/2$ EPR signal

- associated with native Fe-proteins of nitrogenase, *FEBS Lett.* 189, 250-254.
- Hagen, W. R., Wassink, H., Eady, R. R., Smith, B. E. & Haaker, H. (1987) Quantitative EPR of an $S = 7/2$ system in thionine-oxidized MoFe proteins of nitrogenase. A redefinition of the P-cluster concept, *Eur. J. Biochem.* 169, 457-465.
- Kim, J. & Rees, D. C. (1992a) Structural models for the metal centers in the nitrogenase molybdenum-iron protein, *Science* 257, 1677-1682.
- Kim, J. & Rees, D. C. (1992b) Crystallographic structure and functional implications of the nitrogenase molybdenum-iron protein from *Azotobacter vinelandii*, *Nature* 360, 553-560.
- Lowe, D. J., Fisher, K. & Thorneley, R. N. F. (1993) *Klebsiella pneumoniae* nitrogenase: pre-steady-state absorbance changes show that redox changes occur in the MoFe protein that depend on substrate and component ratio; a role for P-centres in reducing dinitrogen?, *Biochem. J.* 292, 93-98.
- Lowe, D. J. & Thorneley, R. N. F. (1984a) The mechanism of *Klebsiella pneumoniae* nitrogenase action. Pre-steady-state kinetics of H_2 formation, *Biochem. J.* 224, 877-886.
- Lowe, D. J. & Thorneley, R. N. F. (1984b) The mechanism of *Klebsiella pneumoniae* nitrogenase action. The determination of rate constants required for the simulation of the kinetics of N_2 reduction and H_2 evolution, *Biochem. J.* 224, 895-901.
- Mensink, R. E. & Haaker, H. (1992) Temperature effects on the MgATP-induced electron transfer between the nitrogenase proteins from *Azotobacter vinelandii*, *Eur. J. Biochem.* 208, 295-299.
- Mensink, R. E., Wassink, H. & Haaker, H. (1992) A reinvestigation of the pre-steady-state ATPase activity of the nitrogenase from *Azotobacter vinelandii*, *Eur. J. Biochem.* 208, 289-294.
- Milburn, M. V., Tong, L., deVos, A. M., Brünger, A., Yamaizumi, Z., Nishimura, S. & Kim, S.-H. (1990) Molecular switch for signal transduction: structural differences between active and inactive forms of protooncogenic *ras* proteins, *Science* 247, 939-945.
- Miller, R. W., Smith, B. E. & Eady, R. R. (1993) Energy transduction by nitrogenase: binding of MgADP to the MoFe protein is dependent on the oxidation state of the iron-sulphur 'P' clusters, *Biochem. J.* 291, 709-711.
- Pai, E. F., Krengel, U., Petsko, G. A., Goody, R. S., Kabsch, W. & Wittinghofer, A. (1990) Refined crystal structure of the triphosphate conformation of H-ras p21 at 1.35 Å resolution: implications for the mechanism of GTP hydrolysis, *EMBO J.* 9, 2351-2359.
- Pierik, A. J., Wassink, H., Haaker, H. & Hagen, W. R. (1993) Redox properties and EPR spectroscopy of the P clusters of *Azotobacter vinelandii* MoFe protein, *Eur. J. Biochem.* 212, 51-61.
- Rayment, I., Holden, H. M., Whittaker, M., Yohn, C.B., Lorenz, M., Holmes, K. C. & Milligan, R. A. (1993a) Structure of the actin-myosin complex and its implications for muscle contraction, *Science* 261, 58-65.
- Rayment, I., Rypniewski, W. R., Schmidt-Bäse, K., Smith, R., Tomchick, D. R., Benning, M. M., Winkelmann, D. A., Wesenberg, G. & Holden, H. M. (1993b) Three-dimensional structure of myosin subfragment-1: a molecular motor, *Science* 261, 50-58.
- Smith, B. E. & Eady, R. R. (1992) Metalloclusters of the nitrogenases, *Eur. J. Biochem.* 205, 1-15.
- Story, R. M. & Steitz, T. A. (1992) Structure of the recA protein-ADP complex, *Nature* 355, 374-376.
- Thorneley, R. N. F., Ashby, G., Howarth, J. V., Millar, N. C. & Gutfreund, H. (1989) A transient kinetic study of the nitrogenase of *Klebsiella pneumoniae* by stopped-flow calorimetry. Comparison with the myosin ATPase, *Biochem. J.* 264, 665-661.
- Thorneley, R. N. F. & Lowe, D. J. (1983) Nitrogenase of *Klebsiella pneumoniae*. Kinetics of the

- dissociation of oxidized iron protein from molybdenum-iron protein: identification of the rate-limiting step for substrate reduction, *Biochem. J.* 215, 393-403.
- Thorneley, R. N. F. & Lowe, D. J. (1985) in *Molybdenum Enzymes* (Spiro, T.G., ed.) pp. 221-284, Wiley and Sons, New York.
- Watt, G. D., Wang, Z.-C. & Knotts, R. R. (1986) Redox reactions of and nucleotide binding to the iron protein of *Azotobacter vinelandii*, *Biochemistry* 25, 8156-8162.
- Wolfe, D., Dean, D. R. & Howard, J. B. (1992) Nucleotide-iron-sulfur cluster signal transduction in the nitrogenase iron-protein: the role of Asp¹²⁵, *Science* 258, 992-995.

Chapter 3

Formation and characterization of a transition state complex of *Azotobacter vinelandii* nitrogenase

Abstract

A stable complex is formed between the nitrogenase proteins of *Azotobacter vinelandii*, aluminium fluoride and MgADP. All nitrogenase activities are inhibited. The complex formation was found to be reversible. An incubation at 50 °C recovers nitrogenase activity. The complex has been characterized with respect to protein and nucleotide composition and redox state of the metal-sulphur clusters. Based on the inhibition by aluminium fluoride together with MgADP, it is proposed that a stable transition state complex of nitrogenase is isolated.

Introduction

In the presence of MgATP and a strong reductant, nitrogenase catalyses the reduction of dinitrogen to ammonia (Hardy & Burns, 1968; Howard & Rees, 1994). The enzyme consists of two proteins: the MoFe protein (Av1), an $\alpha_2\beta_2$ -tetramer of 230 kDa, and the Fe protein (Av2), a γ_2 -dimer of 63 kDa. Each (independently functioning) $\alpha\beta$ -half of the MoFe protein contains an Fe protein binding site and two metal-sulphur clusters: the FeMo cofactor (FeMoco) and the P-cluster (Hagen et al., 1987; Kim & Rees, 1992). The Fe protein contains a single [4Fe-4S] cluster and two binding sites for MgATP or MgADP (Georgiadis et al., 1992).

The generally accepted model for the reduction of dinitrogen by nitrogenase, proposed by Thorneley and Lowe, consists of two electron transfer cycles (Lowe & Thorneley, 1984). In the Fe protein cycle the reduced Fe protein (with MgATP bound) and the MoFe protein associate which yields the active nitrogenase complex. In the nitrogenase complex a single electron is transferred from the Fe protein to the MoFe protein and MgATP is hydrolysed. Hereafter the nitrogenase complex dissociates

into the separate nitrogenase proteins: this is the rate-limiting step of the cycle (Thorneley & Lowe, 1983). Subsequently the Fe protein is reduced first by the present reductant, after which MgADP is rapidly replaced by MgATP, to complete the Fe protein cycle. For the reduction of N_2 to $2 NH_3$ and H_2 (the inevitable side product of the nitrogenase reaction), the MoFe protein must be stepwise reduced in eight consecutive Fe protein cycles: this is described in the MoFe protein cycle (Lowe & Thorneley, 1984).

In order to explain and to be able to simulate the observation that the measured specific H_2 production activity of the *Klebsiella pneumoniae* Fe protein, Kp2, is only 45% of the calculated maximum specific activity, Thorneley and Lowe (1984) assumed that only 45% of all Kp2 present is active. The remaining 55% of total Kp2 is considered to be inactive with respect to electron transfer to Kp1, but is still capable of binding to Kp1 (with lower rate constants for binding to and dissociation from Kp1 than active Kp2 (Thorneley & Lowe, 1984)). This assumption also explains the observation that a ratio $[Kp2]/[Kp1] \geq 4.5$ is needed to obtain maximum electron transfer from the Fe protein to the MoFe protein: if all Kp2 would be active a ratio $[Kp2]/[Kp1] = 2$ would be sufficient (Ashby & Thorneley, 1987).

A close structural similarity between the nucleotide binding sites of Av2 and the H-Ras p21 protein was found (Georgiadis et al., 1992; Howard & Rees, 1994). A comparison between the mechanism of MgATP hydrolysis dependent electron transfer by nitrogenase and the mechanisms of action of molecular switch proteins like the GTPases and the muscle protein myosin was made. Like these proteins nitrogenase could be using nucleotide binding and hydrolysis as a kinetic mechanism in order to switch between different conformations of the protein.

Aluminium fluoride acts as an analogue of phosphate for various GTPases and ATPases, when GDP/ADP is present (Chabre, 1990). The crystal structures of transducin α complexed with MgGDP and aluminium fluoride (1.7 Å resolution) (Sondek et al., 1994), myosin II (*Dictyostelium discoideum*) complexed with MgADP and aluminium fluoride (2.6 Å) (Fisher et al., 1995) and the α -subunit of the G protein G_{i1} complexed with MgGDP and aluminium fluoride (2.2 Å) (Coleman et al., 1994), revealed that in all of these cases GDP/ADP \cdot aluminium fluoride is a transition state analogue of GTP/ATP, rather than an analogue of either the state before (GTP/ATP) or after hydrolysis (GDP/ADP $\cdot P_i$) of GTP/ATP. Aluminium fluoride occupies the position normally filled by the γ -phosphate of GTP/ATP. In contrast to the tetrahedral geometry of a phosphate group the aluminium is octahedrally coordinated to four fluoride ions (in the equatorial plane) and one of the oxygens of the β -phosphate and presumably one oxygen from a water molecule as the axial ligands. This structure resembles the pentacoordinated structure which the γ -phosphate transiently adopts during the transition

state of the hydrolysis of GTP/ATP (Chabre, 1990; Coleman et al., 1994; Sondek et al., 1994; Fisher et al., 1995).

In this paper it is shown that aluminium fluoride together with MgADP inhibits nitrogenase from *A. vinelandii* by stabilizing the normally transient protein complex, which is temporary formed during the Fe protein cycle. The stability and the composition of the nitrogenase · ADP · aluminium fluoride complex were investigated.

Materials and Methods

Azotobacter vinelandii ATCC strain 478 was grown and the nitrogenase component proteins were purified as described elsewhere (Duyvis et al., 1994). Protein concentrations were estimated by the microbiuret method after a precipitation step with deoxycholic acid and trichloroacetic acid (Duyvis et al., 1994). The molar concentrations of Av1 and Av2 were calculated from their molecular masses, 230 Kda and 63 Kda, respectively. Av1 contained 1.8 ± 0.2 Mo/mol Av1; the iron content of the Fe protein was 3.6 ± 0.3 mol Fe/mol Av2 (Duyvis et al., 1994).

The acetylene reduction activity (at 30 °C) of the nitrogenase proteins was determined as described elsewhere (Duyvis et al., 1994). The specific activity of each of the nitrogenase proteins was calculated from the maximum acetylene reduction rate, which was obtained at an optimum [Av2]/[Av1] ratio. Thus, for measurement of the specific activity of Av1, a 10-fold amount of Av2 was added to the reaction mixture. For measurement of the specific activity of Av2, the ratio [Av1]/[Av2] was varied at constant [Av2]; the maximum acetylene reduction rate obtained from this titration (usually at [Av1]/[Av2] \approx 1.5) yielded the specific activity of Av2. The specific activities of Av1 and Av2 were at least 8 mol ethylene produced \cdot s⁻¹ \cdot (mol Av1)⁻¹ and 2 mol ethylene produced \cdot s⁻¹ \cdot (mol Av2)⁻¹, respectively. To investigate the effect of MgADP and aluminium fluoride on the activity of nitrogenase, 1 mM ADP, 1.5 mM MgCl₂, 0.7 mM aluminium fluoride (AlF₃·H₂O) and 7.0 mM KF (in order to dissolve AlF₃·H₂O and obtain AlF₄⁻ the presence of excess F⁻ is required) was added to the incubation mixture; extra P_i (20 mM) was added during the activity measurements.

The ATPase activity of the nitrogenase complex as a function of the ratio [Av2]/[Av1] (Figure 1) was determined under the same conditions as the measurement of the Av1 activity. Samples were taken from the reaction mixture and assayed for creatine by a slightly modified version of the method of Ennor (1957).

For the measurements of electron transfer from Av2 to Av1 a HI-TECH SF-51 stopped-flow spectrophotometer (Salisbury, Wilts, U. K.), equipped with an anaerobic kit and a data acquisition and analysis system, was used. The absorbance changes at 430 nm

were measured. One syringe of the stopped-flow apparatus contained 20 μM Av1 and Av2 in the indicated concentration. To investigate the effect of ADP and aluminium fluoride on the electron transfer 1 mM AlF_4^- (+ 10 mM KF), 1 mM ADP or both were added to this solution. The other syringe contained 10 mM ATP. Both syringes contained 10 mM MgCl_2 , 100 mM NaCl, 5 mM sodium dithionite and 50 mM Tes/NaOH, pH 7.4. The reaction temperature was 22.0 ± 0.1 °C.

The amount of ADP bound in the nitrogenase \cdot ADP \cdot aluminium fluoride complex was measured after addition of HClO_4 (10%) to the complex. After neutralization with KHCO_3 , ADP was converted into ATP using pyruvate kinase (EC 2.7.1.40) and phosphoenolpyruvate. ATP was determined using a bioluminescence assay with luciferin and luciferase (EC 1.13.12.7). The intensity of the emitted light which was liberated by the luciferase reaction was directly proportional to the ATP concentration. An internal standard of ATP was employed to correct for inhibition of luciferase and for emission interference by compounds present in the incubation mixture.

The amounts of Av2 and Av1 present in the nitrogenase \cdot ADP \cdot AlF_4^- complex were determined by a quantitative ELISA (Enzyme Linked ImmunoSorbent Assay) determination, using antibodies against Av1 and Av2, respectively. Purified Av1 and Av2 were used for calibration.

EPR spectra were obtained with a Bruker EPR-200 D spectrometer, with peripheral instrumentation and data acquisition as described elsewhere (Pierik et al., 1993). The concentrations in the EPR sample were: 9 mg protein/ml nitrogenase \cdot ADP \cdot AlF_4^- complex, 2 mM sodium dithionite and 500 mM NaCl in 50 mM Tes/NaOH, pH 7.4. The EPR conditions for the measurements of the FeMoco $S = 3/2$ signal and the signals of oxidized P-clusters were as described by Pierik et al. (1993) and the EPR conditions for the measurements of the Av2 $S = 1/2$ and $S = 3/2$ signals were as described by Hagen et al. (1985).

All buffers used were saturated with argon. ATP (special quality) and ADP, creatine kinase, creatine phosphate and the ATP bioluminescence assay kit were obtained from Boehringer, aluminium fluoride monohydrate ($\text{AlF}_3 \cdot \text{H}_2\text{O}$) from Janssen Chimica.

Results and Discussion

Inhibition of nitrogenase activity by MgADP and aluminium fluoride

The effect of AlF_4^- and MgADP on the nitrogenase activity was investigated, see Table 1. After 5 minutes incubation of the nitrogenase proteins (as indicated) the activity was measured.

Incubation of the nitrogenase proteins ($[Av2]/[Av1] = 3$) with MgADP or P_i did not affect the activity of Av1 and Av2. When the nitrogenase proteins were incubated with both MgADP and AlF_4^- , acetylene reduction was almost completely inhibited. Addition of P_i together with AlF_4^- to the nitrogenase proteins prevented the inhibition of the activity by MgADP and AlF_4^- . This indicates that P_i and AlF_4^- bind at the same position to nitrogenase. When P_i was added after 5 minutes incubation of the nitrogenase proteins with MgADP and AlF_4^- , acetylene reduction was still almost completely inhibited, which shows that P_i cannot exchange with AlF_4^- once MgADP and AlF_4^- are bound to the nitrogenase complex.

Also when excess Av2 ($[Av2]/[Av1] = 10$) was present during incubation with MgADP and AlF_4^- , acetylene reduction was completely inhibited (data not shown). When after the incubation extra Av2 (8.0 μ M) and P_i (20 mM) were added, also no activity was observed, indicating that all Av1 was present in the inhibited nitrogenase \cdot ADP \cdot AlF_4^- complex. It was checked whether Av2 was not inactivated during the incubation with MgADP and AlF_4^- . When after the incubation of the nitrogenase proteins ($[Av2]/[Av1] = 10$) with MgADP and AlF_4^- the original amount of Av1 (0.8 μ M) and P_i (20 mM) were added, nitrogenase activity was observed. This activity corresponded to the nitrogenase activity normally found when $[Av2]/[Av1] = 5$. This indicates that the free Av2 (not bound in the nitrogenase \cdot ADP \cdot AlF_4^- complex) was not inhibited by MgADP and AlF_4^- during the incubation.

Table 1. Inhibition of the acetylene reduction activity of nitrogenase by aluminium fluoride and MgADP.

| Experiment | Additions | Specific activity (%) |
|------------|-----------------------------|-----------------------|
| 1 | - | 100 |
| 2 | P_i | 100 |
| 3 | AlF_4^- | 2 |
| 4 | $AlF_4^- + P_i$ | 100 |
| 5 | AlF_4^- , after 5': P_i | 3 |

The nitrogenase proteins ($[Av1] = 0.8 \mu$ M; $[Av2] = 2.4 \mu$ M) were incubated with ADP (1 mM), $MgCl_2$ (1.5 mM), sodium dithionite (16 mM) and Tes/NaOH (50 mM), pH 7.4, at room temperature for 5 minutes. If present in the incubation mixture: $[AlF_4^-] = 0.7$ mM (plus 7 mM KF) and $[P_i] = 20$ mM. The acetylene reduction activity (at 30 °C) of Av1 was measured without addition of extra Av2. In the absence of aluminium fluoride, at a ratio $[Av2]/[Av1] = 3$, the activity was $100\% = 3.1 \text{ mol } C_2H_4 \text{ produced} \cdot s^{-1} \cdot (\text{mol } Av1)^{-1}$.

Stopped-flow measurements showed that incubation of the nitrogenase proteins with only AlF_4^- before mixing with MgATP did not affect the pre-steady-state MgATP-induced electron transfer reaction. This indicates that AlF_4^- does not rapidly bind and inhibit nitrogenase before MgATP hydrolysis. When the nitrogenase proteins were incubated with both MgADP and AlF_4^- , no electron transfer was observed after mixing with MgATP (data not shown).

The results show that AlF_4^- and MgADP together inhibit the overall nitrogenase activity and the pre-steady-state electron transfer reaction. Addition of MgATP or P_i does not reverse the inhibition. Since both Av2 and Av1 are involved in the inhibition, it seems likely that AlF_4^- and MgADP stabilize a normally transient nitrogenase complex; for catalysis association of Av2 and Av1 and dissociation of the nitrogenase complex are required (Fe protein cycle) (Thorneley & Lowe, 1983; Lowe & Thorneley, 1984).

Inhibition of nitrogenase activity as a function of $[\text{Av2}]/[\text{Av1}]$

In Figure 1 the amplitude of the absorbance increase (430 nm) associated with the MgATP-induced pre-steady-state electron transfer reaction from Av2 to Av1 is shown as a function of the ratio $[\text{Av2}]/[\text{Av1}]$. No MgADP and AlF_4^- were present in the reaction mixture. The absorbance amplitude ($\Delta A_{430} = 0.102$) was maximal when $[\text{Av2}]/[\text{Av1}] \geq 4.5$. Similar data were observed for *K. pneumoniae* nitrogenase by Ashby and Thorneley (1987), and were explained by the assumption that only 45% of the Fe protein is active with respect to electron transfer (Thorneley & Lowe, 1984). The observed rate constant of electron transfer was independent of the ratio $[\text{Av2}]/[\text{Av1}]$: $k_{\text{obs}} \approx 120 \text{ s}^{-1}$ (data not shown).

In the same figure the acetylene reduction activity and the ATPase activity of the nitrogenase complex in the presence of AlF_4^- and MgADP at various $[\text{Av2}]/[\text{Av1}]$ are shown. After 20 minutes incubation of the nitrogenase proteins with MgADP and AlF_4^- , excess Av2 (10-fold $[\text{Av1}]$) and P_i (20 mM) were added to the incubation mixture and the activity was measured. No difference was observed between the inhibition of the activity after 10 minutes or 20 minutes incubation at low ratios ($[\text{Av2}]/[\text{Av1}] \leq 2$); at higher ratios an incubation for 5 minutes already yielded the same inhibition as 20 minutes incubation (data not shown). The 100% acetylene reduction activity was determined in an incubation without AlF_4^- and P_i : 6.9 mol ethylene produced $\cdot \text{s}^{-1} \cdot (\text{mol Av1})^{-1}$. Complete inhibition of the specific activity was observed when $[\text{Av2}]/[\text{Av1}] \geq 3$ during the incubation of the samples with AlF_4^- and MgADP. At lower ratios apparently not all Av1 could be bound in the inhibited nitrogenase $\cdot \text{ADP} \cdot \text{AlF}_4^-$ complex.

The ATPase activity of the nitrogenase complex was inhibited by the presence of AlF_4^- and MgADP and followed the same inhibition pattern as the acetylene reduction activity: at ratio $[\text{Av}2]/[\text{Av}1] \geq 3$ MgATP hydrolysis hardly took place any more, see Figure 1.

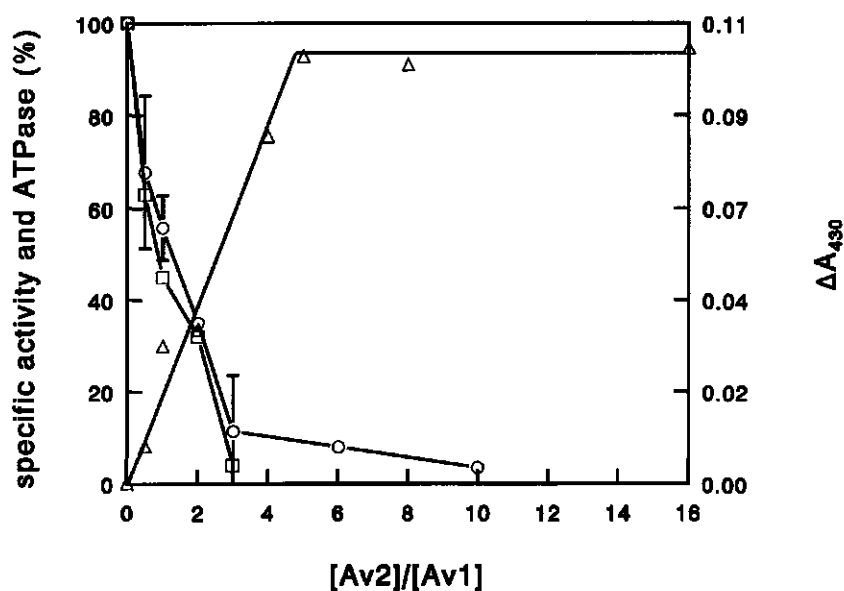


Figure 1. Pre-steady-state electron transfer (ΔA_{430}) as a function of the ratio $[\text{Av}2]/[\text{Av}1]$. The inhibition of the specific (acetylene reduction) activity of Av1 and of the ATPase activity by aluminium fluoride and MgADP, as a function of $[\text{Av}2]/[\text{Av}1]$. Electron transfer (Δ) was measured at 430 nm (ΔA_{430}), in the absence of MgADP and aluminium fluoride. The concentration Av1 after mixing was 10 μM . The acetylene reduction activity (\circ) and ATPase activity (\square) were measured after incubation (at room temperature) of the nitrogenase proteins with aluminium fluoride and MgADP. The concentration Av1 was 0.8 μM . The error bars on the acetylene reduction data points show the deviation from the average of three measurements. In the absence of aluminium fluoride and P_i the 100% activity was 6.9 mol C_2H_4 produced $\cdot \text{s}^{-1} \cdot (\text{mol Av}1)^{-1}$ and the 100% ATPase activity was 50.4 mol ADP produced $\cdot \text{s}^{-1} \cdot (\text{mol Av}1)^{-1}$.

Isolation of the nitrogenase $\cdot \text{ADP} \cdot \text{AlF}_4^-$ complex

The nitrogenase proteins ($[\text{Av}2]/[\text{Av}1] = 6$) were incubated with MgADP and AlF_4^- for 10 minutes at room temperature, to form the inhibited nitrogenase $\cdot \text{ADP} \cdot \text{AlF}_4^-$ complex. The protein complex was bound to DEAE cellulose and free MgADP and AlF_4^- were removed by an 80 mM NaCl (plus 2 mM sodium dithionite in 50 mM

Tes/NaOH, pH 7.4) wash procedure. At 300 mM NaCl the nitrogenase \cdot ADP \cdot AlF_4^- complex eluted (which was verified by an ELISA determination) and at 500 mM NaCl free Av2 eluted from the column. The activity of Av1 in the nitrogenase complex after this treatment was 2% of the specific activity in the absence of MgADP and AlF_4^- (6.9 mol ethylene produced \cdot s $^{-1}$ \cdot (mol Av1) $^{-1}$). The specific activity of the free Av2 was 2.0 mol ethylene produced \cdot s $^{-1}$ \cdot (mol Av2) $^{-1}$, which is as high as the specific activity of Av2 before formation of the nitrogenase \cdot ADP \cdot AlF_4^- complex. If the assumption that inactive Av2 binds to Av1 with a 5-fold higher dissociation constant than active Av2, is correct (Thorneley & Lowe, 1984), more active than inactive Av2 would be expected to be bound in the nitrogenase \cdot ADP \cdot AlF_4^- complex, and the specific activity of the free Av2 would be expected to be lower than the obtained value. We conclude that for the formation of the nitrogenase \cdot ADP \cdot AlF_4^- complex all Av2 is equally active.

After preparation of the inhibited nitrogenase \cdot ADP \cdot AlF_4^- complex, attempts were made to reactivate the protein complex and to measure the specific activity of the nitrogenase proteins. The results are given in Table 2.

Addition of MgCl_2 (10 mM), P_i (20 mM) and NaCl (0.64 M) to the nitrogenase \cdot ADP \cdot AlF_4^- complex did not recover the specific activity of Av1. After incubation of the complex for 5 minutes at 50 °C (in the presence of MgCl_2 , P_i and NaCl) some of the Av1 specific activity was restored: 7% (Table 2, experiment 2).

Incubation of the nitrogenase \cdot ADP \cdot AlF_4^- complex over-night (under argon) at room temperature in the presence of MgCl_2 , P_i and NaCl, increased the specific activity of Av1 to 14%. This shows that some dissociation of the nitrogenase \cdot ADP \cdot AlF_4^- complex occurs in time. Hereafter the mixture was incubated at 50 °C: after 45 minutes, 69% of the specific activity of Av1 was recovered (Table 2, experiment 3).

When, immediately after preparation (as described above), the inhibited nitrogenase \cdot ADP \cdot AlF_4^- complex was incubated at 50 °C (in the presence of MgCl_2 , P_i and NaCl), the specific activity of Av1 increased to 46% in 2 hours (Table 2, experiment 4). Measurement of the nitrogenase activity without adding extra Av2, showed that the Av2 released from the inhibited complex also still had activity: 0.6 mol ethylene produced \cdot s $^{-1}$ \cdot (mol Av2) $^{-1}$. Considering that in the incubation mixture the ratio $[\text{Av2}]/[\text{Av1}]$ will be about 2; and that under these conditions the activity of Av2 is only 50% of its maximum specific activity (Cordewener et al., 1988), the activity found for Av2 is in good agreement with the 46% specific activity found for Av1 after dissociation from the inhibited complex (Table 2, experiment 4).

The results show that the inhibited nitrogenase \cdot ADP \cdot AlF_4^- complex is rather stable: after 20 hours only 14% of the complex was dissociated. The nitrogenase proteins

are not inactivated by the association with MgADP and AlF_4^- : the specific activity of both nitrogenase proteins recovers in time by incubation of the complex at 50 °C.

Table 2. Recovery of the acetylene reduction activity after separation (on DEAE cellulose) of the ADP - aluminium fluoride bound nitrogenase complex from free Av2, MgADP and AlF_4^- .

| Experiment | Incubation | Specific activity (%) |
|------------|---|-----------------------|
| 1 | - | 2 |
| 2 | + P_i + MgCl_2 + NaCl | 0 |
| | 5 min. 50 °C | 7 |
| 3 | overnight (room temperature) | |
| | + P_i + MgCl_2 + NaCl | 14 |
| | 45 min. 50 °C | 69 |
| 4 | + P_i + MgCl_2 + NaCl | 2 |
| | 120 min. 50 °C | 46 |

In experiments 2, 3 and 4: $[\text{P}_i] = 20 \text{ mM}$, $[\text{MgCl}_2] = 10 \text{ mM}$ and $[\text{NaCl}] = 0.64 \text{ M}$. After incubation the specific activity of Av1 was determined. The specific activity of Av1 in the absence of MgADP and AlF_4^- was $6.9 \text{ mol C}_2\text{H}_4 \text{ produced} \cdot \text{s}^{-1} \cdot (\text{mol Av1})^{-1} = 100\%$.

Characterization of the nitrogenase · ADP · AlF_4^- complex

The amounts of Av2, Av1 and ADP in the nitrogenase · ADP · AlF_4^- complex were determined: $2.7 \pm 0.2 \text{ Av2/Av1}$ and $2.0 \pm 0.2 \text{ ADP/Av1}$ were present. Cordewener et al. (1987) observed that two molecules of MgADP bind to Av2, but that only one MgADP molecule binds very tightly to Av2. The less tightly bound MgADP apparently was not present in the nitrogenase · ADP · AlF_4^- complex.

EPR measurements (data not shown) of the nitrogenase · ADP · AlF_4^- complex did not show the $S = 1/2$ and $S = 3/2$ signals of reduced Av2, indicating that Av2 was oxidized in the complex. The FeMoco $S = 3/2$ signal was fully present, comparable to the FeMoco signal of dithionite-reduced Av1. A yet unidentified signal at $g = 5.3$ was observed. This was not a signal associated with partly oxidized P-clusters as observed by Pierik et al. (1993) or Tittsworth & Hales (1993). It is unlikely that an electron was

transferred from Av2 to the P-cluster, since all eight Fe atoms of the P-cluster are thought to be in the ferrous state (Surerus et al., 1992). A possibility might be that in the nitrogenase \cdot ADP \cdot AlF_4^- complex the redox potential of the [4Fe-4S] cluster of Av2 is so low that at the ambient redox potential (about -550 mV) HSO_3^- , present in a sodium dithionite solution, is reduced by Av2 to SO_2^- .

The inhibition of nitrogenase activity by AlF_4^- together with MgADP resembles the action of AlF_4^- together with GDP/ADP on the activity of molecular switch proteins. In analogy to these proteins it is possible that a transition state nitrogenase complex is formed. An important difference with the molecular switch proteins however is that both nitrogenase proteins are necessary for complex formation with AlF_4^- and MgADP, whereas in case of the molecular switch proteins a stable complex is formed from MgGDP/MgADP, AlF_4^- and only the nucleotide binding protein (Chabre, 1990; Coleman et al., 1994; Sondek et al., 1994; Fisher et al., 1995). Since the transition state complex is very stable, it would be worthwhile trying to crystallize the nitrogenase \cdot ADP \cdot AlF_4^- complex and determine its three-dimensional structure.

Acknowledgements

We thank Dr. A. Arendsen and Prof. W. R. Hagen for performing the EPR spectroscopy and Prof. N. C. M. Laane for critically reading the manuscript. This investigation was supported by the Netherlands Foundation for Chemical Research (SON) with financial aid from the Netherlands Organization for Scientific Research (NWO).

References

- Ashby, G. A. & Thorneley, R. N. F. (1987) Nitrogenase of *Klebsiella pneumoniae*. Kinetic studies on the Fe protein involving reduction by sodium dithionite, the binding of MgADP and a conformation change that alters the reactivity of the 4Fe-4S centre, *Biochem. J.* 246, 455-465.
- Chabre, M. (1990) Aluminofluoride and beryllorfluoride complexes: new phosphate analogs in enzymology, *Trends Biochem. Sci.* 15, 6-10.
- Coleman, D. E., Berghuis, A. M., Lee, E., Linder, M. E., Gilman, A. G. & Sprang, S. R. (1994) Structures of active conformations of $G_{\alpha 1}$ and the mechanism of GTP hydrolysis, *Science* 265, 1405-1412.
- Cordewener, J., ten Asbroek, A., Wassink, H., Eady, R., Haaker, H. & Veeger, C. (1987) Binding of ADP and orthophosphate during the ATPase reaction of nitrogenase, *Eur. J. Biochem.* 162, 265-270.
- Cordewener, J., Krüse-Wolters, M., Wassink, H., Haaker, H. & Veeger, C. (1988) The role of MgATP hydrolysis in nitrogenase catalysis, *Eur. J. Biochem.* 172, 739-745.

- Duyvis, M. G., Wassink, H. & Haaker, H. (1994) Pre-steady-state MgATP-dependent proton production and electron transfer by nitrogenase from *Azotobacter vinelandii*, *Eur. J. Biochem.* 225, 881-890.
- Ennor, A. H. (1957) Determination and preparation of N-phosphates of biological origin, *Methods Enzymol.* 3, 850-861.
- Fisher, A. J., Smith, C. A., Thoden, J., Smith, R., Sutoh, K., Holden, H. M. & Rayment, I. (1995) Structural studies of myosin:nucleotide complexes: a revised model for the molecular basis of muscle contraction, *Biophys. J.* 68, 19s-28s.
- Georgiadis, M. M., Komiya, H., Chakrabarti, P., Woo, D., Kornuc, J. J. & Rees, D. C. (1992) Crystallographic structure of the nitrogenase iron protein from *Azotobacter vinelandii*, *Science* 257, 1653-1659.
- Hagen, W. R., Eady, R. R., Dunham, W. R. & Haaker, H. (1985) A novel $S \approx 3/2$ EPR signal associated with native Fe-proteins of nitrogenase, *FEBS Lett.* 189, 250-254.
- Hagen, W. R., Wassink, H., Eady, R. R., Smith, B. E. & Haaker, H. (1987) Quantitative EPR of an $S = 7/2$ system in thionine-oxidized MoFe-proteins of nitrogenase, *Eur. J. Biochem.* 169, 457-465.
- Hardy, R. W. F. & Burns, R. C. (1968) Biological nitrogen fixation, *Annu. Rev. Biochem.* 37, 331-358.
- Howard, J. B. & Rees, D. C. (1994) Nitrogenase: a nucleotide-dependent molecular switch, *Annu. Rev. Biochem.* 63, 235-264.
- Kim, J. & Rees, D. C. (1992) Structural models for the metal centers in the nitrogenase molybdenum-iron protein, *Science* 257, 1677-1682.
- Lowe, D. J. & Thorneley, R. N. F. (1984) The mechanism of *Klebsiella pneumoniae* nitrogenase action. Pre-steady-state kinetics of H_2 formation, *Biochem. J.* 224, 877-886.
- Pierik, A. J., Wassink, H., Haaker, H. & Hagen, W. R. (1993) Redox properties and EPR spectroscopy of the P clusters of *Azotobacter vinelandii* MoFe protein, *Eur. J. Biochem.* 212, 51-61.
- Sondek, J., Lambright, D. G., Noel, J. P., Hamm, H. E. & Sigler, P. B. (1994) GTPase mechanism of G proteins from the 1.7 Å crystal structure of transducin $\alpha \cdot GDP \cdot AlF_4^-$, *Nature* 372, 276-279.
- Surerus, K. K., Hendrich, M. P., Christie, P. D., Rottgardt, D., Orme-Johnson, W. H. & Münck, E. (1992) Mössbauer and integer-spin EPR of the oxidized P-clusters of nitrogenase: P^{ox} is a non-Kramers system with a nearly degenerate doublet, *J. Am. Chem. Soc.* 114, 8579-8590.
- Thorneley, R. N. F. & Lowe, D. J. (1983) Nitrogenase of *Klebsiella pneumoniae*. Kinetics of the dissociation of the iron protein from the molybdenum-iron protein: identification of the rate-limiting step for substrate reduction, *Biochem. J.* 215, 393-403.
- Thorneley, R. N. F. & Lowe, D. J. (1984) The mechanism of *Klebsiella pneumoniae* nitrogenase action. Simulation of the dependences of H_2 -evolution rate on component-protein concentration and ratio and sodium dithionite concentration, *Biochem. J.* 224, 903-909.
- Tittsworth, R. C. & Hales, B. J. (1993) Detection of EPR signals assigned to the 1-equiv-oxidized P-clusters of the nitrogenase MoFe protein from *Azotobacter vinelandii*, *J. Am. Chem. Soc.* 115, 9763-9767.

Chapter 4

Pre-steady-state kinetics of nitrogenase from *Azotobacter vinelandii*.

Evidence for an ATP-induced conformational change of the nitrogenase complex as part of the reaction mechanism

Abstract

The pre-steady-state electron transfer reactions of nitrogenase from *Azotobacter vinelandii* have been studied by stopped-flow spectrophotometry.

With reduced nitrogenase proteins after the initial absorbance increase at 430 nm (which is associated with electron transfer from the Fe protein to the MoFe protein and is complete in 50 ms) the absorbance decreased, which, dependent on the ratio [Av2]/[Av1], was followed by an increase of the absorbance. The mixing of reductant-free nitrogenase proteins with MgATP led, after 20 ms, to a decrease of the absorbance, which could be fitted (from 0.05 s to 1 s) with a single exponential decay with a rate constant $k_{\text{obs}} = 6.2 \pm 0.8 \text{ s}^{-1}$. This reaction of nitrogenase was measured at different wavelengths. The data indicate the formation of a species with a blue shift of the absorbance of metal-sulphur clusters of nitrogenase from 430 nm to 360 nm.

The absorbance decrease at 430 nm observed (after 50 ms) in the case of the reduced nitrogenase proteins, could only be simulated well if after the initial electron transfer from the Fe protein to the MoFe protein and before dissociation of the nitrogenase complex, an additional reaction was assumed. The rate constant of this reaction was of the same order as the rate constant of the MgATP-dependent pre-steady-state proton production by nitrogenase from *A. vinelandii*: $k_{\text{obs}} = 14 \pm 4 \text{ s}^{-1}$ with reduced nitrogenase proteins and $k_{\text{obs}} = 6 \pm 2 \text{ s}^{-1}$ with dithionite-free nitrogenase proteins (Duyvis et al., 1994).

It is proposed that in the presence and absence of reductant the observed absorbance decrease at 430 nm of nitrogenase is caused by a change of the conformation of the nitrogenase complex, as a consequence of hydrolysis of MgATP.

Introduction

Biological nitrogen fixation, which is the reduction of nitrogen to ammonia, is catalysed by the enzyme system nitrogenase. The molybdenum-containing nitrogenase of *Azotobacter vinelandii* consists of two metalloproteins which cooperate in catalysis: the MoFe protein (Av1) and the Fe protein (Av2) (Howard & Rees, 1994).

The MoFe protein is an $\alpha_2\beta_2$ -tetramer and contains two types of metal-sulphur clusters: the FeMo cofactor (FeMoco), which contains Fe, S, Mo and homocitrate, and the P-cluster, which contains Fe and S. FeMoco is generally considered to be the site of substrate reduction. Recent studies have indicated that electrons flow from the Fe protein via the P-cluster to FeMoco (Peters et al., 1995). For both clusters structural models have been proposed by Kim and Rees (1992), based on crystallographic analysis of the MoFe protein, but there is some discussion about the structure of the P-clusters (Bolin et al., 1993; Chan et al., 1993).

The other nitrogenase protein, the Fe protein (Av2), consists of two identical subunits sharing a single [4Fe-4S] cluster and contains two binding sites for MgATP and MgADP. The crystallographic structure of this protein has been determined by Georgiadis et al. (1992). A remarkable similarity between the nucleotide binding sites of the Fe protein and of the molecular switch protein H-Ras p21 was found (Georgiadis et al., 1992). The binding of MgATP or MgADP to the Fe protein leads to a decrease of the redox potential, changes in the EPR spectrum and changes of the conformation of the Fe protein (Howard & Rees, 1994).

During nitrogenase catalysis the Fe protein transfers electrons to the MoFe protein in a MgATP-dependent reaction. The generally accepted kinetic description of the mechanism of action of nitrogenase was developed by Lowe and Thorneley (Thorneley & Lowe, 1983; Lowe & Thorneley 1984a). The model consists of two coupled cycles: the Fe protein cycle and the MoFe protein cycle. In the Fe protein cycle the association of the reduced Fe protein and the MoFe protein to the nitrogenase complex is followed by the transfer of a single electron from the Fe protein to the MoFe protein, with concomitant hydrolysis of MgATP. After this the nitrogenase complex dissociates; this is the rate-limiting step of the cycle (Thorneley & Lowe, 1983). The Fe protein is reduced by the present reductant (flavodoxin or ferredoxin *in vivo*, sodium dithionite *in vitro*) and MgADP is replaced by MgATP. For the complete reduction of N_2 to $2 NH_3$ and H_2 (which is an inevitable side product of the nitrogenase reaction) eight electrons are needed. The sequence of eight Fe protein cycles during which the MoFe protein is stepwise reduced, constitutes the MoFe protein cycle. In this scheme (one of the two independently functioning halves of) the MoFe protein which has been subjected to n Fe protein cycles and is consequently reduced by n electrons, is written as E_n (Lowe &

Thorneley, 1984a). The rate constants of the reactions that constitute the Fe protein cycle are assumed to be independent of the level of reduction of the MoFe protein (Fisher et al., 1991).

The presence of MgATP is an absolute requirement for electron transfer from the Fe protein to the MoFe protein. For MgATP hydrolysis by nitrogenase on the other hand, it is not necessary that electron transfer takes place: nitrogenase hydrolyses MgATP also when no reductant is present and the Fe protein is oxidized (Hadfield & Bulen, 1969).

The precise mechanism of action of MgATP hydrolysis in nitrogenase catalysis is not yet known. If the similarity between the Fe protein of nitrogenase and the molecular switch proteins is more than a structural one, it could be expected that nucleotide binding and hydrolysis are used by nitrogenase to switch between different conformations (Howard & Rees, 1994). Recently we (Duyvis et al., 1996) and Renner and Howard (1996) have independently demonstrated that MgADP plus aluminium fluoride inhibits nitrogenase by stabilizing a complex between both nitrogenase proteins, suggesting a mode of action similar to that observed for molecular switch proteins (Chabre, 1990; Duyvis et al., 1996; Renner & Howard, 1996). However, limited data are available that show that conformational changes occur in the nitrogenase complex during turnover. Mensink & Haaker (1992) concluded from their experiments on the temperature dependence of the extent and rate of MgATP-induced electron transfer that electron transfer occurs via a highly disordered transition state, which indicates a major conformational change. It was proposed that binding of MgATP to the nitrogenase complex causes a change of the conformation of the complex that triggers electron transfer (Mensink & Haaker, 1992; Mensink et al., 1992).

The transfer of the first electron from the Fe protein to the MoFe protein is accompanied by a fast increase of the absorbance at 430 nm, due to oxidation of the Fe protein. Following this absorbance increase smaller absorbance changes are observed (Lowe et al., 1993; Peters et al. 1995), probably caused by subsequent redox changes of the MoFe protein. Lowe et al. (1993) were able to simulate the absorbance changes that occur during the first 0.6 seconds of the reaction of the nitrogenase of *Klebsiella pneumoniae*.

In this paper the absorbance changes associated with pre-steady-state electron transfer reactions by nitrogenase of *A. vinelandii* are presented. The shape of these curves differs significantly from the shape of the curves published for the reaction of *K. pneumoniae* nitrogenase; as a consequence the absorbance changes cannot be simulated using the Lowe-Thorneley model (Lowe et al., 1993). To describe the absorbance changes adequately a reaction associated with an absorbance decrease must be assumed prior to dissociation of the nitrogenase complex. We present evidence that

this reaction is a change of the conformation of the nitrogenase complex from the MgATP-bound to the MgADP-bound conformation.

Materials and methods

Growth and isolation and preparation of nitrogenase

Azotobacter vinelandii ATCC strain 478 was grown and the nitrogenase component proteins were purified and assayed as described elsewhere (Mensink et al., 1992). Specific activities of Av1 and Av2 were at least 8 mol ethylene produced $\cdot s^{-1} \cdot (mol\ Av1)^{-1}$ and 2 mol ethylene produced $\cdot s^{-1} \cdot (mol\ Av2)^{-1}$, respectively. Av1 contained 1.8 ± 0.2 Mo/mol Av1; the iron content of the Fe protein was 3.6 ± 0.3 mol Fe/mol Av2. Dithionite-free Av1 was prepared by running Av1 over a Biogel P-6DG column which was equilibrated with 10 mM $MgCl_2$ and 200 mM NaCl in 50 mM Tes/NaOH, pH 7.4. All buffers used were saturated with argon. ATP (special quality) was obtained from Boehringer.

Spectrophotometry

Stopped flow spectrophotometry was performed with a HI-TECH SF-51 stopped-flow spectrophotometer (Salisbury, Wilts, U. K.) equipped with an anaerobic kit and a data acquisition and analysis system. If not indicated otherwise, the absorbance changes were measured at 430 nm. The reaction temperature was 20.0 ± 0.1 °C. The mixing ratio was 1:1. For measurement of electron transfer, one syringe of the stopped-flow apparatus contained Av1 and Av2 (concentrations as indicated) and the other syringe contained 10 mM ATP; both syringes contained 10 mM $MgCl_2$, 4 mM sodium dithionite and NaCl (concentration as indicated) in 50 mM Tes/NaOH, final pH 7.4. In case of the dithionite-free experiments, one syringe contained dithionite-free Av1 and oxidized Av2 (concentrations as indicated) and the other syringe contained 10 mM ATP; both syringes contained 100 mM NaCl and 10 mM $MgCl_2$ in 50 mM Tes/NaOH, final pH 7.4.

Simulations

The simulations of the absorbance changes associated with electron transfer were performed with the kinetic simulation program KINSIM (Barshop et al., 1983).

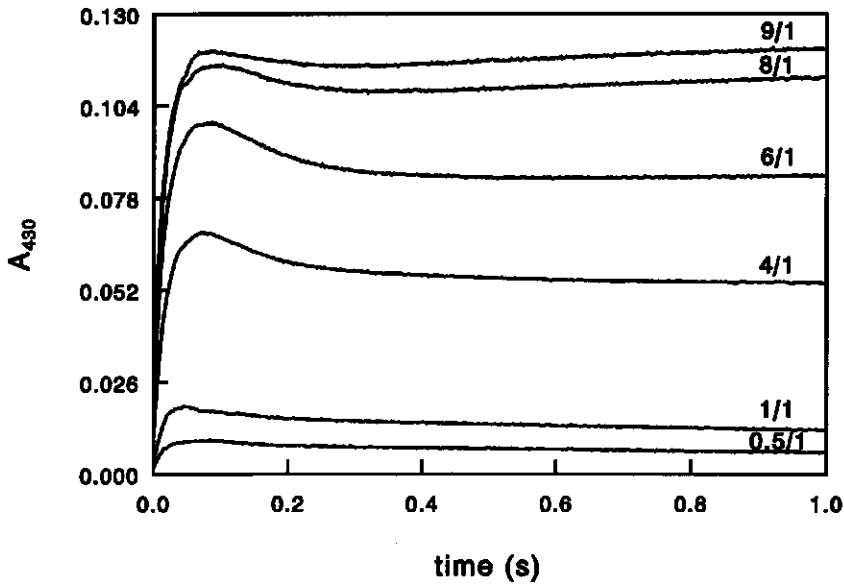


Figure 1. Absorbance changes (430 nm) during the first 1 second of the reaction of nitrogenase at different $[Av2]/[Av1]$ ratios. Concentrations after mixing: 10 μM Av1; 5, 10, 40, 60 and 90 μM Av2; 100 mM NaCl; 4 mM $Na_2S_2O_4$. The ratio $[Av2]/[Av1]$ is indicated for each stopped-flow trace.

Results

Absorbance changes of Azotobacter vinelandii nitrogenase during electron transfer

Figure 1. shows the absorbance changes (at 430 nm) that are observed when consecutive electron transfer steps from the Fe protein to the MoFe protein take place, and the influence of the ratio $[Av2]/[Av1]$ on these absorbance changes. The absorbance increase immediately after the mixing of the nitrogenase proteins with MgATP, caused by the transfer of one electron from the reduced Fe protein to the MoFe protein, was complete within 100 ms at all $[Av2]/[Av1]$ ratios (at 20 °C). The maximum absorbance increase was reached when $[Av2]/[Av1] = 8$ (Av1 is an $(\alpha\beta)_2$ -dimer: each Av1 binds two molecules of Av2); k_{obs} did not depend on the ratio of the nitrogenase proteins ($k_{obs} = 68.3 \pm 11.4 \text{ s}^{-1}$). The absorbance increase at ratio $[Av2]/[Av1] = 9$ could be fitted to a single exponential with $\Delta A_{430} = 0.119$ and rate constant $k_{obs} = 70.5 \text{ s}^{-1}$. The presence of 100 mM NaCl in the reaction mixture, necessary to prevent precipitation of Av1 at low $[Av2]/[Av1]$ ratios, lowers the observed rate constant of electron transfer (in this case

from $\sim 100 \text{ s}^{-1}$ to $\sim 70 \text{ s}^{-1}$) and increases the $[\text{Av}2]/[\text{Av}1]$ ratio at which the maximum absorbance is reached. After 100 ms the absorbance decreases which, dependent on the ratio $[\text{Av}2]/[\text{Av}1]$, was followed by an increase of the absorbance (see Figure 1). These absorbance changes were slower and less pronounced when NaCl was present in the reaction mixture, as can be seen by comparing the stopped-flow traces in Figure 1 (in the presence of 100 mM NaCl) and the stopped-flow trace in Figure 2 (obtained in the absence of salt).

Lowe et al. (1993) simulated the absorbance changes observed in the first 0.6 seconds after the mixing of the nitrogenase proteins from *K. pneumoniae* with MgATP by ascribing the absorbance changes after the initial absorbance increase to the redox changes of Kp1 described in the MoFe protein cycle (Lowe & Thorneley, 1984a). Their simulation used the rate constants for the Fe protein cycle and the MoFe protein cycle given by Lowe and Thorneley (1984a). Different absorbance coefficients were attached to the subsequent redox changes of Kp1 from state E_0 to E_4 . As noticed by the authors, their simulation slightly but reproducibly deviates from the stopped-flow trace between the first 30 and 200 ms. It was suggested that these small deviations are the result of intramolecular reactions (such as electron transfer between the metal-sulphur clusters of Kp1 or from clusters to bound protons) at the E_2 level of reduction of Kp1.

Table 1. Rate constants of the Fe protein cycle, determined for nitrogenase from *Azotobacter vinelandii*, as used in the simulations.

| rate constant | value | reaction | reference |
|---------------|--|--|-------------------------|
| k_{+1} | $5 \times 10^7 \text{ M}^{-1} \cdot \text{s}^{-1}$ | association active complex | Lowe & Thorneley, 1984b |
| k_{-1} | 15 s^{-1} | | Lowe & Thorneley, 1984b |
| k_{+2} | 100 s^{-1} | electron transfer | this study |
| k_{+3} | 3.3 s^{-1} | dissociation of complex | this study |
| k_{-3} | $2.3 \times 10^6 \text{ M}^{-1} \cdot \text{s}^{-1}$ | | this study |
| k_{+4} | 5.6 s^{-1} | reduction $\text{Av}2_{\text{ox}}(\text{MgADP})_2$ | this study |

The rate constant k_{+4} was determined as described by Thorneley & Lowe (1983) and Ashby & Thorneley (1987): given here is the value at 4 mM sodium dithionite. The rate constants k_{+3} and k_{-3} were determined as described by Thorneley & Lowe (1983).

The stopped-flow traces (20 °C) obtained after the mixing of the *A. vinelandii* nitrogenase proteins with MgATP (Figure 1 and Figure 2) had a much more pronounced

shape than the curves obtained with the nitrogenase proteins from *K. pneumoniae* (23 °C) (Lowe et al., 1993). For *A. vinelandii* nitrogenase the absorbance clearly decreased after the initial increase of the absorbance, whereas for the published *K. pneumoniae* ratios ($[Kp2]/[Kp1] = 8/1$ and $1/1$) this was not the case (Lowe et al., 1993).

Table 2. Absorbance coefficients (ϵ_{430}) used for simulation of the absorbance changes at 430 nm observed after the mixing of the nitrogenase proteins from *A. vinelandii* with MgATP.

| species | simulation | | | |
|--|------------------|-------|-------|-------|
| | 1 | 2 | 3 | 4 |
| | ϵ_{430} | | | |
| $[Av2_{ox}(MgATP)_2Av1^*_{red}]_{ATP}$ | 5.0 | 5.0 | 5.9 | 5.5 |
| $[Av2_{ox}(MgADP)_2Av1^*_{red}]_{ADP}$ | - | - | 4.0 | 4.0 |
| E_1 | 0.0 | 0.0 | -0.70 | -0.60 |
| E_2 | -2.2 | 10.0 | 0.25 | 0.3 |
| E_3 | -2.2 | 60.0 | -1.0 | 0.4 |
| E_4 | 4.5 | -55.0 | 6.0 | 4.5 |

$Av1^*$: one of two independently functioning halves of the MoFe protein; $Av1^*_{red}$: MoFe protein with super-reduced FeMoco; $Av2_{ox}$ and $Av2_{red}$: oxidized and reduced Fe protein, respectively; $[Av2(MgATP)_2Av1^*]_{ATP}$ or $[Av2(MgADP)_2Av1^*]_{ADP}$: the nitrogenase complex is in the MgATP-bound or MgADP-bound conformation, respectively. The absorbance coefficients for the appearance of species $[Av2_{ox}(MgATP)_2Av1^*_{red}]_{ATP}$ and $[Av2_{ox}(MgADP)_2Av1^*_{red}]_{ADP}$ are relative to $Av2_{red}(MgATP)_2$ and $Av2_{red}(MgATP)_2Av1^*$; the absorbance coefficients for the appearance of species E_n are relative to E_0 . All absorbance coefficients (ϵ_{430}) are in $mM^{-1} \cdot cm^{-1}$. It was assumed that 62% of all Av2 present was active with respect to electron transfer, and 38% inactive (Thorneley & Lowe, 1984; Duyvis et al., 1996). In simulation 3 an extra reaction ($k = 14 s^{-1}$) is added to the model used in simulations 1 and 2: this reaction is accompanied with an absorbance change at 430 nm, defined by the absorbance coefficient of species $[Av2_{ox}(MgADP)_2Av1^*_{red}]_{ADP}$. In simulation 4 an extra delay ($k = 40 s^{-1}$) is added to the model of simulation 3; this delay is not accompanied with an absorbance change at 430 nm.

We tried to simulate the stopped-flow trace obtained after the mixing of Av1 and Av2 with MgATP in the absence of salt by using the same model and absorbance coefficients and rate constants for the MoFe protein cycle as Lowe et al. (1993). In addition we used the rate constants of the Fe protein cycle as determined for the

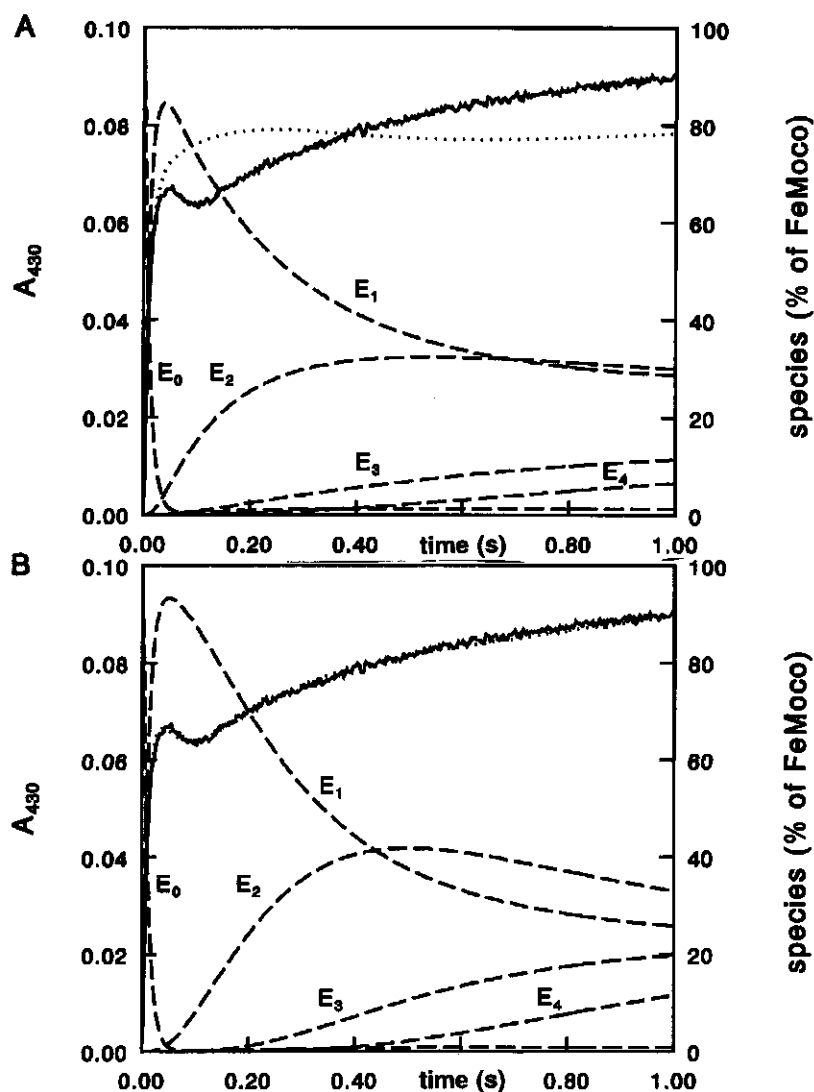


Figure 2. Simulation of the absorbance changes associated with electron transfer from the Fe protein to the MoFe protein. (—): stopped-flow trace (A_{430}) obtained after the mixing of the nitrogenase proteins with MgATP, (· ·): simulation of the absorbance changes, (---): E_n , one of two independently functioning halves of MoFe protein, reduced by n electron equivalents. Concentrations after mixing: 7.7 μ M Av1; 46.2 μ M Av2; 4 mM $\text{Na}_2\text{S}_2\text{O}_4$. The simulation uses rate constants determined for *A. vinelandii* nitrogenase, see Table 1. (A) Simulation of the absorbance changes and the appearance of species E_n , using the model and the absorbance coefficients according to Lowe et al. (1993), see Table 2, simulation 1. (B) Simulation of the absorbance changes and the appearance of species E_n , using the model as in panel (A) with an additional reaction (associated with an absorbance decrease) before dissociation of the nitrogenase complex, see Table 2, simulation 3.

A. vinelandii proteins at 20 °C (see Table 1). The absorbance coefficients used for species E_1 , E_2 , E_3 and E_4 (relative to E_0) are given in Table 2, simulation 1. It is obvious from Figure 2A that the absorbance decrease observed in the stopped-flow trace was absent in the simulation. It was possible, however, to simulate the stopped-flow trace by allowing other absorbance coefficients for the different redox states of Av1, but to obtain a good simulation some of these absorbance coefficients had to be extremely large (see Table 2, simulation 2). Therefore we did not consider this to be the right solution to the problem.

To acquire an adequate simulation of the stopped-flow trace an additional reaction (with an absorbance decrease) with a rate constant of $\sim 14\text{ s}^{-1}$ had to be included in the model of the reaction mechanism: this reaction must take place before dissociation of the nitrogenase complex. With this addition to the model and small changes of the absorbance coefficients of the different redox states of the MoFe protein (see Table 2, simulation 3) a good fit of the stopped-flow trace and the simulated absorbance changes was obtained, see Figure 2B. The stopped-flow traces obtained at different $[Av2]/[Av1]$ ratios could also be simulated with this adjusted model (data not shown). The rate constant of the added reaction was of the same order as the MgATP-dependent pre-steady-state proton production: $k_{\text{obs}} = 14 \pm 4\text{ s}^{-1}$ (reduced nitrogenase proteins) (Duyvis et al., 1994). To be able to simulate their data of pre-steady-state phosphate release caused by the reaction of the nitrogenase proteins from *K. pneumoniae* with MgATP (23 °C), Lowe et al. (1995) assumed a kinetic scheme in which first an electron is transferred ($k_{\text{obs}} = 176\text{ s}^{-1}$), followed by on-enzyme MgATP hydrolysis ($k = 50\text{ s}^{-1}$), after which phosphate is released ($k_{\text{obs}} = 22\text{ s}^{-1}$) and finally the nitrogenase complex dissociates ($k = 6.4\text{ s}^{-1}$). We also added the on-enzyme MgATP hydrolysis step to our kinetic scheme, with a rate constant $k = 40\text{ s}^{-1}$ (20 °C), after electron transfer: with this addition and slightly altered absorbance coefficients (see Table 2, simulation 4) also a good simulation of the stopped-flow data was obtained (data not shown). However, it is not absolutely necessary to add this step to the kinetic scheme because this did not clearly improve the simulation.

Absorbance changes of dithionite-free nitrogenase proteins

The hypothesis that MgATP hydrolysis induces an absorbance decrease at 430 nm in the nitrogenase complex was tested with dithionite-free nitrogenase proteins. After mixing of dithionite-free nitrogenase proteins (oxidized Fe protein, MoFe protein with FeMoco and P-cluster dithionite-reduced (see Materials and Methods)) with MgATP, after a delay of about 20 ms a decrease of the absorbance at 430 nm was observed. An

example of the obtained stopped-flow trace is given in Figure 3. The absorbance decrease could be fitted from 0.05 s to 1 s, to a single exponential: $\Delta A_{430} = 0.011 \cdot \exp(-6.2t)$. The absorbance decrease increased with the component protein ratio and saturated at $[Av2]/[Av1] > 10$ with $\Delta A_{430} = 0.020$ ($[Av1] = 2.7 \mu\text{M}$). The observed rate constant of the absorbance decrease was independent of the ratio $[Av2]/[Av1]$ (data not shown).

The reaction of the dithionite-free nitrogenase proteins with MgATP was measured at different wavelengths. Between 320 and 400 nm the absorbance increased with a maximum at 360 nm, whereas between 400 and 750 nm the absorbance decreased with a minimum around 430 nm (see Figure 3, inset). This indicates that MgATP hydrolysis during the Fe protein cycle induces a blue shift of the absorbance spectrum of the nitrogenase complex; some absorbance of metal-sulphur clusters around 430 nm shifts to 360 nm.

No significant absorbance change was observed when the dithionite-free nitrogenase proteins were mixed with MgADP, nor when either oxidized Av2 or dithionite-free Av1 was mixed with MgATP. The absorbance decrease observed after the

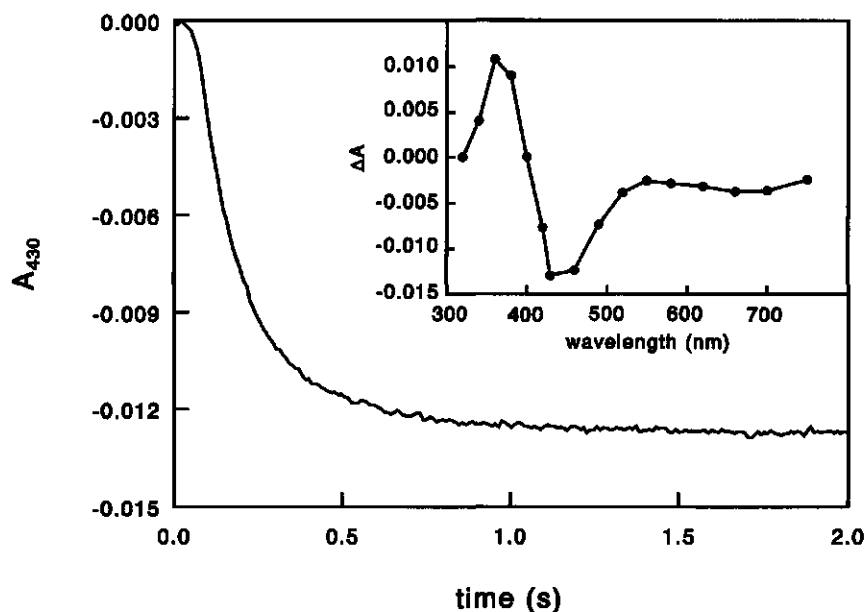


Figure 3. Absorbance changes after the mixing of the dithionite-free nitrogenase proteins with MgATP. Concentrations after mixing: 2.7 μM Av1 and 16 μM Av2. *Inset*, dependence of the amplitude of the absorbance change on the wavelength.

mixing of the dithionite-free nitrogenase complex with MgATP is therefore a property of the nitrogenase complex, not of the individual nitrogenase proteins. No electrons are transferred from the Fe protein to the MoFe protein because the Fe protein is oxidized. EPR measurements indicated that the FeMoco $S = 3/2$ signal did not decrease significantly during the first 2 s. No signals associated with oxidized P-clusters like those reported by Pierik et al. (1993) or Tittsworth and Hales (1993) were observed, even after a prolonged incubation (23 s). It is therefore clear that the absorbance decrease is caused by a reaction other than electron transfer. The rate of the absorbance decrease (after 50 ms) was of the same order as the rate observed for the MgATP-dependent pre-steady-state proton production for dithionite-free nitrogenase proteins: $k_{\text{obs}} = 6 \pm 2 \text{ s}^{-1}$ (Duyvis et al., 1994). This suggests that the absorbance decrease at 430 nm is caused by the same reaction that is causing the MgATP-dependent pre-steady-state proton production.

Discussion

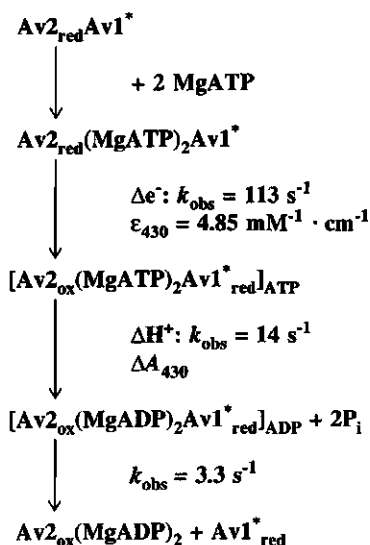
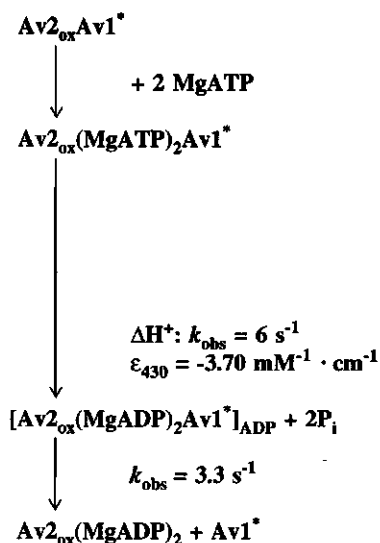
In our previous article (Chapter 2) we suggested that the binding of MgATP to the nitrogenase complex induces electron transfer from the Fe protein to the MoFe protein. After electron transfer MgATP is hydrolysed and the conformation of the nitrogenase complex changes; this change is accompanied by the production of protons (Duyvis et al., 1994). On the basis of the data and simulations presented here we suggest that this conformational change of the nitrogenase complex causes a shift of the absorbance maximum at 430 nm to 360 nm, resulting in a decrease of the absorbance at 430 nm. In this hypothesis a conformational change of the nitrogenase complex could alter the environment of the metal-sulphur clusters of nitrogenase, causing an absorbance change, as observed for various types of chromophores in proteins (Müller et al., 1973; Foguel & Weber, 1995).

The absence of a pronounced absorbance decrease in the *K. pneumoniae* nitrogenase stopped-flow traces (Lowe et al., 1993) in contrast to the traces obtained for *A. vinelandii* nitrogenase, might be caused by a different rate constant of the proposed conformational change of the nitrogenase complex, assuming that such a conformational change exists for *K. pneumoniae* nitrogenase. The absorbance decrease was no longer visible in our simulation if a lower value for the rate constant was chosen (4 s^{-1}) or if a much higher value was chosen: (100 s^{-1}) (data not shown). In the first case the change of the conformation coincided with the dissociation of the nitrogenase complex ($k_{\text{obs}} \approx 3 \text{ s}^{-1}$), and in the other case the absorbance decrease became a contribution to the (lowered) initial absorbance increase, caused by electron transfer.

Lowe et al. (1993) only observed an absorbance decrease after the mixing of the nitrogenase proteins with MgATP under a C_2H_2 atmosphere. This decrease in the absorbance was not followed by an increase. Similar results were obtained with the nitrogenase proteins from *A. vinelandii* under a C_2H_2 atmosphere (data not shown), but this absorbance decrease started only after 200 ms and happened at a much lower rate than the absorbance decrease presented in this paper. Kp1 with C_2H_2 bound cannot be reduced further than the E_3 state (Lowe et al., 1990) and no absorbance increase was observed after the absorbance decrease (Lowe et al., 1993). This shows that the reduction of Kp1 from the E_3 state to the E_4 state in the absence of C_2H_2 causes an increase of the absorbance at 430 nm (Table 2, simulation 1).

The stopped-flow traces obtained with *A. vinelandii* nitrogenase could not be simulated with the model of Lowe et al. (1993); the kinetic scheme had to be adjusted as discussed in Results. Also the absorbance coefficients of the different E_n states were slightly altered (Table 2, simulations 1 and 3). One should not attach too much importance to the value of these absorbance coefficients: what absorbance changes really accompany the reduction of the MoFe protein to each of the subsequent E_n states are not known. We realize that the absorbance changes of the Fe protein caused by oxidation or reduction, also contribute considerably to the stopped-flow traces. It was observed that the rate of reduction of oxidized Av2 after dissociation of the nitrogenase complex has a large influence on the appearance of the stopped-flow traces (data not shown).

On the basis of the described experiments, we suggest the following sequence of events after the mixing of the nitrogenase proteins with MgATP, see Scheme 1. Binding of MgATP to the nitrogenase complex is fast and induces a conformational change of the complex which, if the Fe protein is reduced, allows rapid electron transfer from the Fe protein to the MoFe protein ($k_{obs} \approx 100 \text{ s}^{-1}$, in the absence of salt). In the altered conformation MgATP is hydrolysed and a second conformational change of the nitrogenase complex (to the MgADP-bound conformation) takes place, which changes the environment of the metal-sulphur clusters and causes a blue shift of the absorbance maximum at 430 nm ($k_{obs} \approx 14 \text{ s}^{-1}$). We propose that this reaction is also associated with proton production (Duyvis et al., 1994) and P_i release (Lowe et al., 1995). Hereafter the nitrogenase complex dissociates ($k_{obs} \approx 3 \text{ s}^{-1}$; this rate constant was calculated from the rate of turnover under optimal conditions at 20 °C (Duyvis et al., 1994), assuming that the dissociation of the nitrogenase complex is the rate-limiting step of the catalytic cycle (Thorneley & Lowe, 1983)).

Reduced nitrogenase proteinsReductant-free nitrogenase proteins

Scheme 1. Pre-steady-state reactions of nitrogenase with MgATP. All rate constants were measured for *A. vinelandii* nitrogenase. For the abbreviations used, see Table 2; Δe^- : electron transfer from the Fe protein to the MoFe protein was observed; ΔH^+ : proton production was observed; ΔA_{430} and ϵ_{430} (in $(\text{mM Av1}^*)^{-1} \cdot \text{cm}^{-1}$): an absorbance change at 430 nm was observed.

Acknowledgements

We thank Prof. C. Veeger and Prof. N. C. M. Laane for critically reading the manuscript. This investigation was supported by the Netherlands Foundation for Chemical Research (SON) with financial aid from the Netherlands Organization for Scientific Research (NWO).

References

- Ashby, G. A. & Thorneley, R. N. F. (1987) Nitrogenase of *Klebsiella pneumoniae*. Kinetic studies on the Fe protein involving reduction by sodium dithionite, the binding of MgADP and a conformation change that alters the reactivity of the 4Fe-4S centre, *Biochem. J.* **246**, 455-465.
- Barshop, B. A., Wrenn, R. F. & Frieden, C. (1983) Analysis of numerical methods for computer simulation of kinetic processes: development of KINSIM - a flexible, portable system, *Anal. Biochem.* **130**, 134-145.
- Bolin, J. T., Campobasso, N., Muchmore, S. W., Morgan, T. V. & Mortenson, L. E. (1993)

- Structure and environment of metal clusters in the nitrogenase molybdenum-iron protein from *Clostridium pasteurianum*, in: *Molybdenum enzymes, cofactors and model systems* (Stiefel, E. I., Coucouvanis, D. and Newton, W. E., eds.) pp. 186-195, American Chemical Society, Washington, D. C.
- Chabre, M. (1990) Aluminofluoride and beryllorfluoride complexes: new phosphate analogues in enzymology, *Trends Biochem. Sci.* 15, 6-10.
- Chan, M. K., Kim, J. & Rees, D. C. (1993) The nitrogenase FeMo-cofactor and P-cluster pair: 2.2 Å resolution structures, *Science* 260, 792-794.
- Duyvis, M. G., Wassink, H. & Haaker, H. (1994) Pre-steady-state MgATP-dependent proton production and electron transfer by nitrogenase from *Azotobacter vinelandii*, *Eur. J. Biochem.* 225, 881-890.
- Duyvis, M. G., Wassink, H. & Haaker, H. (1996) Formation and characterization of a transition state complex of *Azotobacter vinelandii* nitrogenase, *FEBS Lett.* 380, 233-236.
- Fisher, K., Lowe, D. J. & Thorneley, R. N. F. (1991) *Klebsiella pneumoniae* nitrogenase. The pre-steady-state kinetics of MoFe-protein reduction and hydrogen evolution under conditions of limiting electron flux show that the rates of association with the Fe-protein and electron transfer are independent of the oxidation level of the MoFe-protein, *Biochem. J.* 279, 81-85.
- Foguel, D. & Weber, G. (1995) Pressure-induced dissociation and denaturation of allophycocyanin at subzero temperatures, *J. Biol. Chem.* 270, 28759-28766.
- Georgiadis, M. M., Komiya, H., Chakrabarti, P., Woo, D., Kornuc, J. J. & Rees, D. C. (1992) Crystallographic structure of the nitrogenase iron protein from *Azotobacter vinelandii*, *Science* 257, 1653-1659.
- Hadfield, K. L. & Bulen, W. A. (1969) Adenosine triphosphate requirement of nitrogenase from *Azotobacter vinelandii*, *Biochemistry* 8, 5103-5108.
- Howard, J. B. & Rees, D. C. (1994) Nitrogenase: a nucleotide-dependent molecular switch, *Annu. Rev. Biochem.* 63, 235-264.
- Kim, J. & Rees, D. C. (1992) Structural models for the metal centers in the nitrogenase molybdenum-iron protein, *Science* 257, 1677-1682.
- Lowe, D. J., Ashby, G. A., Brune, M., Knights, H., Webb, M. R. & Thorneley, R. N. F. (1995) ATP hydrolysis and energy transduction by nitrogenase, in: *Nitrogen fixation: fundamentals and applications* (Tikhonovich, I. A., Provorov, N. A., Romanov, V. I. and Newton, W. E., eds.) pp. 103-108, Kluwer Academic Publishers, Dordrecht, the Netherlands.
- Lowe, D. J., Fisher, K. & Thorneley, R. N. F. (1990) *Klebsiella pneumoniae* nitrogenase. Mechanism of acetylene reduction and its inhibition by carbon monoxide, *Biochem. J.* 272, 621-625.
- Lowe, D. J., Fisher, K. & Thorneley, R. N. F. (1993) *Klebsiella pneumoniae* nitrogenase: pre-steady-state absorbance changes show that redox changes occur in the MoFe protein that depend on substrate and component protein ratio; a role for P-centres in reducing dinitrogen? *Biochem. J.* 292, 93-98.
- Lowe, D. J. & Thorneley, R. N. F. (1984a) The mechanism of *Klebsiella pneumoniae* nitrogenase action. Pre-steady-state kinetics of H₂ formation, *Biochem. J.* 224, 877-886.
- Lowe, D. J. & Thorneley, R. N. F. (1984b) The mechanism of *Klebsiella pneumoniae* nitrogenase action. The determination of rate constants required for the simulation of the kinetics of N₂ reduction and H₂ evolution, *Biochem. J.* 224, 895-901.
- Mensink, R. E. & Haaker, H. (1992) Temperature effects on the MgATP-induced electron transfer between the nitrogenase proteins from *Azotobacter vinelandii*, *Eur. J. Biochem.* 208, 295-299.

- Mensink, R. E., Wassink, H. & Haaker, H. (1992) A reinvestigation of the pre-steady-state ATPase activity of the nitrogenase from *Azotobacter vinelandii*, *Eur. J. Biochem.* 208, 289-294.
- Müller, F., Mayhew, S. G. & Massey, V. (1973) On the effect of temperature on the absorption spectra of free and protein-bound flavines, *Biochemistry* 12, 4654-4662.
- Peters, J. W., Fisher, K., Newton, W. E. & Dean, D. R. (1995) Involvement of the P cluster in intramolecular electron transfer within the nitrogenase MoFe protein, *J. Biol. Chem.* 270, 27007-27013.
- Pierik, A. J., Wassink, H., Haaker, H. & Hagen, W. R. (1993) Redox properties and EPR spectroscopy of the P clusters of the *Azotobacter vinelandii* MoFe protein, *Eur. J. Biochem.* 212, 51-61.
- Renner, K. A. & Howard, J. B. (1996) Aluminum fluoride inhibition of nitrogenase: stabilization of a nucleotide-Fe-protein-MoFe-protein complex, *Biochemistry* 35, 5353-5358.
- Thorneley, R. N. F. & Lowe, D. J. (1983) Nitrogenase of *Klebsiella pneumoniae*. Kinetics of the dissociation of oxidized iron protein from molybdenum-iron protein: identification of the rate-limiting step for substrate reduction, *Biochem. J.* 215, 393-403.
- Thorneley, R. N. F. & Lowe, D. J. (1984) The mechanism of *Klebsiella pneumoniae* nitrogenase action. Simulation of the dependences of H₂-evolution rate on component-protein concentration and ratio and sodium dithionite concentration, *Biochem. J.* 224, 903-909.
- Tittsworth, R. C. & Hales, B. J. (1993) Detection of EPR signals assigned to the 1-equiv-oxidized P-clusters of the nitrogenase MoFe-protein from *Azotobacter vinelandii*, *J. Am. Chem. Soc.* 115, 9763-9767.

Chapter 5

Evidence for multiple steps in the pre-steady-state electron transfer reaction of nitrogenase from *Azotobacter vinelandii*

Abstract

The effect of the NaCl concentration and the reaction temperature on the MgATP-dependent pre-steady-state electron transfer reaction (from the Fe protein to the MoFe protein) of nitrogenase from *Azotobacter vinelandii* was studied by stopped-flow spectrophotometry and rapid-freeze EPR spectroscopy. Besides lowering the reaction temperature, also the addition of NaCl decreased the observed rate constant and the amplitude of the absorbance increase (at 430 nm) which accompanies pre-steady-state electron transfer. The diminished absorbance increase observed at 5 °C (without NaCl) can be explained by assuming reversible electron transfer, which was revealed by rapid-freeze EPR experiments that indicated an incomplete reduction of the FeMo cofactor. This was not the case with the salt-induced decrease of the amplitude of the stopped-flow signal: the observed absorbance amplitude of the electron transfer reaction predicted only 35% reduction of the MoFe protein, whereas rapid-freeze EPR showed 80% reduction of the FeMo cofactor. In the presence of salt, the kinetics of the reduction of the FeMo cofactor showed a lag period which was not observed in the absorbance changes. It is proposed that the pre-steady-state electron transfer reaction is not a single reaction but consists of two steps: electron transfer from the Fe protein to a still unidentified site on the MoFe protein, followed by the reduction of the FeMo cofactor. The consequences of our finding that the pre-steady-state FeMo cofactor reduction does not correlate with the amplitude and kinetics of the pre-steady-state absorbance increase will be discussed with respect to the present model of the kinetic cycle of nitrogenase.

Introduction

Nitrogenase is the enzyme complex which catalyses the reduction of dinitrogen to ammonia. The nitrogenase complex comprises two metalloproteins, the MoFe protein and the Fe protein, which are both necessary for catalysis, as well as MgATP and a strong reductant (Howard & Rees, 1994). The crystal structures of both nitrogenase proteins have been solved (Georgiadis et al., 1992; Kim & Rees, 1992a,b; Bolin et al., 1993; Chan et al., 1993). The MoFe protein (Av1), is a tetramer ($\alpha_2\beta_2$) of 230 kDa. Each $\alpha\beta$ -unit represents a catalytically independent moiety which contains one iron-molybdenum cofactor (FeMoco) and one P-cluster. FeMoco is thought to be the catalytic site for substrate reduction; the P-cluster is close to the putative Fe protein binding site and might be involved in intramolecular electron transfer to FeMoco (Peters et al., 1995). There is some discussion about the structure of the P-cluster (Bolin et al., 1993; Chan et al., 1993). The other nitrogenase protein, the Fe protein (Av2), is a homodimer of 63 kDa, which contains one [4Fe-4S] cluster, and two binding sites for MgATP or MgADP (Georgiadis et al., 1992).

A kinetic model for the reduction of dinitrogen to ammonia by nitrogenase was developed by Thorneley and Lowe (Thorneley & Lowe, 1983; Lowe & Thorneley, 1984). The model consists of an Fe protein cycle and a MoFe protein cycle. The Fe protein cycle involves association of the Fe protein and the MoFe protein to form the nitrogenase complex, the subsequent transfer of a single electron from the Fe protein to the MoFe protein with concomitant hydrolysis of MgATP, followed by dissociation of the nitrogenase complex. The MoFe protein cycle describes the stepwise reduction of the MoFe protein by eight consecutive Fe protein cycles, required for the complete reduction of N_2 to 2 NH_3 and H_2 .

Electron transfer from the Fe protein to the MoFe protein has been monitored by (rapid-freeze) EPR (Orme-Johnson et al., 1972; Smith et al., 1972, 1973; Zumft et al., 1974), following the decrease of the $S = 3/2$ EPR signal of FeMoco (g -values 4.3, 3.7 and 2.01), due to reduction of FeMoco, and the decrease of the $S = 1/2$ EPR signal of the [4Fe-4S] cluster of the Fe protein (g -values 2.05, 1.94 and 1.89), due to oxidation of the Fe protein. Later, the electron transfer from the Fe protein to the MoFe protein was monitored also by stopped-flow spectrophotometry. The absorbance increase at 430 nm, observed after mixing of both nitrogenase proteins with MgATP, is mainly due to the oxidation of the Fe protein in the electron transfer reaction (Thorneley, 1975; Thorneley & Cornish-Bowden, 1977). Lowering the reaction temperature (compared to room temperature) diminishes this absorbance increase at 430 nm (Thorneley et al., 1989; Mensink & Haaker, 1992). Thorneley et al. (1989) suggested that this effect can be explained by assuming that both electron transfer between the component proteins of

nitrogenase and hydrolysis of MgATP are reversible processes; at a lower reaction temperature (6 °C) the back reactions become more important, which causes the lower absorbance increase at 430 nm. Mensink & Haaker (1992) have argued that the kinetic evidence indicates that only electron transfer might be regarded as a reversible reaction, but that the interaction of MgATP with nitrogenase is fast and irreversible.

Several studies have been conducted on the effects of salt on the properties and catalytic activity of the nitrogenase proteins and the complex. The $s_{20,w}$ value for the MoFe protein from *A. vinelandii* is increased by the presence of NaCl (Burns et al., 1985). Binding of NaCl to the Fe protein from *A. vinelandii* is revealed by inhibition of the MgATP-dependent chelation of the iron-sulphur cluster by 2,2-bipyridyl (Deits & Howard, 1990). Salts are also known to be inhibitory in steady-state substrate reduction assays for the nitrogenase complex (Burns et al., 1985; Deits & Howard, 1990). A cross-linking study with the nitrogenase complex from *A. vinelandii* established that NaCl inhibits the association of the component proteins (Willing et al., 1989).

We report here that NaCl suppresses the absorbance increase at 430 nm associated with MgATP-dependent pre-steady-state electron transfer from the Fe protein to the MoFe protein. Rapid-freeze EPR data will be presented which show that the effect of NaCl cannot be attributed to incomplete reduction of FeMoco, and that there is a lag in the reduction of FeMoco, which indicates that a reaction - made slower by the presence of NaCl - precedes the reduction of FeMoco.

Materials and methods

Cell growth and isolation and preparation of nitrogenase

Azotobacter vinelandii ATCC strain 478 was grown and the nitrogenase component proteins were purified and assayed as described elsewhere (Mensink et al., 1992). Specific activities of Av1 and Av2 were at least 8 mol ethylene produced $\cdot s^{-1} \cdot (\text{mol Av1})^{-1}$ and 2 mol ethylene produced $\cdot s^{-1} \cdot (\text{mol Av2})^{-1}$, respectively. Av1 contained 1.8 ± 0.2 Mo/mol Av1. The iron content of the Fe protein was 3.6 ± 0.3 mol Fe/mol Av2.

Stopped-flow and rapid-freeze methods

Stopped-flow spectrophotometry was performed with a HI-TECH SF-51 stopped-flow apparatus (Salisbury, Wilts, U. K.) equipped with an anaerobic kit and a data

acquisition and analysis system. The mixing ratio was 1:1. The absorbance changes were measured at 430 nm. In calculating the absorbance changes a dead reaction time of 1.5 ms was taken into account. Syringe one contained 20 μM Av1 and 120 μM Av2; the other syringe contained 10 mM ATP. Both syringes contained 10 mM MgCl_2 , 5 mM $\text{Na}_2\text{S}_2\text{O}_4$ and 50 mM Tes/NaOH, final pH 7.4. The concentration of NaCl, if present in the reaction mixture, and the reaction temperature were as indicated in the figure legends.

Rapid-freeze experiments were performed with a home-built rapid-mixing apparatus, equipped with 2.5 ml Hamilton syringes (gastight), HPLC valves (Valco) and PEEK tubing (Upchurch Scientific Inc.) to connect the syringes with the mixing chamber and for the aging hose. The end of the aging hose was connected to a nozzle from which the reaction mixture sprayed into a funnel to which an EPR tube was connected with a rubber tubing. With the shortest delay line possible, the minimal reaction time was 17 ms. Both the funnel and the EPR tube were immersed in a cold isopentane solution ($\sim -140^\circ\text{C}$; the isopentane solution was cooled down with $\text{N}_2(\text{l})$ until the solution became viscous). The formed "snow" was packed in the EPR tube and kept in liquid nitrogen for further analysis by EPR spectroscopy. EPR spectra were obtained with a Bruker EPR-200 D spectrometer, with peripheral instrumentation and data acquisition as described elsewhere (Pierik & Hagen, 1991).

For the freeze experiments performed to study the effect of both a high salt concentration and a low reaction temperature, the reaction mixture was not sprayed in a cold isopentane solution, but, after a delay in the aging hose, pushed directly into an EPR tube. The argon flushed aging hose was just prior to the experiment inserted into the argon flushed and isopentane cooled EPR tube about three cm from the bottom of the tube. Immediately after the experiment the tube was immersed into liquid N_2 cooled isopentane. No gas bubbles were present. The freezing time was determined from the reaction of oxidized myoglobin (Fe^{3+}) with sodium azide (Ballou & Palmer, 1974): this was 500 ± 50 ms. The reproducibility of the different samples ($\pm 5\%$, FeMoco signal) was better than with the spray method ($\pm 15\%$, FeMoco signal).

In the (rapid-) freeze experiments one syringe of the rapid-mixing apparatus contained 40 μM Av1 and 240 μM Av2, and the other syringe contained 10 mM ATP. Both syringes contained 5 mM $\text{Na}_2\text{S}_2\text{O}_4$ and 10 mM MgCl_2 in 50 mM Tes/NaOH, final pH 7.4. The concentration of NaCl, if present in the reaction mixture, and the reaction temperature were as indicated in the figure legends. Blanks were obtained by mixing a nitrogenase solution with buffer without MgATP.

The EPR conditions used for the measurements of the FeMoco $S = 3/2$ signal were: microwave frequency, 9.30 GHz; microwave power, 20 mW; modulation frequency, 100 kHz; modulation amplitude, 2.0 mT; temperature 6.3 K. The conditions

used for the measurements of EPR signals of oxidized P-cluster were: microwave frequency, 9.18 GHz; microwave power, 200 mW; modulation frequency, 100 kHz; modulation amplitude, 2.0 mT; temperature 17 K. For the measurements of the Av2 $S = 1/2$ signal the EPR conditions were: microwave frequency, 9.18 GHz; microwave power, 31.7 mW; modulation frequency, 100 kHz; modulation amplitude, 1.25 mT; temperature 17 K.

The concentration of super-reduced FeMoco was calculated from the decrease (with respect to the amplitude at zero reaction time) in the amplitude of the $S = 3/2$ feature at $g = 3.64$ (since the experiments started with dithionite-reduced Av1, electron transfer from Av2 to Av1 causes "super-reduction" of Av1). The decrease in the amplitude of the Av2 $S = 1/2$ signal at $g = 1.94$ was used to estimate the concentration of oxidized Av2. An accurate determination of the concentration of oxidized Av2 was hampered because binding of MgATP or MgADP to Av2 changes the shape of the $S = 1/2$ EPR signal and also causes a different distribution of the Av2 $S = 1/2$ and $S = 3/2$ spin-states (Hagen et al., 1985). The presence of Av1 also interfered with the Av2 $S = 1/2$ signal, because the FeMoco $S = 3/2$ signal has a g -value 2.0. Instead of double-integrating the whole Av2 $S = 1/2$ signal for quantification, we normalized the amplitude of the Av2 $g = 1.94$ feature of the obtained signals, to the amplitude at $g = 1.94$ of free Av2. The ratio between the amplitudes of the $g = 1.94$ feature of Av2 in the absence of a nucleotide, in the presence of MgATP and MgADP is 1 : 0.995 : 1.131, respectively (Prof. W. R. Hagen, personal communication). The error in the data points (see Table 1) was estimated from the difference in the EPR signals of three blanks.

The rate-limiting step(s) of nitrogenase catalysis was obtained from the specific acetylene reduction activity, determined with saturating Av2 ($[Av2]/[Av1] = 20$) and reductant (5 mM sodium dithionite plus 100 μ M flavodoxin), at various salt concentrations and reaction temperatures. It was checked that there was no significant H_2 evolution under all experimental conditions, thus the reported activities are a measure of the flux of electrons through nitrogenase. From the acetylene reduction activity a rate constant for the rate-limiting step(s) of nitrogenase catalysis was calculated.

All buffers used in the experiments were saturated with argon. ATP (special quality) was obtained from Boehringer.

Results

Effect of salt on the pre-steady-state absorbance changes

The electron transfer from the Fe protein to the MoFe protein can be monitored by stopped-flow spectrophotometry. Immediately after mixing of both nitrogenase proteins with MgATP (in the presence of a reductant) the absorbance at 430 nm increases due to the transfer of the first electron from the Fe protein to the MoFe protein. This absorbance increase is mainly caused by the absorbance change associated with the oxidation of the Fe protein in the electron transfer reaction (Thorneley, 1975; Thorneley & Cornish-Bowden, 1977). The molecular absorbance coefficient for electron transfer from Av2 to Av1 is: $\epsilon_{430} = 4.85 \text{ (mM Av1}^*)^{-1} \cdot \text{cm}^{-1}$ (Av1* is one of the two independently functioning halves of the MoFe protein), according to Mensink and Haaker (1992).

The effect of NaCl on the amplitude of the absorbance increase at 430 nm and the observed rate constant, associated with the electron transfer, is shown in Figure 1A. NaCl decreased both the amplitude of the stopped-flow signal (ΔA_{430}) and the observed rate of electron transfer: a Hill plot for the effect of NaCl on the observed rate constant (k_{obs}) is given in Figure 1B. The data fitted to a Hill coefficient of 2.1, which suggests that the inhibition of NaCl on the observed rate of electron transfer occurs in a cooperative fashion. This is an indication that the electron transfer reaction should probably not be represented as a single electron transfer reaction.

No difference was observed between the stopped-flow traces obtained when the nitrogenase proteins were pre-equilibrated with NaCl before mixing with MgATP, and the stopped-flow traces obtained when the nitrogenase proteins (without NaCl) were mixed MgATP and NaCl at once (data not shown). From these observations it must be inferred that the effect of NaCl is complete within the mixing time of the stopped-flow spectrophotometer. This implies that in the model of Deits and Howard (1990) binding of NaCl to the nitrogenase complex and the subsequent dissociation of the component proteins must be fast.

The decrease of the observed rate constant and of the amplitude of the absorbance increase associated with the pre-steady-state electron transfer by NaCl, might be caused by inhibition of the association of the nitrogenase proteins in the presence of salt (Willing et al., 1989). To verify this hypothesis, the effect of the ratio $[\text{Av2}]/[\text{Av1}]$ on k_{obs} and ΔA_{430} was studied in the absence and presence of NaCl. Av1 is an $\alpha_2\beta_2$ -tetramer, and each $\alpha\beta$ -dimer contains one FeMoco and one binding site for Av2. In the absence of salt, the maximum pre-steady-state electron transfer (maximum ΔA_{430}) would be expected at a ratio $[\text{Av2}]/[\text{Av1}] = 2$. However, this was not the case: to obtain the

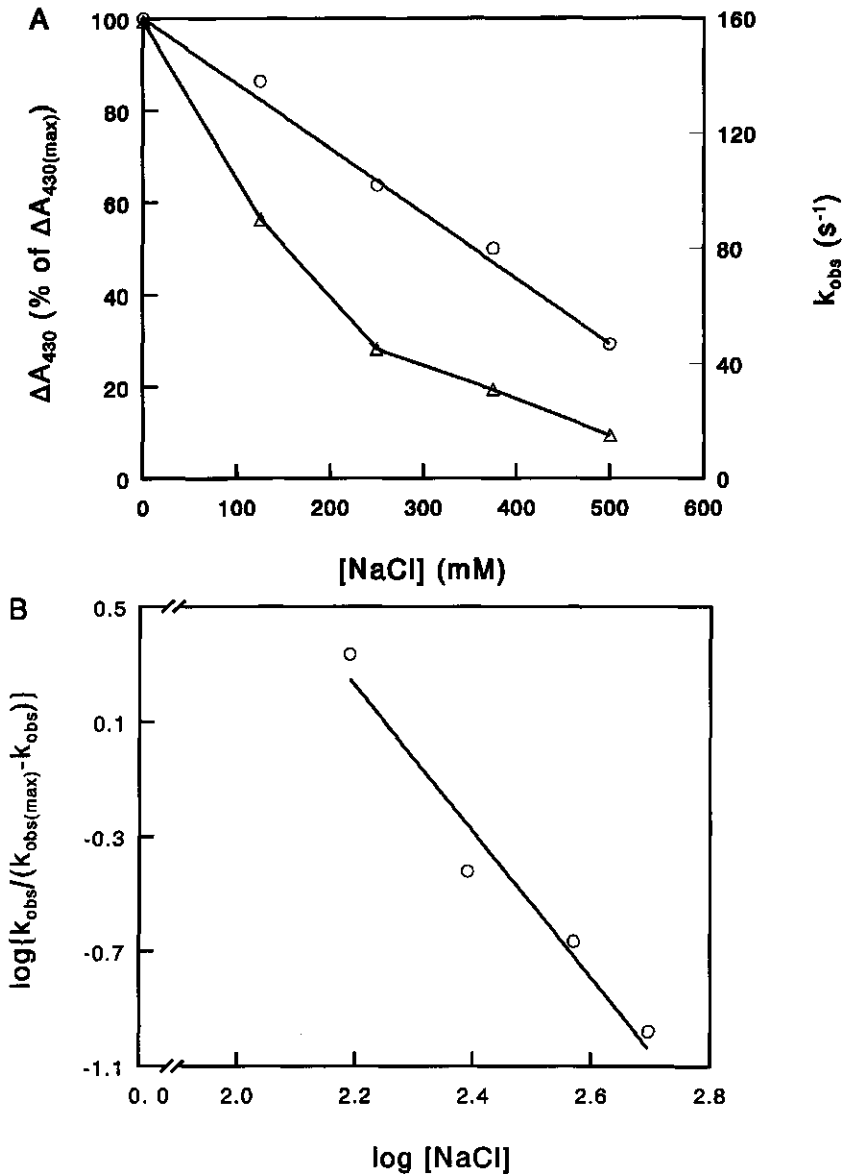


Figure 1. Effect of the NaCl concentration on the absorbance change at 430 nm and the observed rate constant associated with electron transfer. The reaction temperature was 23.0 ± 0.1 °C. (A) The absorbance increase (ΔA_{430}), \circ ; and observed rate constant (k_{obs}), Δ ; caused by the MgATP-dependent electron transfer from Av2 to Av1. The maximum absorbance change, obtained in the absence of NaCl, is: $\Delta A_{430(\max)} = 0.097$ ($[\text{Av1}] = 10 \mu\text{M}$). (B) A Hill plot for the observed rate constant (k_{obs}) of the MgATP-dependent electron transfer. The rate constant observed in the absence of NaCl is: $k_{\text{obs}} = 159 \text{ s}^{-1}$.

maximum amplitude a higher ratio $[Av2]/[Av1]$ was necessary. To explain their observation that the specific activity of the Fe protein from *Klebsiella pneumoniae* is only 45% of the calculated value, Thorneley and Lowe (1984) assumed that only 45% of all Kp2 present is active. The remaining 55% is considered to be capable of binding to Kp1 (with lower rate constants for association and dissociation than active Kp2), but is inactive with respect to electron transfer. This assumption also explains the need for a ratio $[Kp2]/[Kp1] \geq 4.5$ to obtain maximum electron transfer (Ashby & Thorneley, 1987). The nitrogenase proteins from *A. vinelandii* show the same phenomenon. The maximum value for ΔA_{430} was obtained at $[Av2]/[Av1] = 6$, both in the absence and presence of 250 mM NaCl, at 23 °C (data not shown). Thus, it must be concluded that NaCl has no effect on the ratio $[active\ Av2]/[inactive\ Av2]$. However, the absorbance change in the presence of 250 mM NaCl with $[Av2]/[Av1] \geq 6$ was only $\Delta A_{430} = 0.063$ (see Figure 1A), which corresponds with $\epsilon_{430} = 3.15 \pm 0.3\ (mM\ Av1^*)^{-1} \cdot cm^{-1}$ ($[Av1] = 10\ \mu M$). This value differs significantly from the value of $\epsilon_{430} = 4.85 \pm 0.3\ (mM\ Av1^*)^{-1} \cdot cm^{-1}$ which was obtained in the absence of NaCl (Mensink & Haaker, 1992). In the presence of 250 mM NaCl, the observed rate constants increased from $23\ s^{-1}$ at a ratio $[Av2]/[Av1] = 1$, to $34\ s^{-1}$ at $[Av2]/[Av1] = 12$ (data not shown). In this experiment the protein concentration ($[Av1] = 5\ \mu M$) was lower than in the experiment of Figure 1A ($[Av1] = 10\ \mu M$). In the experiment of Figure 1A, at 250 mM NaCl, electron transfer occurred with $k_{obs} = 45\ s^{-1}$ ($[Av2]/[Av1] = 6$). If the concentrations of the nitrogenase proteins are low ($< 0.5\ \mu M$), the so-called dilution effect occurs: the specific activity decreases as the total protein concentration decreases. This effect is due to the rate of association of the (reduced) Fe protein with the MoFe protein becoming rate-limiting at low protein concentrations (Thorneley & Lowe, 1984). Evidently, in the presence of 250 mM NaCl the dilution effect on nitrogenase activity is significant at $[Av1] = 5\ \mu M$. NaCl affects nitrogenase activity by binding to the Fe protein and inhibition of the formation of the nitrogenase complex (Deits & Howard, 1990). The lower observed rate constants of electron transfer at low protein concentrations and at low ratios $[Av2]/[Av1]$ can therefore be explained by an initially smaller amount of binding sites on Av1 being occupied by Av2. During the electron transfer reaction the non-occupied Av2 binding sites on Av1 will eventually also bind Av2, which results in electron transfer. This lowers the observed rate constant of the electron transfer reaction. Without salts there is no additional complex formation at the time scale of the electron transfer reaction. The observed rate constant of electron transfer did not change with the ratio $[Av2]/[Av1]$ when salt was absent from the reaction mixture (data not shown), which must probably be attributed to a larger fraction of Av1 which is complexed to Av2.

Relation between the absorbance changes and the redox state of the metal-sulphur clusters

A decrease of the reaction temperature (in the absence of NaCl) leads to a decrease of the absorbance amplitude and the observed rate constant of electron transfer. This effect on the stopped-flow signal was described earlier (Thorneley et al., 1989; Mensink & Haaker, 1992). It was suggested that electron transfer from the Fe protein to the MoFe protein is reversible at lower temperatures (5 °C) and mainly irreversible above 20 °C. This would explain the diminished absorbance increase and observed rate constant at lower reaction temperatures.

Figure 2 summarizes the influence of the NaCl concentration and the reaction temperature on the absorbance changes at 430 nm, observed after mixing of the nitrogenase proteins with MgATP. Note that the traces A, B, C and D in Figure 2 have different time-axes.

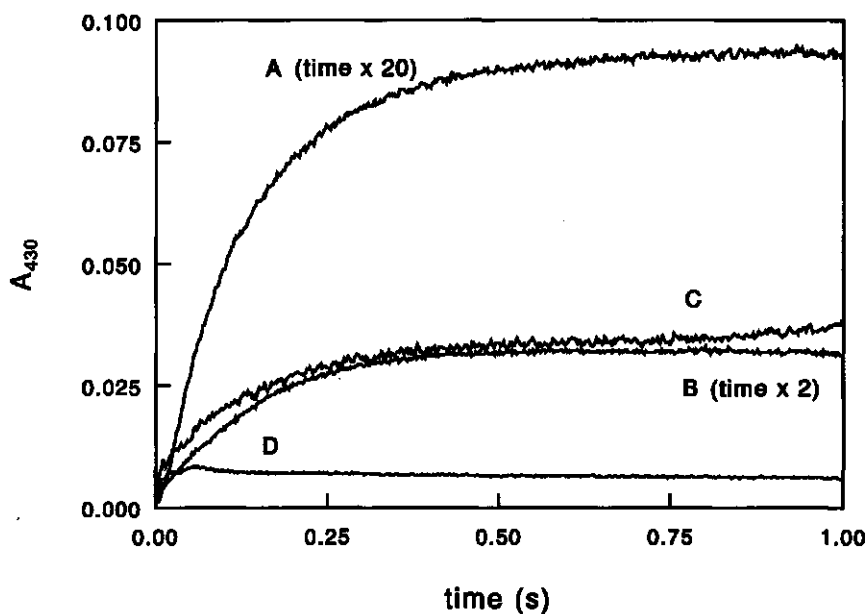


Figure 2. The influence of the temperature and the salt concentration of the reaction mixture on the absorbance changes at 430 nm (A_{430}). (A) and (B) were obtained at 23.0 ± 0.1 °C; (C) and (D) at 5.0 ± 0.1 °C. Reaction mixture (A) and (C) did not contain salt, (B) contained 500 mM NaCl and (D) contained 250 mM NaCl. The traces have different time-axes: the time-axis of trace (A) and trace (B) was multiplied by a factor 20 and 2, respectively (the actual time span of the traces was 50 ms and 0.5 s, respectively), whereas traces (C) and (D) are real 1 s traces.

Table 1. The effect of the temperature and the salt concentration on the pre-steady-state electron transfer and on the redox state of FeMoco, as determined by stopped-flow spectrophotometry and EPR rapid-freeze spectroscopy.

| | condition and reaction time | stopped-flow | | | | EPR | |
|-----|-----------------------------|-------------------------------------|------------------------------------|---|--------------------------|--------------------------|--------------------------------|
| | | k_{obs} rate-limiting step | k_{obs} electron transfer | ΔA_{430} (% of $\Delta A_{430(\text{max})}$) | super-reduced FeMoco (%) | FeMoco (μM) | oxidized Av2 (μM) |
| (A) | 23 °C, no NaCl (0.03 s) | 4.6 | 159 | 98% | 100% | 36 \pm 5 | 42 \pm 25 |
| (B) | 23 °C, 500 mM NaCl (0.5 s) | 1.1 | 13.8 | 33% | 83% | 30 \pm 5 | 51 \pm 25 |
| (C) | 5 °C, no NaCl (0.5 s) | 0.08 | 7.1 | 35% | 40% | 14 \pm 5 | 23 \pm 25 |
| (D) | 5 °C, 250 mM NaCl (8 s) | 0.004 | - | - | 45% | 16 \pm 5 | 47 \pm 25 |

In the stopped-flow experiments the concentrations after mixing were: Av1 = 10 μM (18 μM Mo) and Av2 = 60 μM (54 μM [4Fe-4S] cluster). In the rapid-freeze experiments the concentrations after mixing were: Av1 = 20 μM (36 μM Mo) and Av2 = 120 μM (108 μM [4Fe-4S] cluster). (A), (B), (C) and (D) correspond to traces A, B, C and D in Figure 2. The k_{obs} of the rate-limiting step (calculated from the specific acetylene reduction activity) and the k_{obs} of electron transfer are expressed in s^{-1} . The calculated maximum absorbance increase at 430 nm, $\Delta A_{430(\text{max})} = 0.097$ (Mensink & Haaker, 1992). The heights of the FeMoco S = 3/2 signal (at $g = 3.64$) and the Av2 S = 1/2 signal (at $g = 1.94$) were determined at the reaction time (shown between brackets under "condition") when the absorbance increase (ΔA_{430}) reached the observed maximum.

The EPR rapid-freeze technique was used to check whether reversible electron transfer is manifested in the redox state of the nitrogenase proteins at a low reaction temperature or a high NaCl concentration. It must be realized that the protein concentrations used in the EPR rapid-freeze experiments are two times higher than in the stopped-flow experiments.

Table 1 combines the results of stopped-flow and rapid-freeze EPR experiments.

At 23 °C, in the absence of NaCl, the absorbance increase (see Figure 2, curve A) could be fitted to a single exponential: $\Delta A_{430} = 0.095$, with a rate constant $k_{\text{obs}} = 159 \text{ s}^{-1}$. The absorbance increase was 98% of the calculated maximum value ($\Delta A_{430(\text{max})} = 0.097$, $[\text{Avl}] = 10 \text{ } \mu\text{M}$), see Table 1. The stopped-flow data predicted almost complete reduction of FeMoco. This was confirmed by the EPR rapid-freeze data: all FeMoco (36 μM) was super-reduced at the time when the absorbance maximum was reached (30 ms). The specific activity was $1200 \text{ nmol C}_2\text{H}_2 \cdot \text{min}^{-1} \cdot (\text{mg Avl})^{-1}$, from which the rate constant of the rate-limiting step of catalysis (at 23 °C, in the absence of salt) was calculated: $k_{\text{obs}} = 4.6 \text{ s}^{-1}$, see Table 1.

At 23 °C in the presence of 500 mM NaCl (Figure 2, curve B), the absorbance increase was 33% of the calculated maximum absorbance increase ($\Delta A_{430} = 0.032$), with $k_{\text{obs}} = 13.8 \text{ s}^{-1}$. The specific activity was 25% of the specific activity in the absence of NaCl, at 23 °C, resulting in $k_{\text{obs}} = 1.1 \text{ s}^{-1}$ for the rate-limiting step. The expected super-reduction of FeMoco was not confirmed by the rapid-freeze EPR measurements: at 0.5 s after mixing 83% of FeMoco was super-reduced, whereas, based on the observed absorbance increase, super-reduction of only 33% of FeMoco was expected.

At 5 °C, in the absence of NaCl (Figure 2, curve C), the absorbance increase was 35% of the calculated maximum value ($\Delta A_{430} = 0.034$) with $k_{\text{obs}} = 7.1 \text{ s}^{-1}$. At 0.5 s after mixing, the amount of super-reduced FeMoco, judged by the rapid-freeze EPR data, fairly corresponded with the prediction of the reduction of 35% of all FeMoco present: 40% of the FeMoco $S = 3/2$ signal had disappeared. The specific acetylene reduction activity was only 2% of the specific activity observed at 23 °C, resulting in $k_{\text{obs}} = 0.08 \text{ s}^{-1}$ for the rate-limiting step.

When the reaction temperature was 5.0 °C and 250 mM NaCl was present in the reaction mixture, hardly any activity was measured: $k_{\text{obs}} = 0.004 \text{ s}^{-1}$ for the rate-limiting step (see Table 1). Small absorbance changes could still be observed, see Figure 2, curve D, and Figure 3. Immediately after mixing of the nitrogenase proteins with MgATP the absorbance increased with $\Delta A_{430} = 0.011$ and $k_{\text{obs}} = 199 \text{ s}^{-1}$ (see Figure 2, curve D). The rate constant of this absorbance increase is too high to be related to electron transfer from the Fe protein to the MoFe protein at this low reaction temperature (Mensink & Haaker, 1992) and high salt concentration. This absorbance

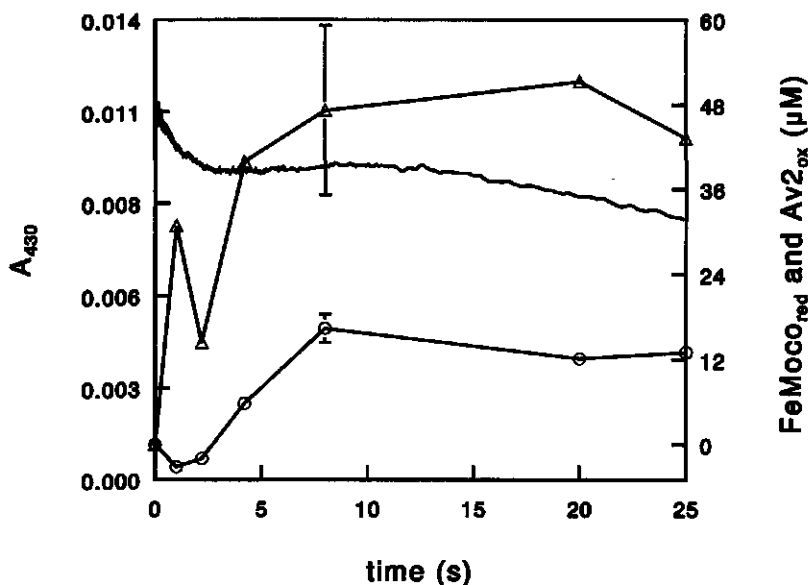


Figure 3. The absorbance changes (A_{430}) and the super-reduction of FeMoco at 5 °C in the presence of 250 mM NaCl. The reaction mixtures in the stopped-flow and the rapid-freeze experiments contained 250 mM NaCl; the reaction temperature was 5.0 ± 0.2 °C. From the rapid-freeze EPR data the amount of super-reduced FeMoco ($\text{FeMoco}_{\text{red}}$) (○); and oxidized Av2 (Av2_{ox}) (△) were determined. The error bar given on one rapid-freeze EPR data point is representative of the error on each of the data points.

increase might be associated with the binding of MgATP to the nitrogenase complex. After 50 ms the absorbance increase was followed by a small decrease, with $\Delta A_{430} = 0.002$ and $k_{\text{obs}} = 1.1 \text{ s}^{-1}$. After the absorbance decrease some minor absorbance changes were observed. The rapid-freeze EPR measurements however indicated significant super-reduction of FeMoco, see Table 1.

In the absence of salt, the absorbance increase at 430 nm is a good measure of the electron transfer from the Fe protein to FeMoco at the MoFe protein. However, in the presence of NaCl, the absorbance increase does not give a good estimation of the amount of super-reduced FeMoco.

The kinetics of the super-reduction of FeMoco was studied in more detail by rapid-freeze EPR. Since the lowest reaction time in the rapid-freeze experiment was ~17 ms (see Materials and Methods) we did not attempt to determine the kinetics of the super-reduction of FeMoco at 23 °C without NaCl. At 23 °C in the presence of 500 mM NaCl,

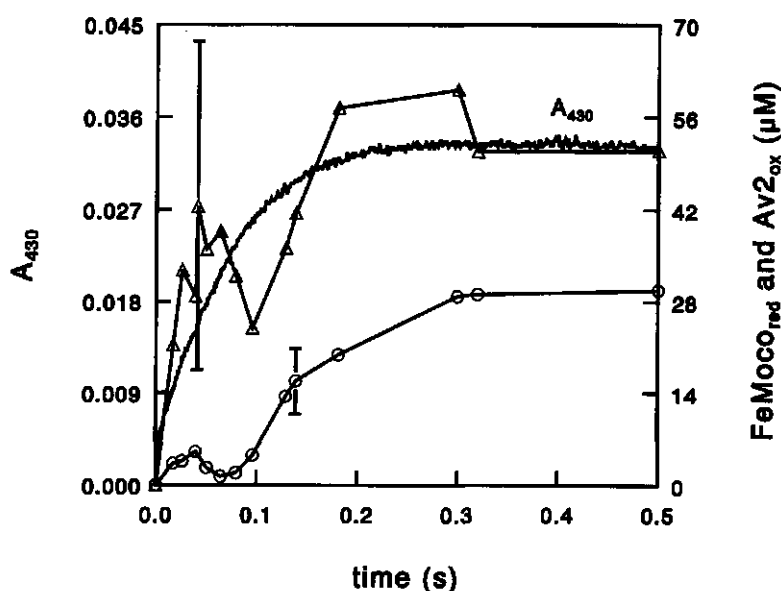


Figure 4. The difference between the kinetics of the absorbance changes (A_{430}) and the kinetics of the super-reduction of FeMoco, at 23 °C in the presence of 500 mM NaCl. Both in the stopped-flow and the rapid-freeze EPR experiment the reaction mixture contained 500 mM NaCl; the reaction temperature was 23.0 ± 0.2 °C. The calculated maximum absorbance change at 430 nm is $A_{430(\text{max})} = 0.097$. From the rapid-freeze EPR data the amount of super-reduced FeMoco ($\text{FeMoco}_{\text{red}}$) (\circ); and oxidized Av2 (Av2_{ox}) (Δ) were determined. The error bar given on one rapid-freeze EPR data point is representative of the error on each of the data points.

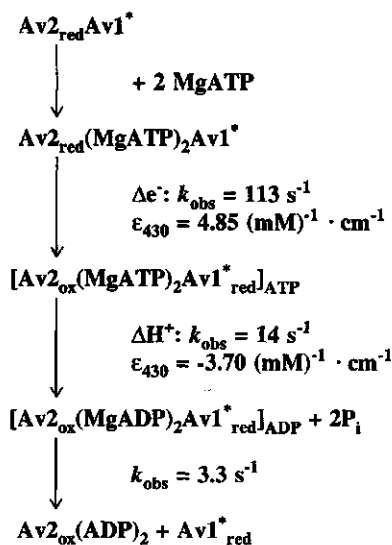
the kinetics of the decrease of the FeMoco $S = 3/2$ signal was different from the kinetics of the absorbance increase, see Figure 4. The absorbance increase started immediately after mixing of the nitrogenase proteins with MgATP, whereas the FeMoco $S = 3/2$ signal started to decrease only after a delay of about 100 ms. The oxidation of Av2 went together with the absorbance increase, see Figure 4. At 5 °C without NaCl, the super-reduction of FeMoco went together with the increase of the stopped-flow signal (data not shown). At 5 °C, in the presence of 250 mM NaCl, the FeMoco $S = 3/2$ signal started decreasing after a delay of 2 s (after mixing of the nitrogenase proteins with MgATP), indicating electron transfer to or from FeMoco, see Figure 3. From 8 s after mixing the height of the FeMoco $S = 3/2$ signal remained more or less constant, at about 55% of its height at zero reaction time (see Table 1 and Figure 4). The Av2 $S = 1/2$ signal started decreasing immediately after mixing of the nitrogenase proteins with MgATP. No indication of EPR signals of oxidized P-clusters as reported by Pierik et al.

(1993) and Tittsworth and Hales (1993), or other signals (in perpendicular and parallel mode EPR) were found in the EPR samples during the reaction.

Discussion

The pre-steady-state absorbance increase (at 430 nm) has been used to monitor the electron transfer from the Fe protein to the MoFe protein of nitrogenase: the oxidation of the [4Fe-4S] cluster of the Fe protein and the super-reduction of FeMoco of the MoFe protein. The absorbance increases because the molecular absorbance coefficient of the redox change of the Fe protein is at least five times larger than the molecular absorbance coefficient of the MoFe protein upon reduction (Ashby & Thorneley, 1987). The lower absorbance increase as observed at a low reaction temperature (5 °C) was explained by a reversible electron transfer between the Fe protein and the MoFe protein (as proposed by Thorneley et al. (1989) and Mensink and Haaker (1992)). Also in the presence of NaCl only a partial electron transfer reaction is predicted from stopped-flow spectrophotometry. The results of the rapid-freeze EPR experiments in the present study, however, indicated significantly more super-reduction of FeMoco under these circumstances and therefore reversible electron transfer between the nitrogenase proteins cannot account for the diminished absorbance change.

As explained in Materials and Methods, the amount of oxidized Av2 could not be determined accurately from the rapid-freeze EPR measurements. The shape of the Av2 $S = 1/2$ signal and the distribution of the Av2 $S = 1/2$ and $S = 3/2$ spin states change when MgATP or MgADP binds to Av2 (Hagen et al., 1985). The FeMoco $S = 3/2$ signal has a g -value 2.0, which interferes with the Av2 $S = 1/2$ signal. This makes quantification of the Av2 $S = 1/2$ signal (by double-integration) highly problematic. However, the amplitude of the $g = 1.94$ feature does not vary too much whether Av2 is free, MgATP- or MgADP-bound, and was used (after normalizing for the amplitude of free Av2) for quantification. The next reason also makes the Av2 data points less accurate than the FeMoco data points. A ratio $[Av2]/[Av1] = 6$ had to be used to saturate the electron transfer reaction; therefore Av2 is partially oxidized under standard conditions whereas almost all FeMoco can be super-reduced. The large scatter (Figure 4, Table 1) in the Av2 data points might also be caused by a change of the distribution of the Av2 $S = 1/2$ and $S = 3/2$ spin states during freezing of the EPR samples. All this makes a calculation of oxidation of Av2 not accurate.



Scheme 1. Pre-steady-state reactions of nitrogenase with MgATP. All rate constants were measured for *A. vinelandii* nitrogenase. Av1^* : one of two independently functioning halves of the MoFe protein; $\text{Av1}_{\text{red}}^*$: MoFe protein with super-reduced FeMoco, Av2_{red} and Av2_{ox} : reduced and oxidized Fe protein, respectively; $[\text{Av2}(\text{MgATP})_2\text{Av1}^*]_{\text{ATP}}$ or $[\text{Av2}(\text{MgADP})_2\text{Av1}^*]_{\text{ADP}}$: the nitrogenase complex is in the MgATP-bound or MgADP-bound conformation, respectively; $\Delta\epsilon^-$: electron transfer from the Fe protein to the MoFe protein is observed; ΔH^+ : proton production is observed; ϵ_{430} (in $(\text{mM Av1}^*)^{-1} \cdot \text{cm}^{-1}$): an absorbance change at 430 nm is observed. The observed rate constants apply for the reactions at 20 °C.

We would like to explain the data presented in this paper with our present scheme of the ATPase reaction of nitrogenase (Duyvis et al., 1996), see Scheme 1. After binding of MgATP to the nitrogenase proteins and subsequent change of the conformation of the nitrogenase complex to the MgATP-bound conformation, Av2 transfers one electron to Av1: $\epsilon_{430} = 4.85 (\text{mM Av1}^*)^{-1} \cdot \text{cm}^{-1}$ (Mensink & Haaker, 1992). After electron transfer MgATP is hydrolysed and the conformation of the nitrogenase complex changes to the MgADP-bound conformation, which causes a decrease of the absorbance at 430 nm: $\epsilon_{430} = -3.70 (\text{mM Av1}^*)^{-1} \cdot \text{cm}^{-1}$. This reaction is followed by dissociation of the nitrogenase complex.

The effect of salt on the kinetics of the electron transfer from Av2 to Av1 can be explained by assuming that the change of the nitrogenase complex to the MgATP-bound conformation and the consequent electron transfer reaction are inhibited by the presence of salt; the hydrolysis of MgATP and subsequent change of the nitrogenase complex to

the MgADP-bound conformation are less inhibited. The absorbance increase associated with electron transfer from Av2 to Av1 does not reach the calculated maximum value, because it is overtaken by the subsequent absorbance decrease, associated with the change to the MgADP-bound conformation of the nitrogenase complex.

The difference in the kinetics of the absorbance increase and of the super-reduction of FeMoco when 500 mM NaCl is present at 23 °C (Figure 4), as well as the delay of the super-reduction of FeMoco at 5 °C with 250 mM NaCl present (Figure 3), both indicate that the electron transfer reaction is not a single one-electron transfer from the [4Fe-4S] cluster of Av2 directly to FeMoco. It is possible that another redox site is involved in the electron transfer reaction. This primary electron acceptor of Av2 might be the P-cluster, as proposed by Peters et al. (1995), but we did not observe any EPR signals confirming this proposal. It has been suggested in the literature that, as all iron atoms of the P-cluster are in the ferrous state (Surerus et al., 1992), the disulphide bridge of the P-cluster might be reduced during catalysis (Chan et al., 1993; Howard & Rees, 1994).

At 5 °C both the electron transfer from Av2 to Av1 and the conformational change of the nitrogenase complex after MgATP hydrolysis (to the MgADP-bound conformation) become slower. Reversibility of the electron transfer reaction might well be the cause of the diminished absorbance increase and the partial super-reduction of FeMoco.

At 5 °C in the presence of 250 mM NaCl (Figure 3), electron transfer to or from FeMoco occurred although no increase of the absorbance was observed. Both the temperature effect and the salt effect contribute to the lowering of the amplitude of the stopped-flow signal.

Acknowledgements

We thank Prof. W. R. Hagen for performing the EPR spectroscopy and Prof. C. Veeger and Prof. N. C. M. Laane for critically reading the manuscript. This investigation was supported by the Netherlands Foundation for Chemical Research (SON) with financial aid from the Netherlands Organization for Scientific Research (NWO).

References

- Ashby, G. A. & Thorneley, R. N. F. (1987) Nitrogenase of *Klebsiella pneumoniae*. Kinetic studies on the Fe protein involving reduction by sodium dithionite, the binding of MgADP and a conformation change that alters the reactivity of the 4Fe-4S centre, *Biochem. J.* 246, 455-465.
- Ballou, D. P. & Palmer, G. A. (1974) Practical rapid-quenching instrument for the study of

- reaction mechanisms by electron paramagnetic resonance, *Anal. Chem.* 46, 1248-1253.
- Bolin, J. T., Campobasso, N., Muchmore, S. W., Morgan, T. V. & Mortenson, L. E. (1993) Structure and environment of metal clusters in the nitrogenase molybdenum-iron protein from *Clostridium pasteurianum*, in: *Molybdenum enzymes, cofactors and model systems* (Stiefel, E. I., Coucouvanis, D. & Newton, W. E., eds.) pp. 186-195, American Chemical Society, Washington.
- Burns, A., Watt, G. D. & Wang, Z. C. (1985) Salt inhibition of nitrogenase catalysis and salt effects on the separate protein components, *Biochemistry* 24, 3932-3936.
- Chan, M. K., Kim, J. & Rees, D. C. (1993) The nitrogenase FeMo-cofactor and P-cluster pair: 2.2 Å resolution structures, *Science* 260, 792-794.
- Deits, T. L. & Howard, J. B. (1990) Effect of salts on *Azotobacter vinelandii* nitrogenase activities. Inhibition of iron chelation and substrate reduction, *J. Biol. Chem.* 265, 3859-3867.
- Duyvis, M. G., Wassink, H. & Haaker, H. (1996) Pre-steady-state kinetics of nitrogenase from *Azotobacter vinelandii*. Evidence for an ATP-induced conformational change of the nitrogenase complex as part of the reaction mechanism, *J. Biol. Chem.* 271, 29632-29636.
- Georgiadis, M. M., Komiya, H., Chakrabarti, P., Woo, D., Kornuc, J. J. & Rees, D. C. (1992) Crystallographic structure of the nitrogenase iron protein from *Azotobacter vinelandii*, *Science* 257, 1653-1659.
- Hagen, W. R., Eady, R. R., Dunham, W. R. & Haaker, H. (1985) A novel $S = 3/2$ EPR signal associated with native Fe-proteins of nitrogenase, *FEBS Lett.* 189, 250-254.
- Howard, J. B. & Rees, D. C. (1994) Nitrogenase: a nucleotide-dependent molecular switch, *Annu. Rev. Biochem.* 63, 235-264.
- Kim, J. & Rees, D. C. (1992a) Structural models for the metal centers in the nitrogenase molybdenum-iron protein, *Science* 257, 1677-1682.
- Kim, J. & Rees, D. C. (1992b) Crystallographic structure and functional implications of the nitrogenase molybdenum-iron protein from *Azotobacter vinelandii*, *Nature* 360, 553-560.
- Lowe, D. J. & Thorneley, R. N. F. (1984) The mechanism of *Klebsiella pneumoniae* nitrogenase action. Pre-steady-state kinetics of H_2 formation, *Biochem. J.* 224, 877-886.
- Mensink, R. E. & Haaker, H. (1992) Temperature effects on the MgATP-induced electron transfer between the nitrogenase proteins from *Azotobacter vinelandii*, *Eur. J. Biochem.* 208, 295-299.
- Mensink, R. E., Wassink, H. & Haaker, H. (1992) A reinvestigation of the pre-steady-state ATPase activity of nitrogenase from *Azotobacter vinelandii*, *Eur. J. Biochem.* 208, 289-294.
- Orme-Johnson, W. H., Hamilton, W. D., Jones, T. L., Tso, M.-Y. W., Burris, R. H., Shah, V. K. & Brill, W. J. (1972) Electron paramagnetic resonance of nitrogenase and nitrogenase components from *Clostridium pasteurianum* W5 and *Azotobacter vinelandii* OP, *Proc. Natl. Acad. Sci. USA* 69, 3142-3145.
- Peters, J. W., Fisher, K., Newton, W. E. & Dean, D. R. (1995) Involvement of the P cluster in intramolecular electron transfer within the nitrogenase MoFe protein, *J. Biol. Chem.* 270, 27007-27013.
- Pierik, A. J. & Hagen, W. R. (1991) $S = 9/2$ EPR signals are evidence against coupling between the siroheme and the Fe/S cluster prosthetic groups in *Desulfovibrio vulgaris* (Hildenborough) dissimilatory sulfite reductase, *Eur. J. Biochem.* 195, 505-516.
- Pierik, A. J., Wassink, H., Haaker, H. & Hagen, W. R. (1993) Redox properties and EPR spectroscopy of the P-clusters of *Azotobacter vinelandii* MoFe protein, *Eur. J. Biochem.* 212, 51-61.
- Smith, B. E., Lowe, D. J. & Bray, R. C. (1972) Nitrogenase of *Klebsiella pneumoniae*: electron-

- paramagnetic-resonance studies on the catalytic mechanism, *Biochem. J.* 130, 641-643.
- Smith, B. E., Lowe, D. J. & Bray, R. C. (1973) Studies by electron paramagnetic resonance on the catalytic mechanism of nitrogenase of *Klebsiella pneumoniae*, *Biochem. J.* 135, 331-341.
- Surerus, K. K., Hendrich, M. P., Christie, P. D., Rottgardt, D., Orme-Johnson, W. H. & Münck, E. (1992) Mössbauer and integer-spin EPR of the oxidized P-clusters of nitrogenase: P^{ox} is a non-Kramers system with a nearly degenerate ground doublet, *J. Am. Chem. Soc.* 114, 8579-8590.
- Thorneley, R. N. F. (1975) Nitrogenase of *Klebsiella pneumoniae*. A stopped-flow study of magnesium-adenosine-triphosphate-induced electron transfer between the component proteins, *Biochem. J.* 145, 391-396.
- Thorneley, R. N. F., Ashby, G., Howarth, J. V., Millar, N. C. & Gutfreund, H. (1989) A transient-kinetic study of the nitrogenase of *Klebsiella pneumoniae* by stopped-flow calorimetry. Comparison with myosin ATPase, *Biochem. J.* 264, 657-661.
- Thorneley, R. N. F. & Cornish-Bowden, A. (1977) Kinetics of nitrogenase of *Klebsiella pneumoniae*. Heterotropic interactions between magnesium-adenosine 5'-diphosphate and magnesium-adenosine 5'-triphosphate, *Biochem. J.* 165, 255-262.
- Thorneley, R. N. F. & Lowe, D. J. (1983) Nitrogenase of *Klebsiella pneumoniae*. Kinetics of the dissociation of oxidized iron protein from molybdenum-iron protein: identification of the rate-limiting step for substrate reduction, *Biochem. J.* 215, 393-403.
- Thorneley, R. N. F. & Lowe, D. J. (1984) The mechanism of *Klebsiella pneumoniae* nitrogenase action. Simulation of the dependences of H_2 -evolution rate on component-protein concentration and ratio and sodium dithionite concentration, *Biochem. J.* 224, 903-909.
- Tittsworth, R. C. & Hales, B. J. (1993) Detection of EPR signals assigned to the 1-equiv-oxidized P-clusters of nitrogenase from *Azotobacter vinelandii*, *J. Am. Chem. Soc.* 115, 9763-9767.
- Willing, A. H., Georgiadis, M. M., Rees, D. C. & Howard, J. B. (1989) Cross-linking of nitrogenase components, *J. Biol. Chem.* 264, 8499-8503.
- Zumft, W. G., Mortenson, L. E. & Palmer, G. (1974) Electron-paramagnetic-resonance studies on nitrogenase. Investigation of the oxidation-reduction behaviour of azoferredoxin and molybdoferredoxin with potentiometric and rapid-freeze techniques, *Eur. J. Biochem.* 46, 525-535.

Chapter 6

Kinetics of nitrogenase from *Azotobacter vinelandii*: is dissociation of the nitrogenase complex necessary for catalysis?

Abstract

The nitrogenase enzyme system consists of two metalloproteins (Fe protein and MoFe protein) which associate and dissociate in order to transfer one electron to N_2 . This cycle, called the Fe protein cycle, is driven by MgATP hydrolysis and is repeated eight times until the substrate (N_2) is completely reduced. The kinetic constants of the first part of the Fe protein cycle: electron transfer from the Fe protein to the MoFe protein, on-enzyme MgATP hydrolysis and P_i/H^+ release, have been determined. The rate-limiting step of the cycle is supposed to be the dissociation of the nitrogenase complex, which is necessary for re-reduction of the Fe protein, followed by the exchange of MgADP for MgATP. This hypothesis was based on experiments with sodium dithionite as reductant. We used three different reductants (sodium dithionite, titanium (III) citrate and flavodoxin hydroquinone) to determine the rate-limiting step of the Fe protein cycle.

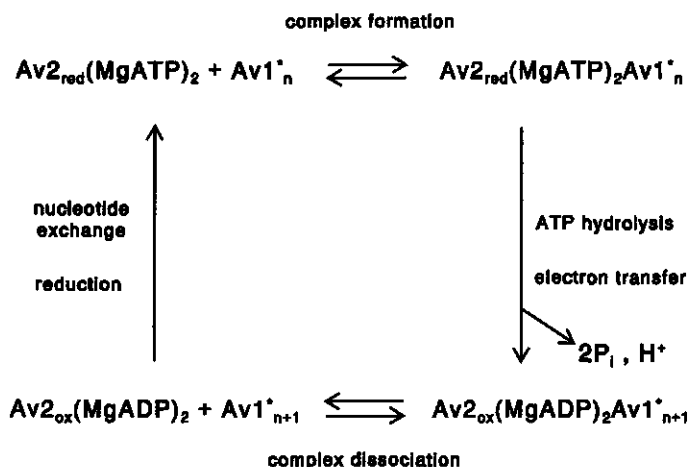
The rate of the reduction of (free) oxidized Fe protein with MgADP bound ($Av2_{ox}(MgADP)_2$) was independent of the reductant used: $k \sim 10^6 \text{ M}^{-1} \cdot \text{s}^{-1}$. In contrast to sodium dithionite, titanium (III) citrate and flavodoxin hydroquinone rapidly reduced $Av2_{ox}(MgADP)_2$ in the nitrogenase complex, without dissociation of the complex preceding the reduction of $Av2_{ox}(MgADP)_2$. Our results also indicated that dissociation of the reduced nitrogenase complex is not required for the exchange of MgADP for MgATP. Pre-steady-state electron uptake experiments indicated that after the reduction of Fe protein in the nitrogenase complex a slow step in the Fe protein cycle occurs. We propose that this slow step (11 s^{-1}) and the preceding P_i/H^+ release (14 s^{-1}) determine the rate of the Fe protein cycle and thus nitrogenase catalysis.

Introduction

The biological reduction of dinitrogen to ammonia is catalysed by nitrogenase, which consists of two oxygen-sensitive metalloproteins that are both necessary for catalysis (Howard & Rees, 1994). For the complete reduction of N_2 to $2 NH_3$ and H_2 (a side product of the nitrogenase reaction) a strong reductant (flavodoxin or ferredoxin *in vivo*, sodium dithionite *in vitro*) and MgATP, which is hydrolysed during catalysis, must be present. In the present investigation the molybdenum-containing nitrogenase from *Azotobacter vinelandii* is studied. The MoFe protein (Av1), a heterodimer of 230 kDa, contains two types of metal-sulphur clusters per $\alpha\beta$ -monomer: the FeMo cofactor (FeMoco) and the P-cluster. FeMoco is generally considered to be the substrate reduction site. The P-cluster might be involved in electron transfer from the Fe protein to FeMoco (Peters et al., 1995). Structural models for FeMoco and the P-cluster have been proposed, based on crystallographic analysis of the MoFe protein of *A. vinelandii* nitrogenase (Kim & Rees, 1992a,b; Chan et al., 1993); however, there still is discussion about the structure of the P-cluster (Bolin et al., 1993). The Fe protein (Av2) is a homodimer of 63 kDa, which contains a single [4Fe-4S] cluster and two nucleotide binding sites. The crystallographic structure of the *A. vinelandii* Fe protein was determined by Georgiadis et al. (1992). Binding of MgATP or MgADP to the Fe protein causes a change of the protein conformation (Walker & Mortenson, 1974; Ljones & Burris, 1978; Ashby & Thorneley, 1987) which leads to, for example, a decrease of the redox potential (Zumft et al., 1974; Braaksma et al., 1982; Watt et al., 1986) and changes in the EPR spectrum (Orme-Johnson et al., 1972; Zumft et al., 1972; Braaksma et al., 1982; Hagen et al., 1985) of the Fe protein. The crystal structure of the Fe protein revealed that the nucleotide binding region of the Fe protein is highly similar to the nucleotide binding region of the H-Ras p21 protein (Georgiadis et al., 1992; Wolle et al., 1992). The H-Ras p21 protein is a member of the group of molecular switch proteins, like myosin (Rayment et al., 1993a,b), the GTPases (Bourne, 1991), etc. These proteins use the binding and hydrolysis of nucleotides in order to switch between two different protein conformations, which determines whether the protein triggers a biochemical process or not. Because of the structural similarities it is meaningful to compare the kinetics of nitrogenase with the kinetics of the molecular switch proteins.

Hageman and Burris (1978) first proposed that the nitrogenase complex dissociates after the transfer of each electron from the Fe protein to the MoFe protein, implicating that for substrate reduction several cycles of association and dissociation of the nitrogenase proteins are necessary. The kinetic description of nitrogenase was further developed by Lowe and Thorneley (Lowe & Thorneley, 1984a; Thorneley & Lowe, 1983, 1985). They proposed a model (based on kinetic data for *Klebsiella pneumoniae*

nitrogenase, with sodium dithionite as the reductant) which comprises two cycles of electron transfer, called the Fe protein cycle and the MoFe protein cycle. In the Fe protein cycle (Scheme 1), after formation of the nitrogenase complex, one electron is transferred from the reduced Fe protein to the MoFe protein with concomitant hydrolysis of MgATP. Subsequently, the nitrogenase complex dissociates into the separate nitrogenase proteins, which is the rate-limiting step of the nitrogenase reaction when all reactants are saturating (Thorneley & Lowe, 1983). After dissociation of the complex the Fe protein must be reduced again by the electron donor after which MgADP is rapidly replaced by MgATP (Ashby & Thorneley, 1987). The MoFe protein cycle describes the stepwise reduction of the MoFe protein by succeeding Fe protein cycles, up to a maximal reduction level of eight electrons, necessary for the reduction of dinitrogen to ammonia and hydrogen.



Scheme 1. The Fe protein cycle (Thorneley & Lowe, 1983). Av1^* : one of the two independently functioning halves of the MoFe protein; Av1^*_{n} : Av1^* is reduced by n electrons.

The molecular mechanism of the MgATP hydrolysis driven electron transfer by nitrogenase is gradually becoming clear. It has been proposed that several conformational changes occur in the nitrogenase complex during the Fe protein cycle: the MgATP-bound conformation allows electron transfer from the Fe protein to the MoFe protein (Duyvis et al., 1994); the hydrolysis of MgATP is followed by a further conformational change and H^+ and P_i release (Duyvis et al., 1994; Lowe et al., 1995), which might be necessary for the electron transfer to continue in the proper direction

(Georgiadis et al., 1992) and for dissociation of the nitrogenase complex. Recently, we (Duyvis et al., 1996a) and Renner and Howard (1996) have independently shown that aluminium fluoride and MgADP or MgATP together can effectively stabilize the nitrogenase complex. In analogy to the interaction of several molecular switch proteins with aluminium fluoride and MgADP/MgGDP this conformation of the nitrogenase complex might be a stabilized transition state (during on-enzyme MgATP hydrolysis and before P_i release). The aim of this work is to describe the rate-limiting step of the Fe protein cycle of nitrogenase from *A. vinelandii*. To that end, several reactions of the Fe protein cycle were studied. These reactions include the proposed rate-limiting step of the Fe protein cycle - dissociation of the nitrogenase complex - and the reduction of oxidized Fe protein with MgADP bound. Three reductants were tested: sodium dithionite, titanium (III) citrate and flavodoxin hydroquinone. With Ti(III) citrate and flavodoxin it was possible to monitor the pre-steady-state and steady-state uptake of electrons by nitrogenase. Evidence is presented that the three tested reductants are able to reduce the Fe protein when it is still bound to the MoFe protein, without dissociation of the nitrogenase complex. Furthermore, it will be shown that nucleotide exchange does not require dissociation of the nitrogenase complex either. It will be discussed whether dissociation of the nitrogenase complex is obligatory at all for the Fe protein cycle of nitrogenase. An extended version of the Fe protein cycle is proposed, which is more in agreement with the present kinetic data than the original Fe protein cycle of Lowe and Thorneley (Thorneley & Lowe, 1983, 1985; Lowe & Thorneley, 1984a).

Materials and methods

Cell growth and isolation and preparation of nitrogenase

A. vinelandii ATCC strain 478 was grown and the separate nitrogenase proteins were isolated as described by Mensink et al. (1992). The molar concentrations of Av1 and Av2 were determined from their molecular masses of 230 kDa and 63 kDa, respectively. The activities of the nitrogenase components were determined from their specific acetylene reduction activity (Braaksma et al., 1982). The specific activities of the Av1 and Av2 preparations used in the experiments were at least 8 mol ethylene produced $\cdot s^{-1} \cdot (\text{mol Av1})^{-1}$ and 2 mol ethylene produced $\cdot s^{-1} \cdot (\text{mol Av2})^{-1}$, respectively. Av1 contained 1.8 ± 0.2 mol Mo/mol Av1; the Fe content of Av2 was 3.7 ± 0.2 mol Fe/mol Av2.

Dithionite-free nitrogenase complex was prepared by running both nitrogenase components together at the indicated ratio over a Biogel P-6DG column (Biorad, 1 cm \times

8 cm), which was equilibrated with argon-saturated 10 mM MgCl_2 and 100 mM NaCl in 50 mM Tes/NaOH, pH 7.4. Dye-oxidized Av2 was prepared with phenazine methosulphate (PMS), following a published procedure (Cordewener et al., 1985).

Chemicals

ADP and ATP (special quality) were obtained from Boehringer; PMS was obtained from Sigma; Ti(III)Cl_3 was obtained from Aldrich.

Stopped-flow experiments

The stopped-flow experiments were performed with a Hi-TECH SF-51 stopped-flow spectrophotometer, equipped with an anaerobic kit and a data acquisition and analysis system. All buffers used in the experiments were saturated with argon. All experiments were performed at $20.0 \pm 0.1^\circ\text{C}$, under argon. In all experiments the mixing ratio was 1:1. In calculating the absorbance changes a dead reaction time of 1.5 ms was taken into account, which was determined from the rate of the reduction of dichlorophenolindophenol by ascorbate, under appropriate conditions.

The electron transfer from Av2 to Av1 and the reduction of oxidized Av2 were measured by monitoring the absorbance changes at 430 nm. The molecular absorbance coefficient for electron transfer was: $\epsilon_{430} = 4.85 \text{ mM}^{-1} \cdot \text{cm}^{-1}$ (Mensink & Haaker, 1992).

The electron uptake by nitrogenase during turnover was measured by monitoring the absorbance changes at 340 nm when titanium (III) citrate was used as the reductant, or 580 nm when flavodoxin hydroquinone (from *A. vinelandii*) was used. The molecular absorbance coefficient for the oxidation of flavodoxin II (hydroquinone to semiquinone) was: $\epsilon_{580} = 5.7 \text{ mM}^{-1} \cdot \text{cm}^{-1}$ (Klugkist et al., 1986). Flavodoxin was reduced by excess $\text{Na}_2\text{S}_2\text{O}_4$ at pH 7.4, and subsequently separated from $\text{Na}_2\text{S}_2\text{O}_4$ on a Biogel P-6DG column, which was equilibrated with argon-saturated 2 mM MgCl_2 in 50 mM Tes/NaOH, pH 7.4. To avoid oxidation of Fld_{HQ} a small amount of $\text{Na}_2\text{S}_2\text{O}_4$ was added. In none of the experiments the Fld_{HQ} oxidation by nitrogenase was affected by $\text{Na}_2\text{S}_2\text{O}_4$ present, because the rate of reduction of Fld_{SQ} by SO_2^- is low ($k = 3 \cdot 10^4 \text{ M}^{-1} \cdot \text{s}^{-1}$). The molecular absorbance coefficient for the oxidation of Ti(III) citrate was: $\epsilon_{340} = 0.73 \text{ mM}^{-1} \cdot \text{cm}^{-1}$ (Seefeldt & Ensign, 1994). Ti(III) citrate was prepared from Ti(III)Cl_3 and sodium citrate, neutralized with an appropriate amount of Tris base, in an anaerobic glove-box (Zehnder, 1976). During the experiments it was observed that citrate

present in the Ti(III) citrate solutions slowly extracted Fe from the Fe protein. For this reason the Ti(III) citrate solutions were always added to the nitrogenase proteins only just before the measurements. With this procedure the experiments could be reproducibly performed within 5 minutes after the addition of Ti(III) citrate to the nitrogenase proteins; in the presence of MgATP however, Fe chelation affected the activity of the Fe protein within 1 minute.

Determination of the rate of reduction of $\text{Av}2_{\text{ox}}$ under different conditions

Determination of the rate of reduction of $\text{Av}2_{\text{ox}}$

The concentrations after mixing were: 92 μM $\text{Av}2_{\text{ox}}$; 7.6 mM $\text{Na}_2\text{S}_2\text{O}_4$ or 0.5-1.0 mM Ti(III) citrate; 5 mM MgCl_2 ; 50 mM Tes/NaOH, final pH 7.4.

Determination of the rate of reduction of $\text{Av}2_{\text{ox}}(\text{MgADP})_2$

$\text{Av}2_{\text{ox}}$ was equilibrated with MgADP before mixing with the reductant and MgADP. Dithionite: the concentrations after mixing were 25 μM $\text{Av}2_{\text{ox}}$, 0.2-16.0 mM $\text{Na}_2\text{S}_2\text{O}_4$, 500 μM ADP, 10 mM MgCl_2 and 50 mM Tes/NaOH, final pH 7.4. Ti(III) citrate: the concentrations after mixing were 94 μM $\text{Av}2_{\text{ox}}$, 0.5-1.0 mM Ti(III) citrate, 1 mM ADP, 5 mM MgCl_2 and 50 mM Tes/NaOH, final pH 7.4. Fld_{HQ} : the concentrations after mixing were 47 μM $\text{Av}2_{\text{ox}}$, 156 μM Fld_{HQ} , 66 μM Fld_{SQ} , 1.5 mM $\text{Na}_2\text{S}_2\text{O}_4$; 1 mM MgADP, 5 mM MgCl_2 and 50 mM Tes/NaOH, final pH 7.4.

Determination of the rate of reduction of $\text{Av}2_{\text{ox}}(\text{MgADP})_2$ in the presence of Av1

Av1 and $\text{Av}2_{\text{ox}}$ were equilibrated with MgADP before mixing with the reductant and MgADP. With dithionite the rate of reduction of $\text{Av}2_{\text{ox}}(\text{MgADP})_2$ was determined from simulations of the absorbance decrease curves in Figure 1B. Dithionite: the concentrations after mixing were: 35 μM Av1; 40 μM $\text{Av}2_{\text{ox}}$; 0-80 μM $\text{Av}2_{\text{red}}$; 5 mM MgADP; 8 mM $\text{Na}_2\text{S}_2\text{O}_4$; 50 mM NaCl; 50 mM Tes/NaOH, final pH 7.4. Ti(III) citrate: the concentrations after mixing were: 35 μM Av1; 30.5 μM $\text{Av}2_{\text{ox}}$; 5 mM MgADP; 1.1 mM Ti(III) citrate; 50 mM NaCl; 50 mM Tes/NaOH, final pH 7.4. With flavodoxin hydroquinone the reduction of $\text{Av}2_{\text{ox}}(\text{MgADP})_2$ was monitored at 418 nm (isosbestic point of the $\text{Fld}_{\text{HQ}}/\text{Fld}_{\text{SQ}}$ couple) and at 580 nm, monitoring the formation of flavodoxin

semiquinone. The concentrations after mixing were: 11 μM Av1; 33 μM Av2_{ox}; 156 μM Fld_{HQ}; 66 μM Fld_{SQ}; 1.5 mM Na₂S₂O₄; 1 mM ADP; 5 mM MgCl₂; 38 mM NaCl; 50 mM Tes/NaOH, final pH 7.4.

The rate of dissociation of the nitrogenase complex (Av1·Av2_{ox}(MgADP)₂) was determined as described for nitrogenase from *Klebsiella pneumoniae* (Thorneley & Lowe (1983)). Three models were tested to simulate the data curves in Figure 1B, according to equations 1, 2 and 3. The simulations yielded the rate constants for the dissociation and the dissociation constants (K_d) of the Av1·Av2_{ox}(MgADP)₂ and the Av1·Av2_{red}(MgADP)₂ complexes. The simulations of the stopped-flow curves were performed with the kinetic simulation program KINSIM (Barshop et al., 1983), and the fit program FITSIM (Zimmerle & Frieden, 1989) (F.T.P. 128.252.135.4). The simulated data points were fit to the experimental data by non-linear regression. The quality of the fit between the simulated data and the experimental data curves (Figure 1B) is reflected in the R-squared value (a value of 1 indicates a perfect fit) and the Mean Square Error (MSE), which is the sum of the squared differences between the experimental and calculated data points, divided by the amount of variables used in the simulation, and which should be close to 0.

Determination of the rate of turnover

The rate of nitrogenase turnover (20 °C) was obtained from the H₂ production activity with saturating Av2 and reductant. The reaction mixture contained 0.55 μM Av1, 11.0 μM Av2, reductant as indicated, and an ATP regenerating system as described by Braaksma et al. (1982). The H₂ production was measured using a H₂ electrode. From the H₂ production the turnover rate of the Fe protein cycle was calculated.

Results

In order to describe the kinetics of nitrogenase from *Azotobacter vinelandii* the rate constants of the individual steps of the Fe protein cycle (Scheme 1) must be determined. The rate-limiting step of the Fe protein cycle is generally accepted to be the dissociation of the nitrogenase complex after electron transfer and MgATP hydrolysis (Thorneley & Lowe, 1983). The rate constant of this step can be determined by measuring the rate of the reduction of oxidized Fe protein with MgADP bound, in the presence of the MoFe protein. It is assumed that when the Fe protein is bound to the MoFe protein, the

[4Fe-4S] cluster of the Fe protein cannot be reduced: therefore the nitrogenase complex must dissociate first. To be able to perform a kinetic analysis of the data curves, the kinetics of the reduction of the free Fe protein must be known. Three reductants were used: sodium dithionite, titanium (III) citrate and flavodoxin hydroquinone (Fld_{HQ}).

Table 1. The reduction of Av2_{ox}, Av2_{ox}(MgADP)₂ and Av2_{ox}(MgADP)₂ in the presence of Av1 by sodium dithionite, titanium (III) citrate, or flavodoxin hydroquinone.

| species | reductant | ϵ_{430} (mM ⁻¹ · cm ⁻¹) | k (× 10 ⁶ M ⁻¹ · s ⁻¹) |
|--|---|--|---|
| Av2 _{ox} | Na ₂ S ₂ O ₄ | 4.50 ± 0.06 | 130 ± 10 |
| Av2 _{ox} | Ti(III) citrate | 4.93 ± 0.15 | 0.4 ± 0.1 |
| Av2 _{ox} (MgADP) ₂ | Na ₂ S ₂ O ₄ | 3.53 ± 0.02 | 3.0 ± 0.5 |
| Av2 _{ox} (MgADP) ₂ | Ti(III) citrate | 4.25 ± 0.12 | 0.9 ± 0.2 |
| Av2 _{ox} (MgADP) ₂ | Fld _{HQ} | - | 6.4 ± 0.1 |
| Av2 _{ox} (MgADP) ₂ + Av1 | Na ₂ S ₂ O ₄ | - | 0.14 ± 0.002 ^a |
| Av2 _{ox} (MgADP) ₂ + Av1 | Ti(III) citrate | - | 0.07 ± 0.02 |
| Av2 _{ox} (MgADP) ₂ + Av1 | Fld _{HQ} | - | 2.95 ± 0.06 |

^aThe rate of the reduction of Av2_{ox}(MgADP)₂ in the presence of Av1 was determined from simulations of the absorbance decrease curves in Figure 1B.

Reduction of oxidized Fe protein

The reduction of the oxidized Fe protein (Av2_{ox}) was studied following published methods (Dixon, 1971; Thorneley et al., 1976; Thorneley & Lowe, 1983). The reduction of Av2_{ox}, observed as a decrease of the absorbance at 430 nm, by excess dithionite ([Na₂S₂O₄] = 7.6 mM, the actual reductant [SO₂^{·-}] = 3.3 μM) occurred in two phases, both of which could be fitted to a single exponential. The second order rate constant for the fast phase was: $k = 1.3 \times 10^8 \text{ M}^{-1} \cdot \text{s}^{-1}$ (Table 1). The molecular absorbance coefficient for the complete reduction of Av2_{ox} was: $\epsilon_{430} = 4.50 \text{ mM}^{-1} \cdot \text{cm}^{-1}$; no correction was made for the iron content of Av2 being 3.7 Fe/Av2 instead of 4 Fe/Av2. 86% of Av2_{ox} was involved in the fast phase and 14% was involved in the slow phase of the reduction. The observations indicate that two different forms of Av2_{ox} were present in the reaction mixture, which were reduced at different rates. However, the

slower reacting Av2_{ox} was always only a small portion of all Av2_{ox} present and will not be further considered.

The observed rate of the reduction of Av2_{ox} by Ti(III) citrate was dependent on the concentration of Ti(III) citrate (0.5 - 1.0 mM) (data not shown). The reduction also occurred in different phases; 85% of all Av2_{ox} was involved in the fast phase of the reduction. With $[\text{Ti(III) citrate}] = 1.0 \text{ mM}$, the first phase could be fitted to a single-exponential with the second order rate constant: $k = 0.4 \times 10^6 \text{ M}^{-1} \cdot \text{s}^{-1}$. For the complete reduction of Av2_{ox} the molecular absorbance coefficient was: $\epsilon_{430} = 4.93 \text{ mM}^{-1} \cdot \text{cm}^{-1}$ (Table 1). The slower reacting phases are not further considered.

Reduction of oxidized Fe protein with MgADP bound

The reduction of Kp2_{ox} by dithionite occurs at a much higher rate than the reduction of Kp2_{ox} with MgADP bound ($\text{Kp2}_{\text{ox}}(\text{MgADP})_2$). The cause of this lower reduction rate was attributed to the change of the conformation of the Fe protein caused by the binding of MgADP (Thorneley et al., 1976; Ashby & Thorneley, 1987). The same applies for the Fe protein from *Azotobacter chroococcum* (Bergström et al., 1988).

The reduction of $\text{Av2}_{\text{ox}}(\text{MgADP})_2$ by dithionite was monitored as a function of the concentration of dithionite (0.2 - 16.0 mM), see Figure 1A. Av2_{ox} was equilibrated with excess MgADP before mixing with dithionite and MgADP. It was verified that the binding of MgADP to Av2_{ox} was saturating. Only one phase of absorbance decrease (430 nm) was observed. The amplitude of this (single-exponential) absorbance decrease was independent of the concentration of dithionite. The molecular absorbance coefficient for the reduction of $\text{Av2}_{\text{ox}}(\text{MgADP})_2$ was: $\epsilon_{430} = 3.53 \text{ M}^{-1} \cdot \text{cm}^{-1}$ (Table 1). Ashby and Thorneley (1987) also found a molecular absorbance coefficient for the reduction of $\text{Kp2}_{\text{ox}}(\text{MgADP})_2$ that was only 80% of the molecular absorbance coefficient for the reduction of Kp2_{ox} . Binding of MgADP lowers the redox potential of Av2 from -375 mV to -473 mV (Braaksma et al., 1982; Watt et al., 1986). The redox equilibrium between HSO_3^- and Av2_{red} however can explain the smaller observed absorbance decrease only partly: under our experimental conditions the redox potential is -525 mV, which allows 88% reduction of $\text{Av2}_{\text{ox}}(\text{MgADP})_2$. This would lower the molecular absorbance coefficient to $\epsilon_{430} = 3.96 \text{ mM}^{-1} \cdot \text{cm}^{-1}$.

Figure 1A shows that the observed rate constant of the reduction of $\text{Av2}_{\text{ox}}(\text{MgADP})_2$ increased with the concentration of dithionite (SO_2^{2-}). The second order rate constant for the reduction of $\text{Av2}_{\text{ox}}(\text{MgADP})_2$ by SO_2^{2-} , calculated from the initial linear dependence of k_{obs} on $[\text{SO}_2^{2-}]$, was: $k = 3.0 \times 10^6 \text{ M}^{-1} \cdot \text{s}^{-1}$ (valid only at low

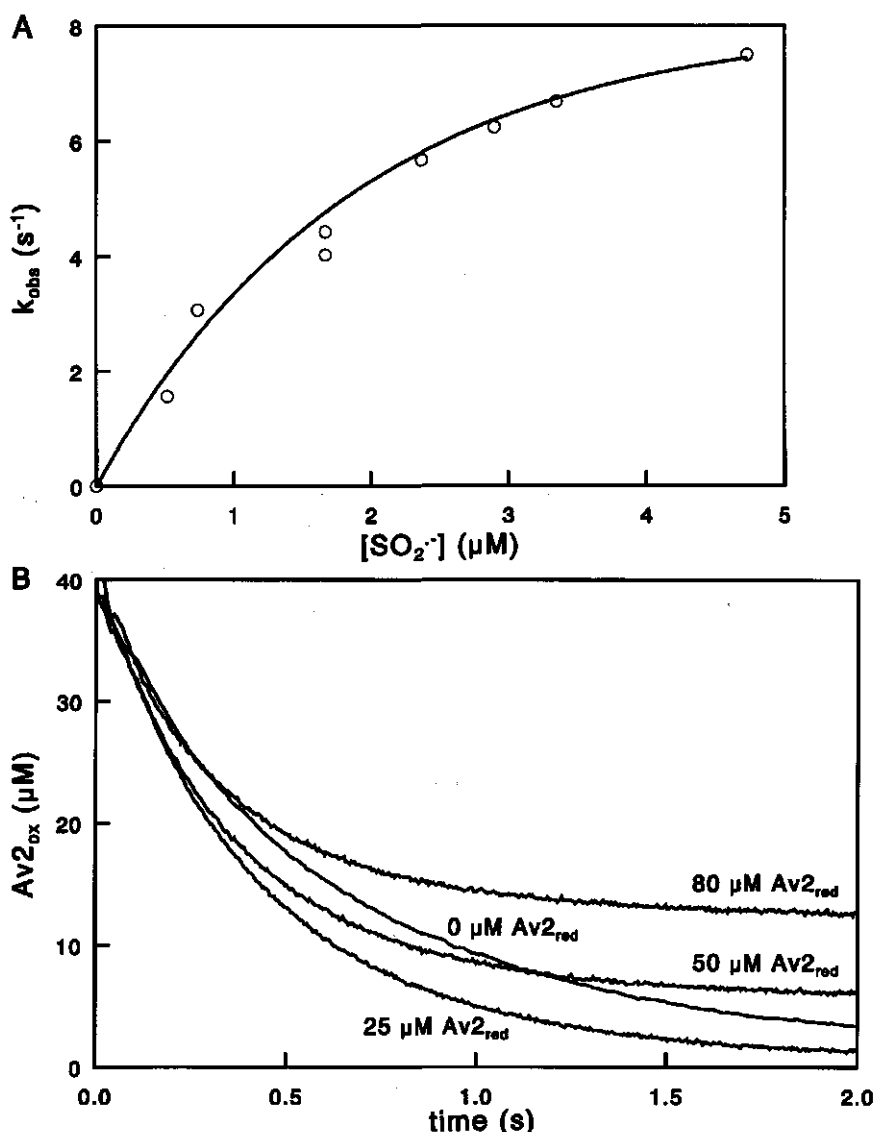


Figure 1. Kinetics of the reduction of $\text{Av2}_{\text{ox}}(\text{MgADP})_2$ by sodium dithionite (monitored by the absorbance decrease at 430 nm). (A) The observed rate constant (k_{obs}) of the reduction of $\text{Av2}_{\text{ox}}(\text{MgADP})_2$ depends on $[\text{SO}_2^{2-}]$. Syringe one contained 50 μM Av2_{ox} ; syringe two contained $\text{Na}_2\text{S}_2\text{O}_4$ (0 - 32 mM); both syringes contained 0.5 mM ADP, 10 mM MgCl_2 and 50 mM Tes/NaOH, final pH 7.4. (B) Determination of the rate of dissociation of the $\text{Av1} \cdot \text{Av2}_{\text{ox}}(\text{MgADP})_2$ complex. Syringe one contained: 70 μM Av1 ; 80 μM Av2_{ox} ; 100 mM NaCl. Syringe two contained 0-160 μM Av2_{red} (in (B) the concentration after mixing is indicated) and 16 mM $\text{Na}_2\text{S}_2\text{O}_4$. Both syringes contained 5 mM MgADP and 50 mM Tes/NaOH, final pH 7.4.

dithionite concentrations), see Table 1. This value is the same as the value reported for the reduction of $\text{Kp2}_{\text{ox}}(\text{MgADP})_2$ (Thorneley & Lowe, 1983; Ashby & Thorneley, 1987), and is close to the values $k = 3.2 \pm 0.2 \times 10^6 \text{ M}^{-1} \cdot \text{s}^{-1}$ and $k = 4.7 \pm 0.5 \times 10^6 \text{ M}^{-1} \cdot \text{s}^{-1}$ for the reduction of $\text{Ac2}_{\text{ox}}(\text{MgADP})_2$ from the vanadium nitrogenase and the molybdenum nitrogenase, respectively, reported by Bergström et al. (1988). Ashby and Thorneley (1987) found a linear dependence of the observed rate constant for the reduction of $\text{Kp2}_{\text{ox}}(\text{MgADP})_2$ on $[\text{S}_2\text{O}_4^{2-}]^{1/2}$ through the origin; for the reduction of $\text{Ac2}_{\text{ox}}(\text{MgADP})_2$ however, Bergström et al. (1988) also observed a deviation from linearity, at dithionite concentrations higher than 4 mM. The authors attributed this deviation from linearity to inhibition of the reduction at high ionic strength. The influence of the ionic strength on the observed rate of reduction of $\text{Av2}_{\text{ox}}(\text{MgADP})_2$ was investigated by addition of sodium sulphate (0–20 mM) to the reaction mixture, at different dithionite concentrations. It was found that Na_2SO_4 decreases k_{obs} to some extent, but this effect was not large enough to completely account for the deviation from linearity in Figure 1A (data not shown). $\text{S}_2\text{O}_4^{2-}$ might inhibit the binding of SO_2^- to Av2 more specifically than SO_4^{2-} does.

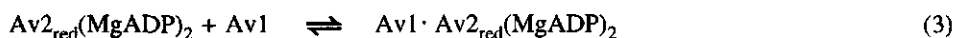
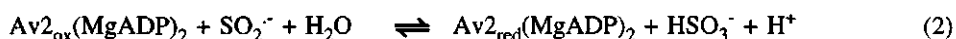
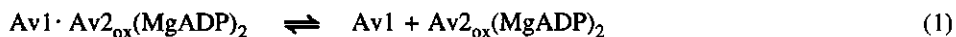
The observed rate of the reduction of $\text{Av2}_{\text{ox}}(\text{MgADP})_2$ by Ti(III) citrate (1.0 mM) was much larger than the rate of reduction of $\text{Av2}_{\text{ox}}(\text{MgADP})_2$ by dithionite; this is caused by the higher concentration of Ti(III) citrate compared to $[\text{SO}_2^-]$. Unlike the reduction of $\text{Av2}_{\text{ox}}(\text{MgADP})_2$ by dithionite, the total absorbance decrease consisted of several single-exponential phases. The slower phases are attributed to Fe chelation of the $[\text{4Fe-4S}]$ cluster of Av2_{ox} by Ti(III) citrate and are not further considered. The second order rate constant of the fast phase was: $k = 0.9 \times 10^6 \text{ M}^{-1} \cdot \text{s}^{-1}$ (Table 1). The molecular absorbance coefficient for the complete reduction of $\text{Av2}_{\text{ox}}(\text{MgADP})_2$ was: $\epsilon_{430} = 4.25 \text{ mM}^{-1} \cdot \text{cm}^{-1}$; this is 86% of the molecular absorbance coefficient found for the reduction of Av2_{ox} by Ti(III) citrate.

The reduction of $\text{Av2}_{\text{ox}}(\text{MgADP})_2$ by Fld_{Hq} (156 μM) was monitored by the absorbance increase at 580 nm, associated with the oxidation of Fld_{Hq} . The second order rate constant for the (single-exponential) reduction of $\text{Av2}_{\text{ox}}(\text{MgADP})_2$ was: $k = 6.4 \times 10^6 \text{ M}^{-1} \cdot \text{s}^{-1}$ (Table 1 and Figure 2).

Determination of the rate of dissociation of the nitrogenase complex

The rate of the dissociation of the nitrogenase complex ($\text{Av1} \cdot \text{Av2}_{\text{ox}}(\text{MgADP})_2$) was determined as described for nitrogenase of *K. pneumoniae* by Thorneley and Lowe (1983). Av1 , Av2_{ox} and MgADP were mixed with dithionite, MgADP and variable concentrations of Av2_{red} . The reduction of $\text{Av2}_{\text{ox}}(\text{MgADP})_2$ was monitored by the

absorbance decrease at 430 nm (Figure 1B). In the model of Thorneley & Lowe (1983), the $\text{Av1} \cdot \text{Av2}_{\text{ox}}(\text{MgADP})_2$ complex must dissociate (equation (1)) before $\text{Av2}_{\text{ox}}(\text{MgADP})_2$ can be reduced (eqn. (2)). $\text{Av2}_{\text{red}}(\text{MgADP})_2$ increases the rate of reduction of $\text{Av2}_{\text{ox}}(\text{MgADP})_2$ by binding to Av1 (eqn. (3)) and thus suppressing the association of Av1 and $\text{Av2}_{\text{ox}}(\text{MgADP})_2$. At increasing concentrations of Av2_{red} , the absorbance decrease curves are increasingly determined by the rate of the dissociation of the $\text{Av1} \cdot \text{Av2}_{\text{ox}}(\text{MgADP})_2$ complex.



The observed rate of reduction of $\text{Av2}_{\text{ox}}(\text{MgADP})_2$ varied from $k_{\text{obs}} = 1.5 \text{ s}^{-1}$ in the absence of Av2_{red} , to $k_{\text{obs}} = 2.9 \text{ s}^{-1}$ in the presence of $80 \text{ } \mu\text{M}$ Av2_{red} . It was observed that the absorbance decrease was smaller at higher concentrations of Av2_{red} , see Figure 1B: at $80 \text{ } \mu\text{M}$ Av2_{red} the absorbance decrease was $\sim 70\%$ of the observed absorbance decrease when no Av2_{red} was added to the reaction mixture. By measuring the redox potential of solutions containing 8 mM dithionite and various concentrations of Av2_{red} , it became clear that during the incubation of Av2_{red} with dithionite (before mixing) the so-called self-oxidation of Av2 (Watt et al., 1986) significantly increased the redox potential of the solution. When no Av2_{red} was present in the solution, the measured redox potential at the time of the experiment was -525 mV ; at $50 \text{ } \mu\text{M}$ Av2 , -509 mV ; at $80 \text{ } \mu\text{M}$ Av2 , -505 mV . The oxidation of $\text{Av2}_{\text{red}}(\text{MgADP})_2$ by HSO_3^- (eqn. (2)) causes the smaller absorbance decrease at higher concentrations of Av2_{red} and was therefore taken into account in the simulations.

The models used to simulate the stopped-flow curves of Figure 1B in order to determine the rate of dissociation of the nitrogenase complex, comprised the reactions in eqns. (1), (2) and (3). In the simulations $k_{\text{obs}} = 6.7 \text{ s}^{-1}$ was used for the reduction of $\text{Av2}_{\text{ox}}(\text{MgADP})_2$; this value was obtained from Figure 1A (8 mM $\text{Na}_2\text{S}_2\text{O}_4$; $3.3 \text{ } \mu\text{M}$ SO_2^{2-}). The rate constant of the dissociation of the $\text{Av1} \cdot \text{Av2}_{\text{ox}}(\text{MgADP})_2$ complex was determined from the simulation that gave the best fit to the data curves. Three models were tested: the results of the simulations are summarized in Table 2.

Table 2. The dissociation of the nitrogenase complex ($Av1 \cdot Av2_{ox}(MgADP)_2$).

| simulation | dissociation | | | | quality of fit | | calculated nitrogenase turnover rate ^c (mol e ⁻ s ⁻¹ . (mol Mo) ⁻¹) |
|------------|-------------------------------|---------------------|--------------------------------|---------------------|--------------------|------------------|---|
| | $Av1 \cdot Av2_{ox}(MgADP)_2$ | | $Av1 \cdot Av2_{red}(MgADP)_2$ | | R-sq. ^a | MSE ^b | |
| | k (s ⁻¹) | K_d (μ M) | k (s ⁻¹) | K_d (μ M) | | | |
| 1 | 2.0 \pm 0.03 | 19.9 \pm 2.0 | 15 ^d | 0.3 ^d | 0.9589 | 19.5 | 1.8 |
| 2 | 9.3 \pm 0.5 | 15.7 \pm 1.4 | 78.9 \pm 95.0 | 12.4 \pm 21.1 | 0.9991 | 0.365 | 6.8 |
| 3 | 2.8 \pm 0.05 | 0.84 \pm 0.02 | 25.5 \pm 11.9 | 0.97 \pm 0.65 | 0.9995 | 0.220 | 2.5 |

^aR-sq. = R-squared value. ^bMSE = Mean Square Error (the sum of the squared differences between the experimental and the calculated data points, divided by the amount of variables used in the simulation). ^cThe nitrogenase turnover rate (mol e⁻ s⁻¹. (mol Mo)⁻¹) was calculated according to the Fe protein cycle in Scheme 1, with $[Av2]/[Av1] = 20$ and $[Na_2S_2O_4] = 20$ mM and the rate constants obtained from the corresponding simulation. ^dIn simulation (1) the dissociation constant (K_d) of the $Av1 \cdot Av2_{red}(MgADP)_2$ complex (eqn. (3)) was fixed at 0.3 μ M.

In the first model (Table 2, simulation 1) it was assumed that the dissociation constant of the $\text{Av1} \cdot \text{Av2}$ complex is determined only by the redox state of the Fe protein and not by the nucleotide bound to the protein. The dissociation constant (K_d) of the $\text{Av1} \cdot \text{Av2}_{\text{red}}(\text{MgADP})_2$ complex (eqn. (3)) was fixed at $0.3 \mu\text{M}$ (which is the value of the K_d of the $\text{Kp1} \cdot \text{Kp2}_{\text{red}}(\text{MgATP})_2$ complex according to Lowe and Thorneley (1984b)). The simulations produced very poor fits to the data curves.

In the second model tested (Table 2, simulation 2) both the dissociation rates of the $\text{Av1} \cdot \text{Av2}_{\text{ox}}(\text{MgADP})_2$ complex and the $\text{Av1} \cdot \text{Av2}_{\text{red}}(\text{MgADP})_2$ complex (eqns. (1) and (3)) were allowed to vary. With these conditions, the simulations yielded good fits to the data curves. For the dissociation of the $\text{Av1} \cdot \text{Av2}_{\text{ox}}(\text{MgADP})_2$ complex $k = 9.3 \text{ s}^{-1}$ and a $K_d = 15.7 \mu\text{M}$ were obtained. For the $\text{Av1} \cdot \text{Av2}_{\text{red}}(\text{MgADP})_2$ complex a dissociation rate $k = 78.9 \text{ s}^{-1}$ and a $K_d = 12.4 \mu\text{M}$ were obtained. The large error in the values of the rate constant of the dissociation and the K_d of the $\text{Av1} \cdot \text{Av2}_{\text{red}}(\text{MgADP})_2$ complex (Table 2, simulation 2) indicates that the simulation is not sensitive to the value of the rate constants of eqn. (3). Surprisingly, although the dissociation of the nitrogenase complex is supposed to be the rate-limiting step of the Fe protein cycle (Thorneley & Lowe, 1983), the rate constant for the dissociation of the nitrogenase complex was found to be nearly two times the observed maximum rate of turnover (with dithionite): $k_{\text{obs}} = 3.0 \text{ s}^{-1}$ (see Table 3; the rate of nitrogenase turnover was determined from the H_2 production by nitrogenase under optimal conditions). In addition, the dissociation constants of the $\text{Av1} \cdot \text{Av2}_{\text{ox}}(\text{MgADP})_2$ and the $\text{Av1} \cdot \text{Av2}_{\text{red}}(\text{MgADP})_2$ complexes were tenfold higher than the corresponding dissociation constants reported for the nitrogenase proteins from *K. pneumoniae*: $1.5 \mu\text{M}$ and $2.2 \mu\text{M}$, respectively (Thorneley & Lowe, 1983). These differences are considered too large and therefore an extended model was examined.

An extra reaction was added to the model: the reduction of Av2_{ox} in the $\text{Av1} \cdot \text{Av2}_{\text{ox}}(\text{MgADP})_2$ complex, besides reduction of $\text{Av2}_{\text{ox}}(\text{MgADP})_2$ after dissociation of the nitrogenase complex (Table 2, simulation 3). With this addition, the simulation yielded $k = 2.8 \text{ s}^{-1}$ for the dissociation of the $\text{Av1} \cdot \text{Av2}_{\text{ox}}(\text{MgADP})_2$ complex and a $K_d = 0.84 \mu\text{M}$, and $k = 25.5 \text{ s}^{-1}$ for the dissociation of the $\text{Av1} \cdot \text{Av2}_{\text{red}}(\text{MgADP})_2$ complex with a $K_d = 0.97 \mu\text{M}$. For the rate of the reduction of $\text{Av2}_{\text{ox}}(\text{MgADP})_2$ in the $\text{Av1} \cdot \text{Av2}_{\text{ox}}(\text{MgADP})_2$ complex $k = 0.14 \times 10^6 \text{ M}^{-1} \cdot \text{s}^{-1}$ was obtained from the simulation (Table 1). The addition of an extra variable increased the quality of the fit (judged by the decrease of the mean square error, the improved quality of the fit was not only caused by the addition of an extra variable to the model). With this model the calculated turnover rate with dithionite as the reductant (2.5 s^{-1}) is better in agreement with the determined turnover rate of 3.0 s^{-1} (Table 3). Also the dissociation constants of the $\text{Av1} \cdot \text{Av2}_{\text{ox}}(\text{MgADP})_2$ complex and the $\text{Av1} \cdot \text{Av2}_{\text{red}}(\text{MgADP})_2$ complex are in the

same range as the constants for the corresponding nitrogenase complexes from *K. pneumoniae*.

Table 3. Turnover of nitrogenase with different reductants.

| reductant | nitrogenase turnover ^a (mol e ⁻ · s ⁻¹ · (mol Mo) ⁻¹) |
|--|---|
| Na ₂ S ₂ O ₄ (16 mM) | 3.0 ± 0.4 |
| Ti(III) citr. (1 mM) | 3.2 ± 0.3 |
| Ti(III) citr. (1 mM) + Fld (50 µM) | 4.4 ± 0.4 |
| Na ₂ S ₂ O ₄ (5 mM) + Fld (50 µM) | 4.8 ± 0.4 |

^aThe rate of nitrogenase turnover is the rate for the completion of one Fe protein cycle (at 20 °C, [Av2]/[Av1] = 20) is expressed in: mol e⁻ · s⁻¹ · (mol Mo)⁻¹, but can also be expressed in s⁻¹, for simplicity. Note that the Mo-content of Av1 was 1.8 Mo/Av1.

The reduction of Av2_{ox}(MgADP)₂ in the presence of Av1 was also studied with Ti(III) citrate (1.0 mM) and Fld_{HQ} (156 µM) as the reductant. With Ti(III) citrate and Fld_{HQ} the observed rate of the reduction of Av2_{ox}(MgADP)₂ in the absence of Av1 was high compared to the rate of association of Av2_{ox}(MgADP)₂ with Av1 and must thus approximate the rate of dissociation of the Av1 · Av2_{ox}(MgADP)₂ complex, also if no Av2_{red} was added to the reaction mixture. With Ti(III) citrate the reduction of Av2_{ox}(MgADP)₂ in the presence of Av1 occurred in two phases, which could each be fitted to a single-exponential, with $k_{\text{obs}} = 70 \text{ s}^{-1}$ (70% of all Av2_{ox}(MgADP)₂) and $k_{\text{obs}} = 8 \text{ s}^{-1}$ (30%). Fld_{HQ} reduced Av2_{ox}(MgADP)₂ (Figure 2) in the presence of Av1 with $k_{\text{obs}} = 460 \text{ s}^{-1}$ (Table 1). Both the reduction by Ti(III) citrate and by Fld_{HQ} occurred at a much higher rate than the observed maximum rate of turnover ($k_{\text{obs}} = 4.8 \text{ s}^{-1}$, Table 3).

These data strongly suggest that Fld_{HQ} and Ti(III) citrate reduce Av2_{ox} in the Av1 · Av2_{ox}(MgADP)₂ complex, without a preceding dissociation of the nitrogenase complex. The simulations suggest that dithionite is also capable of reducing Av2_{ox} in the nitrogenase complex, but at a rate which is about 5% of the rate of reduction of free Av2_{ox}(MgADP)₂ (Table 1). Because the observed maximum rate of turnover of nitrogenase was only 4.8 s^{-1} (Table 3) there must be another slow step in the catalytic cycle that limits the rate of turnover when Ti(III) citrate or Fld_{HQ} is used as the reductant.

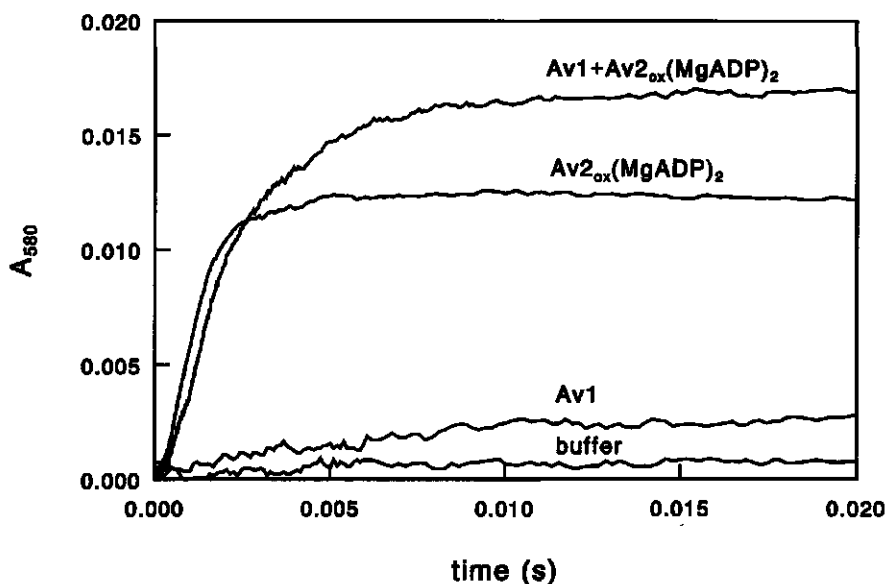


Figure 2. The absorbance changes (A_{580}) associated with the oxidation of flavodoxin hydroquinone by $\text{Av2}_{\text{ox}}(\text{MgADP})_2$, in the absence and in the presence of Av1. Syringe one contained: trace 'Av1 + $\text{Av2}_{\text{ox}}(\text{MgADP})_2$ ': 22 μM Av1, 66 μM Av2_{ox} and 75 mM NaCl; trace ' $\text{Av2}_{\text{ox}}(\text{MgADP})_2$ ': 93 μM Av2_{ox} ; trace 'Av1': 22 μM Av1 and 75 mM NaCl; trace 'buffer': no nitrogenase proteins. The other syringe contained 311 μM Fld_{HQ} , 132 μM Fld_{SQ} and 3 mM $\text{Na}_2\text{S}_2\text{O}_4$. Both syringes contained 1 mM MgADP, 5 mM MgCl_2 and 50 mM Tes/NaOH, final pH 7.4.

Nucleotide exchange

In the catalytic cycle of nitrogenase (Scheme 1) the reduction of the oxidized Fe protein with MgADP bound precedes the exchange of MgADP for MgATP (Ashby & Thorneley, 1987). The requirement of dissociation of the nitrogenase complex ($\text{Av1} \cdot \text{Av2}_{\text{red}}(\text{MgADP})_2$) for the nucleotide exchange was investigated, by the effect of incubation of the nitrogenase proteins with MgADP before mixing with MgATP, on the electron transfer between the nitrogenase proteins. Figure 3 shows that the presence of a low MgADP concentration in the reaction mixture did not affect the absorbance changes that accompany the electron transfer. When the nitrogenase proteins were incubated with MgADP before mixing with MgATP however, the electron transfer trace started with a short lag phase (~ 5 ms) and the observed rate of electron transfer was lowered ($k_{\text{obs}} = 55 \text{ s}^{-1}$). This value is still considerably higher than the rate constant determined for the dissociation of the $\text{Av1} \cdot \text{Av2}_{\text{ox}}(\text{MgADP})_2$ complex ($k = 2.8 \text{ s}^{-1}$; Table 2, simulation 3).

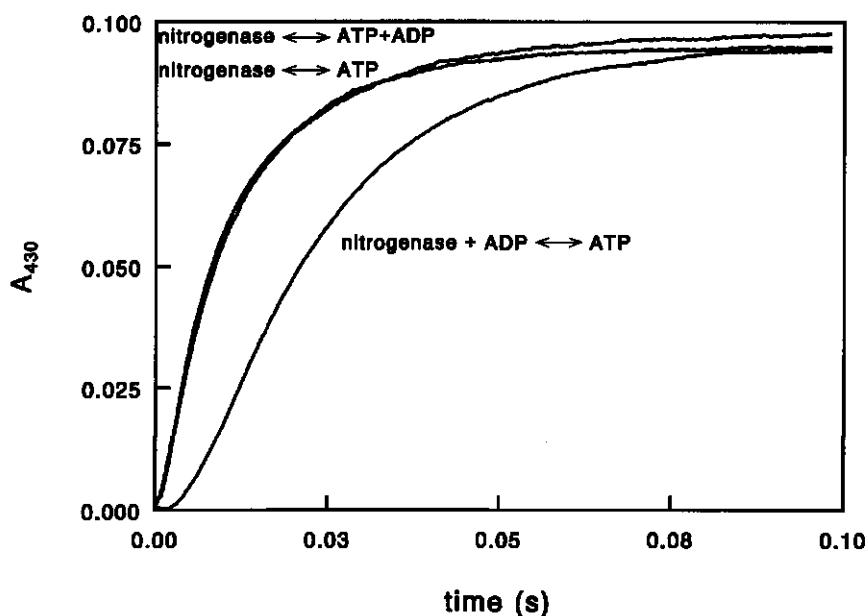


Figure 3. The effect of incubation of the nitrogenase proteins with MgADP on the rate of electron transfer between the nitrogenase proteins. The electron transfer was monitored by the absorbance increase at 430 nm. Syringe one contained 21 μM Av1 and 135 μM Av2; the other syringe contained 20 mM MgATP. Both syringes contained 5 mM $\text{Na}_2\text{S}_2\text{O}_4$, 5 mM MgCl_2 , 60 mM NaCl and 50 mM Tes/NaOH, final pH 7.4. Trace 'nitrogenase \leftrightarrow ATP': no MgADP in the reaction mixture; trace 'nitrogenase + ADP \leftrightarrow ATP': the nitrogenase proteins were incubated with 1 mM MgADP (before mixing with MgATP); trace 'nitrogenase \leftrightarrow ATP + ADP': 1 mM MgADP was added to the ATP solution.

The absorbance amplitude was not affected by the incubation of the nitrogenase proteins with MgADP. The observations indicate that dissociation of the complex is not a prerequisite for the nucleotide exchange.

Electron uptake by nitrogenase during turnover

More evidence that Ti(III) citrate and Fld_{HQ} are capable of reducing Av2_{ox} in the $\text{Av1} \cdot \text{Av2}_{\text{ox}}(\text{MgADP})_2$ complex without a preceding dissociation of the complex, was obtained by studying the oxidation of either reductant during the nitrogenase reaction. The oxidation of Ti(III) citrate was monitored at 340 nm ($\epsilon_{340} = 0.73 \text{ mM}^{-1} \cdot \text{cm}^{-1}$ (Seefeldt & Ensign, 1994)), and the oxidation of Fld_{HQ} at 580 nm ($\epsilon_{580} =$

$5.7 \text{ mM}^{-1} \cdot \text{cm}^{-1}$ (Klugkist et al., 1986)). The molecular absorbance coefficient of dithionite is high ($\epsilon_{315} = 8.0 \text{ mM}^{-1} \cdot \text{cm}^{-1}$ (Dixon, 1971)) and a high concentration is needed to have a sufficient amount of the actual reductant, SO_2^{2-} ; owing to these factors it was impossible to monitor the pre-steady-state oxidation of dithionite.

Mixing of the nitrogenase proteins with MgADP in the presence of Ti(III) citrate did not lead to any absorbance changes at 340 nm. When reduced Av2 and Av1 were mixed with MgATP in the absence of an electron donor, a single turnover of nitrogenase was observed (an absorbance increase at 430 nm, caused by the oxidation of Av2), but no absorbance changes at 340 nm were observed. These data indicate that the contribution of the absorbance changes at 430 nm induced by the electron transfer between the nitrogenase proteins, to the absorbance changes at 340 nm, is minimal.

Figure 4A shows the absorbance changes (A_{340}) caused by oxidation of Ti(III) citrate by nitrogenase. Ti(III) citrate was added to the nitrogenase proteins just before mixing with MgATP. After mixing the absorbance remained constant for about 50 ms before the absorbance decreased, indicating oxidation of Ti(III) citrate. There were three phases of absorbance decrease: a fast phase which was followed by a slow phase and finally a steady-state. This steady-state absorbance decrease (and thus Ti(III) citrate oxidation) was slower than in the fast phase of the pre-steady-state, see Figure 4A. From the tangent to the absorbance changes at 340 nm the rate of the electron uptake was calculated (v): $12.6 \text{ mol e}^- \cdot \text{s}^{-1} \cdot (\text{mol Mo})^{-1}$ in the pre-steady-state and $4.4 \text{ mol e}^- \cdot \text{s}^{-1} \cdot (\text{mol Mo})^{-1}$ in the steady-state.

A similar experiment was performed with Fld_{HQ} as the reductant, see Figure 4B. After a constant phase the oxidation of Fld_{HQ} started (observed as an increase of the absorbance at 580 nm): first there was a fast oxidation phase, which was followed by a slow phase and a steady-state phase. The rate of electron uptake was $4.9 \text{ mol e}^- \cdot \text{s}^{-1} \cdot (\text{mol Mo})^{-1}$ in the pre-steady-state and $3.6 \text{ mol e}^- \cdot \text{s}^{-1} \cdot (\text{mol Mo})^{-1}$ in the steady-state. In this experiment the protein ratio was $[\text{Av2}]/[\text{Av1}] = 6$, which explains the rather low steady-state rate as compared to the value of $4.8 \text{ mol e}^- \cdot \text{s}^{-1} \cdot (\text{mol Mo})^{-1}$, obtained with ratio $[\text{Av2}]/[\text{Av1}] = 20$ (Table 3).

In both cases (Ti(III) citrate and Fld_{HQ}) the pre-steady-state rate of the oxidation of the reductant by nitrogenase was significantly higher than the steady-state rate. With Fld_{HQ} the effect was less extreme than with Ti(III) citrate. These data confirm the observation that the reduction of Av2_{ox} will occur in the nitrogenase complex, before the rate-limiting step of the Fe protein cycle.

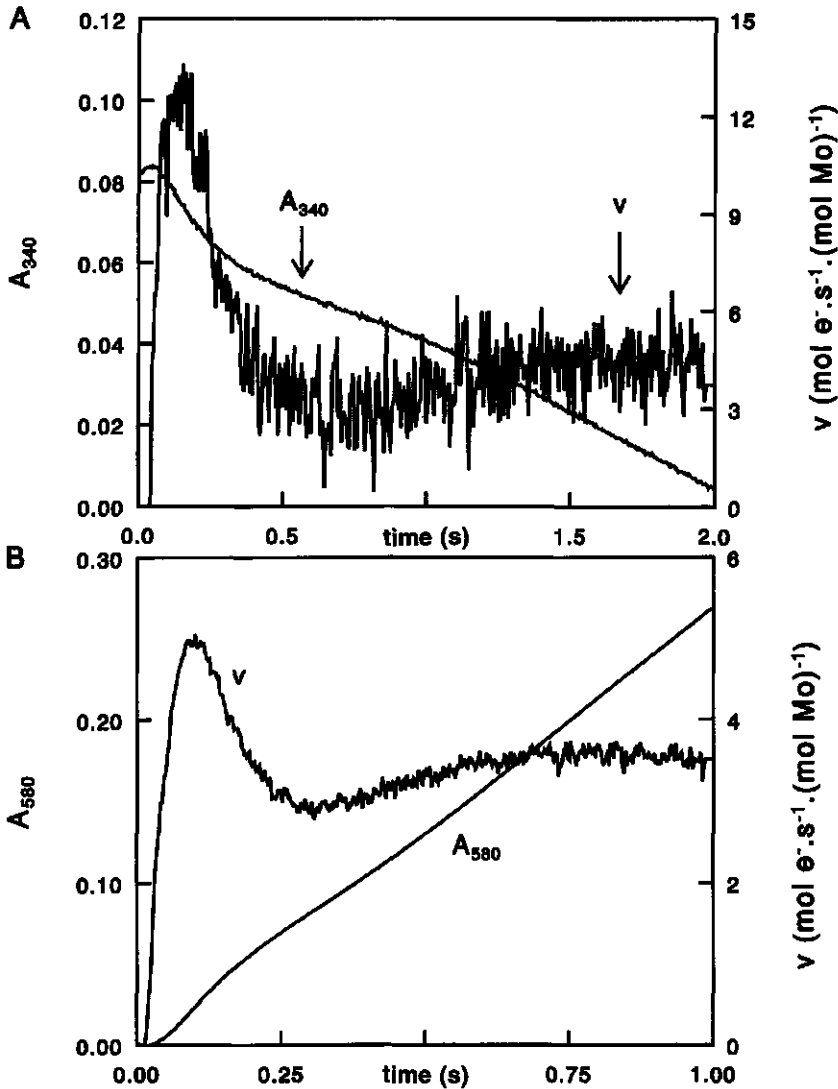


Figure 4. The absorbance changes associated with the oxidation of titanium (III) citrate (A) and flavodoxin hydroquinone (B) by nitrogenase during turnover. (A) The oxidation of Ti(III) citrate was monitored by the absorbance decrease at 340 nm (A_{340}); v ($\text{mol e}^- \cdot \text{s}^{-1} \cdot (\text{mol Mo})^{-1}$) is the rate of the oxidation of Ti(III) citrate. Syringe one contained: 13 μM Av1 and 78 μM Av2 (both dithionite-free) and 2 mM MgCl_2 . Syringe two contained: 10 mM ATP and 20 mM MgCl_2 . Both syringes contained 1 mM Ti(III) citrate, 100 mM NaCl and 50 mM Tes/NaOH, pH 7.4. (B) the oxidation of Fld_{HQ} was monitored by the absorbance increase at 580 nm (A_{580}); v ($\text{mol e}^- \cdot \text{s}^{-1} \cdot (\text{mol Mo})^{-1}$) is the rate of the oxidation of Fld_{HQ} to Fld_{SQ} . Syringe one contained: 16 μM Av1 and 96 μM Av2, 370 μM Fld_{HQ} , 150 μM Fld_{SQ} , 1 mM $\text{Na}_2\text{S}_2\text{O}_4$ and 2 mM MgCl_2 . Syringe two contained: 10 mM ATP and 20 mM MgCl_2 . Both syringes contained 100 mM NaCl and 50 mM Tes/NaOH, pH 7.4.

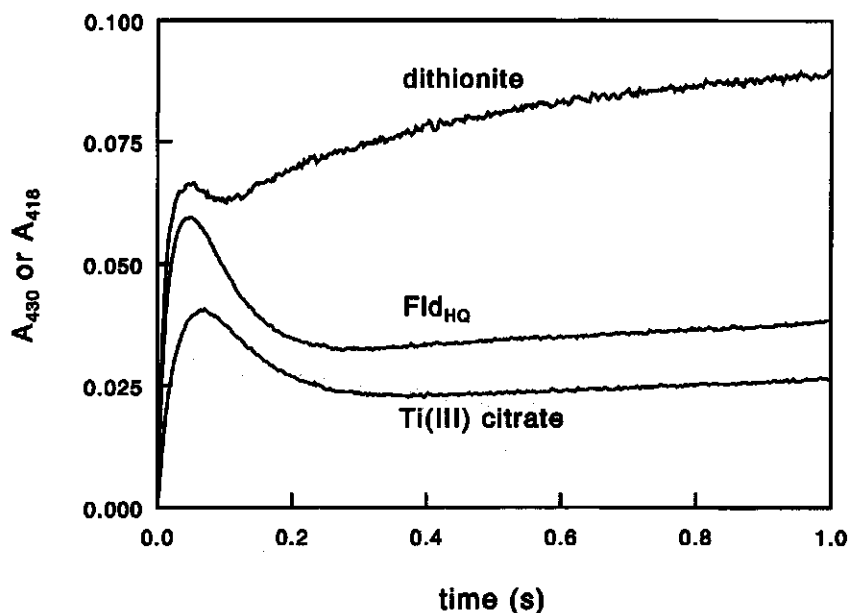


Figure 5. The absorbance changes associated with electron transfer from Av2 to Av1, during the first 1 s of the reaction of nitrogenase with MgATP, in the presence of different reductants. The electron transfer was monitored by the absorbance at 430 nm (sodium dithionite and Ti(III) citrate) or the absorbance at 418 nm (flavodoxin hydroquinone); 418 nm is an isosbestic point of Fld_{HQ}/Fld_{SO}. Dithionite: the protein syringe contained 15.4 μ M Av1 and 92 μ M Av2. Ti(III) citrate: the protein syringe contained 10 μ M Av1 and 100 μ M Av2 (both dithionite-free) and 200 mM NaCl. Fld_{HQ}: the protein syringe contained 16 μ M Av1 and 96 μ M Av2, 370 μ M Fld_{HQ}, 150 μ M Fld_{SO} and 1 mM Na₂S₂O₄. The other syringe always contained 10 mM ATP; both syringes always contained 10 mM MgCl₂ and 50 mM Tes/NaOH, pH 7.4. When dithionite was used as reductant, both syringes also contained 5 mM Na₂S₂O₄; when Ti(III) citrate was used, 1 mM Ti(III) citrate was added to both syringes just before the experiment.

The effect of the reductant on the pre-steady-state electron transfer reaction

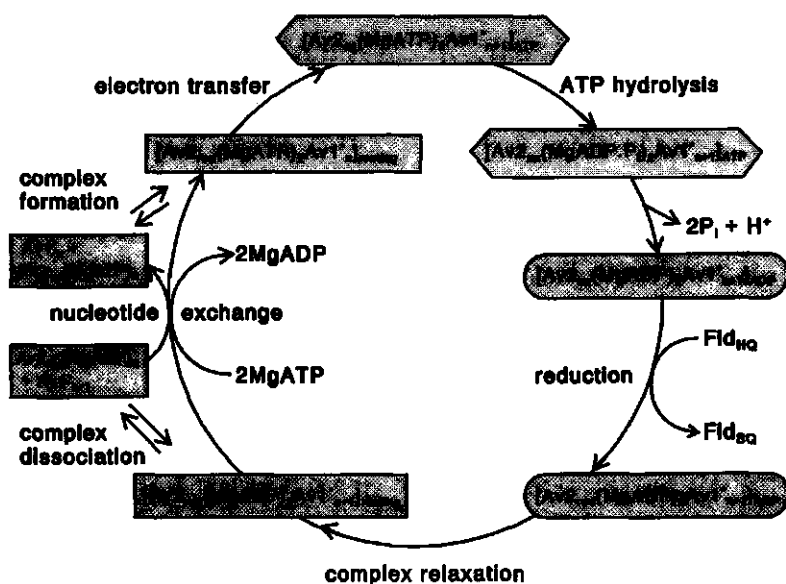
Figure 5 shows the effect of the reductant used on the absorbance changes associated with the electron transfer from Av2 to Av1. The initial absorbance increase after mixing of the nitrogenase proteins with MgATP is mainly due to the oxidation of Av2 by Av1 (Ashby & Thorneley, 1987). The subsequent absorbance decrease was much larger with Ti(III) citrate and Fld_{HQ} as the reductant than with dithionite. This is caused by the higher concentration of reductant when Ti(III) citrate or Fld_{HQ} is used as the reductant, compared to the concentration of SO₂⁻ when dithionite is used as the

reductant; this causes a higher rate of reduction of $\text{Av2}_{\text{ox}}(\text{MgADP})_2$ which results in a larger decrease of the absorbance. When dithionite was used, the absorbance increased again after the absorbance decrease; this was not observed with Ti(III) citrate and Fld_{HQ} (Figure 5). Lowe et al. (1993) attributed the absorbance changes observed after the initial absorbance increase to the consecutive redox changes of the MoFe protein, described in the MoFe protein cycle. The data presented in Figure 5 however show that the absorbance changes observed after the first increase are largely determined by the redox state of Av2, which depends on the reductant used.

Discussion

It is proposed in the literature that the rate-limiting step of the Fe protein cycle (Scheme 1) and thus of nitrogenase catalysis, is the dissociation of the nitrogenase complex after electron transfer and MgATP hydrolysis. Dissociation of the protein complex is thought to be obligatory for the reduction of the Fe protein and for the exchange of MgATP for MgADP . In order to obtain the essential kinetic constants to describe the pre-steady-state and steady-state kinetics of nitrogenase of *A. vinelandii*, the rate of the reduction of $\text{Av2}_{\text{ox}}(\text{MgADP})_2$ and the rate of the dissociation of the $\text{Av1} \cdot \text{Av2}_{\text{ox}}(\text{MgADP})_2$ complex were determined. When the kinetic data (Figure 1B) were analysed according to Scheme 1 the rate constant obtained for the dissociation of the nitrogenase complex was $k = 9.3 \text{ s}^{-1}$ (Table 2, simulation 2). When this rate constant was used, a simulation of the steady-state activity according to Scheme 1 predicted $6.8 \text{ mol e}^- \cdot \text{s}^{-1} \cdot (\text{mol Mo})^{-1}$ for the turnover rate of nitrogenase ($[\text{Av2}]/[\text{Av1}] = 20$, $[\text{Na}_2\text{S}_2\text{O}_4] = 20 \text{ mM}$), which is significantly higher than the observed rate of turnover: $3.0 \text{ mol e}^- \cdot \text{s}^{-1} \cdot (\text{mol Mo})^{-1}$ (Table 3). Furthermore, the dissociation constants of the $\text{Av1} \cdot \text{Av2}_{\text{ox}}(\text{MgADP})_2$ complex as well as the $\text{Av1} \cdot \text{Av2}_{\text{red}}(\text{MgADP})_2$ complex obtained from this simulation were an order of magnitude higher than the dissociation constants of the corresponding nitrogenase complexes from *K. pneumoniae* ($K_d = 1.5 \text{ }\mu\text{M}$ and $2.2 \text{ }\mu\text{M}$, respectively (Thorneley & Lowe, 1983)), which we considered unlikely. An alternative model (Table 2, simulation 3) includes reduction of Av2_{ox} in the $\text{Av1} \cdot \text{Av2}_{\text{ox}}(\text{MgADP})_2$ complex, besides the reduction of $\text{Av2}_{\text{ox}}(\text{MgADP})_2$ after the dissociation of the complex. If this is allowed, the turnover rate predicted by simulation of the kinetic data is $2.5 \text{ mol e}^- \cdot \text{s}^{-1} \cdot (\text{mol Mo})^{-1}$ which is closer to the observed turnover rate. Also the dissociation constants of the $\text{Av1} \cdot \text{Av2}_{\text{ox}}(\text{MgADP})_2$ and $\text{Av1} \cdot \text{Av2}_{\text{red}}(\text{MgADP})_2$ complexes have more likely values. That reduction of Av2_{ox} in the $\text{Av1} \cdot \text{Av2}_{\text{ox}}(\text{MgADP})_2$ complex is possible was shown by the results from the experiments with Ti(III) citrate and Fld_{HQ} : with these reductants dissociation of the

nitrogenase complex is not required for the reduction of Av2_{ox} . The exchange of MgATP for MgADP on the $\text{Av1} \cdot \text{Av2}_{\text{red}}(\text{MgADP})_2$ complex is fast (55 s^{-1}), and also for this reaction dissociation of the nitrogenase complex is not necessary. However, if the catalytic cycle of nitrogenase with Ti(III) citrate or Fld_{Hq} is simulated according to Scheme 1, but with the possibility of reduction and nucleotide exchange in the complex, the predicted turnover rate is $33 \text{ mol e}^- \cdot \text{s}^{-1} \cdot (\text{mol Mo})^{-1}$, which is significantly higher than the observed turnover rate. It is therefore clear that the original Fe protein cycle cannot explain the presented data.



Scheme 2. The extended Fe protein cycle of *A. vinelandii* nitrogenase. Abbreviations as in Scheme 1. $[\text{Av2}(\text{MgATP})_2\text{Av1}^*]_{\text{resting}}$, $[\text{Av2}(\text{MgATP})_2\text{Av1}^*]_{\text{ATP}}$ or $[\text{Av2}(\text{MgADP})_2\text{Av1}^*]_{\text{ADP}}$: the nitrogenase complex is in a resting state, the MgATP -bound or the MgADP -bound conformation, respectively. For details and rate constants, see text.

We propose an extended version of the Fe protein cycle as given in Scheme 2. This scheme is in better agreement with the latest kinetic data than the original Fe protein cycle, Scheme 1. It is known from other ATPases that the hydrolysis of MgATP consists of four distinct steps: the binding of MgATP to the protein, the on-enzyme hydrolysis of MgATP , the release of P_i and H^+ , and the release of MgADP .

In a previous publication we proposed that the binding of MgATP to the reduced nitrogenase complex (in the "resting" state) induces a conformational change of the nitrogenase complex which causes electron transfer from Av2 to Av1: $k_{\text{obs}} \approx 100 \text{ s}^{-1}$ (Duyvis et al., 1994). The release of P_i (Lowe et al., 1995) and H^+ (Duyvis et al., 1994) is observed after a lag phase of 15 - 20 ms: $k_{\text{obs}} \approx 14 \text{ s}^{-1}$. Recently we have shown that a similar lag period is observed before the oxidized nitrogenase complex switches from the MgATP-bound to the MgADP-bound conformation (which was monitored by a blue shift of the absorbance maximum, from 430 nm to 360 nm) (Duyvis et al., 1996b). A kinetic analysis of this lag phase is consistent with a model which comprises rapid formation of the nitrogenase complex, a change of the conformation of the nitrogenase complex upon binding of MgATP allowing electron transfer (100 s^{-1}), a delay reaction (on-enzyme hydrolysis of MgATP, $k \approx 77 \text{ s}^{-1}$) followed by a change from the MgATP-bound to the MgADP-bound conformation of the nitrogenase complex (monitored by H^+ release and a blue shift of the absorbance at 430 nm, $k_{\text{obs}} = 14 \text{ s}^{-1}$). A similar kinetic scheme was used by Lowe et al. (1995) to explain the pre-steady-state P_i release by *K. pneumoniae* nitrogenase. As shown, Ti(III) citrate and $\text{Fld}_{\text{H}_2\text{Q}}$ rapidly reduce Av2_{ox} in the $\text{Av1} \cdot \text{Av2}_{\text{ox}}(\text{MgADP})_2$ complex, before dissociation of the complex. Dithionite also reduces Av2_{ox} in the $\text{Av1} \cdot \text{Av2}_{\text{ox}}(\text{MgADP})_2$ complex before dissociation, but at a lower rate. The nucleotide exchange on the reduced protein complex ($k_{\text{obs}} = 55 \text{ s}^{-1}$) is much faster than the rate-limiting step of the Fe protein cycle. The time courses of the kinetics of Ti(III) citrate or $\text{Fld}_{\text{H}_2\text{Q}}$ oxidation (Figure 4A and 4B) are also consistent with a model where reduction of Av2_{ox} takes place (after a lag period) with a rate higher than the slowest step of the catalytic cycle. Since we have shown that dissociation of the nitrogenase complex is not necessary for reduction of $\text{Av2}_{\text{ox}}(\text{MgADP})_2$ or nucleotide exchange, we propose that a conformational change of the nitrogenase complex from the MgADP-bound conformation to a "resting" state (the "relaxation" step in Scheme 2) is part of the Fe protein cycle. Only after this reaction the nitrogenase complex can dissociate or, after nucleotide exchange, can enter a next round of the Fe protein cycle. An estimate of the rate constant for the proposed complex relaxation reaction was obtained by simulation of the maximum turnover rate of the Fe protein cycle according to Scheme 2. The rate constants of the various reactions of Scheme 2 were as mentioned above. To obtain a turnover rate of $4.8 \text{ mol e}^- \cdot \text{s}^{-1} \cdot (\text{mol Mo})^{-1}$ (at $[\text{Av1}] = 0.5 \text{ } \mu\text{M}$, $[\text{Av2}] = 10 \text{ } \mu\text{M}$ and $[\text{Fld}_{\text{H}_2\text{Q}}] = 50 \text{ } \mu\text{M}$), a rate constant $k = 11 \text{ s}^{-1}$ must be used for the complex relaxation reaction.

Acknowledgements

We thank Prof. C. Veeger and Prof. N. C. M. Laane for critically reading the manuscript. This investigation was supported by the Netherlands Foundation for Chemical Research (SON), with financial aid from the Netherlands Organization for Scientific Research (NWO).

References

- Ashby, G. A. & Thorneley, R. N. F. (1987) Nitrogenase of *Klebsiella pneumoniae*. Kinetic studies on the Fe protein involving reduction by sodium dithionite, the binding of MgADP and a conformation change that alters the reactivity of the 4Fe-4S centre, *Biochem. J.* **246**, 455-465.
- Barshop, B. A., Wrenn, R. F. & Frieden, C. (1983) Analysis of numerical methods for computer simulation of kinetic processes: development of KINSIM - a flexible, portable system, *Anal. Biochem.* **130**, 134-145.
- Bergström, J., Eady, R. R. & Thorneley, R. N. F. (1988) The vanadium- and molybdenum-containing nitrogenases of *Azotobacter chroococcum*. Comparison of mid-point potentials and kinetics of reduction by sodium dithionite of the iron proteins with bound magnesium adenosine 5'-diphosphate, *Biochem. J.* **251**, 165-169.
- Bolin, J. T., Campobasso, N., Muchmore, S. W., Morgan, T. V. & Mortenson, L. E. (1993) Structure and environment of metal clusters in the nitrogenase molybdenum-iron protein from *Clostridium pasteurianum*, in: *Molybdenum enzymes, cofactors and model systems* (Stiefel, E. I., Coucouvanis, D. & Newton, W. E., eds.) pp. 186-195, American Chemical Society, Washington.
- Bourne, H. R., Sanders, D. A. & McCormick, F. (1991) The GTPase superfamily: conserved structure and molecular mechanism, *Nature* **349**, 117-127.
- Braaksma, A., Haaker, H., Grande, H. J. & Veeger, C. (1982) The effect of the redox potential on the activity of the nitrogenase and on the Fe protein of *Azotobacter vinelandii*, *Eur. J. Biochem.* **121**, 483-491.
- Chan, M. K., Kim, J. & Rees, D. C. (1993) The nitrogenase FeMo-cofactor and P-cluster pair: 2.2 Å resolution structures, *Science* **260**, 792-794.
- Cordewener, J., Haaker, H., van Ewijk, P. & Veeger, C. (1985) Properties of the MgATP and MgADP binding sites on the Fe protein of nitrogenase from *Azotobacter vinelandii*, *Eur. J. Biochem.* **148**, 499-508.
- Dixon, M. (1971) The acceptor specificity of flavins and flavoproteins. Techniques for anaerobic spectrophotometry, *Biochim. Biophys. Acta* **226**, 241-258.
- Duyvis, M. G., Wassink, H. & Haaker, H. (1994) Pre-steady-state MgATP-dependent proton production and electron transfer by nitrogenase from *Azotobacter vinelandii*, *Eur. J. Biochem.* **225**, 881-890.
- Duyvis, M. G., Wassink, H. & Haaker, H. (1996a) Formation and characterization of a transition state complex of *Azotobacter vinelandii* nitrogenase, *FEBS Lett.* **380**, 233-236.
- Duyvis, M. G., Wassink, H. & Haaker, H. (1996b) Pre-steady-state kinetics of nitrogenase from *Azotobacter vinelandii*. Evidence for an ATP-induced conformational change of the nitrogenase complex, *J. Biol. Chem.* **271**, 29632-29636.
- Georgiadis, M. M., Komiya, H., Chakrabarti, P., Woo, D., Kornuc, J. J. & Rees, D. C. (1992) Crystallographic structure of the nitrogenase iron protein from *Azotobacter vinelandii*, *Science* **257**, 1653-1659.
- Hageman, R. V. & Burris, R. H. (1978) Nitrogenase and nitrogenase reductase associate and

- dissociate with each catalytic cycle, *Proc. Natl. Acad. Sci. USA* 75, 2699-2702.
- Hagen, W. R., Eady, R. R., Dunham, W. R. & Haaker, H. (1985) A novel $S = 3/2$ EPR signal associated with native Fe-proteins of nitrogenase, *FEBS Lett.* 189, 250-254.
- Howard, J. B. & Rees, D. C. (1994) Nitrogenase: a nucleotide-dependent molecular switch, *Annu. Rev. Biochem.* 63, 235-264.
- Kim, J. & Rees, D. C. (1992a) Structural models for the metal centers in the nitrogenase molybdenum-iron protein, *Science* 257, 1677-1682.
- Kim, J. & Rees, D. C. (1992b) Crystallographic structure and functional implications of the nitrogenase iron-molybdenum protein from *Azotobacter vinelandii*, *Nature* 360, 553-560.
- Kim, J. & Rees, D. C. (1994) Nitrogenase and biological nitrogen fixation, *Biochemistry* 33, 389-397.
- Klugkist, J., Voorberg, J., Haaker, H. & Veeger, C. (1986) Characterization of three different flavodoxins from *Azotobacter vinelandii*, *Eur. J. Biochem.* 155, 33-40.
- Lambeth, D. O. & Palmer, G. (1973) The kinetics and mechanism of reduction of electron transfer proteins and other compounds of biological interest by dithionite, *J. Biol. Chem.* 248, 6095-6103.
- Ljones, T., & Burris, R. H. (1978) Nitrogenase: the reaction between the Fe protein and bathophenanthroline disulfonate as a probe for interactions with MgATP, *Biochemistry* 17, 1866-1872.
- Lowe, D. J., Ashby, G. A., Brune, M., Knights, H., Webb, M. R. & Thorneley, R. N. F. (1995) ATP hydrolysis and energy transduction by nitrogenase, in: *Nitrogen fixation: fundamentals and applications* (Tikhonovich, I. A., Provorov, N. A., Romanov, V. I. and Newton, W. E., eds.) pp. 103-108, Kluwers Academic Publishers, Dordrecht, The Netherlands.
- Lowe, D. J., Fisher, K. & Thorneley, R. N. F. (1993) *Klebsiella pneumoniae* nitrogenase: pre-steady-state absorbance changes show that redox changes occur in the MoFe protein that depend on substrate and component protein ratio: a role for P-centers in reducing dinitrogen? *Biochem. J.* 292, 93-98.
- Lowe, D. J. & Thorneley, R. N. F. (1984a) The mechanism of *Klebsiella pneumoniae* nitrogenase action. Pre-steady-state kinetics of H_2 formation, *Biochem. J.* 224, 877-886.
- Lowe, D. J. & Thorneley, R. N. F. (1984b) The mechanism of *Klebsiella pneumoniae* nitrogenase action. The determination of rate constants required for the simulation of the kinetics of N_2 reduction and H_2 evolution, *Biochem. J.* 224, 895-901.
- Mensink, R. E. & Haaker, H. (1992) Temperature effects on the MgATP-induced electron transfer between the nitrogenase proteins from *Azotobacter vinelandii*, *Eur. J. Biochem.* 208, 295-299.
- Mensink, R. E., Wassink, H. & Haaker, H. (1992) A reinvestigation of the pre-steady-state ATPase activity of nitrogenase from *Azotobacter vinelandii*, *Eur. J. Biochem.* 208, 289-294.
- Orme-Johnson, W. H., Hamilton, W. D., Ljones, T., Tso, M.-Y. W., Burris, R. H., Shah, V. K. & Brill, W. J. (1972) Electron paramagnetic resonance of nitrogenase and nitrogenase components from *Clostridium pasteurianum* W5 and *Azotobacter vinelandii* OP, *Proc. Natl. Acad. Sci. USA* 69, 3142-3145.
- Peters, J. W., Fisher, K., Newton, W. E. & Dean, D. R. (1995) Involvement of the P-cluster in intramolecular electron transfer within the nitrogenase MoFe protein, *J. Biol. Chem.* 270, 27007-27013.
- Rayment, I., Rypniewski, W. R., Schmidt-Bäse, K., Smith, R., Tomchick, D. R., Benning, M. M., Winkelmann, D. A., Wesenberg, G. & Holden, H. M. (1993a) Three-dimensional structure of myosin subfragment-1: a molecular motor, *Science* 261, 50-58.

- Rayment, I., Holden, H. M., Whittaker, M. Yohn, C. B., Lorenz, M., Holmes, K. C. & Milligan, R. A. (1993b) Structure of the actin-myosin complex and its implications for muscle contraction, *Science* 261, 58-65.
- Renner, K. A. & Howard, J. B. (1996) Aluminum fluoride inhibition of nitrogenase: stabilization of a nucleotide-Fe-protein-MoFe-protein complex, *Biochemistry* 35, 5353-5358.
- Seefeldt, L. C. & Ensign, S. A. (1994) A continuous, spectrophotometric activity assay for nitrogenase using the reductant titanium(III) citrate, *Anal. Biochem.* 221, 379-386.
- Thorneley, R. N. F. & Lowe, D. J. (1983) Nitrogenase of *Klebsiella pneumoniae*. Kinetics of the dissociation of oxidized iron protein from molybdenum-iron protein: identification of the rate-limiting step for substrate reduction, *Biochem. J.* 215, 393-403.
- Thorneley, R. N. F. & Lowe, D. J. (1985) Kinetics and mechanism of the nitrogenase enzyme system, in: *Molybdenum enzymes* (Spiro, T. G., ed.) pp. 221-284, Wiley and Sons, New-York.
- Thorneley, R. N. F., Yates, M. G. & Lowe, D. J. (1976) Nitrogenase of *Azotobacter chroococcum*. Kinetics of the reduction of oxidized iron-protein by sodium dithionite, *Biochem. J.* 155, 137-144.
- Walker, G. A. & Mortenson, L. E. (1974) Effect of magnesium adenosine 5'-triphosphate on the accessibility of the iron of Clostridial azoferredoxin, a component of nitrogenase, *Biochemistry* 13, 2382-2388.
- Watt, G. D., Wang, Z.-C. & Knotts, R. R. (1986) Redox reactions of and nucleotide binding to the iron protein of *Azotobacter vinelandii*, *Biochemistry* 25, 8156-8162.
- Wolle, D., Dean, D. R. & Howard, J. B. (1992) Nucleotide-iron-sulfur cluster signal transduction in the nitrogenase iron-protein: the role of Asp¹²⁵, *Science* 258, 992-995.
- Zehnder, A. J. B. (1976) Ph. D. Thesis, Federal Institute of Technology (ETH), Zürich, Switzerland.
- Zimmerle, C. T. & Frieden, C. (1989) Analysis of progress curves by simulations generated by numerical integration, *Biochem. J.* 258, 381-387.
- Zumft, W. G., Cretney, W. C., Huang, T. C., Mortenson, L. E. & Palmer, G. (1972) On the structure and function of nitrogenase from *Clostridium pasteurianum* W5, *Biochem. Biophys. Res. Commun.* 48, 1525-1532.
- Zumft, W. G., Mortenson, L. E. & Palmer, G. (1974) Electron-paramagnetic-resonance studies on nitrogenase. Investigation of the oxidation-reduction behaviour of azoferredoxin and molybdoferredoxin with potentiometric and rapid-freeze techniques, *Eur. J. Biochem.* 46, 525-535.

Chapter 7

Summary and concluding remarks

Nitrogenase has been the subject of many investigations since the early 1960's. The catalytic mechanism of nitrogenase is unique because it couples the transfer of electrons with the hydrolysis of MgATP. The details of the mechanism are still to be revealed. The work described in this thesis aimed at a better understanding of nitrogenase catalysis. Questions we asked ourselves were:

What is the role of MgATP in nitrogenase catalysis?,

and:

What is the sequence of events when electrons are transferred from the Fe protein to the MoFe protein?

We tried to answer these questions mainly by using rapid kinetic methods, studying pre-steady-state reactions in nitrogenase catalysis. A brief introduction to nitrogenase is given in Chapter 1.

The MgATP-dependent pre-steady-state proton production by nitrogenase was studied by monitoring the absorbance changes of a pH indicator, cresol red (*Chapter 2*). The release of protons ($k_{\text{obs}} \approx 14 \text{ s}^{-1}$) was observed after a delay of ~50 ms after mixing of the nitrogenase proteins with MgATP. The MgATP-dependent electron transfer from the Fe protein to the MoFe protein ($k_{\text{obs}} \approx 100 \text{ s}^{-1}$) started immediately after mixing. No proton production with a rate comparable to or higher than the rate of electron transfer was observed. These observations correspond to those of Mensink et al. (1992). The extent of the MgATP-dependent proton production was found to be determined by the redox state of the Fe protein: when the Fe protein was oxidized (and no electrons are transferred but MgATP is still hydrolysed) more protons were released ($k_{\text{obs}} \approx 6 \text{ s}^{-1}$) than in the case when the Fe protein was reduced. This was explained as an indication that during electron transfer, together with the electron, a proton is absorbed by the MoFe protein. Proton production was also observed when the nitrogenase proteins were mixed with MgADP; the characteristics of the proton production, however, differed from the MgATP-induced proton production. It was argued correctly that pH changes during

nitrogenase turnover cannot unambiguously be assigned to a particular event in the nitrogenase catalytic cycle (Lowe et al., 1995): protons might be released due to the binding of MgATP to the nitrogenase complex, MgATP hydrolysis, the release of P_i , the release of MgADP, or during all of these steps. Lowe et al. (1995) studied the MgATP-induced pre-steady-state P_i release by *Klebsiella pneumoniae* nitrogenase, using a fluorescent phosphate probe. The reported P_i release curves are remarkably similar to our proton production curves. To be able to simulate their data, Lowe et al. (1995) had to adjust the Fe protein cycle (Chapter 1, Scheme 1) and use a kinetic scheme in which electron transfer ($k_{\text{obs}} = 176 \text{ s}^{-1}$) precedes the hydrolysis of MgATP ($k_{\text{obs}} = 50 \text{ s}^{-1}$) and the release of P_i from the nitrogenase complex ($k_{\text{obs}} = 22 \text{ s}^{-1}$). As proposed in Chapter 2, it is likely that the binding of MgATP to the nitrogenase complex and a change of the conformation of the nitrogenase complex from an "as-isolated" to a "MgATP-bound" conformation, are the trigger for electron transfer from the Fe protein to the MoFe protein. A recent interesting finding in this respect is that deletion of Leu¹²⁷ from the nucleotide binding region of the (*Azotobacter vinelandii*) Fe protein results in a conformation which closely resembles the MgATP-bound state (Ryle & Seefeldt, 1996), and that this altered Fe protein is capable of transferring one electron to the MoFe protein in the absence of MgATP (Lanzilotta et al., 1996).

When the crystallographic structure of the Fe protein from *A. vinelandii* was solved, it was found that the core of the Fe protein and specifically the nucleotide binding site, is highly similar to the nucleotide binding site of the H-Ras p21 protein (Georgiadis et al., 1992). It was suggested that, like this protein and other molecular switch proteins, nitrogenase could make use of nucleotide binding and hydrolysis to switch between different protein conformations. Non-hydrolysable analogues of ATP or GTP are often used to study the mechanism of nucleotide hydrolysis. Aluminium fluoride is known to act as an analogue of phosphate in the presence of ADP/GDP for various ATPases and GTPases (Chabre, 1990). In Chapter 3 the formation of a stable complex between both nitrogenase proteins, MgADP and aluminium fluoride is described. This complex did not have nitrogenase activity. However, dissociation of the nitrogenase·ADP·aluminium fluoride complex could be stimulated by incubation of the complex at 50 °C in the presence of P_i and NaCl, and nitrogenase activity was recovered. The composition of the nitrogenase·ADP·aluminium fluoride complex was ~2.7 Av2 and ~2.0 ADP per Av1. EPR measurements showed that in the nitrogenase ADP·aluminium fluoride complex the MoFe protein was present in the as-isolated, dithionite-reduced state, whereas the Fe protein was oxidized. The crystal structures of molecular switch proteins complexed with aluminium fluoride and ADP/GDP (transducin α , myosin and $G_{i\alpha}$) revealed that ADP/GDP·aluminium fluoride

mimics a transition state of ATP/GTP hydrolysis. Analogous to these findings, it is likely that we isolated the nitrogenase complex in a conformation which resembles a transition state in MgATP hydrolysis. Shortly after the publication of this work, Renner & Howard published a related study with similar results (1996). It is important to note that the complex with aluminium fluoride and ADP contains both the nitrogenase Fe protein and the MoFe protein, whereas in the case of the molecular switch proteins the nucleotide binding protein alone tightly binds aluminium fluoride and ADP/GDP. Exceptions are elongation factor EF-G, which forms a stable complex with aluminium fluoride, GDP and ribosomes but is not affected by aluminium fluoride in the absence of ribosomes (Mesters et al., 1993), and the Ras-protein, which only forms a complex with aluminium fluoride and GDP in the presence of certain GTPase activating proteins (Mittal et al., 1996). Recently the nitrogenase·ADP·aluminium fluoride complex was crystallized (H. Schindelin, C. Kisker, J. Howard & D. Rees, personal communication to Dr. H. Haaker). Preliminary data showed that the binding of aluminium fluoride and MgADP causes major conformational changes; in the nitrogenase·ADP·aluminium fluoride complex the subunits of the Fe protein are twisted and have moved ~20 Å towards each other, MgADP is bound in the H-Ras-like orientation (along the subunit interface) and the "top" helices in the environment of the [4Fe-4S] cluster are flat, which diminishes the distance between the [4Fe-4S] cluster and the P-cluster by ~5 Å compared to the distance in the proposed docking model for the nitrogenase complex (Kim & Rees, 1992b).

The pre-steady-state electron transfer reactions of nitrogenase are accompanied by changes of the absorbance at 430 nm. The interpretation of these absorbance changes is the subject of *Chapter 4*. The absorbance increase observed immediately after mixing of the nitrogenase proteins with MgATP is associated with the transfer of the first electron from the Fe protein to the MoFe protein and is mainly due to the oxidation of the Fe protein. After the initial absorbance increase (~50 ms) the absorbance decreases, which, dependent on the ratio $[Av2]/[Av1]$, is followed by another absorbance increase. In *Chapter 6* it is shown that this final absorbance increase is largely determined by the redox state of the Fe protein. Lowe et al. (1993) simulated the absorbance changes associated with the pre-steady-state electron transfer reactions of nitrogenase from *K. pneumoniae*, by ascribing the absorbance changes after the initial absorbance increase to successive redox changes of the MoFe protein (see *Chapter 1*, Scheme 2). The absorbance curves obtained for the nitrogenase proteins from *A. vinelandii* had a much more pronounced shape than the curves reported for *K. pneumoniae* nitrogenase (which did not contain a clear absorbance decrease) and, consequently, we were unable to simulate the *A. vinelandii* data with the model used by Lowe et al. (1993). We had to

add an extra step to the kinetic scheme, with a rate constant of $\sim 14 \text{ s}^{-1}$, to obtain an adequate simulation of the absorbance curves. When the reductant-free nitrogenase proteins (oxidized Av2) were mixed with MgATP, the absorbance at 430 nm decreased after a delay of $\sim 20 \text{ ms}$, with $k_{\text{obs}} = 6.6 \text{ s}^{-1}$; it was shown that the absorbance had shifted from 430 nm to 360 nm. It is highly probable that this absorbance decrease is associated with the reductant-independent ATPase activity of nitrogenase. The rate of this absorbance decrease and the rate of the extra reaction added to the kinetic scheme, were of the same order of magnitude as the rates of the MgATP-dependent pre-steady-state proton production in the absence ($k_{\text{obs}} \approx 6 \text{ s}^{-1}$) and in the presence of reductant ($k_{\text{obs}} \approx 14 \text{ s}^{-1}$) described in Chapter 2. It is proposed that the decrease of the absorbance at 430 nm observed during electron transfer and in the absence of reductant, is caused by a change of the conformation of the nitrogenase complex as a consequence of the hydrolysis of MgATP. This change from the MgATP-bound to the "MgADP-bound" conformation of the nitrogenase complex is accompanied by a release of protons.

A high concentration of NaCl and a low reaction temperature both lower the amplitude and the observed rate constant of the initial absorbance increase (430 nm) associated with pre-steady-state electron transfer from the Fe protein to the MoFe protein (Chapter 5). This suggests that, under such conditions, only a part of all MoFe protein present is reduced. Rapid-freeze EPR experiments showed that at 5°C (without NaCl) the reduction of the FeMo cofactor of the MoFe protein was indeed incomplete. This effect can be explained by assuming that the electron transfer between the nitrogenase proteins is a reversible process of which the back reaction becomes significant at low temperatures (Thorneley et al., 1989; Mensink & Haaker, 1992). In the presence of 500 mM NaCl however, the incomplete reduction of the MoFe protein ($\sim 35\%$) as suggested by the amplitude of the stopped-flow signal, was not confirmed by the rapid-freeze EPR data: $\sim 85\%$ of FeMoco was found to be reduced. We concluded that reversibility of electron transfer could not account for the diminished absorbance amplitude observed in the presence of NaCl. It is proposed that NaCl inhibits the rate of electron transfer, but not the rate of MgATP hydrolysis and the subsequent conformational change of the nitrogenase complex. Because the change from the MgATP-bound to the MgADP-bound nitrogenase conformation is accompanied by an absorbance decrease (Chapter 4), the absorbance increase associated with electron transfer is overtaken by this subsequent absorbance decrease and does not reach the maximum value. Deits & Howard (1990) concluded from steady-state experiments that NaCl inhibits substrate reduction without altering the ratio MgATP hydrolysed/electrons transferred. This agrees with our conclusion that electron transfer occurs when the nitrogenase complex is in the MgATP-bound conformation and not after MgATP

hydrolysis (Chapter 2 and Chapter 6). It was observed that in the presence of salt the reduction of FeMoco took place after a lag phase, whereas the absorbance increase associated with electron transfer started immediately after mixing of the nitrogenase proteins with MgATP. We propose that the electron transfer reaction is not a one-step process, but occurs from the Fe protein to FeMoco via an as-yet unidentified site at the MoFe protein. This site might be the P-cluster (Peters et al., 1995), but we were not able to find experimental evidence confirming this suggestion.

The dissociation of the nitrogenase complex after electron transfer and MgATP hydrolysis, is generally considered to be the rate-limiting step of the Fe protein cycle (Chapter 1, Scheme 1) and is thought to be obligatory for the re-reduction of the Fe protein and the exchange of MgADP for MgATP. This hypothesis was based on kinetic experiments with sodium dithionite as reductant. In Chapter 6 the rate-limiting step of the Fe protein cycle was studied, using three different reductants: sodium dithionite, Ti(III) citrate and flavodoxin hydroquinone. The rate of the dissociation of the nitrogenase complex was determined from the rate of reduction of oxidized Fe protein with MgADP bound ($\text{Av}2_{\text{ox}}(\text{MgADP})_2$), in the presence of MoFe protein, by dithionite ($k_{\text{obs}} = 2.8 \text{ s}^{-1}$). Ti(III) citrate and flavodoxin hydroquinone rapidly reduced $\text{Av}2_{\text{ox}}(\text{MgADP})_2$ in the nitrogenase complex, without preceding dissociation of the complex. The observation that dissociation of the nitrogenase complex is the rate-limiting step of nitrogenase catalysis (Thorneley & Lowe, 1983) is probably caused rather by the low concentration of the actual reductant, SO_2^{2-} , when sodium dithionite is used - which enables the nitrogenase complex to dissociate before $\text{Av}2_{\text{ox}}(\text{MgADP})_2$ is reduced - rather than by an impossibility of reduction of $\text{Av}2_{\text{ox}}(\text{MgADP})_2$ in the nitrogenase complex. Our data indicate that the exchange of MgADP for MgATP does not require dissociation of the reduced nitrogenase complex ($\text{Av}1\cdot\text{Av}2_{\text{red}}(\text{MgADP})_2$) either. The uptake of electrons by nitrogenase during turnover was studied by monitoring the absorbance changes associated with the oxidation of Ti(III) citrate and flavodoxin hydroquinone. The presence of a slow phase in the pre-steady-state electron uptake curves indicated that a slow step occurs in the Fe protein cycle after reduction of the oxidized Fe protein. Without adding such a slow reaction ($k = 11 \text{ s}^{-1}$) to the kinetic scheme, simulations of the kinetic cycle with Ti(III) citrate or flavodoxin hydroquinone as the reductant yielded a turnover rate which was unreasonably high compared to the observed rate of nitrogenase turnover. It is proposed that this slow step and the conformational change of the nitrogenase complex after MgATP hydrolysis (14 s^{-1}) together limit the rate of nitrogenase turnover.

The sequence of events during nitrogenase catalysis: a revision of the Fe protein cycle

With the kinetic data described in this thesis it is possible to revise the Fe protein cycle (Chapter 1, Scheme 1) to a version (Chapter 6, Scheme 2) which, according to our kinetic data, better describes the sequence of events during nitrogenase catalysis than the original Fe protein cycle. The binding of MgATP to the nitrogenase complex induces a change from the "resting" conformation to the MgATP-bound conformation of the complex. This conformational change triggers electron transfer from the Fe protein to the MoFe protein ($k_{\text{obs}} \approx 100 \text{ s}^{-1}$). In the MgATP-bound conformation MgATP is hydrolysed ($k \approx 77 \text{ s}^{-1}$), which is followed by a change of the conformation of the nitrogenase complex from the MgATP-bound to the MgADP-bound conformation. This conformational change is accompanied by the production of protons and a decrease of the absorbance at 430 nm ($k_{\text{obs}} \approx 14 \text{ s}^{-1}$). A similar kinetic scheme was used by Lowe et al. (1995) to describe the pre-steady-state P_i release by *K. pneumoniae* nitrogenase. The oxidized Fe protein is rapidly reduced in the nitrogenase complex if Ti(III) citrate or flavodoxin hydroquinone is used, and at a much lower rate if sodium dithionite is used. The slow step in the catalytic cycle might be a relaxation of the nitrogenase complex from the MgADP-bound conformation to the resting state ($k \approx 11 \text{ s}^{-1}$). After this step MgATP is exchanged for MgADP ($k_{\text{obs}} \approx 55 \text{ s}^{-1}$), and the nitrogenase complex enters the next round of electron transfer. In this scheme, dissociation of the nitrogenase complex is a side-reaction of the catalytic cycle and only occurs with sodium dithionite as reductant.

The role of MgATP in nitrogenase catalysis: the Fe protein as a molecular switch protein

When the close structural similarity between the nucleotide binding site of the Fe protein from *A. vinelandii* and the nucleotide binding site of the H-Ras p21 protein was discovered, it was suggested that the Fe protein might act as a molecular switch protein (Georgiadis et al., 1992). It has become clear that the resemblance between the nitrogenase Fe protein and the molecular switch proteins is more than just structural. We have presented kinetic evidence that conformational changes of the Fe protein and thus of the nitrogenase complex, induced by the binding of MgATP and MgATP-hydrolysis, drive the catalytic cycle of nitrogenase. That the MgATP-bound conformation of the Fe protein, as proposed in Chapter 1, is sufficient to induce electron transfer to the MoFe protein, was beautifully illustrated by Ryle & Seefeldt (1996) and Lanzilotta et al.

(1996), who constructed an Fe protein capable of electron transfer in the absence of MgATP. As with many molecular switch proteins, aluminium fluoride and MgADP stabilize the nitrogenase complex in what is probably a transition state of MgATP hydrolysis, thereby inhibiting all nitrogenase activity. The MoFe protein induces MgATP hydrolysis at the Fe protein, which is reminiscent of the way an effector protein induces nucleotide hydrolysis by molecular switch proteins. The function of MgATP hydrolysis might be to secure such a conformation of the nitrogenase complex (the MgADP-bound conformation) that backflow of electrons from the MoFe protein to the Fe protein is prevented (Wolle et al., 1992). The resemblances between the structures and the catalytic mechanisms lead to the conclusion that the nitrogenase Fe protein must be regarded as a molecular switch protein.

References

- Chabre, M. (1990) Aluminofluoride and beryllorfluoride complexes: new phosphate analogs in enzymology, *Trends Biochem. Sci.* 15, 6-10.
- Deits, T. L. & Howard, J. B. (1990) Effect of salts on *Azotobacter vinelandii* nitrogenase activities. Inhibition of iron chelation and substrate reduction, *J. Biol. Chem.* 265, 3859-3867.
- Georgiadis, M. M., Komiya, H., Chakrabarti, P., Woo, D., Kornuc, J. J. & Rees, D. C. (1992) Crystallographic structure of the nitrogenase iron protein from *Azotobacter vinelandii*, *Science* 257, 1653-1659.
- Kim, J. & Rees, D. C. (1992) Crystallographic structure and functional implications of the nitrogenase molybdenum-iron protein from *Azotobacter vinelandii*, *Nature* 360, 553-560.
- Lanzilotta, W. N., Fisher, K., & Seefeldt, L. C. (1996) Evidence for electron transfer from the nitrogenase iron protein to the molybdenum-iron protein without MgATP hydrolysis: characterization of a tight protein-protein complex, *Biochemistry* 35, 7188-7196.
- Lowe, D. J., Ashby, G. A., Brune, M., Knights, H. Webb, M. R. & Thorneley, R. N. F. (1995) ATP hydrolysis and energy transduction by nitrogenase, in: *Nitrogen fixation: fundamentals and applications* (Tikhonovic, I. A., Provarov, N. A., Romanov, V. I. & Newton, W. E., eds.) pp. 103-108, Kluwer Academic Publishers Dordrecht, The Netherlands.
- Lowe, D. J., Fisher, K. & Thorneley, R. N. F. (1993) *Klebsiella pneumoniae* nitrogenase: pre-steady-state absorbance changes show that redox changes occur in the MoFe protein that depend on substrate and component protein ratio; a role for P-centres in reducing dinitrogen? *Biochem. J.* 292, 93-98.
- Mensink, R. E. & Haaker, H. (1992) Temperature effects on the MgATP-induced electron transfer between the nitrogenase proteins from *Azotobacter vinelandii*, *Eur. J. Biochem.* 208, 295-299.
- Mensink, R. E., Wassink, H. & Haaker, H. (1992) A reinvestigation of the pre-steady-state ATPase activity of the nitrogenase from *Azotobacter vinelandii*, *Eur. J. Biochem.* 208, 289-294.

- Mesters, J. R., de Graaf, M. & Kraal, B. (1993) Divergent effects of fluoroaluminates on the peptide chain elongation factors EF-Tu and EF-G as members of the GTPase superfamily, *FEBS Lett.* 321, 149-152.
- Mittal, R., Ahmadian, M. R., Goody, R. S. & Wittinghofer, A. (1996) Formation of a transition-state analog of the Ras GTPase reaction by Ras-GDP, tetrafluoroaluminate, and GTPase activating proteins, *Science* 273, 115-117.
- Peters, J. W., Fisher, K., Newton, W. E. & Dean, D. R. (1995) Involvement of the P-cluster in intramolecular electron transfer within the nitrogenase MoFe protein, *J. Biol. Chem.* 270, 27007-27013.
- Renner, K. A. & Howard, J. B. (1996) Aluminum fluoride inhibition of nitrogenase: stabilization of a nucleotide-Fe protein-MoFe protein complex, *Biochemistry* 35, 5353-5358.
- Ryle, M. J. & Seefeldt, L. C. (1996) Elucidation of a MgATP signal transduction pathway in the nitrogenase iron protein: formation of a conformation resembling the MgATP-bound state by protein engineering, *Biochemistry* 35, 4766-4775.
- Thorneley, R. N. F., Ashby, G. A., Howarth, J. V., Millar, N. C. & Gutfreund, H. (1989) A transient kinetic study of the nitrogenase of *Klebsiella pneumoniae* by stopped-flow calorimetry, *Biochem. J.* 264, 657-661.
- Thorneley, R. N. F. & Lowe, D. J. (1983) Nitrogenase of *Klebsiella pneumoniae*. Kinetics of the dissociation of oxidized iron protein from molybdenum-iron protein: identification of the rate-limiting step for substrate reduction, *Biochem. J.* 215., 393-403.
- Wolle, D., Dean, D. R. & Howard, J. B. (1992) Nucleotide iron-sulfur cluster signal transduction in the nitrogenase iron-protein: the role of Asp¹²⁵, *Science* 258, 992-995.

Samenvatting

Het belang van stikstof voor organismen

Alle organismen hebben het element stikstof (N) nodig. Dit element is een belangrijk bestanddeel van biologische moleculen zoals eiwitten en DNA - moleculen die essentiële onderdelen zijn van elk organisme. Stikstof ondergaat een kringloop tussen atmosfeer, bodem en organismen: de "stikstof kringloop". In de atmosfeer komt stikstof in grote hoeveelheden voor, in de vorm van stikstofgas (N_2). Deze stikstofmoleculen zijn echter zeer stabiel en zijn daarom voor de meeste organismen niet bruikbaar als stikstofbron. Het industriële proces waarin N_2 tot ammoniak (NH_3) wordt omgezet ("stikstofbinding" of "stikstoffixatie") vindt alleen plaats bij hoge temperatuur (300 - 500 °C) en onder zeer hoge druk (meer dan 300 atmosfeer). Planten en veel micro-organismen voorzien in hun stikstofbehoefte door opname van anorganische verbindingen die makkelijker reageren, zoals nitraat (NO_3^-) en ammoniak (NH_3); deze moleculen zijn het uitgangspunt voor de synthese van hun eiwitten en andere complexe organische moleculen. Dieren gebruiken de organische stikstofverbindingen die de plant heeft gesynthetiseerd als stikstofbron. Door verschillende oorzaken verdwijnen de bruikbare stikstofverbindingen (o.a. nitraat, ammoniak en organisch materiaal) in de vorm van N_2 weer in de atmosfeer. De situatie wordt in evenwicht gehouden door een kleine, diverse groep van micro-organismen die beschikken over het enzym *nitrogenase*: dit enzym stelt hen in staat N_2 om te zetten tot NH_3 ("biologische stikstofbinding"), bij kamertemperatuur en een druk van 1 atmosfeer. Uiteindelijk zijn alle organismen voor hun stikstofvoorziening voornamelijk afhankelijk van stikstofbindende organismen. Een bekend voorbeeld is de stikstofbindende bacterie *Rhizobium*, die in knolletjes op de wortels van vlinderbloemige planten leeft. Voor het onderzoek naar het werkingsmechanisme van *nitrogenase*, beschreven in dit proefschrift, werd de vrijlevende stikstofbindende bacterie *Azotobacter vinelandii* op grote schaal gekweekt.

Een *eiwit* is een lange keten van kleine organische moleculen, die aminozuren worden genoemd. Er bestaan 20 verschillende aminozuren; alle organismen gebruiken dezelfde aminozuren als bouwstenen voor hun eiwitten. Doordat aminozuren in willekeurige volgorde aan elkaar kunnen worden gekoppeld tot ketens van verschillende lengte (de meeste eiwitten zijn tussen 50 en 2000 aminozuren lang) is de verscheidenheid aan eiwitten enorm groot. De aminozuurketen is op een specifieke manier in elkaar gevouwen waardoor het eiwit een ruimtelijke structuur, of *conformatie*, heeft. De conformatie bepaalt de biologische functie van het eiwit. Veel eiwitten hebben

om te kunnen functioneren bovendien nog een ander molecuul of een metaalion (zoals b.v. ijzer, koper, zink of magnesium) nodig, dat sterk gebonden is in het eiwit. In vrijwel alle biologische processen spelen eiwitten een cruciale rol. Zo zijn er bijvoorbeeld eiwitten die chemische reacties versnellen, eiwitten met een transport- of opslagfunctie, eiwitten die stevigheid verlenen aan de cel, eiwitten die signalen doorgeven, etcetera. De meeste chemische reacties die in een organisme plaatsvinden verlopen niet of nauwelijks vanzelf en worden daarom gekatalyseerd (\approx versneld) door *enzymen*: de reactiesnelheid kan hierdoor minstens een miljoen maal worden verhoogd. Een enzym is - meestal - een eiwit dat, heel specifiek, één bepaalde chemische reactie katalyseert. Het enzym zelf verandert niet door de reactie en kan de reactie dan ook vele malen herhalen.

Nitrogenase

Het enzym *nitrogenase* katalyseert de chemische omzetting van 1 stikstofmolecuul, N_2 , tot 2 moleculen ammoniak, $2 NH_3$, en één molecuul waterstof, H_2 (een bijproduct van de reactie). Het enzym bestaat uit twee losse eiwitten die samenwerken om deze reactie te laten verlopen: het ijzer-eiwit (Fe-eiwit) en het molybdeen-ijzer-eiwit (MoFe-eiwit) (hoofdstuk 1, figuur 1 en figuur 4). Hun naam ontleen deze eiwitten aan de metalen die ze bevatten. De aanwezigheid van metalen in de nitrogenase eiwitten heeft te maken met het feit dat tijdens de reactie electronen op het stikstofmolecuul moeten worden geplaatst. In het stikstofmolecuul zijn de beide stikstofatomen namelijk ongeladen, terwijl het stikstofatoom in ammoniak drie extra electronen bevat. Men spreekt van *reductie* als electronen worden opgenomen, van *oxidatie* als electronen worden afgestaan. Het Fe-eiwit bevat een structuur die uit vier ijzeratomen (Fe) en vier zwavelatomen (S) bestaat: deze "ijzer-zwavel cluster" kan één electron opnemen en weer afstaan. Het MoFe-eiwit bevat twee soorten metaal-zwavel clusters met een ingewikkelder structuur: de "P-cluster" bestaat uit acht ijzeratomen en zeven of acht zwavelatomen (zie hoofdstuk 1, figuur 3) en de "ijzer-molybdeen cofactor", of "FeMoco", bevat zeven ijzeratomen, één molybdeenatoom (Mo) en zes zwavelatomen (zie hoofdstuk 1, figuur 2). Deze clusters kunnen vermoedelijk meer dan één electron opnemen en afstaan. Tijdens de nitrogenase reactie worden electronen van de ijzer-zwavel cluster in het Fe-eiwit naar het MoFe-eiwit getransporteerd en vervolgens naar het stikstofmolecuul. Tijdens de reactie is N_2 gebonden aan FeMoco in MoFe-eiwit; de functie van de P-cluster staat nog ter discussie.

Het transport van electronen van het Fe-eiwit naar het MoFe-eiwit vindt alleen plaats als het energierijke molecuul ATP (adenosinetrifosfaat) aanwezig is. ATP is de drijvende kracht achter vrijwel alle biologische processen die energie vereisen, zoals

bijvoorbeeld het spannen van een spier. Als een gedeelte van dit molecuul, fosfaat, wordt verwijderd (*hydrolyse* van ATP), komt energie vrij. Dit gebeurt ook tijdens de nitrogenase reactie: ATP bindt op een specifieke plaats aan het Fe-eiwit en als het MoFe-eiwit aanwezig is wordt ATP gehydrolyseerd. Bovendien verandert ATP de conformatie van het Fe-eiwit, wanneer het aan het Fe-eiwit bindt. Het molecuul dat ten gevolge van de hydrolyse van ATP wordt gevormd, ADP (adenosinedifosfaat), verandert de conformatie van het Fe-eiwit ook, maar op een iets andere manier dan ATP.

Een model voor de nitrogenase reactie

In 1983 werd door een engelse groep van biochemici een model voor de opeenvolging van gebeurtenissen tijdens de nitrogenase reactie geponeerd: de "Fe-eiwit cyclus" (hoofdstuk 1, schema 1). In de eerste stap van deze cyclus wordt het *nitrogenase complex* gevormd, door binding van het Fe-eiwit aan het MoFe-eiwit. In dit complex draagt het Fe-eiwit één electron over op het MoFe-eiwit (het Fe-eiwit wordt geoxideerd en het MoFe-eiwit gereduceerd). Tevens wordt ATP gehydrolyseerd. Hierna dissocieert het nitrogenase complex tot de twee afzonderlijke eiwitten: dit is de langzaamste stap van de cyclus (de "snelheidsbeperkende stap"). Om N_2 om te zetten in twee moleculen NH_3 en één molecuul H_2 zijn acht electronen nodig. Het MoFe-eiwit moet dus nog zeven electronen opnemen. De ijzer-zwavel cluster van het Fe-eiwit kan echter maar één electron afstaan, zodat het Fe-eiwit eerst weer gereduceerd moet worden voordat de reactie verder kan verlopen. Dit gebeurt in de laatste stap van de cyclus: het Fe-eiwit wordt door een verbinding die makkelijk electronen afstaat (dithioniet), gereduceerd. Daarna wordt ADP (gevormd door de hydrolyse van ATP) vervangen door ATP: als ADP aan het Fe-eiwit is gebonden vindt namelijk geen electronoverdracht naar het MoFe-eiwit plaats. Hiermee is de cyclus rond. Het MoFe-eiwit doorloopt de Fe-eiwit cyclus in totaal acht keer, zodat het stapsgewijs steeds meer gereduceerd wordt totdat ammoniak tenslotte vrijkomt (hoofdstuk 1, schema 2).

De Fe-eiwit cyclus was het uitgangspunt van het onderzoek dat is beschreven in dit proefschrift. Het doel was een beter inzicht te krijgen in het werkingsmechanisme van nitrogenase, waarbij de volgende vragen werden gesteld:

Welke functie heeft ATP in de nitrogenase reactie?

Wat is precies de volgorde van gebeurtenissen wanneer een electron van het Fe-eiwit op het MoFe-eiwit wordt overgedragen?

Het onderzoek

Zodra ATP aan beide nitrogenase eiwitten wordt toegevoegd, begint het electronentransport van het Fe-eiwit naar het MoFe-eiwit; de overdracht van het eerste electron voltrekt zich binnen 50 milliseconden. De beginfase van de nitrogenase reactie noemt men de "pre-steady-state fase" van de reactie. De electronoverdracht kan op verschillende manieren worden gemeten. Als het Fe-eiwit zijn electron afstaat verandert het enigszins van kleur; de *absorptie* van licht (met een golflengte van 430 nanometer) verandert. Met een "stopped-flow spectrofotometer" kan deze absorptieverandering nauwkeurig in de tijd worden gevolgd. Een andere methode is de nitrogenase eiwitten enige tijd te laten reageren en vervolgens snel te bevriezen, waardoor de reactie stopt ("rapid-freeze"). Met behulp van een andere techniek, "EPR spectroscopie", kan dan worden bepaald of het aantal electronen dat zich op de metaal-zwavel clusters van de nitrogenase eiwitten bevindt, is veranderd ten opzichte van de beginsituatie.

Tijdens de nitrogenase reactie komen protonen vrij, waardoor de oplossing iets zuurder wordt. Dit kan zichtbaar worden gemaakt met behulp van een pH indicator, een stof die van kleur verandert als de zuurgraad (pH) verandert. In *hoofdstuk 2* worden stopped-flow experimenten beschreven waarin de protonproductie tijdens de pre-steady-state fase van de nitrogenase reactie via de kleursveranderingen van een pH indicator werd gevolgd. Uit de experimenten bleek dat de electronoverdracht van het Fe-eiwit naar het MoFe-eiwit veel sneller verliep dan de protonproductie, en dat de protonproductie ~50 ms later dan de electronoverdracht begon. Ook als er geen electronoverdracht plaatsvindt (als het Fe-eiwit geoxideerd is), hydrolyseert nitrogenase ATP: ook onder deze omstandigheden werden protonen geproduceerd. Zonder electronoverdracht was de protonproductie groter dan wanneer er wel electronen werden overgedragen op het MoFe-eiwit. Dit duidt erop dat het MoFe-eiwit tegelijk met een electron een proton opneemt: het neemt als het ware een H-atom op.

Het nitrogenase complex dat tijdens de katalyse uit de beide nitrogenase eiwitten wordt gevormd, bestaat slechts tijdelijk: na de electronoverdracht en de ATP hydrolyse dissocieert het weer. Het is dan ook niet bekend hoe dit complex er uitziet. In *hoofdstuk 3* wordt een tipje van de sluier opgelicht. Er wordt beschreven dat een stabiel complex gevormd kan worden tussen de nitrogenase eiwitten, ADP en aluminiumfluoride. Dit complex vertoonde geen enkele nitrogenase activiteit en er vond geen electronoverdracht plaats. Dissociatie van het complex kon worden gestimuleerd door het te verhitten (50 °C). Deze complexvorming is daarom zo interessant omdat dit een eigenschap is van een zeer grote en diverse groep eiwitten, de "molecular switch" eiwitten. Deze eiwitten gebruiken ATP hydrolyse om te kunnen omschakelen tussen

twee eiwitconformaties, de "ATP-conformatie" en de "ADP-conformatie": hiermee kunnen allerlei biochemische processen in een bepaalde richting gestuurd worden. Het is bekend dat ADP en aluminiumfluoride, in complex met zo'n molecular switch eiwit, samen een actief ATP molecuul nabootsen en daarbij het eiwit in een conformatie "bevriezen" - in een overgangstoestand vlak voordat fosfaat wordt losgelaten. Waarschijnlijk is dit ook het geval bij het stabiele complex van ADP, aluminiumfluoride en de beide nitrogenase eiwitten.

De absorptieveranderingen (430 nm) die worden waargenomen wanneer electronen van het Fe-eiwit op het MoFe-eiwit worden overgedragen, worden beschreven in **hoofdstuk 4**. Meteen na de start van een stopped-flow experiment neemt de absorptie toe ten gevolge van de overdracht van het eerste electron van het Fe-eiwit op het MoFe-eiwit. De daaropvolgende kleinere absorptieveranderingen hebben te maken met de verdergaande reductie van het MoFe-eiwit. Een engelse onderzoeksgroep kon de absorptieveranderingen, waargenomen voor nitrogenase afkomstig uit een andere bacterie (*Klebsiella pneumoniae*), simuleren met de Fe-eiwit cyclus als model voor de katalyse; daarbij werd aangenomen dat elke keer dat een volgend electron op het MoFe-eiwit wordt overgedragen, de absorptie van het MoFe-eiwit enigszins verandert. Omdat de absorptieveranderingen voor nitrogenase uit *Azotobacter vinelandii* essentieel verschilden van die voor *K. pneumoniae* nitrogenase, was het niet mogelijk de absorptieveranderingen voor *A. vinelandii* nitrogenase met dit model te simuleren. Deze absorptieveranderingen konden alleen dán gesimuleerd worden als een extra stap ná de electronoverdracht in de Fe-eiwit cyclus werd geïntroduceerd - een stap met dezelfde snelheid als de snelheid van de protonproductie tijdens de nitrogenase reactie (hoofdstuk 2). Uit een stopped-flow experiment met geoxideerd Fe-eiwit bleek dat ten gevolge van de hydrolyse van ATP de absorptie (bij 430 nm) afneemt, met dezelfde snelheid als protonen werden geproduceerd onder deze omstandigheden (hoofdstuk 2). In hoofdstuk 4 wordt voorgesteld dat na de hydrolyse van ATP de conformatie van het nitrogenase complex verandert, van de "ATP-conformatie" naar de "ADP-conformatie"; deze stap, die langzamer is dan de electronoverdracht, gaat gepaard met een afname van de absorptie en met productie van protonen.

In **hoofdstuk 5** wordt het effect van een lage reactietemperatuur en het effect van een hoge zoutconcentratie op de electronoverdracht beschreven. Een lage reactietemperatuur en een hoge zoutconcentratie vertragen en verkleinen de initiële absorptietoename, die gepaard gaat met oxidatie van het Fe-eiwit; hieruit zou men kunnen afleiden dat de electronoverdracht naar het MoFe-eiwit langzamer en slechts gedeeltelijk verloopt. Rapid-freeze EPR experimenten toonden aan dat dit bij een lage reactietemperatuur inderdaad het geval was; een mogelijke verklaring is dat de electronoverdracht van het Fe-eiwit naar het MoFe-eiwit bij lage temperatuur reversibel

is. Bij een hoge zoutconcentratie bleek echter dat het MoFe-eiwit toch vrijwel volledig werd gereduceerd, in tegenspraak met de verwachting op grond van het stopped-flow experiment. De verminderde absorptietoename wordt verklaard door aan te nemen dat de electronoverdracht langzamer verloopt in de aanwezigheid van zout, terwijl de conformatieverandering van het nitrogenase complex ten gevolge van ATP hydrolyse niet vertraagt. Deze conformatieverandering gaat gepaard met een afname van de absorptie (zoals aangetoond in hoofdstuk 4), zodat de absorptietoename ten gevolge van electronoverdracht in de aanwezigheid van zout wordt "ingehaald" door de absorptieafname. Bij een hoge zoutconcentratie is het stopped-flow signaal dus niet langer een betrouwbare maat voor de electronoverdracht. De rapid-freeze experimenten in aanwezigheid van zout gaven tevens een aanwijzing dat het electron niet in één stap van de ijzer-zwavel cluster van het Fe-eiwit naar FeMoco wordt getransporteerd, maar dat dit in twee stappen gebeurt, via een nog niet geïdentificeerde plaats in het MoFe-eiwit.

In **hoofdstuk 6** wordt de snelheidsbeperkende stap van de Fe-eiwit cyclus, de dissociatie van het nitrogenase complex, bestudeerd. In de Fe-eiwit cyclus wordt het Fe-eiwit na deze stap door dithioniet gereduceerd en wordt ADP vervangen door ATP. Uit experimenten waarin in plaats van dithioniet, titanium(III)citraat of het electronen-transporterende eiwit flavodoxine werd gebruikt om het Fe-eiwit te reduceren, bleek echter dat het Fe-eiwit wel degelijk kon worden gereduceerd terwijl het nog aan het MoFe-eiwit was gebonden. Er werd geconcludeerd dat dissociatie van het nitrogenase complex geen vereiste is om het Fe-eiwit te kunnen reduceren; omdat dithioniet het Fe-eiwit echter op een inefficiënte manier reduceert, heeft het nitrogenase complex de tijd om te dissociëren. Ook bleek dat dissociatie van het nitrogenase complex evenmin noodzakelijk was om ADP te kunnen uitwisselen voor ATP. De resultaten van stopped-flow experimenten waarin de oxidatie van titanium(III)citraat en flavodoxine (in de pre-steady-state fase van de nitrogenase reactie) werd gevolgd, duiden erop dat ná de reductie van het Fe-eiwit nog een langzame stap optrad. Deze stap zou weer een volgende conformatieverandering van het nitrogenase complex kunnen zijn, van de ADP-conformatie naar een rusttoestand.

Conclusie

Hoofdstuk 6 besluit met een voorstel de Fe-eiwit cyclus te herzien. In deze nieuwe cyclus (hoofdstuk 6, schema 2) spelen veranderingen van de conformatie van het nitrogenase complex een belangrijke rol in het reactiemechanisme. De binding van ATP aan het Fe-eiwit brengt het nitrogenase complex in de ATP-conformatie waardoor

electronoverdracht van het Fe-eiwit op het MoFe-eiwit mogelijk is. Daarna wordt ATP gehydrolyseerd. Deze reactie wordt gevolgd door een verandering van de conformatie van het nitrogenase complex, naar de ADP-conformatie. Deze conformatieverandering gaat gepaard met de productie van protonen. Het Fe-eiwit wordt snel gereduceerd in het nitrogenase complex als een efficiënte reductor wordt gebruikt, zoals flavodoxine of titanium(III)citraat. Vervolgens verandert de conformatie van het nitrogenase complex weer, naar een rusttoestand, en wordt ADP vervangen door ATP. Daarna kan het volgende electron naar het MoFe-eiwit overgedragen worden. Dissociatie van het nitrogenase complex is dus geen essentiële stap in deze versie van de Fe-eiwit cyclus.

De voorgestelde serie conformatieveranderingen van het nitrogenase complex tijdens de katalyse en de reactie van nitrogenase met ADP en aluminiumfluoride schetsen het beeld dat nitrogenase kinetische eigenschappen van de molecular switch eiwitten bezit. De molecular switch eiwitten zijn eiwitten - met zeer verschillende herkomst en functies - die werken als een schakelaar. Deze eiwitten gebruiken binding van ATP en ADP (of soortgelijke moleculen zoals GTP en GDP) om hun conformatie te veranderen. De conformatie van het molecular switch eiwit bepaalt of een bepaalde biochemische reactie wordt gekatalyseerd of niet: de ATP-conformatie "zet de reactie aan", in de ADP-conformatie "staat de reactie uit". Het Fe-eiwit doet in feite hetzelfde: de binding van ATP verandert de conformatie van het Fe-eiwit, waardoor het nitrogenase complex de ATP-conformatie aanneemt en electron-overdracht kan plaatsvinden; als ADP aan het Fe-eiwit is gebonden is worden geen electronen getransporteerd naar het MoFe-eiwit en kan het electron niet meer terug van het MoFe-eiwit naar het Fe-eiwit. Het idee dat het Fe-eiwit van nitrogenase tot de groep van molecular switch eiwitten behoort wordt bevestigd door de sterke gelijkenis tussen de structuur van het Fe-eiwit (met name rondom de ATP-bindingsplaats) en de structuur van het humane eiwit Ras p21, een molecular switch eiwit. De overeenkomsten tussen het Fe-eiwit en de molecular switch eiwitten, in katalytisch mechanisme en structuur, leiden tot de conclusie dat het Fe-eiwit van nitrogenase moet worden beschouwd als een molecular switch eiwit.

Curriculum vitae

Martina Gezina Duyvis is geboren op 30 april 1965 te Delft. In 1983 deed zij eindexamen aan het Stedelijk Gymnasium te Breda. Daarna studeerde zij een jaar Plantenziektekunde aan de Landbouwhogeschool te Wageningen. In 1984 zwaaide zij om en begon aan haar studie Moleculaire Wetenschappen, eveneens aan de Landbouwhogeschool. In de doctoraalfase deed zij afstudeervakken bij de vakgroep Moleculaire Fysica (dr. H. van As, prof. T. J. Schaafsma) en de vakgroep Biochemie (dr. A. J. Pierik, prof. W. R. Hagen, prof. C. Veeger). In augustus 1990 studeerde zij af.

Van april 1991 tot april 1995 was zij als onderzoeker in opleiding (oio) verbonden aan de vakgroep Biochemie van de Landbouwniversiteit te Wageningen, in dienst van de Nederlandse Organisatie voor Wetenschappelijk Onderzoek (NWO). Het onderzoek werd gefinancierd door NWO, onder toezicht van de Stichting Scheikundig Onderzoek in Nederland (SON). Het onderzoek werd begeleid door dr. H. Haaker en prof. C. Veeger. De resultaten van het onderzoek zijn beschreven in dit proefschrift.

Publications

Pierik, A. J., Duyvis, M. G., van Helvoort, J. M. L. M., Wolbert, R. B. G. & Hagen, W. R. (1992) The third subunit of desulfoviridin-type dissimilatory sulfite reductases, *Eur. J. Biochem.* 205, 111-115.

Duyvis, M. G., Wassink, H. & Haaker, H. (1994) Pre-steady-state MgATP-dependent proton production and electron transfer by nitrogenase from *Azotobacter vinelandii*, *Eur. J. Biochem.* 225, 881-890.

Duyvis, M. G., Wassink, H. & Haaker, H. (1996) Formation and characterization of a transition state complex of *Azotobacter vinelandii* nitrogenase, *FEBS Lett.* 380, 233-236.

Duyvis, M. G., Wassink, H. & Haaker, H. (1996) Pre-steady-state kinetics of nitrogenase from *Azotobacter vinelandii*: evidence for an ATP-induced conformational change of the nitrogenase complex as part of the reaction mechanism, *J. Biol. Chem.* 271, 29632-29636.

Duyvis, M. G., Mensink, R. E., Wassink, H. & Haaker, H. (1997) Evidence for multiple steps in the pre-steady-state electron transfer reaction of nitrogenase from *Azotobacter vinelandii*, accepted for publication in *Biochim. Biophys. Acta*.

Duyvis, M. G., Wassink, H. & Haaker, H. (1997) Kinetics of nitrogenase from *Azotobacter vinelandii*: is dissociation of the nitrogenase complex necessary for catalysis?, submitted to *Biochemistry*.

Abstracts

Duyvis, M. G., Wassink, H. & Haaker, H. (1993) Pre-steady-state proton production by nitrogenase of *A. vinelandii*, in: *New Horizons in Nitrogen Fixation*. Proceedings of the 9th International Congress on Nitrogen Fixation. (Palacios, R., Mora, J. & Newton, W.E., eds.) p. 133, Kluwer academic Publishers, Dordrecht, The Netherlands.

Hagen, W. R., Pierik, A. J., van Dongen, W. M. A. M., Duyvis, M. G., Verhagen, M. F. J. M. & Haaker, H. (1993) The redox and magnetic properties of the prosthetic groups in the MoFe protein of *Azotobacter vinelandii* nitrogenase, in: *New horizons in nitrogen fixation*. Proceedings of the 9th International Congress on Nitrogen Fixation. (Palacios, R., Mora, J. & Newton, W.E., eds.) p. 137, Kluwer academic Publishers, Dordrecht, The Netherlands.

Nawoord

Op deze laatste bladzijden wil ik graag al diegenen bedanken die mij gesteund hebben bij mijn onderzoek en het schrijven van dit proefschrift.

Ten eerste wil ik Huub Haaker, mijn copromotor, bedanken voor de enthousiaste manier waarop hij mij in het nitrogenase-onderzoek heeft begeleid. Of de tijd dat ik proeven met nitrogenase mocht doen ook voor mij de mooiste tijd van mijn leven was moet natuurlijk nog blijken, maar ik kan wel zeggen dat het erg leuk was. Huub, ik heb veel genoeg beleefd aan de besprekingen van de talloze experimenten, van de vele versies van de hoofdstukken in dit proefschrift, van de theorieën en ideeën waar je nooit gebrek aan had, en aan onze gezamenlijke experimenten. Ik waardeer het zeer dat je steeds zei waar het naar jouw mening op stond. In allerlei opzichten heb ik veel van je geleerd en ik ben blij dat ik in jouw groep mijn promotie-onderzoek kon doen.

Hans Wassink was mijn bondgenoot op het lab. Hij heeft mij geleerd om te gaan met nitrogenase. Hans, bedankt voor je hulp bij al die zuiveringen ("topsport"), kweken en experimenten. Je gezelschap en relativerende opmerkingen in tijden van bijna-wanhoop over onbegrijpelijke resultaten of mislukte proeven, en in tijden dat niets de successen meer in de weg stond, waren voor mij goud waard. Ook wil ik je bedanken voor alle zuiveringen die je in je eentje hebt uitgevoerd, als ik "nog één" stopped-flow of rapid-freeze experiment wilde doen en het eiwit sneller verschoot dan jij het kon zuiveren, en voor de experimenten die je alleen of samen met Huub hebt uitgevoerd om mijn artikelen te vervolmaken. Ik heb genoten van onze samenwerking!

Professor Veeger, mijn promotor, wil ik bedanken voor de gelegenheid mijn promotie-onderzoek op de vakgroep Biochemie te kunnen verrichten en voor zijn kritische kanttekeningen bij de verschillende hoofdstukken van dit proefschrift.

Pendelend tussen zijn groep in Wageningen en zijn werk als hoogleraar in Nijmegen, vond Fred Hagen telkens weer tijd voor EPR-metingen aan mijn nitrogenase samples en voor uitleg van de EPR-spectra, waarvoor ik hem hartelijk wil bedanken.

Colja Laane, hoewel niet "mijn" hoogleraar, was steeds zonder meer bereid mijn artikelen te lezen en van kritisch commentaar te voorzien. Ik wil hem bedanken voor zijn interesse in mijn onderzoek.

Richard Mensink, mijn voorganger in het nitrogenase-onderzoek, wil ik bedanken voor zijn belangstelling voor en bijdrage aan mijn onderzoek. Hoofdstuk 5 van zijn proefschrift was de basis voor hoofdstuk 5 van mijn proefschrift: een deel van Richard's werk heeft in dit hoofdstuk een plaats gevonden.

Het kweken en oogsten van Azotobacter verliep niet altijd vlekkeloos; gelukkig was Fred van den End altijd bereid een deskundige helpende hand te bieden wanneer er problemen waren met de fermentor of de centrifuge.

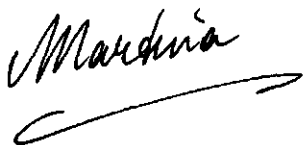
I would like to thank Magda Szafran and Andrey Sergeev, for their pleasant company at the laboratory and their encouragements. Mijn dank geldt ook René Wientjes, Niels Koert, alle studenten die in de afgelopen zes jaar lab 3, lab 3A, lab 4 en lab X bevolkt hebben, en mijn kamergenoten, Hans, René, Axel en Niels, voor de zeer prettige sfeer op het lab.

Ik heb met heel veel plezier op de vakgroep Biochemie gewerkt en niet in de laatste plaats dankzij geweldige collega's. Bedankt voor de gezelligheid, hulp, grappen en belangstelling! Ik ga jullie niet allemaal met name noemen en bedanken, behalve Laura Ausma en Martin Bouwmans, bij wie ik altijd terecht kon voor hulp bij administratieve zaken, van alles en nog wat en voor een praatje, en Adrie Westphal, zonder wiens veelvuldig te hulp schieten dit proefschrift de printer ongetwijfeld nú nog zou blokkeren....

De wekelijkse maaltijden, de zinnige en de onzinnige gesprekken met de Labjournalen - Antonio Pierik, Axel Berg, Frank Vergeldt en Marc Verhagen - waren een feest! Ik ben erg blij met mijn paranimfen, Frank en Axel.

Jos, mama, Suzan en Werner, mijn familie, schoonfamilie en vrienden bedank ik voor hun liefdevolle belangstelling, vriendschap, steun en vertrouwen.

Het is af!

A handwritten signature in black ink, appearing to read 'Mardina', with a long, sweeping horizontal flourish underneath.